Commande coopérative des sytèmes multi-agents avec contraintes de communication

Lara Briñon Arranz

UNIVERSITÉ DE GRENOBLE

THÈSE

Pour obtenir le grade de

DOCTEUR DE L'UNIVERSITÉ DE GRENOBLE

Spécialité : **Automatique et Productique**

Arrêté ministériel : 7 août 2006

Présentée par

Lara BRIÑÓN ARRANZ

Thèse dirigée par **Carlos CANUDAS DE WIT**
et codirigée par **Alexandre SEURET**

préparée au sein du centre de recherche **INRIA Grenoble Rhône-Alpes**, du laboratoire **GIPSA-Lab, Département d'Automatique**
et de l'école doctorale **Électronique, Électrotechnique, Automatique et Traitement du Signal.**

Cooperative control design for a fleet of AUVs under communication constraints

Commande coopérative d'une flotte de véhicules autonomes sous-marins avec contraints de communication

Thèse soutenue publiquement le **18 novembre 2011**,
devant le jury composé de :

Mazen ALAMIR, Président
Directeur de Recherche CNRS, GIPSA-Lab (Grenoble, France)
Rodolphe SEPULCHRE, Rapporteur
Professeur, Université de Liège (Liège, Belgique)
Wilfrid PERRUQUETTI, Rapporteur
Professeur à l'École Centrale de Lille (Lille, France)
Vincent RIGAUD, Examinateur
Responsable Unité Systèmes Sous-Marins , Ifremer (Toulon/La Seyne, France)
Pascal MORIN, Examinateur
Professeur contractuel, Université Pierre et Marie Curie (Paris, France)
Carlos CANUDAS DE WIT, Directeur de thèse
Directeur de Recherche CNRS, GIPSA-Lab (Grenoble, France)
Alexandre SEURET, Co-Directeur de thèse
Chargé de Recherche CNRS, GIPSA-Lab (Grenoble, France)
Jan OPDERBECKE, Invité
Responsable Service Positionnement, Robotique, Acoustique et Optique, Ifremer (Toulon/La Seyne, France)

Acknowledgments

This thesis is the result of the last three years spent at GIPSA-lab and INRIA Grenoble within the NeCS team.

Firstly, I would like to thank my advisor Carlos Canudas de Wit for giving me the opportunity to dive into the world of research and to participate in several enriching projects and meetings during my PhD. I am also thankful to my co-advisor Alexandre Seuret for his inestimable support, his encouraging guidance and for his careful reading of this dissertation. Alex has been more than a motivating tutor, he has also been a friend.

I thank all the members of my thesis committee for their questions and feedback, particularly the reviewers Rodolphe Sepulchre and Wilfrid Perruquetti, whose comments, observations, and suggestions greatly improved this thesis.

Participating in both European project FeedNetBack and French project CONNECT has been a gratifying and interesting experience which provided me colleagues, collaborators, and friends. I would also like to thank all the people who have contributed to the development of this thesis with their useful advices, inspirational discussions, and technical assistance, especially to Federica Garin, Jonathan Dumon, Jan Opderbecke and Alain Sarlette.

Merci aux doctorants de mon équipe pour avoir créé une belle ambiance de travail et aussi à tous les membres du GIPSA-lab et de l'INRIA pour l'environnement motivant qu'ils entretiennent. Un grand merci a Myriam, Elodie et Florence qui ont dépassé leurs compétences administratives pour m'encourager tout au long de ma thèse. Je tiens à remercier sincèrement Nicolas pour m'offrir son aide, supporter mes monologues sans fin, m'encourager dans les moments difficiles et pour me montrer qu'un collègue de bureau peut être beaucoup plus que ça.

El proceso de aprendizaje de estos últimos tres años no sólo reside en la elaboración de esta tesis. Las experiencias de las que he podido nutrirme y que por tanto me han ayudado a finalizar con éxito esta aventura, están protagonizadas por muchos amigos y compañeros a los que deseo agradecer su aportación a todo lo vivido. Gràcies als meus germanets Jordi, Lluc i Marc, con los que descubrí que puedo tener hermanos aún

siendo hija única. Gracias a Rubén que me enseñó el camino del *karma*. Merci à tous ceux qui m'ont soutenu ces trois dernières années, mes chères colocs Ruth, Armelle, Mathilde et les Breners, y mis amigos Elisa, Diego, Alejandro y demás estepicursores, por hacer de Grenoble mi casa, gracias.

No puedo dejar de agradecer a todos aquellos que siempre están dispuestos a perder su tiempo conmigo cuando voy a Madrid por enseñarme a seguir disfrutando de mi ciudad. Y por supuesto a mis amigas repartidas por el mundo cuyo apoyo es incondicional estén donde estén.

Por supuesto, esta tesis se la debo a mis padres, gracias por vuestro apoyo y vuestro ánimo, por enseñarme todo lo que os esforzasteis en hacer que aprendiera y por todo lo que no os disteis cuenta que aprendí de vosotros.

Grazie mille a Alessandro, per avermi insegnato ad apprezzare ogni *pause café*, ogni via, ogni cima, ogni giorno; per insegnarmi che sempre sarà piú perfetto.

Pour finir, un grand merci aux Alpes, et tout ce qu'elles répresentent dans ma vie.

Abstract

This dissertation focuses on cooperative control of multi-agent systems. This topic has been extensively studied in recent literature due to its large number of applications. This thesis is concerned by the design of collaborative control strategies in order to achieve an underwater exploration mission. In particular, the final aim is to steer a fleet of Autonomous Underwater Vehicles, which are equipped by appropriate sensors, to the location of a source of temperature, pollutant or fresh water. In this situation it is relevant to consider constraints in the communication between vehicles which are described by means of a communication graph. The first contributions deal with the development of cooperative formation control laws which stabilize the fleet to time-varying formations and, in addition, which also distribute the vehicles uniformly along the formation. Finally, the source-seeking problem is tackled by interpreting the fleet of vehicles as a mobile sensor network. In particular, it is shown that the measurements collected by the fleet of vehicles allows us to estimate the gradient of a scalar field. Following this idea, a distributed algorithm based on consensus algorithms is proposed to estimate the gradient direction of a signal distribution.

Cette thèse concerne le contrôle coopératif de systèmes multi-agents. Ce sujet a été largement étudié dans la littérature récente en raison de son grand nombre d'applications. Cette thèse propose des nouvelles conceptions de stratégies de contrôle collaboratif afin de réaliser une mission d'exploration sous-marine. En particulier, l'objectif final est de diriger une flotte de véhicules autonomes sous-marins, équipés de capteurs appropriés, jusqu'à l'emplacement d'une source de température, de polluants ou d'eau douce. Dans cette situation, il est pertinent de considérer les contraintes de communication entre véhicules qui sont décrites au moyen d'un graphe de communication. Les premières contributions traitent du développement des lois de commande d'une formation qui stabilisent la flotte vers des formations variant dans le temps, et qui, de plus, distribuent uniformément les véhicules le long de la formation. Enfin, le problème de recherche d'une source est abordé par l'interprétation de la flottille de véhicules comme un réseau de capteurs mobiles. En particulier, il est démontré que les mesures recueillies par la flotte de véhicules permettent d'estimer le gradient de

concentration de la quantité d'intérêt. En suivant cette idée, un algorithme distribué basé sur des algorithmes de consensus est proposé pour estimer la direction du gradient d'une distribution de signal.

Contents

List of Figures

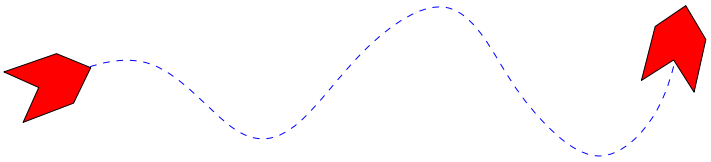

Preface

Statement of problem

The object of this preface is to discuss the problem statement considered in this thesis and give an overview of the dissertation without entering in details.

This thesis deals with control of heterogeneous marine vehicles to achieve a scientific mission composed of several phases. Different classes of surface and underwater vehicles, such as autonomous crafts, Autonomous Underwater Vehicles (AUVs) or underwater gliders, are considered in this context in order to reach several tasks such as, exploration, survey and scientific sensor data sampling. The main objective of this thesis is to develop cooperative control strategies to steer a fleet of AUVs to the location of an underwater source. For instance, the source could be of soft water or chemical pollutants. In this situation, the key problems are concerned by the fields of non linear systems, multi-agent systems, formation control, collaborative control and distributed estimation. With a view to design a solution to these control problems, the dissertation is articulated into three main contributions:

A Formation control

In a first step, we focus on circular formations composed of a group of autonomous underwater vehicles. Consequently, our first contribution consists in designing a feedback control to stabilize a fleet of vehicles to a circular formation, whose center and radius are time-varying. A cooperative term is added in order to dispose the vehicles in a particular configuration along the formation.

B General framework to motion coordination

In order to extend our previous result dealing with time-varying circular formations, we develop a new framework based on affine transformations. This formulation allows us to stabilize the vehicles to a large class, not only circular, of time-varying formations.

C Source-seeking algorithms

The contributions in the field of formation control are the base to tackle the

main objective of this thesis: location and tracking of an underwater source. We present a distributed algorithm to estimate the gradient direction of a signal, by a fleet of vehicles uniformly distributed along a circular formation.

Dissertation Outline

Chapter 1: Introduction

The purpose of this chapter is to put into context the main topics related to this thesis and to give an exhaustive overview of the dissertation. Several contributions are developed in order to achieve the challenges proposed by two projects and their corresponding case study. At first, the case study is explained in detail. General objectives of both projects and technical aspects of underwater missions are exposed.

The second part of the introduction is composed by a review, which deals with multi-agent systems and especially, its application to formation control. These topics are the bases to carry out cooperative tasks, which must be achieved by a group of vehicles or sensors. This survey analyzes the applications of multi-agent systems and different collaborative control strategies present in the literature.

Finally, we recall the main contributions developed, with a view to explain the structure of the dissertation and the main challenges considered.

Chapter 2: Time-varying circular formation control

The first objective of the thesis deals with the control of a fleet of vehicles to reach a time-varying formation. In this context, it is assumed that external or centralized references define the desired shape and location of the formation. A first contribution concerns an extension of existing results in circular control (Paley et al. 2005 [118], Leonard et al. 2007 [86] and Sepulchre et al. 2008 [149, 150]). Two new control laws are developed in order to stabilize the vehicles to a circular motion, whose center tracks a time-varying reference or whose radius depends on time. For both control laws, each vehicle converges independently to the desired formation. Therefore, the phase arrangement of the vehicles along the formation is arbitrary.

A second contribution provides an additional control to ensure that the vehicles are uniformly distributed along the circular formation. Indeed, in the context of source localization by underwater vehicles, which is treated in Chapter 4, this configuration is more adequate to provide efficient source-seeking motions. Consequently, both previous control laws are improved with a collaborative gradient term to achieve the uniform distribution of the AUVs along the circle taking into account communication constraints. The communication topology of the group of vehicles is represented by

a communication graph, and its connectivity determines the stability of the desired configuration.

Chapter 3: Formation control design based on affine transformations

Following the previous formation control approach, a new general framework is introduced. This new formulation allows considering a richer class of formations, not only circular, and also time-varying formations. To do so, the contribution comes from the use of affine transformations, which are composed of linear transformations (scaling and rotation) and translations. The key idea is that a sequence of affine transformations applied to the unit circle defines an elastic formation. In other words, a larger class of time-varying formations with arbitrary shape can be obtained deforming a unit circle. Then, a general control law, based on the circular formation control design, which makes the vehicles reach these elastic formations is provided. The sequence of transformations which defines the final formation is an external reference known to all the vehicles.

This new framework based on affine transformations is pertinent also to define several motions defined only by a desired velocity. The objective now is to make the vehicles converge to the same motion following a velocity reference.

Both approaches are improved with collaborative algorithms in order to achieve several additional aims such as, distribute the vehicles uniformly along the formation and reach an agreement on an unknown parameter which defines the formation.

Chapter 4: Collaborative source-seeking

In this chapter, we tackle the final objective of the thesis dealing with the source-seeking problem. The aim is here to locate the source of some signal distribution, using a fleet of AUVs. In this situation, the vehicles are equipped with sensors. These sensors are able to measure the concentration of the quantity of interest. The fleet of vehicles becomes a mobile wireless sensor network. A first contribution shows that collecting sensor data from vehicles, which are uniformly distributed along a fixed circular formation, the gradient direction of the signal distribution is estimated. Then, a distributed algorithm based on this idea is proposed, in order to take into account the communication constraints. This approach combines the previous results on formation control exposed in Chapters 2 and 3, and existing results on consensus filters (Olfati-Saber and Shamma 2005 [112]) applied to this mobile sensor network situation. A modified algorithm which uses the periodic properties of the circular formation is also proposed with a view to improve the performances of the previous one. Finally, a

comparison of the two distributed source-seeking algorithms is discussed and motivated by simulations.

Chapter 5: Conclusion and Future works

In the last chapter of the thesis, we make a general conclusion, which summarizes the dissertation contributions and describes ongoing and possible future extensions. Appendix A reviews the fundamentals of graph theory and the most important properties of graphs used in this thesis. A summary of the thesis in French is provided in Appendix B.

List of Publications

Proceedings of peer-reviewed international conferences

- Lara Briñón-Arranz, Alexandre Seuret, and Carlos Canudas de Wit, ***Translation Control of a Fleet Circular Formation of AUVs under Finite Communication Range***. In Proceedings of the 48th IEEE Conference on Decision and Control, held jointly with the 28th Chinese Control Conference, Shanghai, China, 2009.

- Lara Briñón-Arranz, Alexandre Seuret, and Carlos Canudas de Wit, ***Contraction Control of a Fleet Circular Formation of AUVs under Limited Communication Range***. In Proceedings of the 2010 American Control Conference, Baltimore, USA, 2010.

- Lara Briñón-Arranz, Alexandre Seuret, and Carlos Canudas de Wit, ***General Framework using Affine Transformations to Formation Control Design***. In Proceedings of the 2nd IFAC Workshop on Distributed Estimation and Control in Networked Systems, Annecy, France, 2010.

- Lara Briñón-Arranz, Alexandre Seuret, and Carlos Canudas de Wit, ***Elastic Formation Control based on Affine Transformations***. In Proceedings of the 2011 American Control Conference, San Francisco, USA, 2011.

- Lara Briñón-Arranz, Alexandre Seuret and Carlos Canudas de Wit, ***Collaborative Estimation of Gradient Direction by a Formation of AUVs under Communication Constraints***. In Proceedings of the 50th IEEE Conference on Decision and Control, held jointly with the European Control Conference in the invited session *Consensus Algorithms, Cooperative Control, and Distributed Optimization*, Orlando, USA, 2011.

- Lara Briñón-Arranz, Alexandre Seuret and Carlos Canudas de Wit, ***Collaborative Estimation of Gradient Direction by a Formation of AUVs***. 5th International ICST Conference on Performance Evaluation Methodologies and Tools, Cachan, France, 2011.

Peer-reviewed national conference papers

- Lara Briñón-Arranz, Alexandre Seuret and Carlos Canudas de Wit, ***Translation Control of a Fleet Circular Formation of Vehicles under Communication Constraints***. 6th National Conference on Control Architectures of Robots, Grenoble, France, 2011

Technical reports

- Lara Briñón-Arranz, Alexandre Seuret, Brandon J. Moore and Carlos Canudas de Wit, ***Formation control***. D02.01 Cooperative Control and Estimation Algorithms, Deliverable FeedNetBack project, 26 February 2010

- Alexandre Seuret, Daniel Simon, Emilie Roche, Lara Briñón-Arranz and Gabriel Rodrigues de Campos, ***Multi-agent systems architecture***. D01.03 Building blocks and architectures, Deliverable FeedNetBack project, 26 February 2010

- Lara Briñón-Arranz, Alexandre Seuret, Brandon J. Moore and Carlos Canudas de Wit, ***Collaborative control for AUVs***. D02.02 Cooperative Control and Estimation Algorithms, Deliverable FeedNetBack project, 24 August 2011

Journal articles under preparation

- Lara Briñón Arranz, Alexandre Seuret and Carlos Canudas de Wit, ***Distributed Source-Seeking by a Circular Formation of Autonomous Underwater Vehicles***.

- Lara Briñón Arranz, Alexandre Seuret and Carlos Canudas de Wit, ***Distributed Consensus with Reference Velocity for a Time-varying Circular Formation of AUVs***.

Chapter 1

Introduction

Underwater exploration is the relatively recent process of investigating the depths of the sea to understand its physical and chemical characteristics and to learn about the life forms that inhabit this realm. Deep-sea exploration is a novel phenomenon (compared to many other sciences) because the necessary technology to assure human safety in deep water has been recently developed. Over the last decades, alternative technologies, which use vehicles without crew, such as subsurface floats, Remotely Operated Vehicles (ROVs) and Autonomous Underwater Vehicles (AUVs), have emerged to complement the existing sensing techniques. All these vehicles are equipped with different sensors in order to collect information from a region of interest. This information provides fundamental support to understand the oceans' processes from a biological point of view (ecosystem productivity), or to predict physical properties of the ocean, such as temperature and current. For this purpose, control strategies to command mobile vehicles must be developed to steer the vehicles towards places where their data would be most useful [39].

Mobile sensor networks are often used in environmental applications such as ocean sampling, surveillance, mapping, space exploration and communication, see [39, 86, 177, 167] and the references therein. In these kinds of missions, the mobile sensor platforms are commanded to measure an unknown scalar field. For instance, a chemical concentration, a pollutant, or temperature. Since each platform can only take one measurement at a time, the platforms should move in a formation to estimate the field of interest. It seems appropriate that a group of vehicles collaborate in order to carry out the exploration task while optimizing time and energy. Collaboration means that each vehicle is able to communicate some information to the rest of the group and this data is used to determine some action or particular behavior in order to accomplish the exploration task.

Within this context, the present thesis discusses the problem of an underwater exploration mission carried out by a group of AUVs in a cooperative way. The aim

is to design control strategies to accomplish the different scientific challenges found in such missions:

Control of multi-agent systems: A multi-agent system, more precisely defined in Section 1.2, is a system composed by a group of autonomous individuals interacting with each other. Therefore, a fleet of AUVs can be treated as a multi-agent system in which each vehicle is considered as an agent with communication capabilities.

Formation control design: In order to accomplish an exploration task, a reasonable choice is to coordinate the agents to form a particular configuration. The control algorithms to reach this purpose, must assure some performances, such as the inter-distance between the vehicles in the formation. The most important aim is to move the group of vehicles while keeping the formation.

Control design under communication constraints: In a collaborative mission, the individuals exchange information to achieve a particular task. The data transmitted is subject to different communication problems due to the communication channel, especially in underwater environments, such as noise in the signal transmitted, packet loss, time delays during the transmission and fading problems of the power of the signal.

This dissertation deals with these problems in the context of an underwater mission in which a fleet of AUVs has to collaborate to locate a source.

1.1 Context of the thesis

This thesis is part of two research projects: the European project FeedNetBack[1] and the French project CONNECT[2], funded by the ANR (National Research Agency). Both projects deal with networked control systems (NCS) and they are particularly interested in the problem of controlling multi-agent systems, *i.e.*, systems composed of several sub-systems interconnected by an heterogeneous communication network. The main challenge of these projects is to learn how to design controllers taking into account constraints on the network topology, and of the possibility to share computational resources during the system operation, while preserving closed-loop system stability.

The FeedNetBack project involves several academic partners, and also industrial participants in order to carry out the technological applications. A common case study of both projects focuses on cooperative control design of a group of unmanned marine

[1] http://www.feednetback.eu/

[2] http://www.gipsa-lab.inpg.fr/projet/connect/

vehicles, *i.e.*, Autonomous Underwater Vehicles (AUVs) and Autonomous Surface Vessels (ASVs). This case study, detailed later, concerns the partner IFREMER[3] which is charged with the technical aspects relating to the underwater vehicles. It will accomplish a demonstration using real vehicles. One of the academic participants which is concentrated in the technical innovations of this case study, is the research institute INRIA (Institut National de Recherche en Informatique et en Automatique) via the NeCS Team[4], in the heart of which, this thesis has been made. The CONNECT project also considers the possibility to evaluate the proposed control structures through a graphical interface developed by PGES and simulations effectuated with a complex simulator which is built by PROLEXIA.

1.1.1 Case study

Multi-agent networked systems, particularly underwater systems, which has presently used or intended by the offshore industry and marine research, are subject to severe technological constraints. The advantage of using several simple vehicles instead of one complex, expensive and high capability system, is that a fleet is able to realize tasks that can not easily be achieved by a single vehicle. This case study involves heterogeneous marine vehicles (surface and underwater vehicles such as autonomous crafts, AUVs or underwater gliders) to achieve a scientific mission composed of several phases (exploration and survey, scientific sensor data sampling). The proposed case study copes with a main mission whose objective is to carry out a gradient search and following an underwater source by a fleet of AUVs. The nature of the source to be detected, can be very different: fresh water, a chemical source, methane vent, etc. The technical details corresponding to this case study are reported in [113].

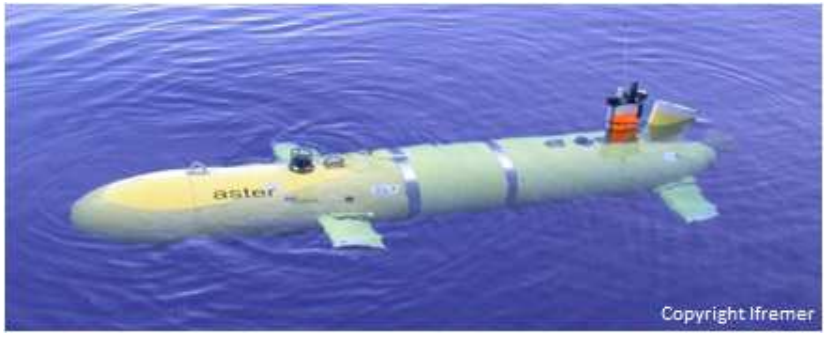

Figure 1.1: *The underwater vehicle AsterX*

[3]Institut français de recherche pour l'exploitation de la mer, http://wwz.ifremer.fr/institut
[4]http://necs.inrialpes.fr/

AsterX

The underwater vehicle considered in this case study and hence, in this thesis, is the AsterX, which belongs to IFREMER (see Figure 1.1). The AsterX is an autonomous underwater vehicle which is actuated by a main screw propeller for moving in the longitudinal direction. The steering of the vehicle around its roll, pitch and yaw angles is achieved through two fins in the front part of the vehicle (canard fins), and two couples of fins at the tail of the vehicle (horizontal and vertical plan). Depending on the payload its weight is between 580 and 800 kg in air, with a diving depth of 3000 metres. Its cruising speed is between 0.5 to 2.5 metres per second. Vehicle length is 4.5 meters and its autonomy is 11 hours executing a mission [135].

This AUV has several navigation sensors: a Doppler loch to measure the speed, an inertial measurement unit (composed of a gyroscope, accelerometers and magnetometers) to compute in real time its attitude (roll, pitch and yaw angle) and update its position, and also an acoustic sensor for absolute positioning.

Underwater scenario and mission

The objective of the mission is to locate and follow a source by considering sensed data provided by dedicated scientific sensors located on-board the AUVs, which measure the concentration of the source flow. The configuration of the vehicles must be such that spatial estimates of the gradient of the signal concentration can be computed cooperatively. The cooperative control laws designed to reach this aim, should consider communication constraints due to the underwater scenario.

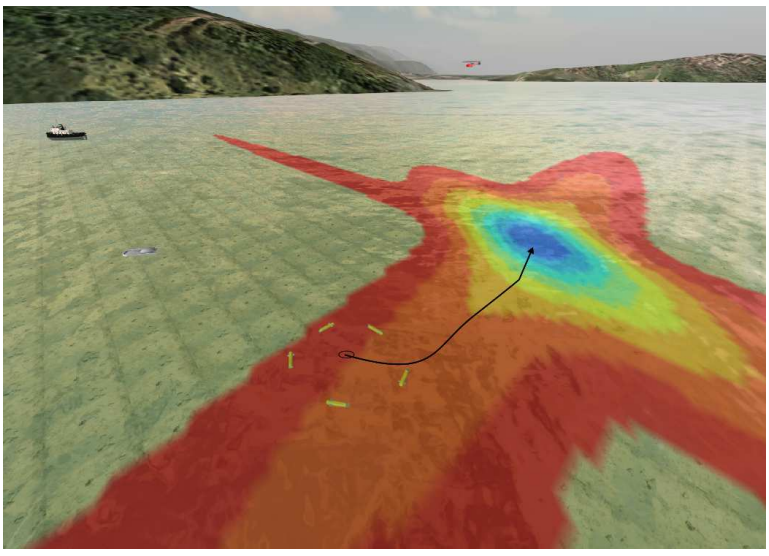

Figure 1.2: *Underwater source detection and tracking*

To perform missions involving several vehicles, coordinated motion is required, especially when the goal of the mission is sensor driven. In the case presented here, the detection of the source can be performed with sensor information collected by the vehicles measuring concentration in the source plume, as shown in Figure B.2. This picture represents the objective of the case study and it is produced by the graphical interface developed by PGES and the simulator which is provided by PROLEXIA. The colored elliptical forms symbolize the level curves of the scalar field of interest. The fleet of AUVs, organized in a particular formation, will compute in a collaborative way the best direction to move the center of the formation towards the source location. It is up to the fleet to maneuvre so as to seek the region of higher concentrations of the signal distribution, and thus, to carry out the localization of the source.

Phases of the mission and challenges

In recent years, it can be noticed the deterioration of marine waters due to multiple pollutants. This case study, developed in coordination with IFREMER, aims to locate the sources of the leaks, following a shipwreck, or, conversely, sources of fresh water for domestic consumption. The different steps considered to reach this objective are detailed below.

The initial configuration is a fleet of five autonomous underwater vehicles equipped with salinity sensors, which must locate a source of fresh water without human intervention. Cooperation strategies with the pooling of information from each vehicle, must be developed to exploit the advantages of using a fleet of vehicles and, to reduce the time of exploration.

A first challenge is due to the difficulty of establishing reliable communication in underwater environment. This is a key point for ensuring an effective cooperation. Indeed, the data rate is only of a few hundred $bits/s$, the transmission delay is around a second and about 10% of items are lost. In this situation, all control strategies developed have to take into account communication constraints.

The source localization task will be carried out in two phases. Therefore, a second challenge concerns the design of formation control laws appropriate to achieve the objectives of each phase. The first one corresponds to the exploration phase. During this exploration stage, the vehicles move in a V-shaped formation [103], in order to collect information and to detect the signal distribution emitted by the source. Once an agent detects a significant change in salinity, it transmits this information to the others. Then the fleet starts a phase of consolidation.

In this second phase, the fleet is regrouping into a particular shape, for instance circular. With such formation, the movement might be slower than with the V-formation. However, a circular formation has greater flexibility to move in all directions. Also,

the distribution of AUVs along the formation is pertinent to collect spacial distributed measurements which can allow a more precise localization of the source. It is also possible to envisage many class of formations: it might be interesting to deform the shape of the formation to adapt it to the environment, to follow a path or to avoid obstacles.

With a view to form and maintain this formation, the vehicles must exchange messages according to their relative position to the center of the formation. A centralized design can be considered such that a surface vehicle provides all necessary informations to the fleet. Exchanges of data between the AUVs allow considering a decentralized approach in which any vehicle is designed as a leader. In order to deal with communication constraints, such as limited communication area of the AUVs, only the nearest neighbors are taken into account to exchange informations.

In order to fulfill the objective of source-seeking, a decision algorithm must be developed. It will be also based on data exchanges between neighbors to ensure the same robustness with respect to communications. The objective of this final task is to allow all vehicles to agree on a direction for the formation to move towards the source using the measurements collected by the vehicles. One can imagine extending this type of algorithms for other applications such as contours seeking to delineate the extent and evolution of a polluted area.

1.1.2 General objectives

The general common objectives of both FeedNetBack and CONNECT projects, corresponding to the underwater vehicles case study previously presented, are focused on the following five key challenges:

Architecture: The need to coordinate the actions of the vehicles over channels with limited capacity.

Control and Complexity: Centralised versus decentralized control strategies, which are at the heart of this application.

Control and Communication: The available bandwidth is severely limited (few bits per second), communication is subject to long and variable propagation delays, multi-path, fading and high bit error rates.

Control and Computation: The case study will make use of the adaptive sampling strategies, and distributed collaborative computation.

Control and Energy: In this application battery power is limited and usually batteries cannot generally be recharged. Energy resources must be shared between different functions.

According to these general objectives, the following control strategy, based on a technical report of the FeedNetBack project [152], to achieve a collaborative search of an underwater source using a fleet of AUVs is proposed in this thesis. The first challenge is to describe an adequate architecture to deal with a cooperative approach taking into account all the elements of the problem statement and all the constraints. In consequence, three main control loops are considered, as shown in Figure 1.3. Knowing that this project aims to study fleets of vehicles working together to reach a common objective, in terms of control and coordination of fleets, this thesis considers the fleet to be composed of a homogeneous set of vehicles, *i.e.*, all vehicles have the same dynamic model.

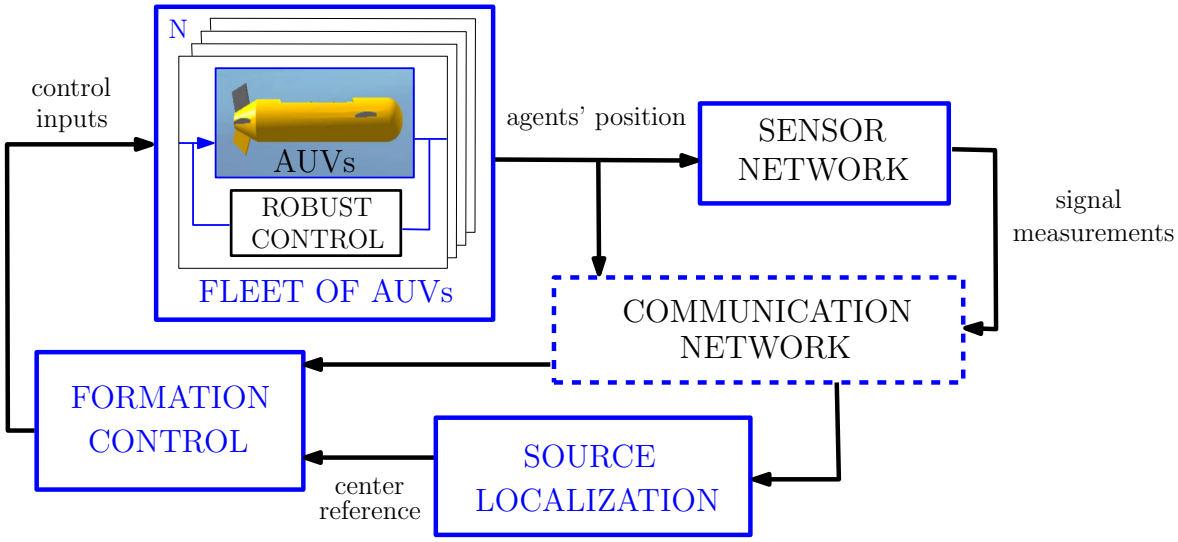

Figure 1.3: *Architecture of the control strategy*

The first aim is to develop a local control loop, called robust control, which stabilizes each AUV. This control law takes into account the dynamic model of the vehicles in order to control their orientation, velocity and deep. The motion along the three axes is uncoupled so that, three different controllers are computed for the control of the forward speed, the yaw angle and, the altitude respectively. The thesis of Roche [136], which is also part of both FeedNetBack and CONNECT projects, deals with robust control design for trajectory tracking of a single AUV via a variable sampling interval approach.

Considering several identical vehicles, the external loop carries out the search task. A cooperative control is implemented to reach a coordination motion of the fleet such that, the group of AUVs is disposed in a particular configuration. The desired formation is defined by several parameters such as, its center and radius in the case of

a circular formation. A collaborative control law stabilizes the fleet to a formation tracking the time-varying parameters which define it. This work is realized in two dimensions, hence it is assumed that all the vehicles are moving at the same deep. Linear velocity and orientation are the control variables which depend on the AUV state (position and velocity) and on the external references which define the desired formation. The uniform distribution of the vehicles along the formation is also considered. In order to take into account communication constraints, a decentralized algorithm is designed to stabilize the vehicles to the desired pattern (uniform distribution), only using information from their closer neighbors.

Finally, the trajectory of the formation center is obtained by a distributed control using the measurements of the signal distribution by a fleet of AUVs. The expected data is measured by detection sensors. The trajectory to be followed by the fleet shifts from the predefined search pattern to a sensor-based trajectory control in order to detect the source of the measured data.

The implementation of control loops on a network of digital controllers induces some additional disturbances with respect to the initial continuous time design, more precisely due to sampling, delays, jitter, quantification and data loss. Consequently, it is appropriate to take into account these communication constraints in order to design the different control strategies previously defined.

In order to consider the underwater communication problems, the development of efficient underwater acoustic communication protocols is needed. Current underwater acoustic modems are based on very classical single-carrier modulation with a very low bit rate. For achieving high data rate and large system capacity, Orthogonal Frequency Division Multiplexing (OFDM) has been claimed to be an efficient communication technology [78]. It allows designing low complexity receivers to deal with highly dispersive channels. This fact motivates the use of OFDM in underwater environments. Moreover, the multiple access channel technique called OFDMA (Orthogonal Frequency Division Multiplex Access) can significantly reduce the latency induced by TDMA (Time Division Multiplex Access) based protocols currently used [76, 77]. Using this protocol the quality of the transmitted signal decay with the distance. Therefore, we consider that each vehicle is able to communicate only in a region defined by a critical communication distance ρ.

With a view to deal with these general objectives, the multi-agent systems and its applications, particularly the formation control problem, are considered in this thesis. Therefore, an overview on this kind of systems is presented in the following section.

1.2 Survey on formation control of multi-agent systems

Cooperative behavior in large groups of individuals appears abundantly in nature. There exist well known examples of such behaviors such as, schools of fish, flocks of birds, collective food-gathering in ant colonies. The reader might refer to [158] to find more examples. The fundamental property of this cooperation is that the group behavior is not dictated by one of the individuals. On the contrary, the behavior results implicitly from the local interactions between the individuals and their neighbors. For instance every fish in a school knows where the other fish in its neighborhood are heading, but it does not known the average heading of all fishes. Nonetheless the fishes in the school stay together and moves as a group in a certain direction [37, 134], see Figure 1.4.

Figure 1.4: *School of fish. This image is used under the CC-BY-2.0 licence (http://creativecommons.org/licenses/by/2.0/deed.fr), it is posted to Flickr by JordanSu.*

Many engineering systems also consist of large groups of cooperating dynamic systems. They are called *multi-agent systems*. One has to refer to a topic of research that emerges in the 1980's with the thesis of Tsitsiklis [168], which was one of the first contributions in the field. Even if this thesis is more concerned by computer science and distributed programming, the implication to the field of automatic control was significant at this time and leads to open problems in many areas such as *distributed*

optimization, *consensus algorithms*, *formation control*, etc.

Cooperative control has been extensively studied in the past few years. This field includes consensus algorithms, collaborative control of multi-agent systems, motion coordination, distributed optimization and distributed estimation in sensor networks. Engineering motivations for studying cooperative control approaches stem from increasing interest in groups of embedded systems, such as multi-vehicle and sensor networks.

Particularly, consensus problems have a long history in the field of computer science. A consensus algorithm is an interaction rule that specifies the information exchange between an individual and all of its neighbors on the network whose proposal is to converge to an agreement value. There exist a huge number of contributions to this problem including consensus algorithms with time-delays, switching topology or consensus filters, among many others [109, 111, 112, 130, 151]. These distributed agreement problems are directly related with cooperative multi-agent applications. Moreover, consensus algorithms represent an excellent tool to develop more complex cooperative control laws. Furthermore, a decentralized algorithm presents several advantages in comparison with a centralized approach, especially if the multi-agent system is subject to communication limitations.

Hence, before going to the details of the technical achievements of the present dissertation, it is necessary to provide a precise definition of *multi-agent systems* and *formation control*.

1.2.1 Multi-agents systems

Multi-agent systems (MAS) has received a lot of attention in recent years. A MAS is a system composed of multiple interacting intelligent agents. MAS can be used to solve problems that are difficult or impossible for an individual agent or a monolithic system to solve. Intelligence may include some methodical, functional, procedural or algorithmic search, find and processing approaches. Topics where multi-agent systems research may deliver an appropriate approach include on-line trading [137], disaster response [144], and modelling social structures [161].

A broad definition of *agent* was introduced in [53]. This book presents and reviews the concept of multi-agent systems and its applications. The author define an agent as a physical or virtual entity having several important characteristics:

- **Reactivity capabilities**: An agent is able to act and has a behaviour to satisfy its goals.
- **Autonomy**: An agent is at least partially autonomous.
- **Perception**: It is able to perceive its environment.

- **Local views**: No agent has a full global view of the system, or the system is too complex for an agent to make practical use of such knowledge.

- **Communication capabilities**: An agent is able to communicate with others agents.

A multi-agent system is composed of an environment, objects and agents, relations between all the entities, a set of operations that can be performed by the entities and the changes of the environment in time and due to these actions. In this situation, the agents are the only ones to act.

As a comment, it is worth noting that multi-agent systems research does not only refer to automatic control. Among other fields, MAS often addressed computer science [53, 169], distributed computation [11, 14], game theory [15], social science [40], etc. A multi-agent system may contain combined computer's agents, human teams and agent-human teams.

In automatic control, the interests of MAS is particularly relevant when one has to face with systems consisting of multiple vehicles (which are considered to be the agents) with several sensors and actuators that are intended to perform a coordinated task. This is currently an important and challenging field of research motivated by a large number of applications in many areas. Potential applications for multi-agent systems include surveillance, collaborative search and rescue, environmental monitoring, exploration and distributed reconfigurable sensor networks. To enable these applications, various cooperative control capabilities have been analyzed, including formation control, rendezvous, attitude alignment, flocking, congestion control in communication networks, task and role assignment, air traffic control, coverage and cooperative search.

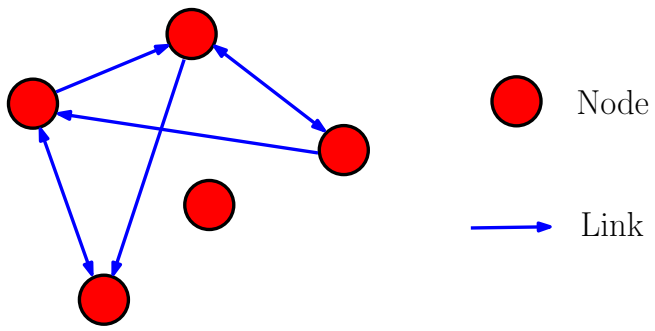

Figure 1.5: *Diagram of a multi-agent system*

Summarizing, a multi-agent system is a group of nodes (agents) representing vehicles, sensors, plants, etc., which are able to exchange information in order to reach a common goal. Schematically, MAS can be represented by a network of nodes in-

terconnected via a communication topology as shown in Figure 1.5. Interconnections between agents in a MAS are usually modeled by directed or undirected graphs [12].

This paragraph presents some basic tools of graph theory. For an extensive analysis, see Appendix A. The communication topology for the groups of agents is represented by means of a graph $\mathcal{G}(V, E)$ where $V = \{1, 2, ..., N\}$ is the set of vertices (agents) and E the set of edges (communication links) such that $(k, j) \in E$ if agent k communicates with agent j. In this thesis all communication graphs considered are undirected. It means that the communication between agents is bidirectional, *i.e.*, if agent k communicates with agent j, agent j transmits also to agent k. When there is a communication link between agent k and agent j, both agents are called neighbors. The set of neighbors of agent k is denoted by $\mathcal{N}_k$ and the degree of agent k is represented by $d_k = |\mathcal{N}_k|$. The Laplacian matrix $\mathbf{L}$ of a undirected graph $\mathcal{G}$ is defined as:

$$L_{k,j} = \begin{cases} d_k, & \text{if} \quad k = j \\ -1, & \text{if} \quad j \in \mathcal{N}_k \\ 0 & \text{otherwise} \end{cases} \tag{1.1}$$

The Laplacian matrix allows us to include, in a compact form, communication constraints to different control laws for MAS, see [12].

Classical objectives for MAS

a) *Consensus and average consensus*

The term consensus refers to an agreement in the value of a variable reached by a multi-agent system. The average consensus refers to the agreement protocol in which the final value of the consensus variable is the average of the initial values.

b) *Synchronization*

A multi-agent system reaches synchronization if the state of all the agents is the same asymptotically. This definition can be interpreted as a consensus algorithm but synchronization is usually applied in manifolds with particular symmetries, such as in the case of oscillators.

c) *Formation control*

A collection of interacting agents disposed in a particular configuration whose objective is to achieve a common goal is defined as a formation. There exist several formation control strategies in order to make the agents converge to a particular configuration or to maintain inter-agent distances, for instance.

d) *Exploration task and coverage*

The purpose of exploration is to collect information by searching or traveling

around an area of interest. In particular, coverage is a collaborative task in which the agents reach their optimal locations in order to maximize the monitored area.

In the sequel, an overview of different models for MAS gives several examples of these main challenges.

Models of nodes

In the literature, different models to represent the dynamics of multi-agent systems have been used. The description provided in this thesis deals only with continuous models. Consider a MAS formed by $k = 1, \ldots, N$ agents. The state of agent k is represented by $x_k \in \mathbb{R}^m$ where m is the dimension of the state. The control input of the system is denoted by u_k.

The possible kinematics models of nodes can be classed as follows:

A) Linear models

i) *General linear models*

A general linear kinematic model for the agents is described by the following equations:

$$\dot{x}_k = \mathbf{A}x_k + \mathbf{B}u_k \tag{1.2a}$$

$$y_k = \mathbf{C}x_k \tag{1.2b}$$

where $\mathbf{A}, \mathbf{B}, \mathbf{C}$ are matrices. The consensus algorithm corresponding to this model can be writing as [171, 172]:

$$u_k = -\mathbf{K} \sum_{j \in \mathcal{N}_k} (y_k - y_j)$$

where $\mathbf{K}$ is a control matrix.

This model is used in the literature mainly to deal with formation control design such as in [51, 52, 62, 65, 92].

ii) *Single integrator model*

A particular case of a kinematic linear model is the simple integrator:

$$\dot{x}_k = u_k \tag{1.3}$$

To achieve the agreement of the state of the agents the commonly used consensus algorithm in this case is expressed by, see [8, 111, 151]:

$$u_k = -\sum_{j \in \mathcal{N}_k} (x_k - x_j)$$

Apart from consensus algorithms, there are many different applications for MAS which contemplate this simple model to represent a group of agents. Some of these applications are formation control [103], rendezvous [36], cycle pursuit [79, 95], coverage [35, 122, 145] among many others [66, 71].

An important application of this model is the study of the coupled oscillators. The mathematical analysis of these systems composed of phase oscillators interacting each others allows us to learn about the synchronization problem. Kuramoto introduces the first notions to understand this kind of systems and analyzes its collective behavior in [83], where the following synchronization algorithm for coupled oscillators was presented:

$$u_k = -\sum_{j \in \mathcal{N}_k} sin(x_k - x_j)$$

Many extensions dealing with Kuramoto oscillators have been developed in recent literature, see [27, 83, 106, 157], among many others. The knowledge provided by these works can be exploited to synchronize and stabilize different patterns in a MAS configuration, [118].

iii) *Double integrator model*

In many cases, several vehicles can be governed by controlling the acceleration of its actuators, for instance the time-derivative of the angular speed of motors. Thus, a double integrator model is very used in the literature of MAS:

$$\ddot{x}_k = u_k \tag{1.4}$$

The consensus algorithm for double integrator dynamics is given by [129]:

$$u_k = -\sum_{j \in \mathcal{N}_k} [(x_k - x_j) + \alpha(\dot{x}_k - \dot{x}_j)]$$

where α is a control parameter. There exists several extensions of this consensus algorithm taking into account different constraints, see [128].

As in the case of simple integrator, this model is utilized in several approaches of cooperative control such as distributed formation control [110, 138], rendezvous [159] and flocking [108]. This model allows the agents to reach an agreement in their velocities. This particular case of consensus problems is called flocking and, by definition, it is not possible to be applied to simple integrator dynamics of the agents.

B) Nonlinear models

i) *General nonlinear models*

Linear models are sometimes too simplistic to model the dynamics of a real agent. For example, the dynamics of a sensor network might have many non-linearities and it is not realistic to represent the dynamics of some kind of vehicles such as, planes, marine vehicles and two-wheel vehicles, by linear models. Therefore, several authors have studied the previously presented coordinated algorithms for MAS by a nonlinear approach. A general nonlinear model is described by:

$$\dot{x}_k = f(x_k, u_k) \tag{1.5a}$$
$$y_k = h(x_k, u_k) \tag{1.5b}$$

where $f(\cdot)$ and $h(\cdot)$ are functions that could satisfy some particular conditions according to the problem considered.

Consensus algorithms on nonlinear spaces are studied in [142, 146, 147]. The applications of this model are focus on formation control [9, 10, 50, 114, 125], motion planing [57], extremum-seeking problem [82] and plume tracking [140].

ii) *Unicycle kinematics*

A particular nonlinear model extensively considered in the robotics and automatic control is the unicycle model. This non-holonomic model is used to represent dynamics of ground vehicles, Autonomous Underwater Vehicles (AUVs) and Unmanned Aerial Vehicles (UAVs). The state of the agent k is denoted by vector $(x_k, y_k, \theta_k)^T$ where $(x_k, y_k)^T \in \mathbb{R}^2$ is its position vector, $\theta_k \in S^1$ is its heading angle and v_k, u_k are the control inputs:

$$\dot{x}_k = v_k \cos\theta_k \tag{1.6a}$$
$$\dot{y}_k = v_k \sin\theta_k \tag{1.6b}$$
$$\dot{\theta}_k = u_k \tag{1.6c}$$

Basically, all the previous collaborative algorithms developed using simple and double integrator kinematics to model the agents have been investigated using this non-holonomic model. Formation control [24, 32, 33, 45, 69, 120, 149, 150], rendezvous [46], trajectory tracking [80, 81], motion planing [43], synchronization [119], coverage [84, 94], exploration task [86] and source-seeking problems [28, 30, 104] are the main cooperative problems studied in the current literature.

1.2.2 Motion coordination

The previous review on MAS summarizes some of the most important and commonly studied applications in the field of cooperative control. This thesis deals with a system formed by multiple vehicles whose common goal is to coordinate its motion to achieve a task. In this situation, the collaborative approaches coping with motion coordination are specially examined in the sequel.

Motion coordination is a phenomenon in biological systems as has been remarked before, see Figure 1.4. Moreover, it is a useful tool for groups of vehicles, mobile sensors, and embedded robotic systems. A motion coordination task is defined as a collaborative behavior of a group of mobile agents in order to reach a common aim. In other words, achieving a coordination task corresponds to moving the agents and changing their state to maximize or minimize an objective function [97]. Several objective functions can be specified to describe different behaviors and tasks. In addition, the geometry and symmetric proprieties of the desired configuration, are directly related to control design for motion coordination [142].

A review on motion coordination considering some aggregate objective functions is presented in [97]. The authors consider three main objectives: deployment, consensus and cohesiveness. In the context of mobile agents, deployment means placing the agents in the optimal positions to achieve maximum coverage (monitoring or vision of the environment) [7, 35, 133]. The consensus is a useful algorithm to reach rendezvous, *i.e.*, all the agents converge to the same location [36, 46, 174]. Finally, the cohesiveness, is characterized by a repulsion/attraction function which makes the agents in the network maintain desired relative distances between its neighbors or achieve collision avoidance [108, 164].

In this dissertation, other collaborative behaviors are considered as a motion coordination such as, motion planing, collaborative path following, cooperative target tracking and formation control. A multi-agent motion planing is a cooperative algorithm for generating the motion of a group of vehicles in an environment that might change over time, in which each agent takes into account the information of its neighbors to compute its motion [43, 54, 160]. Coordinated path following is a control strategy where multiple vehicles are required to follow pre-specified spatial paths while keeping a desired inter-vehicle formation pattern in time [60]. The target tracking problem can be accomplished by a group of mobile vehicles or sensors. In this case, the objective for the agents is to locate and follow the trajectory of a moving target. There exist many different approaches to deal with this topic in the literature, the reader can refer to [96] and [170], and the references therein.

For many applications it is interesting to impose a particular configuration for the agents. The next subsection reviews the main strategies dealing with formation control.

1.2.3 Formation control

Formation control is an important issue in coordinated control for multi-agent systems. A formation is defined as a group of autonomous agents (vehicles, sensors or robots) with communication capacities, which form a particular configuration (*i.e.*, desired positions and orientations), in which the agents collaborate to achieve a common goal. Keeping a group of vehicles in formation presents several advantages as, for instance, reducing the system cost, reconfiguration ability and structure flexibility of the system, increasing the robustness of the system and improving the properties of the communication topology. There are many areas of application for the formation control field. Surveillance, target tracking and environmental monitoring are some examples.

In the survey [26], the authors study in detail the different strategies dealing with formation control presented in the literature. The analysis of the several approaches is very exhaustive, therefore, in the sequel, a classification of the different formation control designs based on [26] is elaborated, adding other approaches and references in order to complete this overview.

Formation control via behavior-based approach and potential field approach: In [5, 24], several motor schemas implement the overall behavior of a robot in order to move it to a goal location while avoiding obstacles, collisions with other robots and remaining in formation. Each schema generates a vector representing the desired behavioral response (direction and magnitude of movement). Others works combined the behavior-based approach with potential fields as in [48, 126]. The group formation behavior is based on social potential fields. Artificial potential trenches are used to represent the formation trajectory of the group in [59]. The authors of [102] apply this method to a non-linear dynamic system for obstacle avoidance and trajectory generation.

Formation control via generalized coordinates: In this strategy, the agent's position, its orientation and the shape with respect to a reference point in the formation are defined by the generalized coordinates. These coordinates can be used to specify the formation trajectories. This methodology is developed in several works [63, 153].

Formation control via leader-follower approach: In this approach one agent is designated as being the leader and the mission of the rest of vehicles (followers) is to maintain a desired distance to the leader. Hence, the followers receive information from the leader in order to keep the desired formation, see Figure 1.6.

In [45], a controller is designed using input/output feedback and an application of this strategy can be found in [162]. Other strategy to produce formation motions (*i.e.*,

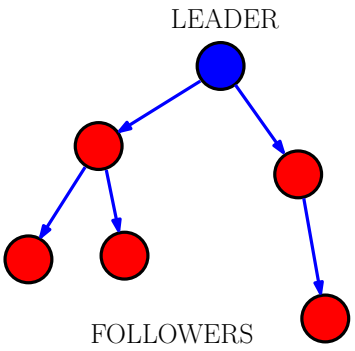

Figure 1.6: *Illustration of the leader-follower structure*

flight formations) is the virtual-leader approach [125] where a suitable inter-distance (and orientation) is set between agents. The motion of the formation results from the motion of the leader. Several extensions to multiple non-holonomic mobile robots are presented in [25, 32, 33, 42, 49].

Formation control via virtual structure method: This method is developed to enforce a group of agents to stay in a rigid formation. The controller of each agent is designed to track the dynamics defined for the virtual structure. It means that, for a desired formation, the control laws designed minimize the error between the desired positions in the virtual structure and the real position of the agents, as shown in Figure 1.7. Introduced by [87, 163], this approach is usually applied to spacecraft or satellite formation flying control [9, 10].

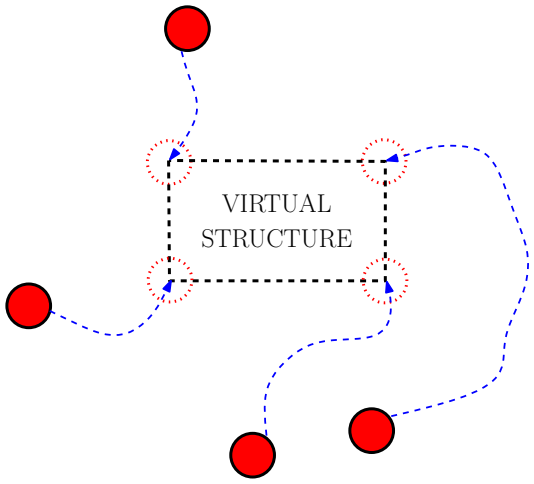

Figure 1.7: *Illustration of the virtual structure method*

Formation control induced by flocking: The paper [134] deals with animal behavior models during the motion of a flock of birds, a herd of land animals, or a school of fish. In this work, Reynolds introduces three heuristic rules that led to creation of the first computer animation of flocking:

1. Flock Centering: attempt to stay close to near by flockmates.
2. Obstacle Avoidance: avoid collisions with near by flockmates.
3. Velocity Matching: attempt to match velocity with near by flockmates.

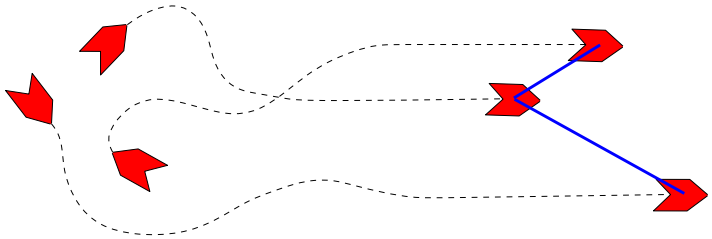

Figure 1.8: *Illustration of flocking*

Based on this previous nearest-neighbor interaction rules, several works dealing with flocking motions have been developed for double-integrator dynamics of the agents, [108, 164, 165]. A common definition of this class of motion is: a group of mobile agents that align their velocity vectors, and stabilize their inter-agent distances, using decentralized algorithms and taking into account the communication topology, as shown in Figure 1.8.

Rendezvous: The multi-agent rendezvous problem, which was posed in [1], copes with the collective behavior of a group of mobile agents, and cooperative algorithms that cause all members of the group to eventually rendezvous at single unspecified location, as defined in [88], see Figure 1.9. The same authors of this previous work analyze the rendezvous strategies based on a sequence of *stop-and-go* maneuvers, in the synchronous [89] and asynchronous case [90]. The rendezvous problem can also be studied through consensus algorithms, see [71, 111]. A review of the various approaches of this problem for linear models of motion can be found in [132]. A detailed analysis of this class of coordinated algorithms to achieve rendezvous using proximity graphs is provided in [36] and several improvements are presented in [46].

Cyclic pursuit: The authors of [95] propose a collaborative strategy for multi-vehicle systems based on the notion of cyclic pursuit from mathematics. They focus on circular

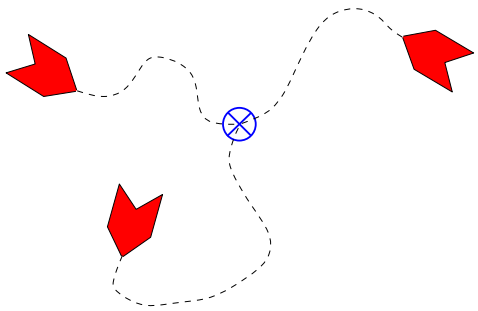

Figure 1.9: *Illustration of rendezvous*

formations of a group of N ordered identical vehicles. Cyclic pursuit means that each agent k pursuit agent $k+1$ modulo N, then each agent is required to sense information from only one other agent, see Figure 1.10. Based on a cyclic pursuit strategy, in [79] a cooperative control of a multi-agent system to achieve a target-capturing task in 3-D space is presented.

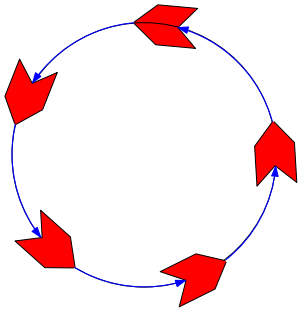

Figure 1.10: *Illustration of cyclic pursuit*

There are certainly other approaches of formation control that this survey has not discussed in detail. Nevertheless, this review allows the reader to understand the state-of-the-art on MAS and justify the main directions followed in this thesis to deal with the challenges presented in the case study.

1.3 Contributions of the thesis

The community of automatic control has specially focused on multi-agent systems in the last twenty years. The different aspects presented in previous overview has been extensively studied due to the advantages of multi-agent systems, with respect to use one single vehicle or sensor, in a large number of applications.

In the context of underwater exploration, designing collaborative missions allows collecting information from extensive areas in a shorter time. The main advantage of

using multiple systems in a coordinated motion is the extension of the sensor range with respect to area coverage or depth coverage. This is especially important if properties which shall be measured fluctuate with time.

According to the case study presented in this chapter, the main challenges addressed in this dissertation are summarized as follows:

- Formation control of AUVs
- Collaborative control
- Source-seeking problem
- Control design under communication constraints

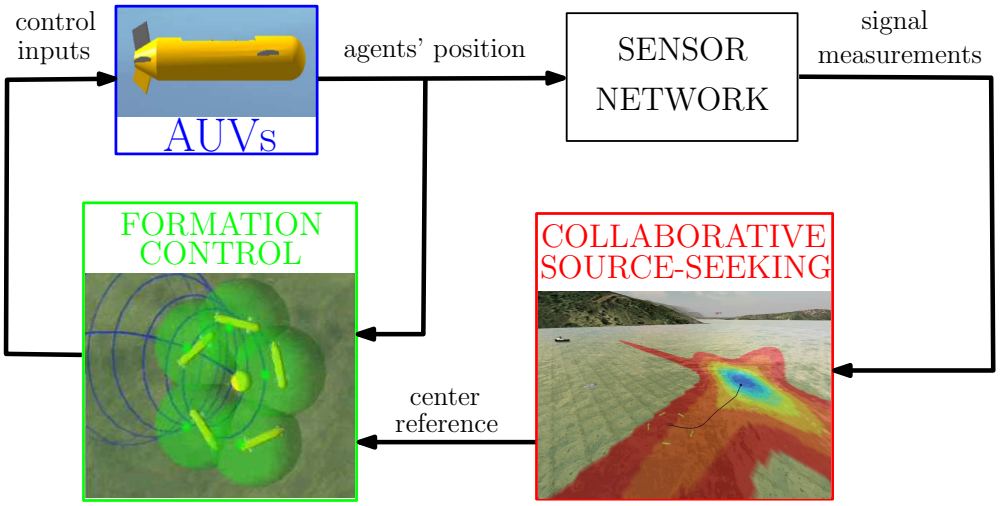

Figure 1.11: *Illustration of the contributions of this thesis*

Figure 1.11 displays a diagram representing the main objectives which will be discussed along this thesis. The first control loop corresponds to the formation control problem. The multi-agent system, in this case representing a group of AUVs, is governed by a control law which uses the agents' positions and orientations, and given references of the formation parameters. This algorithm stabilizes the fleet to time-varying formations tracking external references of the parameters which define the desired configuration, as its center for instance. Moreover, collaborative algorithms are developed to distribute the vehicles in a particular pattern along the formation.

The second control loop is designed to reach the final objective, the collaborative localization and tracking of a source. The AUVs are now considered as a mobile sensor network obtaining measurements of a scalar field. These measurements will be used to compute a distributed algorithm to achieve the source-seeking problem defined.

Finally, this algorithm provides the adequate reference to move the formation towards the location of the source.

At the end of this thesis, it will be seen how several tools in the domain of the automatic control allow us to find a solution for the problems discussed at the beginning of this chapter.

Chapter 2

Time-varying circular formation control

In order to face the challenges mentioned in Chapter 1, the control strategy designed in this thesis is structured in three phases. As shown in Figure 2.1, the first step focuses on the formation control problem. This chapter deals with designing formation control laws for a fleet of Autonomous Underwater Vehicles (AUVs). A formation is a configuration conformed by a group of vehicles with communication capacities, in which the vehicles collaborate to achieve a common goal. This first contribution concentrates on control design to reach circular formations.

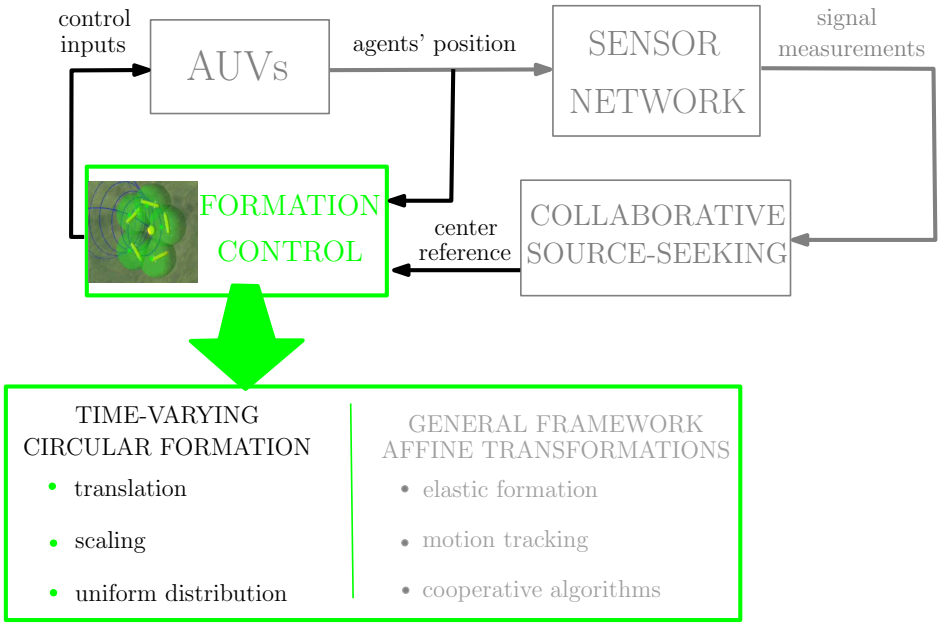

Figure 2.1: *Contributions of Chapter 2*

The circle has several interesting symmetric properties and its geometrical form can be simply characterized by its center and its radius. For this reason, the circular motion of vehicles is a large analyzed topic in the literature. There exist several approaches which tackle this question. Collaborative cyclic pursuit strategy studied in [95] (see the survey on formation control in Subsection 1.2.3), circumnavigation of a single vehicle presented in [44] and collective circular motion from [86] are some examples.

Based on previous circular formation control results studied in the literature, in this chapter different control laws are developed to stabilize the fleet of agents to time-varying circular formations. Firstly, a control design to make the vehicles converge to a circular motion following a time-varying reference of its center is provided. In a second time, the agents are stabilized to a circular motion which changes its radius according to an external reference. Both control laws are improved adding a potential function in order to distribute the agents along the common formation in a collaborative way.

2.1 Problem statement

In this chapter, circular formations of autonomous agents in a 2-dimensional space are considered. It is assumed that the agents have no physical extension, that is, that their positions are single points. Consider a group of N identical vehicles modeled with unicycle kinematics subject to a simple non-holonomic constraint, adequate for the underwater vehicles as presented in previous survey of multi-agent systems, such that the dynamics of agents where $k = 1, \ldots, N$ are defined by:

$$\dot{x}_k = v_k \cos\theta_k \tag{2.1a}$$

$$\dot{y}_k = v_k \sin\theta_k \tag{2.1b}$$

$$\dot{\theta}_k = u_k \tag{2.1c}$$

where $\mathbf{r}_k = (x_k, y_k)^T \in \mathbb{R}^2$ is the position vector of agent k, $\theta_k \in S^1$ is its heading angle and v_k, u_k are the control inputs.

The objective is to design control strategies to make converge the group of AUVs, represented by system (2.1), to circular formations, whose parameters center and radius are time-varying. Following assumptions are considered in the sequel to deal with this first contribution:

- Each vehicle $k = 1, \ldots, N$ knows its absolute vector position $\mathbf{r}_k$ with respect to the inertial frame.

- The time-varying references which define the parameters of the circular formation, *i.e.*, its center and its radius, are known to all the vehicles.

- Each vehicle is able to communicate in a region delimited by a critical communication distance ρ. This is motivated by the underwater communication constraints and the communication protocol used, as explained in Chapter 1. This critical radius is the same for all the vehicles.
- Others communication problems such as, noise, packet loss and time delays, are not considered.

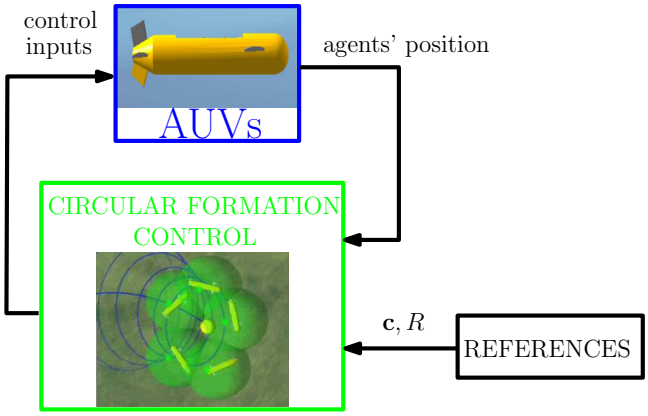

Figure 2.2: *Problem statement of Chapter 2*

Under these assumptions, this chapter presents control laws to stabilize a group of vehicles to circular motions tracking time-varying references, as is represented in Figure 2.2. In addition, a collaborative algorithm allows distributing the vehicles in a particular desired pattern along the circular formation.

2.2 Collective motions

A particular class of motion coordination for multi-agent systems is studied in [86, 115, 119, 148, 149, 150] under different constraints. These previous works study the problem of design feedback control laws that stabilize a collective motion. The evolution of the dynamics of a system consisting of several mobile agents coordinating their motion using relative positions and orientations with respect to their neighbors is called a collective motion.

The authors of [74] has analyzed in detail model (2.1) which is extensively used to represent the dynamics of multi-agent systems. These authors have emphasized the Lie group structure that underlies the state space. The configuration space of a group of N agents consists in the same number of replicas of the group $SE(2)$. When the control law only depends on relative phases and relative positions, the closed-loop vector field is

invariant under an action of the symmetry group $SE(2)$ and the closed-loop dynamics evolve on a reduced quotient manifold. This manifold is called the shape space, and it corresponds to the space of all relative phases and relative positions [150].

Parallel and circular collective motions of a group of vehicles modeled with unicycle kinematics (2.1) are analyzed under a Lyapunov approach. Parallel motions are catarecterized by a common orientation for all the agents, and the circular motions are defined by circular orbits of the agents around a fixed point. This cooperative approach only depends on relative orientation and relative position, *i.e.*, on the variables $\theta_{kj} = \theta_k - \theta_j$ and $\mathbf{r}_{kj} = \mathbf{r}_k - \mathbf{r}_j$ where $k, j = 1, \ldots, N$. As is explained in [143], circular and parallel motions are the only possible coordinated motions on the symmetry group $SE(2)$ because the closed-loop vector field is invariant under an action of $SE(2)$.

In [86], the authors develop collaborative control laws to stabilize the group of agents to parallel and circular formations. A feedback control law that stabilizes circular motion of a group of N vehicles around its center of mass is provided. Each vehicle moves in the plane subject to planar steering control, modeled by (2.1) with unit constant velocity, such that $v_k = 1$. Two examples of constant control input are shown to help understand this model:

- $u_k = \omega_0 \neq 0$: the vehicles travel on fixed circles of radius $1/|\omega_0|$ and the sense of rotation is given by the sign of ω_0
- $u_k = \omega_0 = 0$, each vehicle follows a straight trajectory in the direction of the initial heading.

The motion of the group can be related to the vehicle headings due to the unit speed and unit mass assumptions. In [86], the authors suggest a control law for stabilization to a circular formation centered at the center of mass $\mathbf{c}_m$ defined as:

$$\mathbf{c}_m = \frac{1}{N} \sum_{k=1}^{N} \mathbf{r}_k$$

All previously cited works on circular formation use a complex notation due to the isometry between $\mathbb{R}^2$ and $\mathbb{C}$. In order to be consistent with the notation which is used in this thesis, the results obtained in [86] will be presented in $\mathbb{R}^2$. Let the relative position vector from the center of mass to vehicle k be defined as

$$\tilde{\mathbf{r}}_k = \mathbf{r}_k - \mathbf{c}_m = \frac{1}{N} \sum_{j=1}^{N} (\mathbf{r}_k - \mathbf{r}_j)$$

Note that each $\tilde{\mathbf{r}}_k$ depends only on the relative positions of the agents.

With a view to stabilize the agents to a circular formation the authors propose the following theorem:

Theorem 2.1 *(Leonard et al. [86]) Consider the vehicle model* (2.1) *with* $v_k = 1$ *for all* $k = 1, \ldots, N$. *Then the control law:*

$$u_k = \omega_0(1 + \kappa \tilde{\boldsymbol{r}}_k^T \dot{\boldsymbol{r}}_k) \tag{2.2}$$

where $\kappa > 0$ *is a scalar gain, ensures that all the agents converge to a circular formation centered at* $\boldsymbol{c}_m$ *and of radius* $1/|\omega_0|$.

Proof 2.1 *The stability of the circular motion of the group around a common point can be studied using standard Lyapunov functions. The proof is based on the following Lyapunov function:*

$$S(\boldsymbol{r}, \theta) = \frac{1}{2} \sum_{k=1}^{N} \left\| \dot{\boldsymbol{r}}_k - \omega_0 \boldsymbol{R}_{\frac{\pi}{2}} \tilde{\boldsymbol{r}}_k \right\|^2 \geq 0 \tag{2.3}$$

where the matrix $\boldsymbol{R}_{\frac{\pi}{2}} \in \mathbb{R}^{2\times 2}$ *represents a matrix rotation through an angle* $\frac{\pi}{2}$ *counter-clockwise around the origin (of the corresponding reference frame) such that:*

$$\boldsymbol{R}_{\frac{\pi}{2}} = \begin{pmatrix} 0 & -1 \\ 1 & 0 \end{pmatrix}$$

and the vectors of positions and headings are defined as $\boldsymbol{r} = (\boldsymbol{r}_1^T, \ldots, \boldsymbol{r}_N^T)^T$ *and* $\theta = (\theta_1, \ldots, \theta_N)^T$ *respectively. This function has minimum zero for circular motion around the fixed center of mass because at the equilibrium, when* $S(\boldsymbol{r}, \theta) = 0$, *the dynamics of the vehicles satisfy:*

$$\dot{\boldsymbol{r}}_k - \omega_0 \boldsymbol{R}_{\frac{\pi}{2}} \tilde{\boldsymbol{r}}_k = 0$$

In consequence, the relative position vector from the center of mass to agent $k = 1, \ldots, N$ *is perpendicular to its position vector due to* $\dot{\boldsymbol{r}}_k^T \tilde{\boldsymbol{r}}_k = 0$. *In this situation, the vehicle* k *describes circular trajectories around the center of mass.*

The derivative of the Lyapunov function is expressed as follows:

$$\begin{aligned} \dot{S}(\boldsymbol{r}, \theta) &= \sum_{k=1}^{N} \left(\ddot{\boldsymbol{r}}_k - \omega_0 \boldsymbol{R}_{\frac{\pi}{2}} \dot{\tilde{\boldsymbol{r}}}_k \right)^T \left(\dot{\boldsymbol{r}}_k - \omega_0 \boldsymbol{R}_{\frac{\pi}{2}} \tilde{\boldsymbol{r}}_k \right) \\ &= \sum_{k=1}^{N} \left(u_k \boldsymbol{R}_{\frac{\pi}{2}} \dot{\boldsymbol{r}}_k - \omega_0 \boldsymbol{R}_{\frac{\pi}{2}} \dot{\boldsymbol{r}}_k \right)^T \left(\dot{\boldsymbol{r}}_k - \omega_0 \boldsymbol{R}_{\frac{\pi}{2}} \tilde{\boldsymbol{r}}_k \right) \\ &= \sum_{k=1}^{N} \omega_0 \tilde{\boldsymbol{r}}_k^T \dot{\boldsymbol{r}}_k (\omega_0 - u_k) \end{aligned}$$

Thanks to the control law (2.2) *this derivative becomes:*

$$\dot{S}(\boldsymbol{r}, \theta) = \sum_{k=1}^{N} \omega_0 \tilde{\boldsymbol{r}}_k^T \dot{\boldsymbol{r}}_k (\omega_0 - \omega_0(1 + \kappa \tilde{\boldsymbol{r}}_k^T \dot{\boldsymbol{r}}_k)) = -\kappa \sum_{k=1}^{N} \left(\omega_0 \tilde{\boldsymbol{r}}_k^T \dot{\boldsymbol{r}}_k \right)^2 \leq 0$$

By the LaSalle Invariance principle, solutions for the reduced system on shape space converge to the largest invariant set Λ where

$$\omega_0 \tilde{\boldsymbol{r}}_k^T \dot{\boldsymbol{r}}_k \equiv 0$$

and the conclusion is that solutions converge to a circular relative equilibrium. It means that the agents converge to a circular motion centered at the center of mass $\boldsymbol{c}_m$ and with radius $1/|\omega_0|$. The details of the proof can be found in [149].

□

Note that this circular formation control law depends only on relative positions $\mathbf{r}_{kj}$ which stress the notion of collective motion and the center of the final formation $\mathbf{c}_m$ results from a consensus algorithm [149].

There exist several extensions of this theorem under limited communication [119, 150], considering the effect of underwater currents [120, 121] and collective motions in three-dimensional space [69]. In the sequel, two other extensions will be presented. These contributions allows moving and contracting/expanding circular formations.

2.2.1 Circular motion control with fixed center

Based on the same ideas from collective motions, the authors of [118] present a feedback control in order to stabilize a single vehicle to a circular motion with fixed center and constant radius. Each vehicle k knows its absolute position $\mathbf{r}_k$ and its dynamics are modeled by (2.1) with constant velocity $v_k = 1$ for all $k = 1, ..., N$. The authors propose a beacon control law composed of Hamiltonian and dissipative terms, such as:

$$u_k = -\omega_0(1 + \mathbf{r}_k^T \dot{\mathbf{r}}_k)$$

where $\omega_0 \neq 0$ is the angular velocity. In consequence, the following theorem is presented:

Theorem 2.2 *(Paley et al. [118]) Consider the vehicle model* (2.1) *with $v_k = 1$ for all $k = 1, \ldots, N$. Then the control law:*

$$u_k = -\omega_0(1 + \boldsymbol{r}_k^T \dot{\boldsymbol{r}}_k) \tag{2.4}$$

where $\omega_0 > 0$ ensures that all the agents converge to a clockwise circular motion with radius $1/\omega_0$ about the origin of the coordinate system $\boldsymbol{c}_0 = (0, 0)^T$.

Proof 2.2 *In order to proof this result Lyapunov techniques are used. Consider the following Lyapunov function given by*

$$S_k(\boldsymbol{r}_k, \theta_k) = \frac{1}{2}\|\boldsymbol{r}_k - R_0 \boldsymbol{R}_{\frac{\pi}{2}} \dot{\boldsymbol{r}}_k\|^2$$

where $R_0 = 1/|\omega_0|$ is the radius of the desired circular motion.

The relative position of the vehicles with respect to a center point $\boldsymbol{c}_0$ is defined as $\tilde{\boldsymbol{r}}_k = \boldsymbol{r}_k - \boldsymbol{c}_0$. Without loss of generality, the center point corresponds to the origin of the coordinate system. Therefore, the following change of coordinates is proposed:

$$x_k = R_k \cos\varphi_k \tag{2.5a}$$

$$y_k = R_k \sin\varphi_k \tag{2.5b}$$

where $R_k \in \mathbb{R}^+$ and

$$\phi_k = \theta_k - \psi_k + \frac{\pi}{2}$$

In the new coordinates (R_k, ϕ_k, φ_k) the system (2.1) with control (2.4) becomes:

$$R_k = \sin\phi_k \tag{2.6}$$

$$\dot{\phi}_k = -\omega_0(1 + R_k \sin\phi_k) + \frac{\cos\phi_k}{R_k} \tag{2.7}$$

and

$$\dot{\varphi}_k = -\frac{\cos\phi_k}{R_k}$$

In the shape coordinates the circular motion equilibrium is a fixed point. Using these relations, the previous Lyapunov potential can be rewritten as

$$S_k(R_k, \phi_k) = \frac{1}{2}\left(R_k^2 + R_0^2 - 2R_k R_0 \cos\phi_k\right)$$

and differentiating

$$\dot{S}_k(R_k, \phi_k) = -R_k \sin^2\phi_k \leq 0$$

By the LaSalle invariance principle the vehicles converge to the largest invariant set for which $\dot{S}_k(R_k, \phi_k) = 0$. This set corresponds to the fixed point $(R_k, \phi_k) = (R_0, 0)$, hence the vehicles converge to a circular motion centered at the origin of the reference frame and with radius R_0.

□

Remark 2.1 *Note that this beacon control law stabilizes a group of agents to a clockwise circular motion centered at the origin of the coordinates system. This result can be generalized considering an arbitrary fixed center $\boldsymbol{c}$ and an angular velocity $\omega_0 \neq 0$. Under these hypothesis the previous control law (2.4) becomes:*

$$u_k = \omega_0(1 + \dot{\boldsymbol{r}}_k^T(\boldsymbol{r}_k - \boldsymbol{c}))$$

This circular motion control law ensures that a group of vehicles converge to a fixed circular motion centerd at $\boldsymbol{c}$. The direction of rotation is determined by the sign of ω_0.

2.3 Translation of a circular motion

Based on previous collaborative works on multi-agent circular formation [86, 149, 150], this section presents a first contribution dealing with formation control design and a first step to tackle the source-seeking problem.

Moving a formation of agents is pertinent to some applications where the agents should perform collaborative tasks requiring the formation to displace towards an a priori unknown direction. For instance, in source seeking applications, the formation is driven following the source gradient direction (which is computed on-line, and instrumented as an additional outer loop) [64, 104]. The target tracking problem also requires to consider time-varying formations. In this application, the agents attempt encircling the target. Therefore, a circular formation in whose center is located the target, seems very appropriate to the target tracking problem. Some cooperative approaches to carry out this challenge using a fleet of vehicles have been studied in the literature [80, 117]. Hence, a circular formation can be useful to track the trajectory of a time-varying target [85].

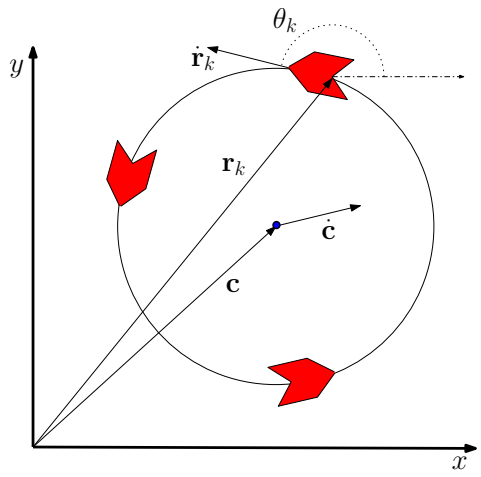

Figure 2.3: *Translation of a circular formation*

This section presents a control strategy such that a multi-agent system defined by (2.1) converges to a circular motion which tracks a time-varying center, as described in Figure 2.3. At the first stage, the desired time-varying center $\mathbf{c}(t)$ is assumed to be a given external reference which is shared to all the agents in the formation.

To solve the problem of moving a circular formation, one has to focus on the two following issues:

a) Improving the previous circular control law from [118] to stabilize the fleet of agents to the same time-varying circular motion.

b) Defining the class of functions $\mathbf{c}(t)$ for which the translation of the circular motion is possible.

2.3.1 Additional constraints on the center reference

A uniform circular motion describes the motion of a body traversing a circular path at constant speed. The velocity of a point rotating with constant angular velocity around a center point is perpendicular to the relative vector from the center to the moving point and its magnitude is constant. Nevertheless, due to the rigid body kinematics during a combined motion composed by a uniform rotation and a constant translation the velocity of a point turning around a moving center is not constant anymore.

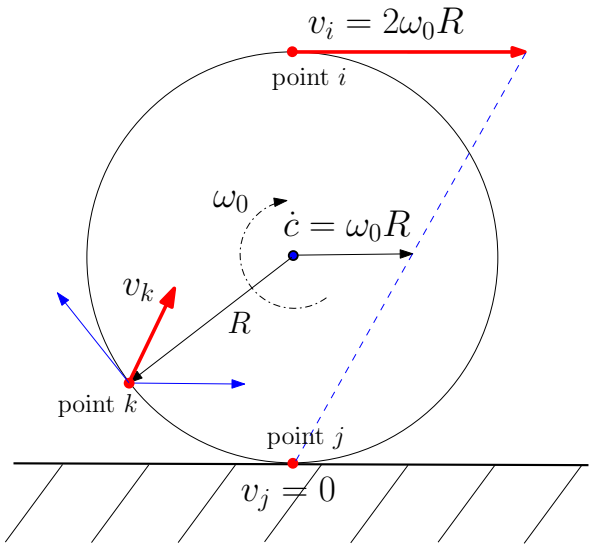

Figure 2.4: *A wheel, rolling without slipping, with the velocity of three points shown*

For instance, in a circular motion of a wheel of radius R, without slipping, represented in Figure 2.4, the center of the mass is moving with constant linear velocity which magnitude, $\dot{c} = R\omega_0$, is equal to the tangent velocity. The parameter $\omega_0 \neq 0$ represents the angular velocity. The velocity of each point in the circle is a vectorial sum of the velocity of the center of mass and the tangential velocity. Therefore, the velocities of all the points are different during the motion.

In conclusion, considering constant angular velocity, in order to track a time-varying center the magnitude of the velocity vector of vehicles describing circular trajectories around a moving center is time-varying. This fact leads to a contradiction with the choice of constant linear velocity of the agents.

The results exposed in [86, 149] to obtain time-invariant circular formations and the beacon control law from [118] dealing with circular motions, presented in Section 2.2,

represent the vehicles with a unicycle model (2.1) with unit linear velocity, *i.e.* $v_k = 1, \forall k$. This assumption is pertinent to model several kind of underwater vehicles as gilders, see [86]. The constant speed consideration is consistent with the circular motion of the agents around a fixed point. According to the relation $v = R\omega_0$ satisfied during a circular motion, in order to extend the algorithms based on constant speed to time-varying circular formations the only choice is to consider time-varying angular velocity of rotation ω_0. In this chapter, the parameter ω_0 is assumed to be constant, therefore the velocity v_k becomes a new and necessary control input to overcome this mechanical constraint.

Another constraint belonging to AUV characteristics is that its velocity should never be zero, otherwise the vehicle will sink to the bottom of the sea. According with the previous example of a wheel motion, the zero velocity corresponds to the contact point between the wheel and the floor. To avoid this situation, it is easy to see in Figure 2.4, that there is a constraint related to the velocity of the center of mass. The motion of a circular formation of AUVs, turning and tracking a time-varying center, is consistent with the rigid body kinematics described in Figure 2.5.

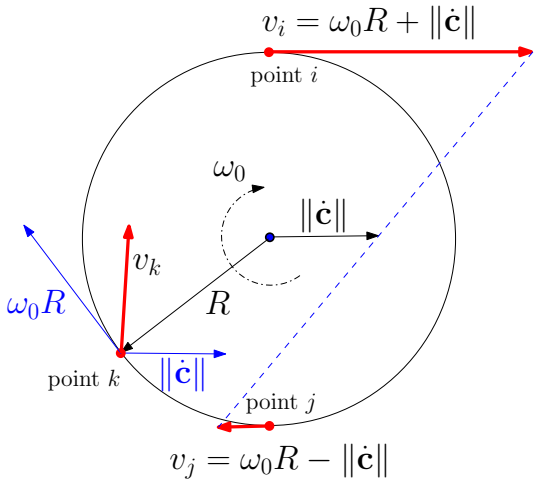

Figure 2.5: *Combination of a translational motion and a rotational motion*

Nevertheless, this fact implies also conditions on the velocity of the reference of the circular formation center, denoted by $\dot{\mathbf{c}}$, in order to keep the formation and avoid the zero velocity of the agents. The situation in which the AUVs are not moving must be avoided. In reality, a minimum value of the velocity have to be guaranteed to allow the vehicle to turn. In other words, the vehicle is only able to change its heading angle during the motion. In the sequel, we will show how to deal with this problem.

2.3.2 Introduction of a new system of coordinates

We want to stabilize system (2.1) to a circular motion of radius R and the given time-varying reference of its center $\mathbf{c}(t)$. The methodology proposed in this thesis to design a time-varying circular control law is structured in the following steps:

- **Change of coordinates:** the position vector of each agent is expressed in a transformed system which is moving with the desired time-varying center.
- **Fixed circular control law:** the transformed system is stabilized to a circular motion with fixed center thanks to the beacon control law from [118].
- **Inverse transformation:** the control inputs of the original system are expressed depending on the previous control law for the transformed system.

The main idea and thus, the main contribution, is to express the multi-agent system in a relative frame whose origin is the time-varying desired center $\mathbf{c} = (c_x, c_y)^T$. This transformed system, in which the agents' position are expressed with respect to the circle center, will be stabilized to a circular motion centered at $\mathbf{c}$ and with radius R, using the circular motion control law from [118]. The different steps of the control design are explained schematically in Figure 2.6.

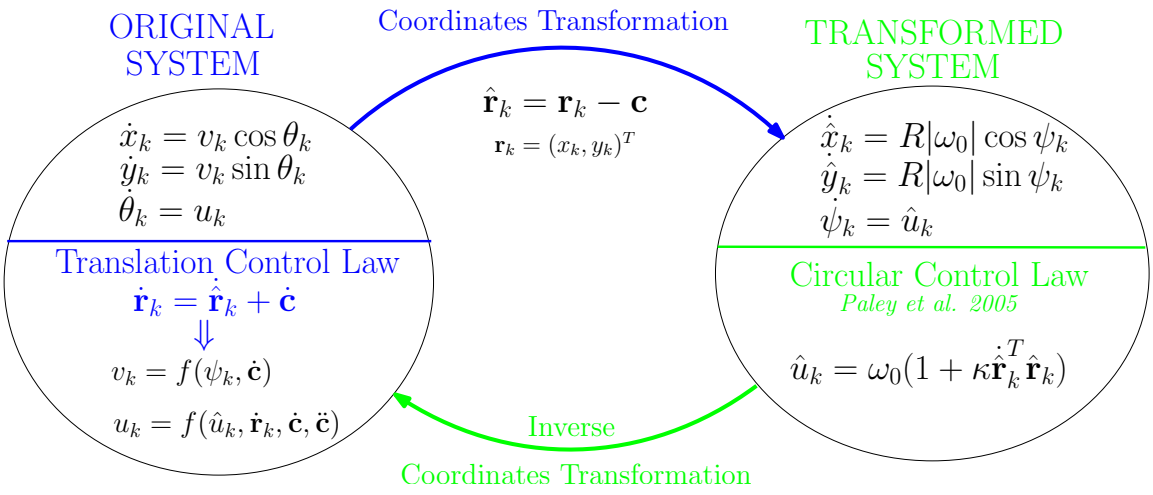

Figure 2.6: *Change of coordinates process*

In order to express the position vector $\mathbf{r}_k$ of each agent k in the relative frame which is moving with the center of the circular motion $\mathbf{c}$, the following change of coordinates is defined:

$$\hat{\mathbf{r}}_k = \mathbf{r}_k - \mathbf{c} \tag{2.8}$$

where $\hat{\mathbf{r}}_k \in \mathbb{R}^2$ represents the relative position vector.

The circular control law from [118] can be applied to a multi-agent system modeled by (2.1) with constant velocity $v_k = v$. Therefore, to apply this circular control law to the transformed system expressed in the relative reference frame with respect to the moving center, the dynamics of the relative positions must have constant velocity. The agents defined by the transformed system will converge to a circular motion with radius $R = v/|\omega_0|$ where $\omega_0 \neq 0$ is the angular velocity. Then, the transformed system is enforced to have constant linear velocity equal to $v = R|\omega_0|$. Consequently, we impose to the transformed system the following dynamics:

$$\dot{\hat{x}}_k = R|\omega_0| \cos\psi_k \tag{2.9a}$$

$$\dot{\hat{y}}_k = R|\omega_0| \sin\psi_k \tag{2.9b}$$

$$\dot{\psi}_k = \hat{u}_k \tag{2.9c}$$

where ψ_k represents the angular orientation of the transformed velocity vector $\dot{\hat{\mathbf{r}}}_k = (\dot{\hat{x}}_k, \dot{\hat{y}}_k)^T$ and $\hat{u}_k$ is the control input.

The resulting transformed system, is time-invariant since the center becomes fixed in the new transformed frame. Hence, circular control law from

2.3.3 Translation control law

The problem is to design a control law such that the group of AUVs forms a circle that tracks the time-varying center $\mathbf{c}(t)$. The trajectory of the center $\mathbf{c}(t)$, is considered here as an external reference. The radius of the circle R, and the rotation velocity ω_0, are constant given parameters. Applying the previous circular control law from [118] but expressed in the new transformed frame, the system (2.9) converges to a circle centered at $\mathbf{c}(t)$ with radius R.

Consider the vector which contains all the transformed position vectors $\hat{\mathbf{r}}$ and the vector containing all the inner new variables ψ_k, denoted by $\hat{\mathbf{r}} = (\hat{\mathbf{r}}_1^T, \ldots, \hat{\mathbf{r}}_N^T)^T$ and $\psi = (\psi_1, \ldots, \psi_N)^T$ respectively. The convergence of the transformed system to a circular motion is analyzed using the following Lyapunov function, based on the analysis of the circular control laws proposed in [86, 118]:

$$S(\hat{\mathbf{r}}, \psi) = \frac{1}{2} \sum_{k=1}^{N} \left\| \dot{\hat{\mathbf{r}}}_k - \omega_0 \mathbf{R}_{\frac{\pi}{2}} \hat{\mathbf{r}}_k \right\|^2 \geq 0 \tag{2.10}$$

Analyzing the equilibrium points of this Lyapunov function, when $S(\hat{\mathbf{r}}, \psi) = 0$ the dynamics of the transformed system (2.9) satisfy $\dot{\hat{\mathbf{r}}}_k - \omega_0 \mathbf{R}_{\frac{\pi}{2}} \hat{\mathbf{r}}_k = 0$. Thus, the transformed position vector and its velocity vector are perpendicular because $\dot{\hat{\mathbf{r}}}_k^T \hat{\mathbf{r}}_k = 0$. This condition leads to the kinematic relation for the rotation of the rigid body, it means that the transformed vectors $\hat{\mathbf{r}}_k$ are turning around the frame origin $\mathbf{c}$ at the equilibrium.

Evaluating the derivative of $S(\hat{\mathbf{r}}, \psi)$ along the solutions of the resulting closed-loop system (2.9) leads to:

$$\begin{aligned}\dot{S}(\hat{\mathbf{r}}, \psi) &= \sum_{k=1}^{N} \left(\ddot{\hat{\mathbf{r}}}_k - \omega_0 \mathbf{R}_{\frac{\pi}{2}} \dot{\hat{\mathbf{r}}}_k\right)^T \left(\dot{\hat{\mathbf{r}}}_k - \omega_0 \mathbf{R}_{\frac{\pi}{2}} \hat{\mathbf{r}}_k\right) \\ &= \sum_{k=1}^{N} \left(\hat{u}_k \mathbf{R}_{\frac{\pi}{2}} \dot{\hat{\mathbf{r}}}_k - \omega_0 \mathbf{R}_{\frac{\pi}{2}} \dot{\hat{\mathbf{r}}}_k\right)^T \left(\dot{\hat{\mathbf{r}}}_k - \omega_0 \mathbf{R}_{\frac{\pi}{2}} \hat{\mathbf{r}}_k\right) \\ &= \sum_{k=1}^{N} \omega_0 \hat{\mathbf{r}}_k^T \dot{\hat{\mathbf{r}}}_k (\omega_0 - \hat{u}_k)\end{aligned}$$

Based on the circular control laws from [86, 118] and according with previous Lyapunov function, the following control law is proposed for the transformed system:

$$\hat{u}_k = \omega_0 (1 + \kappa \dot{\hat{\mathbf{r}}}_k^T \hat{\mathbf{r}}_k) \tag{2.11}$$

where $\kappa > 0$ is a control parameter. Note that for $\kappa = 0$, the control law becomes $\hat{u}_k = \dot{\psi}_k = \omega_0 \neq 0$ thus, each transformed position vector $\hat{\mathbf{r}}_k$ will undergo circular motion with direction of rotation determined by the sign of ω_0. The gain κ regulates the contribution to the control of a dissipation term which steers vector $\hat{\mathbf{r}}_k$ such that, it is perpendicular to its velocity vector $\dot{\hat{\mathbf{r}}}_k$.

Considering the proposed control law (2.11), the previous derivative of the Lyapunov function becomes:

$$\dot{S}(\hat{\mathbf{r}}, \psi) = -\kappa \sum_{k=1}^{N} (\omega_0 \hat{\mathbf{r}}_k^T \dot{\hat{\mathbf{r}}}_k)^2 \leq 0 \tag{2.12}$$

In conclusion, $S(\hat{\mathbf{r}}, \psi)$ is a suitable Lyapunov function for this transformed system, and the solutions converge to the largest invariant set Λ, for which $\dot{S} = 0$.

After the previous detailed analysis a first contribution of this thesis can be presented as a theorem:

Theorem 2.3 *(Briñón-Arranz et al. 2009 [16]) Consider a twice differentiable function $\boldsymbol{c}(t) : \mathbb{R} \to \mathbb{R}^2$, with bounded first and second time-derivatives. Let $R > 0$ be the radius of the desired circular motion, the control parameters be such that $\omega_0 \neq 0$, $\kappa > 0$ and the following condition is satisfied:*

$$R|\omega_0| > \sup_{t \geq 0} \{\|\dot{\boldsymbol{c}}(t)\|\} \tag{2.13}$$

where $\sup\{\cdot\}$ represents the supremum of a real number.

Then, the control law

$$v_k = \left\| R|\omega_0|(\cos\psi_k, \sin\psi_k)^T + \dot{\boldsymbol{c}} \right\| \tag{2.14a}$$

$$\dot{u}_k = \left(1 - \frac{\dot{\boldsymbol{r}}_k^T \dot{\boldsymbol{c}}}{v_k^2}\right) \dot{\psi}_k - \frac{\dot{\boldsymbol{r}}_k^T \boldsymbol{R}_{\frac{\pi}{2}} \ddot{\boldsymbol{c}}}{v_k^2} \tag{2.14b}$$

$$\dot{\psi}_k = \omega_0 \left(1 + \kappa R|\omega_0|(\cos\psi_k, \sin\psi_k)(\boldsymbol{r}_k - \boldsymbol{c})\right) \tag{2.14c}$$

with the inner state of the dynamic controller initialized as

$$\psi_k(0) = \theta_k(0) \tag{2.15}$$

makes all the agents defined by (2.1) *converge to a circular motion of radius R, and whose center tracks the time-varying reference $\boldsymbol{c}(t)$. The direction of rotation is determined by the sign of ω_0.*

Proof 2.3 *The previous Lyapunov function $S(\hat{\boldsymbol{r}}, \psi)$ is positive semidefinite and from* (2.12) *is nonincreasing along the solutions. Thanks to the change of coordinates* (2.8)*, the dynamic closed-loop equation corresponding to the transformed system is time-invariant with respect to the reference $\boldsymbol{c}(t)$, hence LaSalle Principle can be applied. Therefore, solutions for the reduced system on shape space converge to the largest invariant set Λ where*

$$\kappa \hat{\boldsymbol{r}}_k^T \dot{\hat{\boldsymbol{r}}}_k \equiv 0 \quad \forall k = 1, \ldots, N$$

In this set, $\dot{\psi}_k = \omega_0$, i.e.*, the transformed position vector describes circles of radius $R|\omega_0|/|\omega_0|$. The transformed system* (2.8) *asymptotically reaches the circular motion centered at $\boldsymbol{c}$, radius R and with fixed angular velocity ω_0. Hence, the dynamics of the agents satisfy:*

$$\dot{\boldsymbol{r}}_k = \dot{\boldsymbol{c}} + \omega_0 \boldsymbol{R}_{\frac{\pi}{2}} (\boldsymbol{r}_k - \boldsymbol{c})$$

which is the kinematic relation for the combined motion of a translation and a rotation of the rigid body.

The next step of the proof concerns the design of the control inputs (v_k, u_k) of the original system. According to the change of coordinates (2.8)*, differentiating the definition of $\hat{\boldsymbol{r}}_k$ gives*

$$\dot{\boldsymbol{r}}_k = \dot{\hat{\boldsymbol{r}}}_k + \dot{\boldsymbol{c}}$$

This equation provides both expressions of the control inputs. Expressing previous equation in terms of its components, gives:

$$v_k \cos\theta_k = R|\omega_0| \cos\psi_k + \dot{c}_x$$
$$v_k \sin\theta_k = R|\omega_0| \sin\psi_k + \dot{c}_y$$

Therefore, the control input v_k is thus straightforwardly given by (2.14a). *A more particular attention is addressed to the input u_k. Using previous equations the following equality holds:*

$$\tan\theta_k = \frac{\dot{\hat{y}}_k + \dot{c}_y}{\dot{\hat{x}}_k + \dot{c}_x} = \frac{R|\omega_0|\sin\psi_k + \dot{c}_y}{R|\omega_0|\cos\psi_k + \dot{c}_x} \tag{2.16}$$

and differentiating

$$\begin{aligned} \dot{\theta}_k(1+\tan^2\theta_k) &= \frac{(\ddot{\hat{y}}_k + \ddot{c}_y)(\dot{\hat{x}}_k + \dot{c}_x) - (\dot{\hat{y}}_k + \dot{c}_y)(\ddot{\hat{x}}_k + \ddot{c}_x)}{(\dot{\hat{x}}_k + \dot{c}_x)^2} \\ \dot{\theta}_k v_k^2 &= (\hat{u}_k\dot{\hat{y}}_k + \ddot{c}_y)(\dot{\hat{x}}_k + \dot{c}_x) - (\dot{\hat{y}}_k + \dot{c}_y)(-\hat{u}_k\dot{\hat{x}}_k + \ddot{c}_x) \end{aligned}$$

To fit with the change of coordinates previous relation becomes:

$$\dot{\theta}_k v_k^2 = \hat{u}_k(v_k^2 - \dot{x}_k\dot{c}_y - \dot{y}_k\dot{c}_x) + \dot{x}_k\ddot{c}_y - \dot{y}_k\ddot{c}_x$$

Then, from $u_k = \dot{\theta}_k$ the control input u_k proposed in (2.14b) *is retrieved. In order to satisfy the relation* (2.16) *for all t, the initial conditions of the inner variable ψ_k must be imposed as a function of the initial values of the system state. Let us consider that the initial velocity of the center is equal to zero, such as $\dot{\boldsymbol{c}}(0) = (0,0)^T$. Therefore, since equation* (2.16) *is satisfied, following relation holds:*

$$\psi_k(0) = \theta_k(0)$$

Note that this control law has singular points when $\|\dot{\boldsymbol{r}}_k\| = 0$. This situation is equivalent to:

$$v_k = \left\| R|\omega_0|(\cos\psi_k, \sin\psi_k)^T + \dot{\boldsymbol{c}} \right\| = 0$$

This singular point occurs if there exists a time t_c such that:

$$\begin{cases} \|\dot{\boldsymbol{c}}(t_c)\| = R|\omega_0| \\ \angle\dot{\boldsymbol{c}}(t_c) = -\psi_k(t_c) \end{cases}$$

where $\angle$ represents the argument of a vector. The equation (2.17) *is a sufficient condition to avoid the singular points.*

□

Remark 2.2 *Physically, the singular points of the control law* (2.14) *represent the contact point in a wheel motion, as seen previously in Figure 2.4. To understand this singularity, consider the example of the cycloid whose first derivative is not defined at some instants.*

Remark 2.3 *The translation control law presented in Theorem 2.3 is an extension of the circular control proposed in [118]. In this paper, the authors present a control law which stabilizes a vehicle to a circular motion with fixed center and constant radius using its absolute position. The improvement with respect to this work comes from the fact that is possible to stabilize the agents to circular motions whose center is time-varying. Note that if the reference of the center* $\boldsymbol{c}$ *becomes time-invariant,* i.e., $\dot{\boldsymbol{c}}(t) = \ddot{\boldsymbol{c}}(t) = 0$ *for all* t*, according to equation* (2.16) *the angles* ψ_k *and* θ_k *become equal. Thus, the control law* (2.14) *is the same control as in Theorem 2.2, this means:*

$$\begin{aligned} v_k &= R|\omega_0| \\ \dot{u}_k &= \hat{u}_k = \omega_0(1 + \kappa \dot{\boldsymbol{r}}_k^T(\boldsymbol{r}_k - \boldsymbol{c})) \end{aligned}$$

Therefore, this result dealing with a circular formation with time-varying center encompass the previous circular motion control problem from [118].

Theorem 2.3 presents a control law which stabilizes the fleet of agents defined by (2.1) to a time-varying circular motion. It is worth noting that the center is an external reference. This reference and its first and second derivatives are given and known to all the agents.

With respect to [118], our approach also considers that each agent knows its absolute position vector $\mathbf{r}_k$. This assumption is consistent with the real AUVs. As explained in Chapter 1, the autonomous underwater vehicles belonging to IFREMER have a precise inertial measurement unit for navigation. This system provides a very accurate measurements of the absolute position of the vehicle. Otherwise, the agents do not need to transmit any information to its neighbors, because each vehicle governed by the control law (2.14) converges to the desired moving circular motion independently. Hence, this result is not cooperative contrary to the circular control laws presented in [86, 150, 149]. A cooperative translation control for a circular formation is presented in Section 2.5.

2.3.4 Tracking on $SE(2)$

Previous subsection presents the first contribution of this thesis dealing with time-varying circular control. The control law from Theorem 2.3 stabilizes the vehicles to a circular motion with time-varying center. Due to the methodology applied and the change of coordinates defined by (2.8) the inner variable ψ_k must be initialized as a function of the initial conditions of the heading angle θ_k. In consequence, the control law is not robust to uncertainties in $\theta_k(0)$.

In order to avoid this problem, we propose a new control strategy. This approach considers that both the dynamics of the transformed system and the time-varying

center of the circular motion are references to the original system. The transformed system, previously defined by (2.8), is stabilized to a fixed circular motion. The control design becomes a tracking problem between both systems. This new strategy follows three phases:

- **Reference model:** a relation between the original system (position vector of each agent) and the reference system (relative position vector) is determined.
- **Fixed circular control law:** the reference system is stabilized to a circular motion with fixed center thanks to the beacon control law from [118].
- **Tracking approach:** the control inputs of the original system are defined by tracking the dynamics of the reference system and the velocity of the desired motion center.

In this case, the transformed system defined by (2.8) is considered as a reference system. The dynamics of the reference system satisfy (2.9) and the closed-loop dynamics are imposed by the control law (2.11). In this situation, the following theorem presents the main result of this chapter.

Theorem 2.4 *Consider a twice differentiable function $\boldsymbol{c}(t) : \mathbb{R} \to \mathbb{R}^2$, with bounded first and second time-derivatives. Let $R > 0$ be the radius of the desired circular motion, the control parameters be such that $\omega_0 \neq 0$, $\kappa > 0$, $\beta > 0$ and the following condition is satisfied:*

$$v_k > 0 \quad \forall k = 1, \ldots, N \tag{2.17}$$

Then, for all initial conditions $\boldsymbol{r}(0), \theta(0)$, the control law

$$\dot{v}_k = -\beta v_k + \frac{\hat{u}_k \dot{\boldsymbol{r}}_k^T \boldsymbol{R}_{\frac{\pi}{2}} \dot{\hat{\boldsymbol{r}}}_k + \dot{\boldsymbol{r}}_k^T (\ddot{\boldsymbol{c}} + \beta(\dot{\hat{\boldsymbol{r}}}_k + \dot{\boldsymbol{c}}))}{v_k} \tag{2.18a}$$

$$u_k = \frac{\hat{u}_k \dot{\boldsymbol{r}}_k^T \dot{\hat{\boldsymbol{r}}}_k + \dot{\boldsymbol{r}}_k^T \boldsymbol{R}_{\frac{\pi}{2}}^T (\ddot{\boldsymbol{c}} + \beta(\dot{\hat{\boldsymbol{r}}}_k + \dot{\boldsymbol{c}}))}{v_k^2} \tag{2.18b}$$

where $\dot{\hat{\boldsymbol{r}}}_k$ and $\hat{u}_k$ are defined by (2.9) and (2.11) respectively, makes all the agents defined by (2.1) converge to a circular motion of radius R, and whose center tracks the time-varying reference $\boldsymbol{c}(t)$. The direction of rotation is determined by the sign of ω_0.

Proof 2.4 *According to previous results, the convergence of the reference system to a fixed circular motion can be analyzed with the Lyapunov function:*

$$S(\hat{\boldsymbol{r}}, \psi) = \frac{1}{2} \sum_{k=1}^{N} \left\| \dot{\hat{\boldsymbol{r}}}_k - \omega_0 \boldsymbol{R}_{\frac{\pi}{2}} \hat{\boldsymbol{r}}_k \right\|^2 \geq 0$$

Thanks to this potential function, it has already proved that with the control law (2.11) *its derivative satisfies* $\dot{S}(\hat{\boldsymbol{r}}, \psi) \leq 0$. *Therefore, the reference system* (2.9) *converge to the largest invariant set where* $\dot{S}(\hat{\boldsymbol{r}}, \psi) = 0$ *and consequently, the dynamics of the reference system satisfy the following equation*

$$\dot{\hat{\boldsymbol{r}}}_k = \omega_0 \boldsymbol{R}_{\frac{\pi}{2}} \hat{\boldsymbol{r}}_k$$

which corresponds to a circular motion.

According to relation (2.8), *the objective now is to make converge the dynamics of the original system to a combined motion defined by the dynamics of the reference system and the velocity of the desired center, i.e.:*

$$\dot{\boldsymbol{r}}_k \to \dot{\hat{\boldsymbol{r}}}_k + \dot{\boldsymbol{c}}$$

In order to achieve this objective the tracking error is defined as follows:

$$\boldsymbol{e}_k = \dot{\boldsymbol{r}}_k - (\dot{\hat{\boldsymbol{r}}}_k + \dot{\boldsymbol{c}})$$

With a view to make the error converge to zero, we wish to impose the error dynamics $\dot{\boldsymbol{e}}_k = -\beta \boldsymbol{e}_k$ *where* $\beta > 0$. *Then, the error converge exponentially to zero. Thanks to previous definition of the error the following equation holds when* $t \to \infty$*:*

$$\dot{\boldsymbol{r}}_k = \dot{\hat{\boldsymbol{r}}}_k + \dot{\boldsymbol{c}} \quad \forall k = 1, \ldots, N$$

Taking into account the circular control law (2.11), *the closed-loop dynamics of the reference system converge to* $\dot{\boldsymbol{r}}_k = \omega_0 \boldsymbol{R}_{\frac{\pi}{2}} \hat{\boldsymbol{r}}_k$, *hence previous equality can be written as follows:*

$$\dot{\boldsymbol{r}}_k = \omega_0 \boldsymbol{R}_{\frac{\pi}{2}} \hat{\boldsymbol{r}}_k + \dot{\boldsymbol{c}}$$

and thanks to the relation between both systems (change of coordinates) the agents converge to a time-varying circular motion since:

$$\dot{\boldsymbol{r}}_k = \underbrace{\omega_0 \boldsymbol{R}_{\frac{\pi}{2}} (\boldsymbol{r}_k - \boldsymbol{c})}_{\textit{circular motion}} + \underbrace{\dot{\boldsymbol{c}}}_{\textit{translation}}$$

The following step is to express the control inputs (v_k, u_k) *depending on the reference system. The dynamics of the error equation determines the control law for the original system* (2.1) *since:*

$$\begin{aligned}
\dot{\boldsymbol{e}}_k &= \ddot{\boldsymbol{r}}_k - \ddot{\hat{\boldsymbol{r}}}_k - \ddot{\boldsymbol{c}} \\
-\beta(\dot{\boldsymbol{r}}_k - \dot{\hat{\boldsymbol{r}}}_k - \dot{\boldsymbol{c}}) &= \frac{\dot{v}_k}{v_k} \dot{\boldsymbol{r}}_k + u_k \boldsymbol{R}_{\frac{\pi}{2}} \dot{\boldsymbol{r}}_k - \hat{u}_k \boldsymbol{R}_{\frac{\pi}{2}} \dot{\hat{\boldsymbol{r}}}_k - \ddot{\boldsymbol{c}} \\
\frac{\dot{v}_k}{v_k} \dot{\boldsymbol{r}}_k + u_k \boldsymbol{R}_{\frac{\pi}{2}} \dot{\boldsymbol{r}}_k &= -\beta(\dot{\boldsymbol{r}}_k - \dot{\hat{\boldsymbol{r}}}_k - \dot{\boldsymbol{c}}) + \hat{u}_k \boldsymbol{R}_{\frac{\pi}{2}} \dot{\hat{\boldsymbol{r}}}_k + \ddot{\boldsymbol{c}}
\end{aligned}$$

Multiplying the above equation by $\dot{\boldsymbol{r}}_k^T$ *and by* $\dot{\boldsymbol{r}}_k^T \boldsymbol{R}_{\frac{\pi}{2}}^T$ *both following expressions hold:*

$$\begin{aligned} \dot{v}_k v_k &= -\beta v_k^2 + \beta \dot{\boldsymbol{r}}_k^T (\dot{\hat{\boldsymbol{r}}}_k + \dot{\boldsymbol{c}}) + \hat{u}_k \dot{\boldsymbol{r}}_k^T \boldsymbol{R}_{\frac{\pi}{2}} \dot{\hat{\boldsymbol{r}}}_k + \dot{\boldsymbol{r}}_k^T \ddot{\boldsymbol{c}} \\ u_k v_k^2 &= \beta \dot{\boldsymbol{r}}_k^T \boldsymbol{R}_{\frac{\pi}{2}}^T (\dot{\hat{\boldsymbol{r}}}_k + \dot{\boldsymbol{c}}) + \hat{u}_k \dot{\boldsymbol{r}}_k^T \dot{\hat{\boldsymbol{r}}}_k + \dot{\boldsymbol{r}}_k^T \boldsymbol{R}_{\frac{\pi}{2}}^T \ddot{\boldsymbol{c}} \end{aligned}$$

By definition, this control law enforces exponential convergence of the tracking error dynamics away from the singularity $v_k = 0$*. If condition* (2.17) *is satisfied then, the control inputs of* (2.18) *are respectively obtained.*

Note that Theorem 2.4 presents a dynamic control law in which the control inputs are $(\dot{v}_k, u_k)$*.*

□

This new result does not depend on the initial conditions of the reference system. Therefore, for any initial conditions of the original and reference system, $\theta_k(0)$ and $\psi_k(0)$ respectively, each vehicle k converges to a circular motion with radius R and the time-varying center $\mathbf{c}(t)$.

2.3.5 Simulation results

This section presents the simulation results of the multi-agents system composed of AUVs modeled by (2.1) in order to validate the previous theoretical analysis of the translation control law.

The simulation shown in Figure 2.7 displays a fleet of five agents governed by the translation control law from Theorem 2.4. The controller parameters are $\omega_0 = \kappa = \beta = 1$, the radius of the desired circular motion is $R = 2$ and the reference of the center is given by:

$$\mathbf{c}(t) = (0.2t, 3\sin(0.08t))^T$$

Figure 2.7 shows a simulation of five agents which describes a circular motion tracking the time-varying reference of its center denoted by the blue line. The trajectory of only one agent is represented by the red line. Each vehicle converges to this motion independently of the others vehicles in the fleet for any initial conditions. Thus, according to definition of *formation* introduced in the survey of previous Chapter 1, the fleet of agents does not exactly move in formation. However, for each instant t, all the agents describe a circular trajectory with center $\mathbf{c}(t)$ and radius R, therefore, the vehicles are in the same circle. Nevertheless, the distribution of the agents does not follow a particular pattern. This problem will be considered in the last section of this chapter.

Figure 2.8 shows the evolution of the control inputs v_k and u_k for all the agents, obtained from the same simulation. The oscillations of both variables are due to the

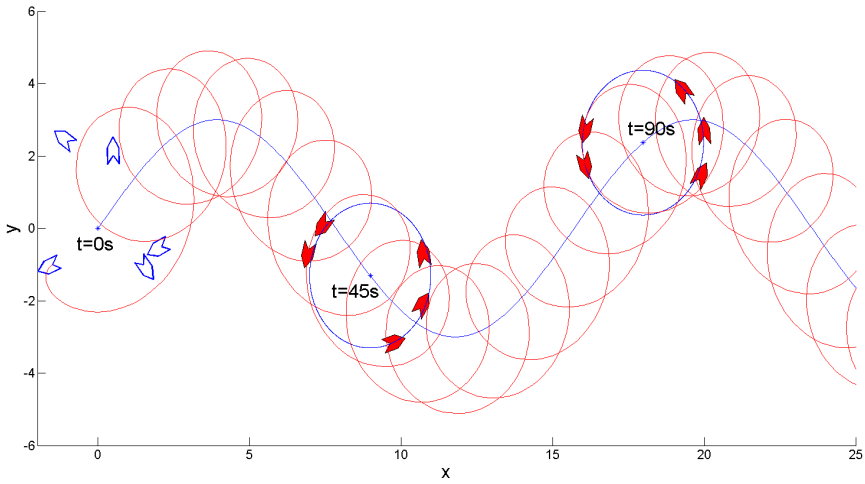

Figure 2.7: *Simulation of five agents governed by the control law* (2.18). *The figure represents three snapshots: the void blue agents correspond to the initial conditions and the red ones to two different instants, at* $t = 45s$ *and at* $t = 90s$. *The red line describes the trajectory of one agent tracking the reference of the center in blue.*

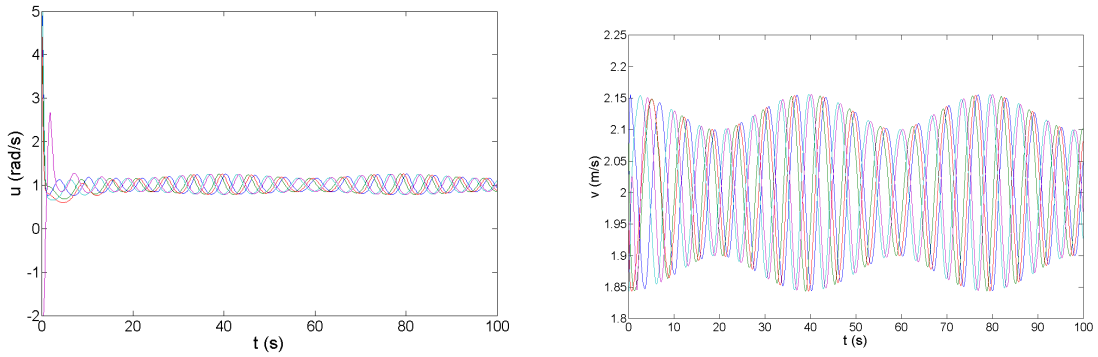

(a) Control inputs u_k

(b) Control inputs v_k

Figure 2.8: *Evolution of the control inputs* u_k *(a) and* v_k *(b) corresponding to the previous simulation of five agents shown in Figure 2.7.*

time-varying reference of the center. The velocity v_k of the vehicles oscillates around the value of the tangent velocity $R|\omega_0| = 2$. The mean value of the input u_k is logically equal to the angular velocity $\omega_0 = 1$.

2.4 Scaling of a circular motion

This subsection presents a second contribution based on previous circular control from [86, 118]. After the first result concerning the translation of a circular motion proposed before, the problem considered here is to design a control law such that the group of AUVs forms a circle whose center $\mathbf{c}$ is fixed and whose radius tracks a time-varying reference $R(t)$, as described in Figure 2.9. Using the same idea as in the translation case, this extension to the scaling (contraction and expansion) of a circular motion is the logical following step taking into account that the main parameters of a circle are its center and its radius.

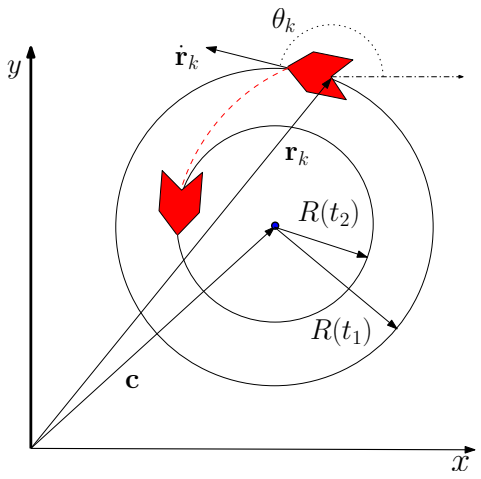

Figure 2.9: *Scaling of a circular formation*

Changing the size of a formation can be useful in several situations. For instance, it can be seen as a collision avoidance method such that the circular formation of AUVs reduces its radius in order to go through a narrow place. On the other hand, a scaling algorithm provides a solution to solve communication problems between the agents with low communication range. For example, in order to guaranty the communication between all the agents and theirs two neighbors in a circular formation the radius of the circle should satisfy a geometrical condition with respect to the communication range of the agents. These communication constraints and the influence in the radius of the circle will be considered in the next section.

In the sequel, a new control law is developed so that the agents converge to a circular motion with fixed center and whose radius tracks a time-varying reference.

2.4.1 Coordinates transformation

As we explained before, in the field of circular control there exist several methods in which, a unicycle model (2.1) with constant unit velocity, is consider to model the agents. As in the translation case, considering constant angular velocity, the velocity of the agents must be considered as a control input.

Basic mathematics show that for a uniform circular motion, there exists a relation between the linear and the angular magnitudes, such that, the magnitude of the tangential velocity of a point in a circular motion is equal to $v = R|\omega_0|$. Hence, is obvious that if the radius $R(t)$ is time-varying, considering a constant angular velocity ω_0, the velocity of the agents v_k must be time-varying too. Note that another approach, which was not considered here, could deal with this scaling problem if the angular velocity becomes a control input and the velocity remains constant.

This situation is the base of the work [120] in which the authors stabilize a fleet of vehicles to a fixed circular formation in a flowfield. The velocity of the vehicles is constant therefore to keep the circular formation in the presence of currents, the vehicles rotate with non constant angular velocity depending on the spacial distribution of the flowfield.

To raise the scaling of a circular motion, the same method presented previously in Figure 2.6 for the translation control of a circular motion will be followed. The main idea, is to transform the multi-agent system (2.1) into a time-invariant system with respect to the radius $R(t)$. Then, the dynamics of this transformed system are enforced to have constant velocity in order to apply the circular control law from [118]. In this case the new variable $\hat{\mathbf{r}}_k$ is defined such that:

$$\hat{\mathbf{r}}_k = \frac{(\mathbf{r}_k - \mathbf{c})}{R} \tag{2.19}$$

The aim is to ensure the convergence of the transformed system defined by (2.19) to a circle which has a fixed center $\mathbf{c}$ and unit radius, as shown in Figure 2.10. According to the relation in a circular motion $v = R|\omega_0|$, to stabilize the transformed system to a circle with unit radius the velocity should be equal to $|\omega_0|$. Therefore the dynamics of the transformed position vector are defined as:

$$\dot{\hat{x}}_k = |\omega_0| \cos\psi_k \tag{2.20a}$$

$$\dot{\hat{y}}_k = |\omega_0| \sin\psi_k \tag{2.20b}$$

$$\dot{\psi}_k = \hat{u}_k \tag{2.20c}$$

where ψ_k represents the angular orientation of the transformed velocity vector.

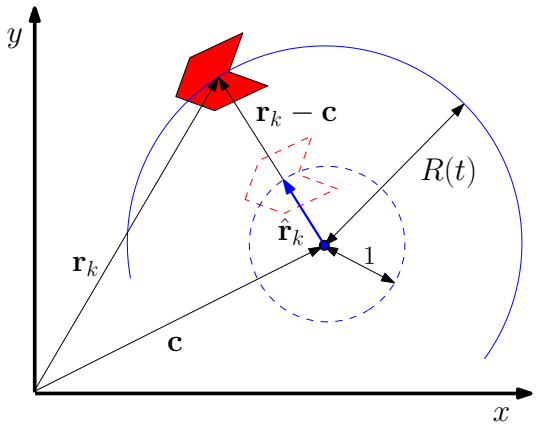

Figure 2.10: *Coordinates transformation for the scaling problem*

2.4.2 Scaling control law

Consider the problem of tracking a circular formation defined by a fixed and given center $\mathbf{c}$ and a time-varying radius. Assume that the reference defined the radius of the circular motion $R(t)$ is always positive and its first and second time-derivative are known and bounded. Moreover, the following assumption is required:

Assumption 2.1 *Let $t_s > 0$ be a sufficiently large time to be defined latter. Assume the reference of the radius $R(t)$ satisfies the conditions:*

$$\forall t < t_s, \quad R(t) = R_0 > 0, \quad \dot{R}(t) = \ddot{R}(t) = 0$$

This assumption corresponds to a class of initialisation of the multi-agent system. The idea is to allow the agents to reach a circular motion with constant radius and then to start tracking the time-varying reference of the radius (see Figure 2.12). This assumption is not restrictive since this initialization protocol could be used in practice.

Based on the previous translation control design, the convergence of the transformed system to a fixed circular motion with unit radius is analyzed using the same Lyapunov function:

$$S(\hat{\mathbf{r}}, \psi) = \frac{1}{2} \sum_{k=1}^{N} \left\| \dot{\hat{\mathbf{r}}}_k - \omega_0 \mathbf{R}_{\frac{\pi}{2}} \hat{\mathbf{r}}_k \right\|^2 \geq 0$$

Following the same reasoning, in the minimum of this Lyapunov function corresponding to $S(\hat{\mathbf{r}}, \psi) = 0$, the dynamics of the transformed system (2.20) satisfy $\dot{\hat{\mathbf{r}}}_k - \omega_0 \mathbf{R}_{\frac{\pi}{2}} \hat{\mathbf{r}}_k = 0$. Thus, the transformed position vector and its velocity vector are perpendicular because $\dot{\hat{\mathbf{r}}}_k^T \hat{\mathbf{r}}_k = 0$. This condition leads to the kinematic relation for the rotation of the rigid body, it means that the transformed vectors $\hat{\mathbf{r}}_k$ are turning around $\mathbf{c}$.

Evaluating the derivative of $S(\hat{\mathbf{r}}, \psi)$ along the solutions of the resulting closed-loop system (2.20) leads to:

$$\begin{aligned}\dot{S}(\hat{\mathbf{r}}, \psi) &= \sum_{k=1}^{N} \left(\ddot{\hat{\mathbf{r}}}_k - \omega_0 \mathbf{R}_{\frac{\pi}{2}} \dot{\hat{\mathbf{r}}}_k\right)^T \left(\dot{\hat{\mathbf{r}}}_k - \omega_0 \mathbf{R}_{\frac{\pi}{2}} \hat{\mathbf{r}}_k\right) \\ &= \sum_{k=1}^{N} \left(\hat{u}_k \mathbf{R}_{\frac{\pi}{2}} \dot{\hat{\mathbf{r}}}_k - \omega_0 \mathbf{R}_{\frac{\pi}{2}} \dot{\hat{\mathbf{r}}}_k\right)^T \left(\dot{\hat{\mathbf{r}}}_k - \omega_0 \mathbf{R}_{\frac{\pi}{2}} \hat{\mathbf{r}}_k\right) \\ &= \sum_{k=1}^{N} \omega_0 \hat{\mathbf{r}}_k^T \dot{\hat{\mathbf{r}}}_k (\omega_0 - \hat{u}_k)\end{aligned}$$

Based on the circular control law from [86] and according to the previous Lyapunov function, the same control law (2.11) is proposed to control the transformed system. Note again that for $\kappa = 0$, each transformed position vector $\hat{\mathbf{r}}_k$ will undergo circular motion which direction of rotation is determined by the sign of $\omega_0 \neq 0$. The gain κ regulates the contribution to the control of a dissipation term which steers vector $\hat{\mathbf{r}}_k$ such that it is perpendicular to its velocity vector $\dot{\hat{\mathbf{r}}}_k$.

Considering the proposed control law (2.11), the previous derivative of the Lyapunov function becomes:

$$\dot{S}(\hat{\mathbf{r}}, \psi) = -\kappa \sum_{k=1}^{N} (\omega_0 \hat{\mathbf{r}}_k^T \dot{\hat{\mathbf{r}}}_k)^2 \leq 0 \tag{2.21}$$

In conclusion, $S(\hat{\mathbf{r}}, \psi)$ is a suitable Lyapunov function for this transformed system. Thus, the solutions converge to the largest invariant set Λ, for which $\dot{S} = 0$.

Theorem 2.5 *(Briñón-Arranz et al. 2010 [17]) Consider three positive scalars $\epsilon > 0$ and $R_2 > R_1 > 0$. Let $\omega_0 \neq 0$ and $\kappa > 0$ be two control parameters. Let $R : \mathbb{R} \to [R_1, R_2]$ be a twice differentiable function, with bounded first and second time-derivatives, which satisfies Assumption 2.1 and the condition:*

$$\forall t, \quad \dot{R}(t) < \frac{R(t)|\omega_0|}{(1+\epsilon)} \tag{2.22}$$

Then the control law:

$$v_k = \left\| R|\omega_0|(\cos\psi_k, \sin\psi_k)^T + \frac{\dot{R}}{R}(\boldsymbol{r}_k - \boldsymbol{c}) \right\| \tag{2.23a}$$

$$u_k = \left(1 - \frac{\dot{R}}{R} \frac{\dot{\boldsymbol{r}}_k^T (\boldsymbol{r}_k - \boldsymbol{c})}{v_k^2}\right) \dot{\psi}_k + \frac{R\ddot{R} - 2\dot{R}^2}{(Rv_k)^2} (\boldsymbol{r}_k - \boldsymbol{c})^T \boldsymbol{R}_{\frac{\pi}{2}} \dot{\boldsymbol{r}}_k \tag{2.23b}$$

$$\dot{\psi}_k = \omega_0 \left(1 + \kappa \frac{|\omega_0|}{R} (\cos\psi_k, \sin\psi_k)^T (\boldsymbol{r}_k - \boldsymbol{c})\right) \tag{2.23c}$$

with the initial conditions $\psi_k(0)$ *as:*

$$\psi_k(0) = \theta_k(0) \tag{2.24}$$

makes all the agents defined by (2.1) *converge to a circular motion of center* $\boldsymbol{c}$*, and whose radius follows the time-varying reference* $R(t)$*. The direction of rotation is determined by the sign of* ω_0*.*

Proof 2.5 *The proof of this theorem follows the same steps that in the case of the translation control law. First, the stability of the transformed system with the control law* (2.23c) *is established through the previous Lyapunov function* $S(\hat{\boldsymbol{r}}, \psi)$*. The Lyapunov function is positive definite and from* (2.29)*,* S *is nonincreasing along the solutions. Thanks to the change of coordinates* (2.19)*, the dynamic closed-loop system corresponding to the transformed system is time-invariant, hence LaSalle Principle can be applied again. Therefore, solutions for the reduced system on shape space converge to the largest invariant set* Λ *where*

$$\kappa \hat{\boldsymbol{r}}_k^T \dot{\hat{\boldsymbol{r}}}_k \equiv 0 \quad \forall k$$

In this set, $\dot{\psi}_k = \omega_0$*,* i.e.*, the transformed position vector describes circles of unit radius. The transformed system* (2.19) *asymptotically reaches the circular formation centered at* $\boldsymbol{c}$ *and of unit radius with fixed angular velocity* ω_0*. Hence, the dynamics of the agents satisfy:*

$$\dot{\boldsymbol{r}}_k = \underbrace{\omega_0 \boldsymbol{R}_{\frac{\pi}{2}}(\boldsymbol{r}_k - \boldsymbol{c})}_{\textit{circular motion}} + \underbrace{\frac{\dot{R}}{R}(\boldsymbol{r}_k - \boldsymbol{c})}_{\textit{scaling term}}$$

The fist term describes the kinematic relation of a circular motion and the scaling term, enforces the velocity vector $\dot{\boldsymbol{r}}_k$ *to change its direction according to the derivative of the radius,* i.e. *if* $\dot{R} < 0$ *the velocity vector is deviated leading to the contraction term, and the case of* $\dot{R} > 0$ *corresponds to an expansion motion.*

The next step involves expressing the original control inputs v_k *and* u_k *in terms of the inner state variable* $\dot{\psi}_k$*. According to the change of coordinates* (2.19)*, differentiating the definition of* $\hat{\boldsymbol{r}}_k$ *gives*

$$\dot{\boldsymbol{r}}_k = R\dot{\hat{\boldsymbol{r}}}_k + \dot{R}\hat{\boldsymbol{r}}_k = R\dot{\hat{\boldsymbol{r}}}_k + \frac{\dot{R}}{R}(\boldsymbol{r}_k - \boldsymbol{c})$$

This equation provides both expressions of the control inputs. Expressing previous equation in terms of its components, gives:

$$v_k \cos\theta_k = R|\omega_0| \cos\psi_k + \frac{\dot{R}}{R}(x_k - c_x)$$
$$v_k \sin\theta_k = R|\omega_0| \sin\psi_k + \frac{\dot{R}}{R}(y_k - c_y)$$

Therefore, the control input v_k is thus straightforwardly given by (2.23a). *A more particular attention is addressed to $\dot{\theta}_k$. Using previous equations the following equality holds:*

$$\tan\theta_k = \frac{R\dot{\hat{y}}_k + \dot{R}\hat{y}_k}{R\dot{\hat{x}}_k + \dot{R}\hat{x}_k} = \frac{R|\omega_0|\sin\psi_k + \frac{\dot{R}}{R}(y_k - c_y)}{R|\omega_0|\cos\psi_k + \frac{\dot{R}}{R}(x_k - c_x)} \tag{2.25}$$

and differentiating

$$\dot{\theta}_k(1+\tan^2\theta_k) = \frac{(R\ddot{\hat{y}}_k + 2\dot{R}\dot{\hat{y}}_k + \ddot{R}\hat{y}_k)(R\dot{\hat{x}}_k + \dot{R}\hat{x}_k) - (R\dot{\hat{y}}_k + \dot{R}\hat{y}_k)(R\ddot{\hat{x}}_k + 2\dot{R}\dot{\hat{x}}_k + \ddot{R}\hat{x}_k)}{(R\dot{\hat{x}}_k + \dot{R}\hat{x}_k)^2}$$

Developing previous expression the following equation holds:

$$\begin{aligned}\dot{\theta}_k v_k^2 &= (\hat{u}_k R\dot{\hat{x}}_k + 2\dot{R}\dot{\hat{y}}_k + \ddot{R}\hat{y}_k)(R\dot{\hat{x}}_k + \dot{R}\hat{x}_k) - (R\dot{\hat{y}}_k + \dot{R}\hat{y}_k)(-\hat{u}_k R\dot{\hat{y}}_k + 2\dot{R}\dot{\hat{x}}_k + \ddot{R}\hat{x}_k)\\ &= \hat{u}_k\left(R^2(\dot{\hat{x}}_k^2 + \dot{\hat{y}}_k^2) + \dot{R}R(\dot{\hat{x}}_k\hat{x}_k + \dot{\hat{y}}_k\hat{y}_k)\right) + (R\ddot{R} - 2\dot{R}^2)(\dot{\hat{x}}_k\hat{y}_k - \dot{\hat{y}}_k\hat{x}_k)\end{aligned}$$

To fit with the change of coordinates previous relation becomes:

$$\dot{\theta}_k v_k^2 = \hat{u}_k\left(v_k^2 - \frac{\dot{R}}{R}(\dot{x}_k(x_k - c_x) + \dot{y}_k(y_k - c_y))\right) + \frac{R\ddot{R} - 2\dot{R}^2}{R^2}(\dot{x}_k(y_k - c_y) - \dot{y}_k(x_k - c_x))$$

Then, from $u_k = \dot{\theta}_k$, the control input u_k proposed in (2.23b) *is retrieved. In order to satisfy the relation* (2.25) *for all t, the initial conditions of the inner variable ψ_k must be imposed as a function of the initial values of θ_k. Therefore, since equation* (2.25) *is satisfied and considering Assumption 2.1, following relation holds:*

$$\psi_k(0) = \theta_k(0)$$

Note that this control law, as in the translation control design, has singular points when $v_k = 0$. This singular point occurs if there exists a time t_c such that:

$$\begin{cases} \angle(\boldsymbol{r}_k(t_c) - \boldsymbol{c}) = -\psi_k(t_c) \\ \frac{|\dot{R}(t_c)|}{R(t_c)}\|\boldsymbol{r}_k(t_c) - \boldsymbol{c}\| = R(t_c)|\omega_0| \end{cases} \tag{2.26}$$

To avoid the singular situation when $v_k = 0$, the initialization protocol described in Assumption 2.1 is required. Thanks to Theorem 2.5, considering a constant radius $R(t) = R_0$ described in Assumption 2.1, the multi-agents system converges asymptotically to a circle centered at $\boldsymbol{c}$ and with radius R_0. The transformed system converges to a circular motion also centered at $\boldsymbol{c}$ and whit unit radius. This means that there exists a time t_s such that:

$$\forall t > t_s, \quad \|\hat{\boldsymbol{r}}_k(t)\| - 1 = \left\|\frac{\boldsymbol{r}_k(t) - \boldsymbol{c}}{R(t)}\right\| - 1 < \epsilon$$

This inequality can be rewritten as:

$$\forall t > t_s, \quad \|\boldsymbol{r}_k(t) - \boldsymbol{c}\| < R(t)(1+\epsilon)$$

This result is logical, because this inequality expresses the asymptotic convergence of the original system to a circular motion of radius $R(t)$. Starting from the singular point (2.26) *and taking into account this previous inequality, the following expression holds:*

$$\forall t > t_s, \quad \frac{|\dot{R}(t)|}{R(t)}\|\boldsymbol{r}_k(t) - \boldsymbol{c}\| < \frac{|\dot{R}(t)|}{R(t)}R(t)(1+\epsilon) = |\dot{R}(t)|(1+\epsilon)$$

If condition (2.27) *is satisfied, this previous inequality can be rewritten:*

$$\forall t > t_s, \quad \frac{|\dot{R}(t)|}{R(t)}\|\boldsymbol{r}_k(t) - \boldsymbol{c}\| < (1+\epsilon)\frac{R(t)|\omega_0|}{1+\epsilon} = R(t)|\omega_0|$$

which is in contradiction with (2.26). *Thus, the singular point $v_k = 0$ is avoided. Note that this initialization protocol, described graphically in Figure 2.11, is not very restrictive, and it could correspond to an engineering requirement.*

□

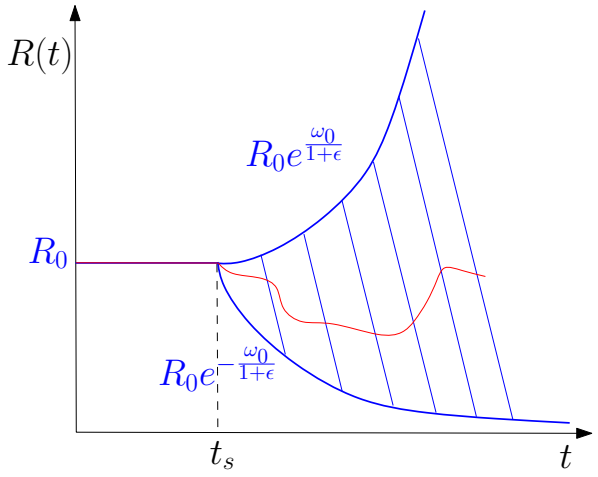

Figure 2.11: *Graphical interpretation of the condition which is imposed to the reference of the radius in Theorem 2.5. After a given instant t_s, the radius $R(t)$ is contained in the blue striped region.*

Remark 2.4 *The scaling control law presented in Theorem 2.5 is an extension of the circular control proposed in [118]. In this paper, the authors present a control law which stabilizes a vehicle to a circular motion with fixed center and constant radius using its absolute position. The improvement with respect to this work comes from the fact that is possible to stabilize the agents to circular motions whose radius is time-varying. Note that if radius R becomes time-invariant,* i.e., *$\dot{R}(t) = \ddot{R}(t) = 0$ for all t, according to equation* (2.23b) *and the initial condition* (2.24) *the angles ψ_k and θ_k become equal.*

Thus, the control law (2.23) *is the same control as in Theorem 2.2 with a different gain, such that:*

$$\begin{aligned} v_k &= R|\omega_0| \\ u_k &= \hat{u}_k = \omega_0 \left(1 + \frac{\kappa}{R^2}\dot{\boldsymbol{r}}_k^T(\boldsymbol{r}_k - \boldsymbol{c})\right) \end{aligned}$$

Remark 2.5 *The domain of the reference of the radius for Theorem 2.5 is limited by* $R_2 \leq v_{max}/|\omega_0|$ *where* v_{max} *represents the maximum speed for the vehicles which depends on the mechanical performances. Therefore, the maximum radius of the circle is related to the physical constraints of the AUVs.*

2.4.3 Tracking on $SE(2)$ for the scaling problem

The control law from Theorem 2.5 stabilize the vehicles to a circular motion with time-varying center. Due to the methodology applied and the change of coordinates defined by (2.19) the inner variable ψ_k must be initialized as a function of the initial conditions of the heading angle θ_k. In consequence, the control law is not robust to uncertainties in $\theta_k(0)$.

Based on previous translation control design, we use the same methodology in order to stabilize a fleet of agents modeled by (2.1) to a circular motion with time-varying radius. Following a tracking process, the transformed system defined by the change of coordinates (2.19) is considered as a reference to the original system (2.1). The dynamics of the reference system satisfy (2.20) and the closed-loop dynamics are imposed by the control law (2.11). In this situation, the following theorem presents another contribution of this chapter.

Theorem 2.6 *(Extension of Briñón-Arranz et al. 2010 [17]) Consider a twice differentiable function* $R(t) : \mathbb{R} \to \mathbb{R}^+$*, with bounded first and second time-derivatives. Let* $\boldsymbol{c}$ *be the center of the desired circular motion, the control parameters be such that* $\omega_0 \neq 0$*,* $\kappa > 0$*,* $\beta > 0$*, and the following condition is satisfied:*

$$v_k > 0 \quad \forall k = 1, \ldots, N \tag{2.27}$$

Then, for all initial conditions $\boldsymbol{r}(0), \theta(0)$*, the control law*

$$\dot{v}_k = -\beta v_k + \frac{\hat{u}_k R \dot{\boldsymbol{r}}_k^T \boldsymbol{R}_{\frac{\pi}{2}} \dot{\hat{\boldsymbol{r}}}_k + \frac{\ddot{R}+\beta\dot{R}}{R}\dot{\boldsymbol{r}}_k^T(\boldsymbol{r}_k - \boldsymbol{c}) + (2\dot{R} + \beta R)\dot{\boldsymbol{r}}_k^T \dot{\hat{\boldsymbol{r}}}_k}{v_k} \tag{2.28a}$$

$$u_k = \frac{\hat{u}_k R \dot{\boldsymbol{r}}_k^T \dot{\hat{\boldsymbol{r}}}_k + \frac{\ddot{R}+\beta\dot{R}}{R}\dot{\boldsymbol{r}}_k^T \boldsymbol{R}_{\frac{\pi}{2}}^T(\boldsymbol{r}_k - \boldsymbol{c}) + (2\dot{R} + \beta R)\dot{\boldsymbol{r}}_k^T \boldsymbol{R}_{\frac{\pi}{2}}^T \dot{\hat{\boldsymbol{r}}}_k}{v_k^2} \tag{2.28b}$$

where $\dot{\hat{\boldsymbol{r}}}_k$ *and* $\hat{u}_k$ *are defined by* (2.20) *and* (2.11) *respectively, makes all the agents defined by* (2.1) *converge to a circular motion centered at* $\boldsymbol{c}$*, and whose radius tracks*

the time-varying reference $R(t)$. The direction of rotation is determined by the sign of ω_0.

Proof 2.6 *The proof of this theorem follows the same steps that in the case of the translation control law. Based on the previous translation control design, the convergence of the transformed system to a fixed circular motion with unit radius is analyzed using the same Lyapunov function:*

$$S(\hat{\boldsymbol{r}}, \psi) = \frac{1}{2} \sum_{k=1}^{N} \left\| \dot{\hat{\boldsymbol{r}}}_k - \omega_0 \boldsymbol{R}_{\frac{\pi}{2}} \hat{\boldsymbol{r}}_k \right\|^2 \geq 0$$

Following the same reasoning, in the minimum of this Lyapunov function corresponding to $S(\hat{\boldsymbol{r}}, \psi) = 0$, the dynamics of the transformed system (2.20) satisfy

$$\dot{\hat{\boldsymbol{r}}}_k = \omega_0 \boldsymbol{R}_{\frac{\pi}{2}} \hat{\boldsymbol{r}}_k$$

Thus, the transformed position vector and its velocity vector are perpendicular because $\dot{\hat{\boldsymbol{r}}}_k^T \hat{\boldsymbol{r}}_k = 0$. This condition leads to the kinematic relation for the rotation of the rigid body, it means that the transformed vectors $\hat{\boldsymbol{r}}_k$ are turning around $\boldsymbol{c}$.

Evaluating the derivative of $S(\hat{\boldsymbol{r}}, \psi)$ along the solutions of the resulting closed-loop system (2.20) leads to:

$$\begin{aligned}
\dot{S}(\hat{\boldsymbol{r}}, \psi) &= \sum_{k=1}^{N} \left(\ddot{\hat{\boldsymbol{r}}}_k - \omega_0 \boldsymbol{R}_{\frac{\pi}{2}} \dot{\hat{\boldsymbol{r}}}_k \right)^T \left(\dot{\hat{\boldsymbol{r}}}_k - \omega_0 \boldsymbol{R}_{\frac{\pi}{2}} \hat{\boldsymbol{r}}_k \right) \\
&= \sum_{k=1}^{N} \left(\hat{u}_k \boldsymbol{R}_{\frac{\pi}{2}} \dot{\hat{\boldsymbol{r}}}_k - \omega_0 \boldsymbol{R}_{\frac{\pi}{2}} \dot{\hat{\boldsymbol{r}}}_k \right)^T \left(\dot{\hat{\boldsymbol{r}}}_k - \omega_0 \boldsymbol{R}_{\frac{\pi}{2}} \hat{\boldsymbol{r}}_k \right) \\
&= \sum_{k=1}^{N} \omega_0 \hat{\boldsymbol{r}}_k^T \dot{\hat{\boldsymbol{r}}}_k (\omega_0 - \hat{u}_k)
\end{aligned}$$

Based on the circular control laws from [86, 118] and according to the previous Lyapunov function, the control law (2.11) is proposed to control the transformed system. Note again that for $\kappa = 0$, each transformed position vector $\hat{\boldsymbol{r}}_k$ will undergo circular motion which direction of rotation is determined by the sign of $\omega_0 \neq 0$. The gain κ regulates the contribution to the control of a dissipation term which steers vector $\hat{\boldsymbol{r}}_k$ such that it is perpendicular to its velocity vector $\dot{\hat{\boldsymbol{r}}}_k$.

Considering the proposed control law (2.11), the previous derivative of the Lyapunov function becomes:

$$\dot{S}(\hat{\boldsymbol{r}}, \psi) = -\kappa \sum_{k=1}^{N} (\omega_0 \hat{\boldsymbol{r}}_k^T \dot{\hat{\boldsymbol{r}}}_k)^2 \leq 0 \tag{2.29}$$

In conclusion, $S(\hat{\boldsymbol{r}}, \psi)$ is positive definite and is nonincreasing along the solutions. Thanks to the change of coordinates (2.19), the dynamic closed-loop system corresponding to the transformed system is time-invariant, hence LaSalle Principle can be

applied again. Therefore, solutions for the reduced system on shape space converge to the largest invariant set Λ *where*

$$\kappa \hat{\boldsymbol{r}}_k^T \dot{\hat{\boldsymbol{r}}}_k \equiv 0 \quad \forall k$$

In this set, $\hat{u}_k = \dot{\psi}_k = \omega_0$, i.e., *the transformed position vector describes circles of unit radius. The transformed system* (2.20) *asymptotically reaches a circular motion centered at* $\boldsymbol{c}$*, with unit radius and fixed angular velocity* ω_0.

The objective now is to make converge the original system to the reference system according to relation (2.19)*, i.e.:*

$$\dot{\boldsymbol{r}}_k \to \dot{R}\hat{\boldsymbol{r}}_k + R\dot{\hat{\boldsymbol{r}}}_k$$

In order to achieve this objective the tracking error is defined as follows:

$$\boldsymbol{e}_k = \dot{\boldsymbol{r}}_k - \dot{R}\hat{\boldsymbol{r}}_k - R\dot{\hat{\boldsymbol{r}}}_k$$

In order to make the error converge to zero, such that $\boldsymbol{e}_k \to 0$*, we impose the error dynamics* $\dot{\boldsymbol{e}}_k = -\beta \boldsymbol{e}_k$ *where* $\beta > 0$*. Then, the error converge exponentially to zero. Thanks to previous definition of the error the following equation holds when* $t \to \infty$*:*

$$\dot{\boldsymbol{r}}_k = \dot{R}\hat{\boldsymbol{r}}_k + R\dot{\hat{\boldsymbol{r}}}_k \quad \forall k = 1, \ldots, N$$

Hence, when the reference system is stabilized, the dynamics of the agents satisfy:

$$\dot{\boldsymbol{r}}_k = \underbrace{\omega_0 \boldsymbol{R}_{\frac{\pi}{2}}(\boldsymbol{r}_k - \boldsymbol{c})}_{\textit{circular motion}} + \underbrace{\frac{\dot{R}}{R}(\boldsymbol{r}_k - \boldsymbol{c})}_{\textit{scaling term}}$$

The fist term describes the kinematic relation of a circular motion and the scaling term, enforces the velocity vector $\dot{\boldsymbol{r}}_k$ *to change its direction according to the derivative of the radius,* i.e. *if* $\dot{R} < 0$ *the velocity vector is deviated leading to the contraction term, and the case of* $\dot{R} > 0$ *corresponds to an expansion motion.*

The dynamics of the error equation determines the control law for the original system (2.1) *since:*

$$\begin{aligned}
\dot{\boldsymbol{e}}_k &= \ddot{\boldsymbol{r}}_k - \ddot{R}\hat{\boldsymbol{r}}_k - 2\dot{R}\dot{\hat{\boldsymbol{r}}}_k - R\ddot{\hat{\boldsymbol{r}}}_k \\
-\beta(\dot{\boldsymbol{r}}_k - \dot{R}\hat{\boldsymbol{r}}_k - R\dot{\hat{\boldsymbol{r}}}_k) &= \frac{\dot{v}_k}{v_k}\dot{\boldsymbol{r}}_k + u_k \boldsymbol{R}_{\frac{\pi}{2}}\dot{\boldsymbol{r}}_k - \hat{u}_k \boldsymbol{R}_{\frac{\pi}{2}}\dot{\hat{\boldsymbol{r}}}_k - \ddot{R}\hat{\boldsymbol{r}}_k - 2\dot{R}\dot{\hat{\boldsymbol{r}}}_k \\
\frac{\dot{v}_k}{v_k}\dot{\boldsymbol{r}}_k + u_k \boldsymbol{R}_{\frac{\pi}{2}}\dot{\boldsymbol{r}}_k &= -\beta(\dot{\boldsymbol{r}}_k - \dot{R}\hat{\boldsymbol{r}}_k - R\dot{\hat{\boldsymbol{r}}}_k) - \hat{u}_k \boldsymbol{R}_{\frac{\pi}{2}}\dot{\hat{\boldsymbol{r}}}_k - \ddot{R}\hat{\boldsymbol{r}}_k - 2\dot{R}\dot{\hat{\boldsymbol{r}}}_k
\end{aligned}$$

Multiplying by the above equation by $\dot{\boldsymbol{r}}_k^T$ *and by* $\dot{\boldsymbol{r}}_k^T \boldsymbol{R}_{\frac{\pi}{2}}^T$ *both following expressions hold:*

$$\begin{aligned}
\dot{v}_k v_k &= -\beta v_k^2 + \beta \dot{\boldsymbol{r}}_k^T(\dot{R}\hat{\boldsymbol{r}}_k + R\dot{\hat{\boldsymbol{r}}}_k) + \hat{u}_k \dot{\boldsymbol{r}}_k^T \boldsymbol{R}_{\frac{\pi}{2}}\dot{\hat{\boldsymbol{r}}}_k + \ddot{R}\dot{\boldsymbol{r}}_k^T\hat{\boldsymbol{r}}_k + 2\dot{R}\dot{\boldsymbol{r}}_k^T\dot{\hat{\boldsymbol{r}}}_k \\
u_k v_k^2 &= \beta \dot{\boldsymbol{r}}_k^T \boldsymbol{R}_{\frac{\pi}{2}}^T(\dot{R}\hat{\boldsymbol{r}}_k + R\dot{\hat{\boldsymbol{r}}}_k) + \hat{u}_k \dot{\boldsymbol{r}}_k^T \dot{\hat{\boldsymbol{r}}}_k + \ddot{R}\dot{\boldsymbol{r}}_k^T \boldsymbol{R}_{\frac{\pi}{2}}^T\hat{\boldsymbol{r}}_k + 2\dot{R}\dot{\boldsymbol{r}}_k^T \boldsymbol{R}_{\frac{\pi}{2}}^T\dot{\hat{\boldsymbol{r}}}_k
\end{aligned}$$

By definition, this control law enforces exponential convergence of the tracking error dynamics away from the singularity $v_k = 0$. If condition (2.27) *is satisfied then, the control inputs of* (2.28) *are respectively obtained.*

Note that Theorem 2.6 presents a dynamic control law in which the control inputs are $(\dot{v}_k, u_k)$.

□

This result is independent on the initial conditions of the reference system. Therefore, for any initial conditions of the original and reference system, $\theta_k(0)$ and $\psi_k(0)$ respectively, each vehicle k converges to a circular motion centered at $\mathbf{c}$ with the time-varying radius $R(t)$.

Remark 2.6 *The domain of the reference of the radius for Theorem 2.6 is limited by* $R_{max} = v_{max}/|\omega_0|$ *where* v_{max} *represents the maximum speed for the vehicles which depends on the mechanical performances. Therefore, the maximum radius of the circle is related to the physical constraints of the AUVs.*

2.4.4 Simulation results

This section presents the simulation of a fleet of AUVs modeled by (2.1) governed by the scaling control law (2.28). The control parameters are $\omega_0 = -1$ and $\kappa = \beta = 1$. The reference of the radius is given by:

$$R(t) = \begin{cases} 7 \quad \text{if} \quad t \leq 30 \\ 30.25 - 0.7t \quad \text{if} \quad 30 < t \leq 35 \\ 4 \quad \text{if} \quad 35 < t \leq 60 \\ 24.33 - 0.33t \quad \text{if} \quad 30 < t \leq 35 \\ 1 \quad \text{if} \quad 35 < t \leq 60 \end{cases}$$

In order to apply Theorem 2.6, the first and second time-derivatives of the reference which defines the radius must be well-defined and bounded. Therefore, a filter is added to the previous signal to avoid the singularities in the references $R(t)$, $\dot{R}(t)$ and $\ddot{R}(t)$. The chosen filter is given by the transfer function $F(s) = 1/(s^3 + 2s^2 + 2s + 1)$.

Figure 2.12 (a) shows the evolution of the relative position magnitudes $\|\mathbf{r}_k - \mathbf{c}\|$ of five agents controlled by the control law (2.28) from Theorem 2.6. The five agents converge to a circular motion following the time-varying reference of its radius $R(t)$. Figure 2.12 (b) shows the trajectory of only one agent governed by the control law defined in Theorem 2.6 during the contraction motion defined by the time-varying reference $R(t)$ from Figure 2.12 (a). The contraction of the circular motion is achieved for any random initial conditions (position and heading of the agents).

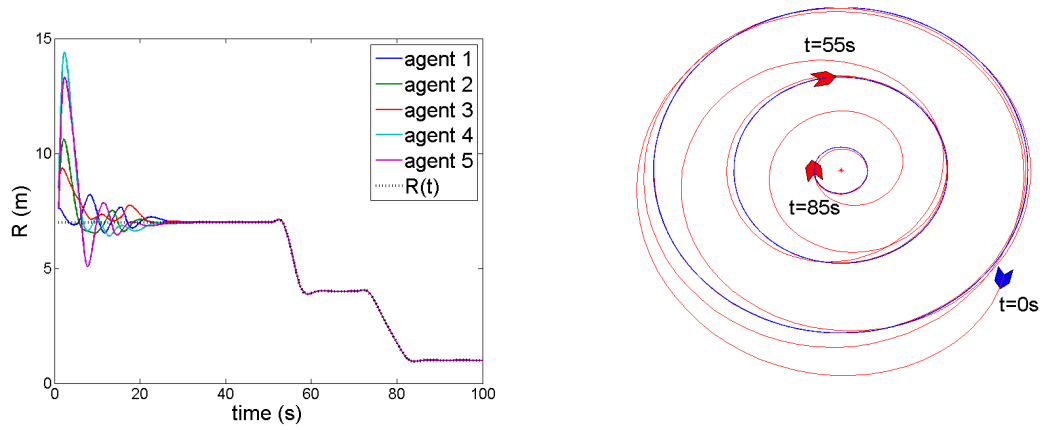

(a) Relative distances between each agent and the center of the circular formation

(b) Trajectory of one agent following the reference of the radius $R(t)$

Figure 2.12: *Simulation of five agents governed by* (2.28) *tracking a time-varying reference for the radius.*

Two previous sections present both contributions of this chapter dealing with time-varying motions: translation and scaling of a circular motion. The combination of both motions will be tacked in next Chapter 3. The contributions of this following chapter are based on the methodology developed in these previous sections in order to consider the main transformations of a formation.

The translation and scaling control laws are not cooperative because each agent is able to reach the desired circular motion even if there does not exist communication between the agents. The following section improves both control laws with a collaborative term in order to distribute the agents according to a desired pattern.

2.5 Uniform distribution along a circular formation

Both previous control laws do not take into consideration communication constraints, because each agent converges independently to the desired circular motion. Therefore, the phase arrangement of the particles is arbitrary. In other words, in order to stabilize the agents to a circular *formation* the translation and scaling control laws must include a cooperative term to distribute the agents along the same circle following a particular pattern. Moreover, in the context of source-seeking for underwater vehicles, ensuring that the agents are uniformly distributed along the formation might be more appropriate to produce efficient search motions.

The objective is now, to design an extension of both translation and scaling control laws in order to distribute uniformly the agents along the circular formation. Fig-

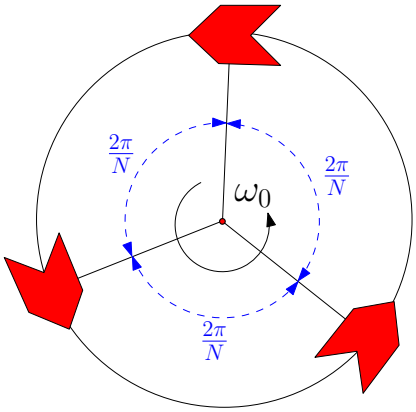

Figure 2.13: *Uniform distribution of the vehicles along a circular formation*

ure 2.14 shows the uniform distribution of three vehicles along a circular orbit, *i.e.*, the phase difference between adjacent vehicles is $\frac{2\pi}{N}$ where N is the number of vehicles.

A first method would be to deploy a centralized controller. This controller would deliver to each agent the control law to reach the uniform distribution. However, this is not fit with an underwater situation in which the signal transmitted decays with the distance. Hence, it is assumed that no agent has global knowledge of its neighbors' position. Several works follow the main idea from [86] to stabilize the vehicles to a circular motion tackling also the problem of distribute the agents along the circle in a particular pattern. These results are based on the synchronization problem of oscillators and the symmetric proprieties of the manifold S^1, see [142]. In the sequel, a review about control of symmetric patterns in a circular formation is presented.

2.5.1 Control of symmetric patterns

A first analysis of the stabilization of a group of agents to a uniform distribution along a circular formation is presented in [118]. The authors design a methodology to stabilize the *splay state* formation of a group of agents. This configuration is characterized by a circular motion around the fixed center of mass of the group, with all vehicles being evenly spaced on the circle. An extension to several kinds of patterns is studied in [149] for all-to-all communication topology. Based on these results, the circular control presented in [86] is improved in order to stabilize the vehicles to a fixed circular motion with uniform distribution. This approach requires the communication topology to be time-invariant and connected. Moreover, the communication is assumed to be bidirectional. Transmitting the relative headings of the vehicles, the authors can stabilize particular phase-locked patterns or arrangements of the agents in a circular formation. This is achieved adding a gradient control term to the previous circular control law

presented in Theorem 2.1 from [86] as follows:

$$u_k = \omega_0(1 + \kappa \tilde{\mathbf{r}}_k^T \dot{\mathbf{r}}_k) - \frac{\partial U}{\partial \theta_k} \tag{2.30}$$

The potential function $U(\theta)$ depends on the heading angles of all the agents represented by the vector $\theta = (\theta_1, \ldots, \theta_N)^T$ and satisfy $\nabla U \mathbf{1} = 0$, where $\nabla U = (\frac{\partial U}{\partial \theta_1}, \ldots, \frac{\partial U}{\partial \theta_N})$ represents the gradient of the potential function and $\mathbf{1} \in \mathbb{R}^N$ is the vector of ones. Then, the potential is invariant to rigid rotation of all the vehicles' headings. Moreover, the circular motion of the group in a phase-locked heading arrangement is a critical point of $U(\theta)$.

The control of relative headings can be studied under two different approaches, all-to-all communication assumption and limited communication. Considering limited communication means that each agent may receive information from only some of the other agents [109]. It is known that designing collaborative controllers leads to more difficulties than in the case of all-to-all communication assumption. In both cases, presented in detail in [149] and [150] respectively, the potential function enables us to stabilize symmetric patterns of the vehicles in circular formations.

The results of both works are expressed in $\mathbb{C}$. In order to define these results in the $\mathbb{R}^2$ formulation the following notation is introduced. The Laplacian matrix considered is $\bar{\mathbf{L}} = \mathbf{L} \otimes \mathbf{I}_2$ where $\otimes$ is the classical Kronecker product and $\mathbf{I}_N \in \mathbb{R}^{N \times N}$ is the identity matrix. Let $b_{mk} = (\cos m\theta_k, \sin m\theta_k)^T$ be the vector which contains the orientation angle of the agents and $\mathbf{B}_m = (b_{m1}^T, \ldots, b_{mN}^T)^T$ contains all the heading angles of the system.

Symmetric (M, N)-patterns of the agents are characterized by $2 \leq M \leq N$ heading clusters separated by a multiple of $\frac{2\pi}{M}$, see [149]. To avoid local minimums and to include higher harmonics, the moment of the phase distribution on the circle is defined as:

$$p_m = \frac{1}{mN} \sum_{k=1}^{N} b_{mk}$$

where $m \in \mathbb{N}$. Let the potential $U_m(\theta) = \frac{N}{2}\|p_m\|^2$ satisfy $\nabla U_m \mathbf{1} = 0$. Considering all-to-all communication topology, the unique minimum of this potential corresponds to the balancing modulo $\frac{2\pi}{m}$, reached when $p_m = 0$. Its unique maximum is the synchronization modulo $\frac{2\pi}{m}$, reached when the phase difference between any two phases is an integer multiple of $\frac{2\pi}{m}$. Therefore, the function $U(\theta)$ defined as:

$$U(\theta) = K \sum_{m=1}^{\lfloor N/2 \rfloor} U_m(\theta) \tag{2.31}$$

where $K > 0$ and $\lfloor N/2 \rfloor$ is the largest integer less than or equal to $N/2$, is called splay state potential, whose global minimum is the splay state, equivalent to the symmetric (N, N)-pattern. The splay state formation control law has the form from (2.30).

Assuming all-to-al communication, the potential function is given by (2.31) and the control law can be written as:

$$u_k = \omega_0(1 + \kappa\tilde{\mathbf{r}}_k^T\dot{\mathbf{r}}_k) + \frac{K}{N}\sum_{j=1}^{N}\sum_{m=1}^{\lfloor N/2\rfloor}\frac{\sin m\theta_{kj}}{m}$$

where the relative headings $\theta_{kj} = \theta_k - \theta_j$ are the additional transmitted informations.

Theorem 2.7 *(Sepulchre et al. 2007 [149]) Each (M, N)-pattern circular formation of radius $1/|\omega_0|$ is an isolated relative equilibrium of the particle model (2.1) and is exponentially stabilized by the control law (2.30) where the potential function is defined by (2.31).*

Proof 2.7 *In order to analyze the stability of the motion, the authors of [149] propose a combined Lyapunov function:*

$$V(\boldsymbol{r}, \theta) = \kappa S(\boldsymbol{r}, \theta) + U(\theta) \geq 0$$

where $S(\boldsymbol{r}, \theta) = \frac{1}{2}\sum_{k=1}^{N}\left\|\dot{\boldsymbol{r}}_k - \omega_0\boldsymbol{R}_{\frac{\pi}{2}}\tilde{\boldsymbol{r}}_k\right\|^2$ as it was defined in (2.3). This function reach its minimum for circular motion around the fixed center of mass as it was proved in Theorem 2.1. Moreover, the agents are distributed in an (M, N)-pattern corresponding to the minimum of the potential function $U(\theta)$. The derivative of the Lyapunov function can be written by:

$$\dot{V}(\boldsymbol{r}, \theta) = \kappa\dot{S}(\boldsymbol{r}, \theta) + \nabla U(\theta) = \sum_{k=1}^{N}\left(\kappa\omega_0\tilde{\boldsymbol{r}}_k^T\dot{\boldsymbol{r}}_k - \frac{\partial U}{\partial\theta_k}\right)(\omega_0 - u_k)$$

and thanks to control law (2.30) then $\dot{V}(\boldsymbol{r}, \theta) \leq 0$.

By the LaSalle Invariance principle, solutions for the reduced system on shape space converge to the largest invariant set Λ where

$$\omega_0\tilde{\boldsymbol{r}}_k^T\dot{\boldsymbol{r}}_k - \frac{\partial U}{\partial\theta_k} \equiv 0$$

for all $k = 1, \ldots, N$, and the conclusion is that solutions converge to an (M, N)-pattern circular equilibrium. It means that the agents converge to a circular motion centered at the center of mass $\boldsymbol{c}_0$ and with radius $1/|\omega_0|$. Moreover, the (M, N)-pattern is exponentially stable.

□

This result is extended to the limited communication case in [116, 150]. In order to isolate symmetric patterns of curve-phases, the authors restrict the interconnection topology to d_0-circulant graphs, see [41] and Appendix A. All d_0-circulant graphs

are d_0-regular, which means that $d_k = d_0$ for all k. Both adjacency and Laplacian matrices of a circulant graph are circulant, *i.e.*, they are completely defined by their first row. Each subsequent row of a circulant matrix is the previous row shifted one position to the right with the first element equal to the last element of the previous row. For example, the complete graph (all-to-all communication) is $(N-1)$-circulant and the cyclic graph (ring topology) is 2-circulant. For instance, the Laplacian matrix corresponding to a ring topology of a fleet of $N = 5$ agents is defined as:

$$\mathbf{L} = \begin{pmatrix} 2 & -1 & 0 & 0 & -1 \\ -1 & 2 & -1 & 0 & 0 \\ 0 & -1 & 2 & -1 & 0 \\ 0 & 0 & -1 & 2 & -1 \\ -1 & 0 & 0 & -1 & 2 \end{pmatrix}$$

The function $U(\theta)$ takes into account the communication constraints through the Laplacian matrix of the communication graph of the multi-agent system. Based on previous analysis for the all-to-all communication assumption, the previous potential function is generalized to arbitrary connected topologies:

$$U(\theta) = \frac{K}{N} \sum_{m=1}^{\lfloor N/2 \rfloor} \frac{\mathbf{B}_m \bar{\mathbf{L}} \mathbf{B}_m}{2m^2}$$

The splay state corresponding to the uniform distribution, is locally asymptotically stable for d_0-circulant graphs. An extensive analysis is detailed in [116] and [150].

Our objective is to apply this methodology to the previous translation and scaling control laws. In the sequel, two improved circular control laws to stabilize the agents to a uniform distributed circular formation tracking a time-varying center and a time-varying radius respectively will be presented. The splay state control laws are studied in the case of fixed communication topology and a new contribution for limited communication range is presented.

2.5.2 Fixed communication graphs

A fixed communication topology of a sensor network or a group of vehicles is represented by a time-invariant communication graph $\mathcal{G}$. The constant Laplacian matrix of $\mathcal{G}$ describes the communication links between agents. In this case, previous splay state formation control law can be easily applied to the translation and scaling problems.

In order to apply previous cooperative approaches to our two contributions, the potential $U(\theta)$ becomes a function depending on the transformed heading angle $\psi = (\psi_1, \ldots, \psi_N)^T$. In a fixed circular formation centered at the origin, the distribution of the position vectors $\mathbf{r}_k$ is equivalent to the distribution of the velocity vectors $\dot{\mathbf{r}}_k$ because

when the vehicles are in the circle the equation $\dot{\mathbf{r}}_k^T \mathbf{r}_k = 0$ is satisfied. This is means that the angle corresponding to the position vectors is equal to $\theta_k + \frac{\pi}{2}$. In the case of a time-varying circle, the transformed system is stabilized to a fixed circle, therefore the transformed position vectors $\hat{\mathbf{r}}_k$ are perpendicular to their velocity vectors. Hence, our objective is to achieve the uniform distribution of the *virtual* agents defined by the respective transformed systems (2.9) and (2.20) along a fixed circle using a potential function $U(\psi)$.

In this situation, the Laplacian matrix considered now is $\bar{\mathbf{L}} = \mathbf{L} \otimes \mathbf{I}_2$ where $\otimes$ is the classical Kronecker product and $\mathbf{I}_N \in \mathbb{R}^{N\times N}$ is the identity matrix. Let $b_{mk} = (\cos m\psi_k, \sin m\psi_k)^T$ be the vector which contains the orientation angle of the virtual agents and $\mathbf{B}_m = (b_{m1}^T, \ldots, b_{mN}^T)^T$ contains all the heading angles of the transformed system.

Translation control: Considering the previous notation and applying the splay state potential function mentioned before to our new formulation, the following corollary holds:

Corollary 2.1 *(Extension of Briñón-Arranz et al. 2009 [16]) Consider a twice differentiable function $\boldsymbol{c}(t) : \mathbb{R} \to \mathbb{R}^2$, with bounded first and second time-derivatives and the radius of desired formation $R > 0$. Let the control parameters be such that $\omega_0 \neq 0$, $\kappa > 0$, $\beta > 0$ and the condition (2.17) is satisfied. Let $\mathcal{G}$ be a fixed d_0-circulant graph, and $\boldsymbol{L}$ be its corresponding Laplacian matrix. Then the control law (2.18) now with:*

$$\begin{cases} \hat{u}_k = \omega_0(1 + \kappa \dot{\hat{\boldsymbol{r}}}_k^T \hat{\boldsymbol{r}}_k) - \frac{\partial U}{\partial \psi_k} \\ U(\psi) = \frac{K}{N} \sum_{m=1}^{\lfloor N/2 \rfloor} \frac{1}{2m^2} \boldsymbol{B}_m \bar{\boldsymbol{L}} \boldsymbol{B}_m \end{cases} \tag{2.32}$$

makes all the agents defined by (2.1) converge to a circular motion of radius R and of center the time-varying reference $\boldsymbol{c}(t)$. Moreover the splay state is a critical point of $U(\psi)$. For $K > 0$, the set of curve-phase arrangements that are synchronized modulo $2\pi/N$ is locally exponentially stable.

Proof 2.8 *Based on Theorem 2.7, the stability of the motion is analyzed by the composed Lyapunov function*

$$V(\hat{\boldsymbol{r}}, \psi) = \kappa S(\hat{\boldsymbol{r}}, \psi) + U(\psi)$$

where $S(\hat{\boldsymbol{r}}, \psi)$ is defined in (2.10). The time derivative of this function along the solutions of (2.9) is given by $\dot{V}(\hat{\boldsymbol{r}}, \psi) = \kappa \dot{S}(\hat{\boldsymbol{r}}, \psi) + \nabla U(\psi)$. The potential $U(\psi)$ is invariant to rigid rotation, thus $\sum_{k=1}^{N} \frac{\partial U}{\partial \psi_k} = 0$ and by definition

$$\nabla U(\psi) = \sum_{k=1}^{N} \frac{\partial U}{\partial \psi_k} \dot{\psi}_k$$

Then, the derivative of the composed Lyapunov function is rewritten as:

$$\begin{aligned}\dot{V}(\hat{\boldsymbol{r}},\psi) &= \kappa\sum_{k=1}^{N}\left(\omega_0\hat{\boldsymbol{r}}_k^T\dot{\hat{\boldsymbol{r}}}_k\right)(\omega_0-\hat{u}_k)+\sum_{k=1}^{N}\frac{\partial U}{\partial\psi_k}\hat{u}_k\\ &= \sum_{k=1}^{N}\left(\kappa\omega_0\hat{\boldsymbol{r}}_k^T\dot{\hat{\boldsymbol{r}}}_k-\frac{\partial U}{\partial\psi_k}\right)(\omega_0-\hat{u}_k)\end{aligned}$$

According to the control law (2.32) *the following inequality holds:*

$$\dot{V}(\hat{\boldsymbol{r}},\psi)=-\sum_{k=1}^{N}\left(\kappa\omega_0\hat{\boldsymbol{r}}_k^T\dot{\hat{\boldsymbol{r}}}_k-\frac{\partial U}{\partial\psi_k}\right)^2\leq 0$$

Therefore, solutions converge to the largest invariant set, Λ*, for which* $\dot{V}=0$*. The details of the proof can be found in [150].*

□

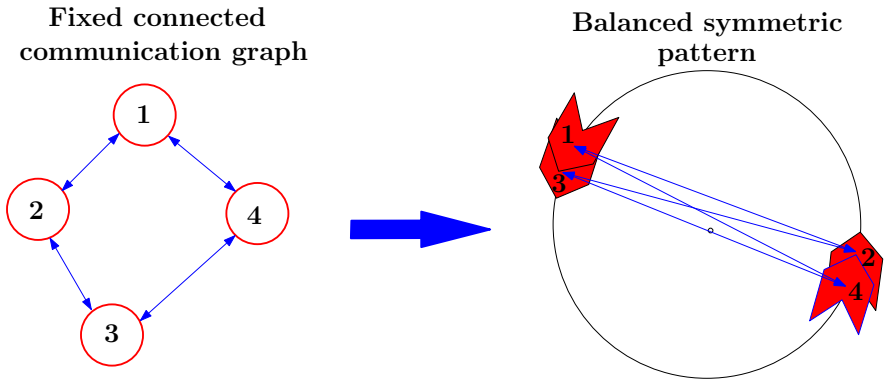

Figure 2.14: *An equilibrium configuration, balanced symmetric pattern, for a fixed connected communication graph in the case of even number of agents.*

Remark 2.7 *Corollary 2.1 does not exclude convergence to formations which corresponds to other critical points of* $U(\psi)$ *[150]. For instance, when the fleet has a even number of vehicles, the system could be stabilized to another critical point of the potential function corresponding to a different* (M,N)*-pattern to the splay state (uniform distribution) as is shown in Figure 2.14. This is due to the local stability of the splay state in the case of fixed communication graph.*

Remark 2.8 *If the graph* $\mathcal{G}$ *is complete (all-to-all communication), then the set of curve-phase arrangements that are balanced modulo* $2\pi/N$ *is a global maximum of* $U(\psi)$ *in the reduced space of relative curve-phases; this is asymptotically stable for* $K>0$*. Moreover if* $K<0$ *the control law of Corollary 2.1 forces convergence to the synchronized circular formation [149].*

Scaling control: Following the same reasoning, we can add the potential function whose critical point correspond to the splay state, to the scaling control law to achieve the uniform distribution of the vehicles along a circle with time-varying radius. Based on Theorem 2.6, and applying previous results on uniform distribution the following corollary holds:

Corollary 2.2 *(Extension of Briñón-Arranz et al. 2010 [17]) Consider a twice differentiable function $R(t) : \mathbb{R} \to \mathbb{R}^+$, with bounded first and second time-derivatives. Let the control parameters be such that $\omega_0 \neq 0$, $\kappa > 0$, $\beta > 0$, and assuming the condition* (2.27) *is satisfied. Let $\mathcal{G}$ be a fixed d_0-circulant graph, and $\boldsymbol{L}$ be its corresponding Laplacian matrix. Then the control law* (2.28) *now with:*

$$\begin{cases} \hat{u}_k = \omega_0 \left(1 + \kappa \dot{\hat{\boldsymbol{r}}}_k^T \hat{\boldsymbol{r}}_k\right) - \frac{\partial U}{\partial \psi_k} \\ U(\psi) = \frac{K}{N} \sum_{m=1}^{\lfloor N/2 \rfloor} \frac{1}{2m^2} \boldsymbol{B}_m \bar{\boldsymbol{L}} \boldsymbol{B}_m \end{cases} \tag{2.33}$$

makes all the agents defined by (2.1) *converge to a circular motion of center $\boldsymbol{c}$ and the time-varying radius $R(t)$. Moreover, for $K > 0$, the set of curve-phase arrangements that are balanced modulo $2\pi/N$ is locally exponentially stable.*

The proof is similar that in Corollary 2.1.

2.5.3 Limited communication range

Applying the method from [149, 150] to distribute the agents along the circular formation to both present translation and scaling control laws is straightforward, as shown in the previous subsection for the case of fixed communication graph. Nevertheless, the splay state corresponding to the uniform distribution, is only locally stable, then, others configurations could be stabilized depending on the initial conditions of the system as shown in Figure 2.14. The authors of [116] conclude that the simulations suggest a large region of attraction for each (M, N)-formation for the complete graph but not necessarily for d_0-circulant graphs with $d_0 < N-1$. To demonstrate convergence of the closed-loop system with limited communication, they have selected initial conditions near the desired (M, N)-formation.

Moreover in practice, considering fixed communication graphs is not realistic because the distance between two linked agents is not considered, [111, 109, 130]. In the case of underwater communication, the quality of the link is strongly affected by the distance between two agents [155]. Therefore, in an underwater scenario, it might be more interesting to consider distance-dependent communication graphs. This means that each agent can only receive information from its closed neighbors.

Moreover, in the context of the project CONNECT the multiple access channel technique called OFDMA (Orthogonal Frequency Division Multiplex Access) is applied

in order to reduce the latency induced by TDMA (Time Division Multiplex Access) based protocols, as it has been explained in Chapter 1. Using this protocol the quality of the transmitted signal decay with the distance.

In this situation, a communication area for each vehicle is introduce in our approach. The communication area for any agent is defined by ρ which is the critical communication distance given by the characteristics of the communication devices and the environment of the AUVs. Then, the radius ρ demarcates a circular communication region for each vehicle. For simplicity, it is assumed to be the same radius ρ for all AUVs. This assumption is consistent whit the real modems installed in the IFREMER's AUV AsterX. However, we assume that there is a perfect communication inside this region. Time-delays, packet loss, damping effect and noise are not considered in our approach.

Assuming bidirectional communication, the condition to get a communication link between vehicle k and vehicle j is expressed as:

$$k \in \mathcal{N}_j \quad \Longleftrightarrow \quad j \in \mathcal{N}_k \quad \Longleftrightarrow \quad \|\mathbf{r}_k - \mathbf{r}_j\| \leq \rho$$

The distance-dependent communication graph is now time-varying because the position of vehicles is changing in time. Based on graph theory, the time-varying Laplacian matrix $\mathbf{L}(t)$ corresponding to a distance-dependent communication graph is defined as follows:

$$L_{k,j} = \begin{cases} d_k, & \text{if} \quad k = j \\ -1, & \text{if} \quad \|\mathbf{r}_k - \mathbf{r}_j\| \leq \rho \\ 0 & \text{otherwise} \end{cases} \tag{2.34}$$

The above graph is also called *proximity graph* in the literature [36, 73].

Note that, for simplicity, in the simulation figures, the communication region defined by the critical radius ρ is designed as a circle of radius $\rho/2$ to ameliorate the visualization, as in Figure 2.15 for example.

Translation control: The splay state formation control law does not change with respect to the fixed communication assumption. Nevertheless, a new condition is imposed to assure almost a d_0-circular graph, see Appendix A. It corresponds to a geometrical condition which relates the critical communication distance ρ to the radius of the circular formation R and the number of agents N, as show in Figure 2.15.

The cooperative translation control for the distance-dependent communication assumption is presented in the following corollary:

Corollary 2.3 *(Extension of Briñón-Arranz et al. 2009 [16]) Consider a twice differentiable function $\mathbf{c}(t) : \mathbb{R} \to \mathbb{R}^2$, with bounded first and second time-derivatives and the radius of desired formation $R > 0$. Let the control parameters be such that $\omega_0 \neq 0$,*

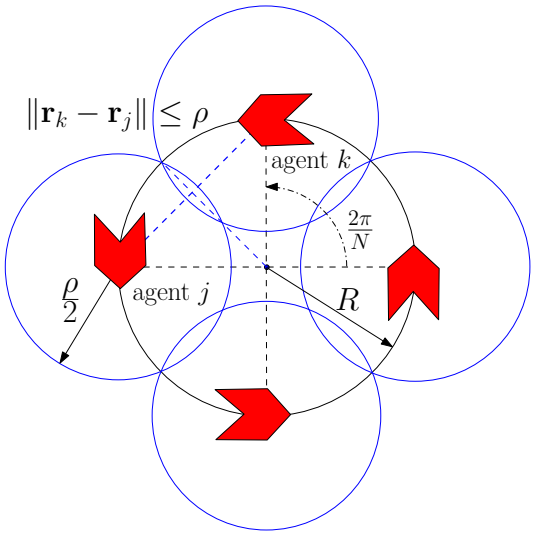

Figure 2.15: *Geometrical condition to assure a circular communication graph for a group of agents in a circular formation with communication radius ρ.*

$\kappa > 0$, $\beta > 0$, and the condition (2.17) *is satisfied. Let $\mathcal{G}(t)$ be the communication graph, $\boldsymbol{L}(t)$ be its corresponding Laplacian matrix and the critical communication distance ρ satisfies:*

$$\rho > 2R \sin \frac{\pi}{N} \tag{2.35}$$

Then the control law (2.18) *with* (2.32)*, makes all the agents defined by* (2.1) *converge to a circular motion of radius R and of center the time-varying reference $\mathbf{c}(t)$. Moreover, for $K > 0$, the splay state is the only critical point of $U(\psi)$ exponentially stable.*

Proof 2.9 *The stability of the uniformly distributed circular formation is analyzed by the composed Lyapunov function*

$$V(\hat{\boldsymbol{r}}, \psi) = \kappa S(\hat{\boldsymbol{r}}, \psi) + U(\psi)$$

whose derivative satisfies $\dot{V}(\hat{\boldsymbol{r}}, \psi) \leq 0$. Thanks to Theorem 2.4, the control law (2.18) *makes all the agents reach the circle whit radius R and centered at $\mathbf{c}(t)$. Then, consider the potential function [150]:*

$$U(\psi) = \frac{K}{N} \sum_{m=1}^{[N/2]} \frac{1}{2m^2} \sum_{k=1}^{N} U_m^k(\psi)$$

where $U_m^k(\psi)$ is be expressed as:

$$U_m^k(\psi) = d_k - \sum_{j=1, j\neq k}^{N} L_{k,j}(t) \cos m\psi_{kj}$$

where $\psi_{kj} = \psi_k - \psi_j$ *denotes the relative angle between agents* k *and* j*. Note that* $\sum_{k=1}^{N} U_m^k = \boldsymbol{B}_m \bar{\boldsymbol{L}} \boldsymbol{B}_m$*. The objective of the collaborative control is to minimize the function* $U(\psi)$*, or equivalently to maximize the functions* $U_m^k(\psi)$ *to achieve the uniform distribution. Without loss of generality, consider agent* k*.* $U_m^k(\psi)$ *represents the potential functions associated to agent* k*. The maximum of these functions is obtained when the relative angles between agent* k *and its neighbors is* π/m*. This means that the angle between agent* k *and its neighbors will tend to* π/m*. This works for all* m *and this finally leads to an increase of the angles between connected agents until the communication between them is lost. As shown in Figure 2.16, the geometry of the problem ensures that the connection between agent* k *and a neighbor* j *is lost when:*

$$R \sin \frac{\psi_{kj}}{2} = \frac{\rho}{2}$$

where $\psi_{kj} = (\psi_k + \frac{\pi}{2}) - (\psi_j + \frac{\pi}{2})$ *On the other side,* $U_m^k(\psi)$ *is discontinuous because of the definition of the Laplacian matrix* $\boldsymbol{L}$*. Note that the communication with any agent, for instance* j*, leads to a contribution in the potential function of the following type:*

$$1 - cos\psi_{kj} \geq 0$$

Thus, if a communication link is broken, a positive contribution is removed. Therefore, the potential functions decrease discontinuously. Finally the agents are deployed along the circle. The condition (2.35) *ensures that this expansion guarantees that the agents are connected at least in* d_0*-circular graph.*

Applying Theorem 2.7, the fact that $\mathcal{G}$ *is a circular graph implies that the splay state,* (N, N)*-pattern, corresponding to the uniform distribution is locally asymptotically stable. No other local critical point is achieved because other critical points of the potential function require that a link between agents is broken and consequently an increase of the potential function. Therefore all the agents are uniformly distributed along the circle. Thanks to change of coordinates* (2.9)*, the dynamic closed-loop system corresponding to our approach (time-varying center) is time-invariant, hence LaSalle principle can be applied.*

□

Remark 2.9 *The set of curve-phase arrangements that are balanced modulo* $2\pi/N$ *(uniform distribution) is asymptotically stable for* $K > 0$*. Moreover if* $K < 0$ *the control law of Corollary 2.3 forces convergence to the synchronized circular formation [150].*

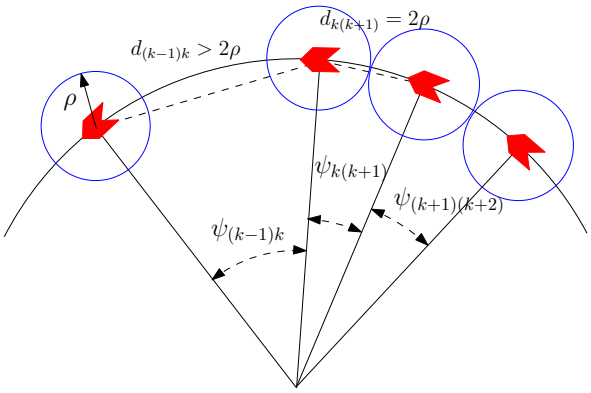

Figure 2.16: *Formation of communication chains during the contraction motion*

Scaling control: The previous analysis for the translation control problem can be applied directly to the scaling control law. In this case, the geometrical condition imposed to ρ is related to the maximum value of the reference which defines the radius. The following corollary summarize this result:

Corollary 2.4 *(Based on Briñón Arranz et al. 2010 [17]) Consider a twice differentiable function $R(t) : \mathbb{R} \to (0, R_{max}$, with bounded first and second time-derivatives. Let the control parameters be such that $\omega_0 \neq 0$, $\kappa > 0$, $\beta > 0$, and assuming the condition (2.27) is satisfied. Let $\mathcal{G}(t)$ be the communication graph, $\boldsymbol{L}(t)$ be the corresponding Laplacian matrix and the critical communication distance ρ satisfies:*

$$\rho > 2R_{max} \sin \frac{\pi}{N} \tag{2.36}$$

Then the control law (2.28) with (2.33) ensures that all agents reach the circular formation centered at $\boldsymbol{c}$ and whose radius tracks reference $R(t)$. Moreover, for $K > 0$ the uniform distribution of the agents along the circle is achieved.

The proof is similar that the previous one from Corollary 2.3.

2.5.4 Simulation results

In the sequel, several computing simulations are shown to validate the cooperative control laws improved in this section. We are interested to show the different capabilities of these control laws to achieve the uniform distribution of the agents along time-varying circular formations. The problem of fixed communication graph is applied only to the translation control (the same observations can be obtained with the scaling control law). The simulations highlight the local stability of the critical points of $U(\psi)$. A specially attention is addressed to the case of limited communication which is studied for the both translation and scaling control laws.

Fixed communication graph

The simulation shown in Figure 2.17, displays a fleet of six agents governed by the translation control law from Corollary 2.1. The controller parameters are $\omega_0 = \kappa = \beta = 1$, and $K = 0.1$, the radius of the desired circular formation is $R = 2$ and the reference of the center is given by

$$\mathbf{c}(t) = (0.2t, 3\sin(0.08t))^T$$

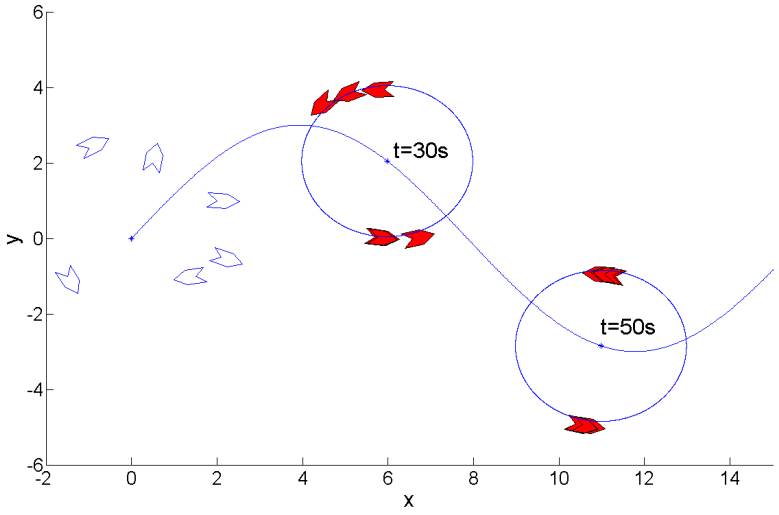

Figure 2.17: *Simulation of six agents governed by the control law from Corollary 2.1 with circular communication graph, tracking the reference of the center formation in blue. The figure displays three snapshots: the void blue agents correspond to the initial conditions and the red ones to two different instants, at $t = 30s$ and at $t = 50s$.*

The vehicles are stabilized to a time-varying circular formation. The cooperative term of the control law utilizes the transformed angles ψ_k transmitted taking into account the fixed circular communication graph. According to Corollary 2.1 in this simulation a 2-circulant graph (ring topology) is considered. Thanks to the connectivity properties of its Laplacian matrix, a critical point of the potential $U(\psi)$ is reached. Nevertheless, this equilibrium point corresponds to the $(2, 6)$-pattern and the desired splay state is not achieved.

Figure 2.18 shows the evolution in time of the control inputs v_k and u_k for all the agents, obtained from the same simulation. The oscillations of both variables are due to the time-varying reference of the center. The velocity v_k of the vehicles oscillates around the value of the tangent velocity magnitude $R|\omega_0| = 2$. The mean value of the input u_k is logically equal to the angular velocity $\omega_0 = 1$. The phases are balanced

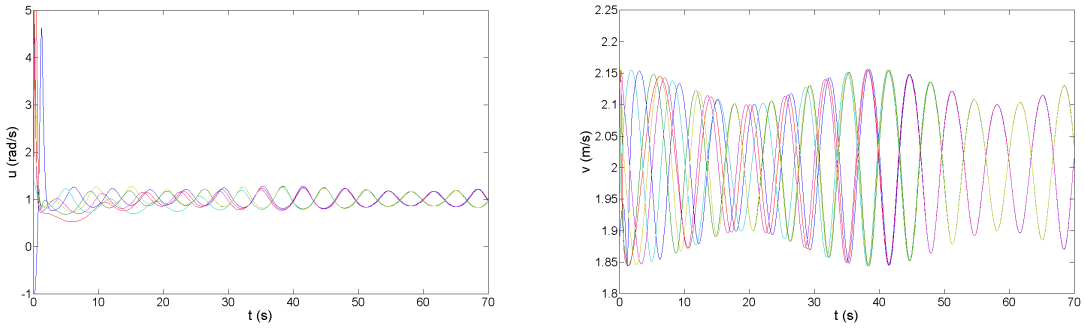

(a) Control inputs u_k (b) Control inputs v_k

Figure 2.18: *Evolution in time of the control inputs (a) u_k and (b) v_k corresponding to the previous simulation of six agents shown in Figure 2.17.*

modulo $\frac{2\pi}{2}$ then, there are two groups of three agents whose phases are synchronized as show in Figure 2.18 (a).

Limited communication graph

In this case, the communication graph considered is distance-dependent and its corresponding Laplacian matrix is defined by (2.34). The following simulations show the influence of the critical communication radius ρ according to conditions (2.35) and (2.36) respectively.

The simulation shown in Figure 2.19, displays a fleet of six agents governed by the translation control law from Corollary 2.3. The control parameters and the reference of the center $\mathbf{c}(t)$ are the same that in the previous simulation. The critical communication radius $\rho = 3$ satisfies condition (2.35). Therefore, the agents are uniformly distributed along the circle.

Figure 2.20 shows the evolution of the control inputs v_k and u_k for all the agents, obtained from this simulation. In this case, the phases are balanced modulo $\frac{2\pi}{6}$ because the stable splay state is reached.

In order to confirm the influence of the communication radius ρ to achieve the uniform distribution, Fig. 2.21 shows a simulation of five agents governed by the cooperative control law from Corollary 2.4. The control parameters are $\omega_0 = -1$, $\kappa = \beta = 1$, and $K = 0.1$ and the desired circular formation is centered at $\mathbf{c} = (1, 1)^T$. The reference of the radius is given by:

$$R(t) = \begin{cases} R_2 & \text{if} \quad t \leq 30 \\ R_2 - \frac{R_2 - R_1}{80-30}(t-30) & \text{if} \quad 30 < t \leq 80 \\ R_1 & \text{if} \quad t > 80 \end{cases}$$

where $R_2 = 7$ and $R_1 = 2$. The communication radius $\rho = 1.5$ satisfies the following

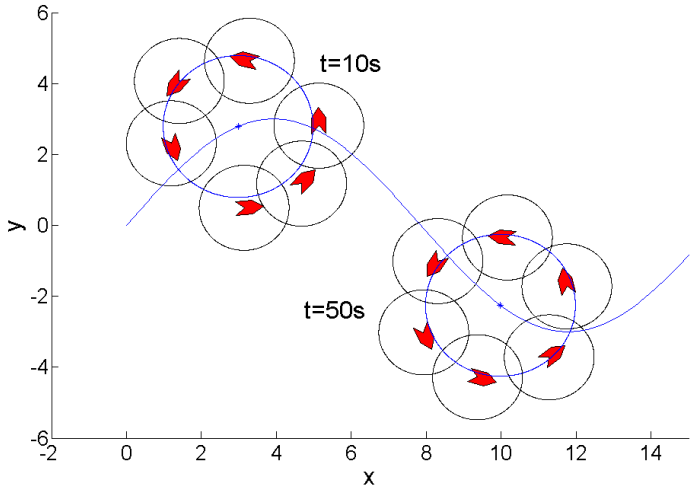

Figure 2.19: *Simulation of six agents governed by the control law from Corollary 2.3 tracking the reference of the center formation in blue. The black circles represent the communication region of the agents. The figure displays two snapshots corresponding to different instants, at $t = 10s$ the uniform distribution is not achieved yet and at $t = 50s$ the splay state formation is stabilized.*

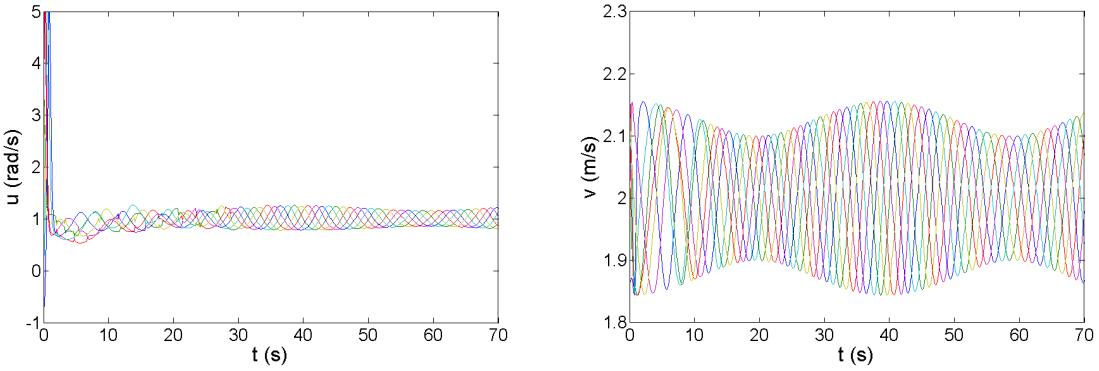

(a) Control inputs u_k (b) Control inputs v_k

Figure 2.20: *Evolution of the control inputs (a) u_k and (b) v_k corresponding to the previous simulation of six agents shown in Fig 2.19.*

inequalities:

$$2R_1 \sin\frac{\pi}{2} < \rho < 2R_2 \sin\frac{\pi}{2}$$

Therefore, according to condition (2.36), the simulation shows how the uniform distribution is not achieved whereas this condition is not satisfied.

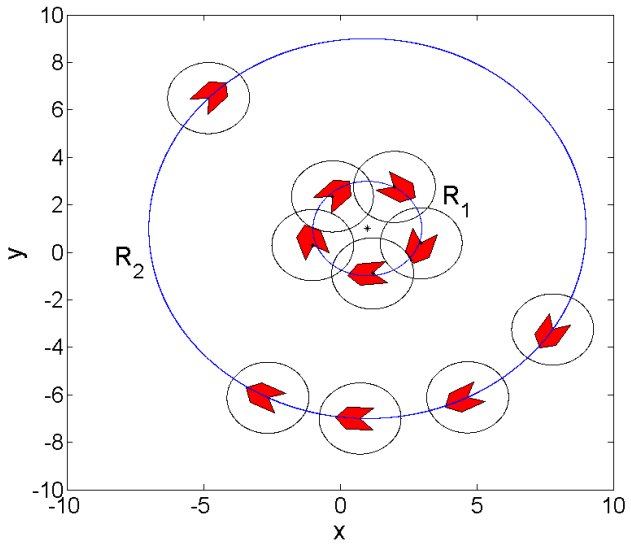

Figure 2.21: *Simulation of five agents governed by the control law from Corollary 2.4 which converge to a circular formation tracking a time-varying radius. The black circles represent the communication region of the agents. The figure displays two snapshots corresponding to different instants, at $t = 20s$ the uniform distribution is not achieved yet and at $t = 85s$ the splay state formation is stabilized.*

2.6 Conclusions

This chapter presents the first contributions of this thesis dealing with control of a fleet of non-holonomic agents in order to reach a time-varying circular formation. These contributions are the initial step to achieve the final objective which is to steer a fleet of AUVs to the location of an underwater source in a collaborative way. The control laws presented in this chapter, has been developed to move the center of a circular formation and to change its radius following a time-varying reference, respectively. In the next chapter, a method based on these previous contributions which allows considering a large class of formations, not only circular, will be presented.

In both cases, the functions which define the center and radius of the circular motion are given external references. Its first and second derivatives are know for all the vehicles in the fleet. The problems of delays, references corrupted by noise and packet loss are not considered here.

In order to achieve both objectives, translation and scaling, a control design based on a model matching approach is developed. The main idea is to transform the original system representing the group of vehicles to a transformed system which is time-invariant with respect to the reference (center or radius) which depends on time. This

new system is stabilized to a fixed circular motion. The transformed system is a reference now to the original one and a tracking process is followed to obtain the corresponding control inputs for the vehicles. This method allows us to stabilize the fleet of agents to time-varying circular motions defined only by few parameters, its center and its radius. Moreover, thanks to our control strategy, existing cooperative approaches can be applied directly to improve both time-varying circular motion control laws.

In addition, this Chapter 2 deals with collaborative control strategies in order to reach the uniformly distribution of the agents along the circular formation. A cooperative control term based on potential functions has been added to both translation and scaling control laws to achieve the uniform distribution. The communication constraints are considered using a communication graph. The notion of uniform distribution can be applied to another class of formations. This will constitute a contribution of following chapter. Moreover, it will be shown that the uniform distribution of the vehicles along a circular formation is decisive with a view to drive the fleet in a source-seeking scenario.

Chapter 3

Formation control design based on affine transformations

The previous chapter presents two contributions to the field of formation control: translation and scaling (contraction and expansion) of a circular formation. Even if these two items are fundamental for the final objective, the source-seeking problem, it might be interesting to not restrict the formation control law to circular formations. In order to express these previous contributions in a compact form and with a view to extend these results to more complex time-varying formations, a new framework based on affine transformations is introduced.

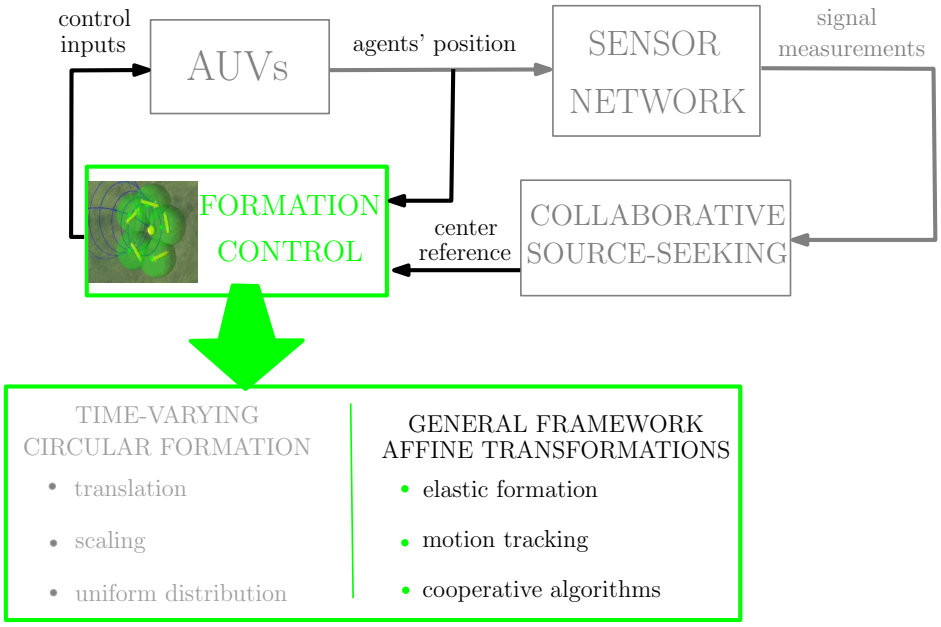

Figure 3.1: *Contributions of Chapter 3*

This chapter focuses on the design of a novel formation control law using a different approach. The objective is to generalize the previous control laws, employing affine transformations, as shown in Figure 3.1. In the sequel, a new general formation control law is developed to stabilize a group of vehicles to a richer class of formations, not only circular, and time varying formations. The shape of the formation is defined by a transformation matrix which is a given reference known to all the agents in the fleet. In addition, a cooperative control is provided to distribute the agents uniformly along the formation taking into account the communication constraints, as in previous chapter. Finally, distributed algorithms are designed to improve the general formation control law in the case that the reference of the formation center is unknown.

3.1 Problem statement

In this chapter, a large class of planar formations of autonomous agents in a 2-dimensional space are considered. As in previous Chapter 2, it is assumed that the agents have no physical extension, that is, that their positions are single points. Consider a group of N identical vehicles modeled with unicycle kinematics subject to a simple non-holonomic constraint. The dynamics of agents are defined by:

$$\dot{x}_k = v_k \cos\theta_k \tag{3.1a}$$

$$\dot{y}_k = v_k \sin\theta_k \tag{3.1b}$$

$$\dot{\theta}_k = u_k \tag{3.1c}$$

where $(x_k, y_k)^T \in \mathbb{R}^2$ is the position vector of each agent $k = 1, \ldots, N$, $\theta_k \in S^1$ is its heading angle and v_k, u_k are the control inputs.

The aim now is to design control strategies to make the group of AUVs represented by the system (3.1) converge to several classes of formations defined by a combination of affine transformations. A general transformation matrix, which is a combination of affine transformation matrices, will be defined in the next section. These matrices can be time-varying. The following assumptions are considered in the sequel to deal with this new contribution:

- Each vehicle $k = 1, \ldots, N$ knows its absolute vector position $(x_k, y_k)^T$ with respect to the inertial frame.
- The general matrix, which defines the desired motion, is known to all the vehicles.
- The communication topology of the fleet of vehicles is defined by an undirected graph $\mathcal{G}$.
- Communication problems such as, packet loss and time delays are not considered.

Under these assumptions, this chapter presents two control strategies dealing with the stabilization of the vehicles to an *elastic formation* and the *motion-tracking* control design. Both contributions which will be mathematically defined in the sequel, are developed using the same methodology based on affine transformations. In addition, several collaborative algorithms will be presented to improve both results. For instance, a cooperative control design will be introduced in order to distribute the vehicles in a particular desired pattern along the formation and another cooperative approach will allow the agents to reach the same formation following a reference velocity.

3.2 Definition of affine transformations

The affine transformations are used in the fields of Computer sciences and Robotics, [2, 70, 72, 107]. They are very useful to express in a simpler manner the coordinates of a manipulator robot [58] or to relate the local reference frame of a camera to an other system of coordinates, for instance. In general, an affine transformation is composed of linear transformations, such that rotation and scaling, and translations. Since a translation is an affine transformation but not a linear transformation, homogeneous coordinates are normally used to represent the translation operator by a matrix and thus, to make it linear.

Homogeneous coordinates are a system of coordinates used in projective geometry much as Cartesian coordinates are used in Euclidean geometry. They have the advantage that the coordinates of points, including points at infinity, can be represented using finite coordinates. Formulas involving homogeneous coordinates are often simpler and more symmetric than their Cartesian counterparts. Homogeneous coordinates have a range of applications, including computer graphics and 3-D computer vision, where they allow affine transformations and, in general, projective transformations to be easily represented by a matrix.

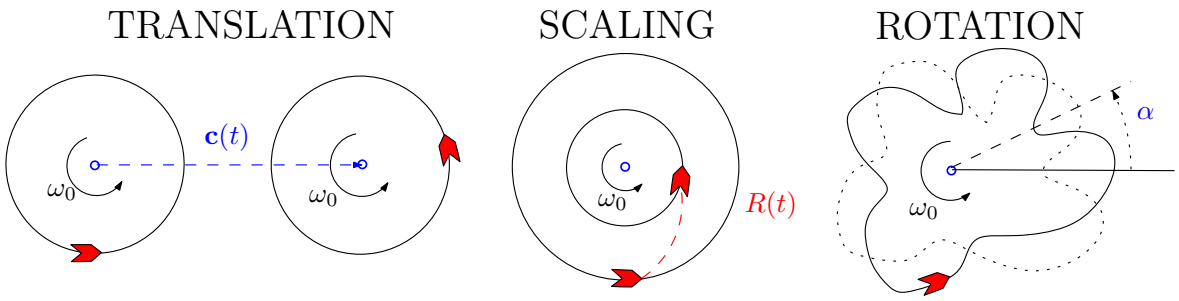

Figure 3.2: *Affine transformations applied to formations*

The three main affine transformations are translation, rotation and scaling. To ex-

press these transformations in a matrix way, the homogeneous coordinates are defined, see [56]. The homogeneous coordinates of a vector $\mathbf{z} = (z_x, z_y)^T \in \mathbb{R}^2$ can simply be defined as the new vector $\mathbf{z}^h = (z_x, z_y, 1)^T$. Let the vectors $e_1 = (1, 0, 0)^T$, $e_2 = (0, 1, 0)^T$, $e_3 = (0, 0, 1)^T$ be a canonic base of the space $\mathbb{R}^2$ expressed in homogeneous coordinates. In the sequel, the basic affine transformations and some of their properties are presented.

Translation: The translation in the plane $\mathcal{T}$ of a point $\mathbf{z}$ by a vector $\mathbf{c} = (c_x, c_y)^T$ corresponds to the following operation $\mathcal{T}(\mathbf{z}) = \mathbf{z} + \mathbf{c}$. This can be expressed in a matrix multiplication of the form $\mathbf{z}' = \mathbf{T}_c \mathbf{z}^h$ where

$$\mathbf{T}_c = \begin{pmatrix} 1 & 0 & c_x \\ 0 & 1 & c_y \\ 0 & 0 & 1 \end{pmatrix}$$

and $\mathbf{z}'$ is expressed in homogeneous coordinates. Its inverse exists and satisfies $\mathbf{T}_c^{-1} = \mathbf{T}_{-c}$. Note that $\mathbf{c}$ can be time-varying. The translation is pertinent to move the center of formations, see Figure 3.2.

Scaling: A non-uniform scaling expressed in homogeneous coordinates is a transformation such that $\mathbf{z}' = \mathbf{S}\mathbf{z}^h$ where

$$\mathbf{S} = \begin{pmatrix} s_x & 0 & 0 \\ 0 & s_y & 0 \\ 0 & 0 & 1 \end{pmatrix}$$

and $s_x > 0$, $s_y > 0$. Its inverse matrix contains the inverse of its elements. The parameters of the scaling can be time-varying. Some examples of scaling can even lead to ellipses or other closed curves, as shown in Figure 3.2.

Rotation: A rotation through an angle α counterclockwise around the origin can be written in a matrix form as previously, $\mathbf{z}' = \mathbf{R}_\alpha \mathbf{z}^h$, where

$$\mathbf{R}_\alpha = \begin{pmatrix} \cos\alpha & -\sin\alpha & 0 \\ \sin\alpha & \cos\alpha & 0 \\ 0 & 0 & 1 \end{pmatrix}$$

Its inverse exists and satisfies $\mathbf{R}_\alpha^{-1} = \mathbf{R}_\alpha^T = \mathbf{R}_{-\alpha}$. The angle α can be time-varying. A rotation applied to a formation, can change its orientation with respect to the frame origin, as shown in Figure 3.2.

3.3 Elastic formation control

For many applications it should be very appropriate to obtain formations with shapes different from a circle. A result dealing with formation control design to stabilize a group of agents to closed curves is presented in [119]. In this paper, the agents converge to the set of trajectories that orbit a single closed curve. In this approach, the authors require the curve to be convex with definite curvature.

The idea presented in this chapter is to obtain formations with arbitrary shape, not only circular, and/or time-varying, by deforming a circular formation. The resulting configurations belong to a richer class of formations, defined mathematically in the following subsection, and they are called *elastic formations*.

3.3.1 Definition of elastic formation

A circular formation in the plane can be defined by three basic parameters, its center, its radius and the angular velocity of rotation. In order to modify these parameters, the affine transformations are introduced. The objective now is to define a mathematical formulation of *elastic formations*. Considering the previous contributions, translation and scaling of a circle, the main idea is to deform the unit circle in order to obtain the desired *elastic formation*. In this context, the unit circle $\mathcal{C}_0$ is defined as a circumference centered at the origin of the frame and with unit radius.

A sequence of affine transformations, which are generated by a combination of the previous ones, is defined as follows:

$$\mathbf{G} = \prod_{i}^{I} \prod_{j}^{J} \prod_{k}^{K} \mathbf{S}_i \mathbf{R}_{\alpha_j} \mathbf{T}_{c_k} \tag{3.2}$$

where the subscripts denote the different transformations of the same type which are applied. Note that, is this case, the product of matrices is not commutative. For instance, the matrix $\mathbf{G} = \mathbf{S}_1\mathbf{S}_2\mathbf{R}_\alpha\mathbf{T}_c$ is a combination of one translation, one rotation and two different scaling. Note that the matrix multiplication is not commutative. However, the general transformation $\mathbf{G}$ considered here, is a sequence of the three affine transformations and the order defined in (3.2) can be changed, for instance, to $\mathbf{G} = \mathbf{R}_\alpha\mathbf{S}_1\mathbf{T}_c\mathbf{S}_2$, which defines another different elastic formation.

As it is shown in the previous section, the affine transformations are invertible, therefore the inverse matrix of the general transformation exists and is denoted by $\mathbf{G}^{-1}$. Thanks to previous definitions, $\mathbf{G}$ and $\mathbf{G}^{-1}$ are differentiable, if their parameters are differentiable. Note that the operators derivative and invertible are not commutative, therefore:

$$(\frac{d}{dt}\mathbf{G})^{-1} \neq \frac{d}{dt}(\mathbf{G}^{-1}) = \dot{\mathbf{G}}^{-1}$$

Each combination of affine transformations, expressed by a general matrix $\mathbf{G}$, define an elastic formation $\mathcal{F}$.

Definition 3.1 *An elastic formation $\mathcal{F}$ is a curve which results of applying a sequence of affine transformations $\boldsymbol{G}$ defined by (3.2), to the unit circle $\mathcal{C}_0$ such that:*

$$\mathcal{F} = \boldsymbol{G} \circ \mathcal{C}_0$$

This elastic formation can be time-varying if at least one element of the transformation matrices is time-varying. The final formation depends on the sequence used to define $\mathbf{G}$. The term elastic denote the capability of the formation to move and change its shape in order, for instance, to avoid an obstacle (see Figure 3.5), to achieve the source seeking problem, to delimit a polluted region, or to avoid unnecessary energy waste.

3.3.2 Coordinates transformation

Thanks to the general transformation matrix denoted by $\mathbf{G}$ previously presented, several elastic formations can be defined according to Definition 3.1. This transformation matrix allows us to relate the unit circle to a complex desired elastic formation transforming the reference frame, as shown in Figure 3.3.

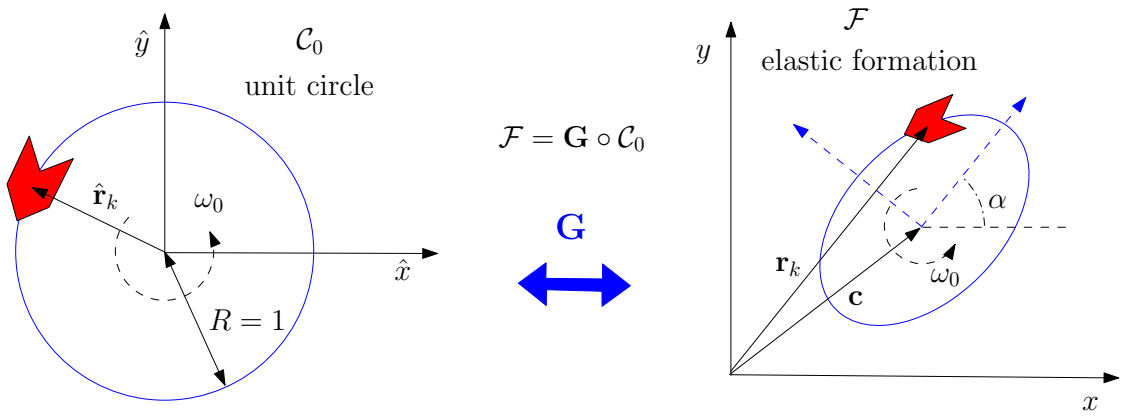

Figure 3.3: *General transformation of the unit circle to an elastic formation*

Consequently, the control strategy proposed here is composed by the following steps. First, the position vector of each vehicle is expressed in a transformed reference frame $(\hat{x}, \hat{y})$, according to the general transformation matrix $\mathbf{G}$. Then, the circular control law presented in Theorem 2.2 is applied to the new transformed system in order to stabilize the *virtual* agents to the unit circle. Finally, the control law expressed in the original frame (x, y) is calculated applying the inverse transformation and the vehicles

converge to the desired formation which is defined by matrix $\mathbf{G}$ applied to the unit circle, as shown in Figure 3.3.

A similar methodology has been used to reach arbitrarily shaped formations of mobile robots also in [138, 139]. The authors develop a distributed algorithm to stabilize a group of agents to a formation with arbitrary shape as result of deforming a regular polygon. In these papers, the agents are modeled by holonomic double integrator model. The objective of this chapter is to deal with this problem considering a non-holonomic kinematic model for the vehicles.

In the sequel, in order to apply the affine transformations, all the vectors are expressed in homogeneous coordinates. The position vector of the agent k in homogeneous coordinates is now defined as $\mathbf{r}_k = (x_k, y_k, 1)^T$. The first step is to express this position vector in the transformed reference frame. According to the definition of an elastic formation $\mathcal{F} = \mathbf{G} \circ \mathcal{C}_0$, the following coordinates transformation is introduced:

$$\hat{\mathbf{r}}_k = \mathbf{G}^{-1}\mathbf{r}_k \tag{3.3}$$

where $\hat{\mathbf{r}}_k = (\hat{x}_k, \hat{y}_k, 1)^T$ is the transformed position vector expressed in homogeneous coordinates.

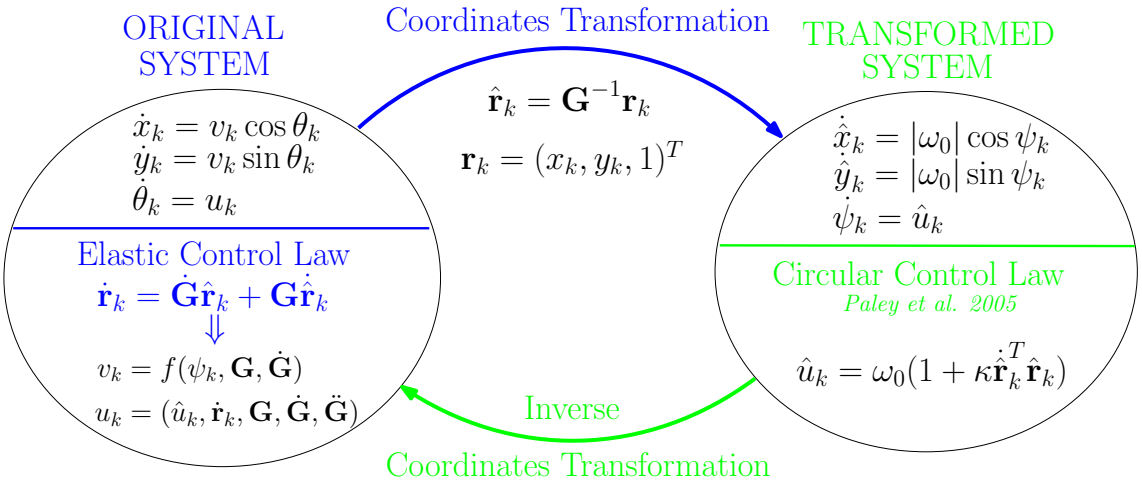

Figure 3.4: *Change of coordinates process*

Recalling the main idea, explained schematically in Figure 3.4, the objective is first, to stabilize the new transformed system to a circle with unit radius $R_0 = 1$, centered at the origin of the transformed reference frame and with angular velocity $\omega_0 \neq 0$. Then, the circular control law from [118] is applied to this transformed system. Finally, applying the inverse transformation, control laws are expressed in the original framework.

In order to implement the circular formation control law, the new transformed system must have constant linear velocity equal to $|\omega_0|$. The reasoning is the same that in the previous chapter for the translation and scaling of the circular formation. By definition, the linear velocity of a point in the fixed unit circle is $v = R_0|\omega_0|$. Therefore the dynamics of the transformed position vector are imposed as:

$$\dot{\hat{x}}_k = |\omega_0| \cos\psi_k \tag{3.4a}$$

$$\dot{\hat{y}}_k = |\omega_0| \sin\psi_k \tag{3.4b}$$

$$\dot{\psi}_k = \hat{u}_k \tag{3.4c}$$

where ψ_k represents the angular orientation of the transformed velocity vector $(\dot{\hat{x}}_k, \dot{\hat{y}}_k)^T$ and $\hat{u}_k$ denotes the control input.

3.3.3 Elastic motion control law

The problem now is to design a control law such that the fleet of AUVs converges to an elastic motion defined by a matrix transformation $\mathbf{G}$ which is a sequence of translation, scaling, and rotation matrices. The parameters of the desired motion are considered as given external references therefore, the matrix $\mathbf{G}$ is known to all the agents. The velocity of rotation of the agents around the motion center ω_0 is also a given parameter. In a first step, the control law presented in this chapter is not cooperative. Cooperative control laws to make converge the multi-agent system to an elastic *formation* will be presented in following subsections.

Following the main idea introduced previously, the first step to design a control law to stabilize the agents to an elastic motion is to control the transformed system such that it converges to the unit circle. Then, all previous analysis for both time-varying circular control laws from Chapter 2 are pertinent also in this case. The same Lyapunov function that in the translation and scaling problems, but expressed according with the new formulation based on homogeneous coordinates, can be written as:

$$S(\hat{\mathbf{r}}, \psi) = \frac{1}{2} \sum_{k=1}^{N} \left\| \dot{\hat{\mathbf{r}}}_k - \omega_0 \mathbf{R}^* \hat{\mathbf{r}}_k \right\|^2 \geq 0 \tag{3.5}$$

where the matrix $\mathbf{R}^* \in \mathbb{R}^{3\times3}$ represents a rotation matrix through an angle $\frac{\pi}{2}$ counter-clockwise around the origin (of the corresponding reference frame) denoted by $\mathbf{R}_{\frac{\pi}{2}}$ but the element which corresponds to the homogeneous coordinates becomes a zero, such that:

$$\mathbf{R}^* = \begin{pmatrix} 0 & -1 & 0 \\ 1 & 0 & 0 \\ 0 & 0 & 0 \end{pmatrix}$$

At the equilibrium of this Lyapunov function, when $S(\hat{\mathbf{r}}, \psi) = 0$, the dynamics of the transformed system (3.4) satisfy $\dot{\hat{\mathbf{r}}}_k = \omega_0 \mathbf{R}^* \hat{\mathbf{r}}_k$ which corresponds to the kinematic relation for the rotation of the rigid body. Its means that, the *virtual* transformed agents (*i.e.*, the position vectors expressed in the transformed frame) are turning around the origin of the transformed reference frame with rotation velocity equal to ω_0 at the equilibrium.

Evaluating the derivative of $S(\hat{\mathbf{r}}, \psi)$ along the solutions of the resulting closed-loop system (3.4) leads to:

$$\dot{S}(\hat{\mathbf{r}}, \psi) = \sum_{k=1}^{N} \left(\mathbf{R}_{\frac{\pi}{2}} \dot{\hat{\mathbf{r}}}_k \dot{\psi}_k - \omega_0 \mathbf{R}_{\frac{\pi}{2}} \dot{\hat{\mathbf{r}}}_k \right)^T \left(\dot{\hat{\mathbf{r}}}_k - \omega_0 \mathbf{R}^* \hat{\mathbf{r}}_k \right) = \sum_{k=1}^{N} \omega_0 \hat{\mathbf{r}}_k^T \dot{\hat{\mathbf{r}}}_k (\omega_0 - \hat{u}_k)$$

According to the circular control from [118] and the new control laws presented in both previous Theorems 2.4 and 2.6, we impose the closed-loop dynamics of the transformed system (3.4) by the following control law:

$$\hat{u}_k = \omega_0 (1 + \kappa \dot{\hat{\mathbf{r}}}_k^T \hat{\mathbf{r}}_k) \tag{3.6}$$

Replacing this expression in the derivative of the Lyapunov function the following inequality holds:

$$\dot{S}(\hat{\mathbf{r}}, \psi) = -\kappa \sum_{k=1}^{N} \left(\omega_0 \hat{\mathbf{r}}_k^T \dot{\hat{\mathbf{r}}}_k \right)^2 \leq 0 \tag{3.7}$$

Therefore $S(\hat{\mathbf{r}}, \psi)$ is a suitable Lyapunov function for this transformed system. Thus, the solutions converge to the largest invariant set Λ, for which $\dot{S} = 0$. Then, the transformed system (3.4) asymptotically converges to a circular motion centered at the origin of the transformed system of coordinates, with unit radius and with constant angular velocity ω_0. Thanks to the change of coordinates (3.3), the dynamic closed-loop equation corresponding to the transformed system is time-invariant in the transformed reference frame, hence LaSalle Principle can be applied. As stated above, this result is a generalization of circular motions, adapting the circular control law from [118] to a new framework.

Using the previous definitions of elastic formations and the general transformation matrix, a new general control law is proposed in the following theorem:

Theorem 3.1 *(Briñón-Arranz et al. 2011 [21]) Let $\boldsymbol{G}$ be a twice differentiable matrix function with bounded derivatives resulting of a sequence of affine transformations as defined in* (3.2) *and $\mathcal{F} = \boldsymbol{G} \circ \mathcal{C}_0$ be the desired elastic formation. Let $\omega_0 \neq 0$, $\kappa > 0$ be two control parameters such that the following condition is satisfied:*

$$|\omega_0| \neq \left\| \boldsymbol{G}^{-1} \dot{\boldsymbol{G}} \boldsymbol{G}^{-1} \boldsymbol{r}_k \right\| \tag{3.8}$$

Then the control law:

$$v_k = \left\| \dot{\boldsymbol{G}}\boldsymbol{G}^{-1}\boldsymbol{r}_k + |\omega_0|\,\boldsymbol{G}(\cos\psi_k, \sin\psi_k, 0)^T \right\| \tag{3.9a}$$

$$u_k = \frac{1}{v_k^2}\left(\ddot{\boldsymbol{G}}\boldsymbol{G}^{-1}\boldsymbol{r}_k + 2\dot{\boldsymbol{G}}\dot{\boldsymbol{G}}^{-1}\boldsymbol{r}_k + 2\dot{\boldsymbol{G}}\boldsymbol{G}^{-1}\dot{\boldsymbol{r}}_k\right)^T \boldsymbol{R}_{\frac{\pi}{2}}\dot{\boldsymbol{r}}_k + \frac{\dot{\psi}_k}{v_k^2}\left(\dot{\boldsymbol{G}}^{-1}\boldsymbol{r}_k + \boldsymbol{G}^{-1}\dot{\boldsymbol{r}}_k\right)^T \boldsymbol{R}_{\frac{\pi}{2}}^T\boldsymbol{G}^T\boldsymbol{R}_{\frac{\pi}{2}}\dot{\boldsymbol{r}}_k \tag{3.9b}$$

$$\dot{\psi}_k = \omega_0\left(1 + \kappa|\omega_0|(\cos\psi_k, \sin\psi_k, 0)\,\boldsymbol{G}^{-1}\boldsymbol{r}_k\right) \tag{3.9c}$$

with the inner state of the dynamic controller initialized as

$$\psi_k(0) = \arctan\frac{e_2^T\frac{d}{dt}(\boldsymbol{G}^{-1}\boldsymbol{r}_k)(0)}{e_1^T\frac{d}{dt}(\boldsymbol{G}^{-1}\boldsymbol{r}_k)(0)} + \epsilon\pi \tag{3.10}$$

where $\epsilon = 0$ if $e_1^T\frac{d}{dt}(\boldsymbol{G}^{-1}\boldsymbol{r}_k)(0) > 0$ and $\epsilon = 1$ otherwise, makes all the agents defined by (3.4) *converge to the elastic formation $\mathcal{F}$. The direction of rotation is determined by the sign of ω_0.*

Proof 3.1 *The proof of this theorem follows the same steps that in both cases of translation and scaling control laws. First, thanks to the previous Lyapunov function $S(\hat{\boldsymbol{r}}, \psi)$, the stability of the transformed system with the control law* (3.9c) *is proved. The Lyapunov function is positive definite and from* (3.5)*, is also nonincreasing along the solutions. Considering the change of coordinates* (3.3)*, the dynamic closed-loop equation corresponding to the transformed system is time-invariant to the transformed reference frame, hence LaSalle Principle can be applied again. Therefore, solutions for the reduced system on shape space converge to the largest invariant set Λ where*

$$\kappa\hat{\boldsymbol{r}}_k^T\dot{\hat{\boldsymbol{r}}}_k \equiv 0 \quad \forall k$$

In this set, $\dot{\psi}_k = \omega_0$, i.e.*, the transformed position vector describes circles of unit radius. The transformed system* (3.4) *is stabilized asymptotically to a circula motion with unit radius, whose center is the origin of the transformed reference frame and with fixed angular velocity ω_0.*

Applying the circular control law from [118] expressed in the transformed framework, the system (3.4) *converges to $\mathcal{C}_0$. Now the following step is to come back to the original framework to express the control inputs of the original system v_k, u_k with respect to the transformed control input $\dot{\psi}_k$. According to the change of coordinates* (3.3)*, differentiating the definition of $\hat{\boldsymbol{r}}_k$ gives*

$$\dot{\boldsymbol{r}}_k = \dot{\boldsymbol{G}}\hat{\boldsymbol{r}}_k + \boldsymbol{G}\dot{\hat{\boldsymbol{r}}}_k = \dot{\boldsymbol{G}}\boldsymbol{G}^{-1}\hat{\boldsymbol{r}}_k + \boldsymbol{G}\dot{\hat{\boldsymbol{r}}}_k$$

This equation provides both expressions of the control inputs. Expressing previous equation in terms of its components, gives:

$$\begin{aligned} v_k \cos\theta_k &= e_1^T(\boldsymbol{G}\dot{\hat{\boldsymbol{r}}}_k + \dot{\boldsymbol{G}}\hat{\boldsymbol{r}}_k) \\ v_k \sin\theta_k &= e_2^T(\boldsymbol{G}\dot{\hat{\boldsymbol{r}}}_k + \dot{\boldsymbol{G}}\hat{\boldsymbol{r}}_k) \end{aligned}$$

Therefore, the control input v_k is thus straightforwardly given by (3.9a)*. A more particular attention is addressed to $\dot{\theta}_k$. Using previous equations the following equality holds:*

$$\tan\theta_k = \frac{e_2^T(\boldsymbol{G}\dot{\hat{\boldsymbol{r}}}_k + \dot{\boldsymbol{G}}\hat{\boldsymbol{r}}_k)}{e_1^T(\boldsymbol{G}\dot{\hat{\boldsymbol{r}}}_k + \dot{\boldsymbol{G}}\hat{\boldsymbol{r}}_k)} \tag{3.11}$$

Differentiating and according with the change of coordinates, then, from $u_k = \dot{\theta}_k$, the control input u_k proposed in (3.9b) *is retrieved. In order to satisfy the relation* (3.11) *for all t, the initial conditions of the inner variable ψ_k must be imposed as a function of the initial values of θ_k. Therefore, since equation* (3.11) *is satisfied, following relation holds:*

$$\psi_k(0) = \arctan \frac{e_2^T \frac{d}{dt}(\boldsymbol{G}^{-1}\boldsymbol{r}_k)(0)}{e_1^T \frac{d}{dt}(\boldsymbol{G}^{-1}\boldsymbol{r}_k)(0)} + \epsilon\pi$$

where $\epsilon = 0$ if $e_1^T \frac{d}{dt}(\boldsymbol{G}^{-1}\boldsymbol{r}_k)(0) > 0$ and $\epsilon = 1$ otherwise.

Note that, this control law, as in the previous translation and scaling previous cases, has singular points when $v_k = 0$, such that:

$$v_k = \left\| \dot{\boldsymbol{G}}\boldsymbol{G}^{-1}\boldsymbol{r}_k + \omega_0 \boldsymbol{G}(\cos\psi_k, \sin\psi_k, 0)^T \right\| = 0$$

This singular point occurs if there exists a time t_c such that:

$$\begin{cases} \left\| \boldsymbol{G}^{-1}(t_c)\dot{\boldsymbol{G}}(t_c)\boldsymbol{G}^{-1}(t_c)\boldsymbol{r}_k(t_c) \right\| = |\omega_0| \\ \angle \boldsymbol{G}^{-1}(t_c)\dot{\boldsymbol{G}}(t_c)\boldsymbol{G}^{-1}(t_c)\boldsymbol{r}_k(t_c) = \psi_k(t_c) \end{cases}$$

where $\angle$ represents the argument of a vector. The equation (3.8) *is a sufficient condition to avoid the singular points.*

□

Remark 3.1 *Equation* (3.8) *is a condition imposed to the transformation matrix $\boldsymbol{G}$ to restrict the variation of its time-varying parameters with respect to the angular velocity ω_0. In the time-invariant case, such that matrix $\boldsymbol{G}$ is not time-varying, this condition becomes $|\omega_0| \neq 0$. In each particular case, condition* (3.8) *can be expressed in a simple manner, and correspond to an initialization protocol or a physical limitation.*

For instance, to avoid $v_k = 0$ in the case of a time-varying translation $\boldsymbol{G} = \boldsymbol{T}_{c(t)}$, the velocity of the moving center cannot be equal to the linear velocity of the agents in the circle, as it has been shown in Chapter 2. The condition (3.8) *becomes $R|\omega_0| \neq \|\dot{\boldsymbol{c}}\|$ where R is the radius of the circle and $\dot{\boldsymbol{c}}$ the velocity of its center.*

Theorem 3.1 presents a general control law expressed in the new framework, to stabilize a group of agents to an elastic formation. The matrix $\mathbf{G}$ is a given reference for all the agents. Note that each agent converges to the formation independently of the rest of the fleet.

3.3.4 Tracking strategy

The control law from Theorem 3.1 stabilize the vehicles to an elastic motion defined by the transformation matrix (3.2). Due to the methodology applied and the change of coordinates defined by (3.3) the inner variable ψ_k must be initialized as a function of the initial conditions of the heading angle θ_k. In consequence, the control law is not robust to uncertainties in $\theta_k(0)$.

Based on previous translation and scaling control design from Chapter 2, we use the same methodology in order to stabilize a fleet of agents modeled by (3.1) to an elastic motion with time-varying parameters. Following a tracking process, the transformed system defined by the change of coordinates (3.3) is considered as a reference to the original system (3.1). The dynamics of the reference system satisfy (3.4) and the closed-loop dynamics are imposed by the control law (3.6). In this situation, the following theorem presents another contribution of this chapter.

Theorem 3.2 *(Extension of Briñón-Arranz et al. 2011 [21]) Let $\boldsymbol{G}$ be a twice differentiable matrix function with bounded derivatives resulting of a sequence of affine transformations as defined in* (3.2) *and $\mathcal{F} = \boldsymbol{G} \circ \mathcal{C}_0$ be the desired elastic motion. Let $\omega_0 \neq 0$, $\kappa > 0$, $\beta > 0$ be three control parameters and the following condition is satisfied:*

$$v_k > 0 \quad \forall k = 1, \ldots, N \tag{3.12}$$

Then, for all initial conditions $\boldsymbol{r}(0), \theta(0)$, the control law:

$$\dot{v}_k = -\beta v_k + \frac{\hat{u}_k \dot{\boldsymbol{r}}_k^T \boldsymbol{G}\boldsymbol{R}_{\frac{\pi}{2}} \dot{\hat{\boldsymbol{r}}}_k + \dot{\boldsymbol{r}}_k^T \left(\ddot{\boldsymbol{G}}\boldsymbol{G}^{-1}\boldsymbol{r}_k + \beta \dot{\boldsymbol{G}}\boldsymbol{G}^{-1}\boldsymbol{r}_k + 2\dot{\boldsymbol{G}}\dot{\hat{\boldsymbol{r}}}_k + \beta \boldsymbol{G}\dot{\hat{\boldsymbol{r}}}_k) \right)}{v_k} \tag{3.13a}$$

$$u_k = \frac{\hat{u}_k \dot{\boldsymbol{r}}_k^T \boldsymbol{R}_{\frac{\pi}{2}}^T \boldsymbol{G}\boldsymbol{R}_{\frac{\pi}{2}} \dot{\hat{\boldsymbol{r}}}_k + \dot{\boldsymbol{r}}_k^T \boldsymbol{R}_{\frac{\pi}{2}}^T \left(\ddot{\boldsymbol{G}}\boldsymbol{G}^{-1}\boldsymbol{r}_k + \beta \dot{\boldsymbol{G}}\boldsymbol{G}^{-1}\boldsymbol{r}_k + 2\dot{\boldsymbol{G}}\dot{\hat{\boldsymbol{r}}}_k + \beta \boldsymbol{G}\dot{\hat{\boldsymbol{r}}}_k) \right)}{v_k^2} \tag{3.13b}$$

where $\dot{\hat{\boldsymbol{r}}}_k = (\dot{\hat{x}}_k, \dot{\hat{y}}_k, 1)^T$ and $\hat{u}_k$ are defined by (3.4) *and* (3.6) *respectively, makes all the agents defined by* (3.1) *converge to the elastic motion defined by $\mathcal{F}$. The direction of rotation is determined by the sign of ω_0.*

Proof 3.2 *The proof of this theorem follows the same steps that in both cases of translation and scaling control laws. First, thanks to the previous Lyapunov function $S(\hat{\boldsymbol{r}}, \psi)$,*

the stability of the transformed system with the control law (3.6) *is proved. The Lyapunov function is positive definite and from* (3.7)*, is also nonincreasing along the solutions. Considering the change of coordinates* (3.3)*, the dynamic closed-loop equation corresponding to the transformed system is time-invariant to the transformed reference frame, hence LaSalle Principle can be applied. Therefore, solutions for the reduced system on shape space converge to the largest invariant set* Λ *where*

$$\kappa \hat{\boldsymbol{r}}_k^T \dot{\hat{\boldsymbol{r}}}_k \equiv 0 \quad \forall k$$

In this set, $\hat{u}_k = \dot{\psi}_k = \omega_0$, i.e., *the transformed position vector describes circles of unit radius. The transformed system* (3.4) *is stabilized asymptotically to a circular motion with unit radius, whose center is the origin of the transformed reference frame and with fixed angular velocity* ω_0*. Applying the circular control law from [118] expressed in the transformed framework, the system* (3.4) *converges to* $\mathcal{C}_0$*.*

The objective now is to make converge the original system to the reference system (transformed system). The original system is related to the transformed system through the matrix $\boldsymbol{G}$*, i.e.:*

$$\dot{\boldsymbol{r}}_k \to \dot{\boldsymbol{G}}\hat{\boldsymbol{r}}_k + \boldsymbol{G}\dot{\hat{\boldsymbol{r}}}_k$$

In order to achieve this objective the tracking error is defined as follows:

$$\boldsymbol{e}_k = \dot{\boldsymbol{r}}_k - (\dot{\boldsymbol{G}}\hat{\boldsymbol{r}}_k + \boldsymbol{G}\dot{\hat{\boldsymbol{r}}}_k)$$

In order to make the error converge to zero, such that $\boldsymbol{e}_k \to 0$*, we wish to impose the error dynamics* $\dot{\boldsymbol{e}}_k = -\beta \boldsymbol{e}_k$*, where* $\beta > 0$*. Therefore, the error converge exponentially to zero. Thanks to previous definition of the error the following equation holds when* $t \to \infty$*:*

$$\dot{\boldsymbol{r}}_k = \dot{\boldsymbol{G}}\hat{\boldsymbol{r}}_k + \boldsymbol{G}\dot{\hat{\boldsymbol{r}}}_k \quad \forall k = 1, \ldots, N$$

The dynamics of the error equation determines the control law for the original system (3.1) *since:*

$$\begin{aligned}
\dot{\boldsymbol{e}}_k &= \ddot{\boldsymbol{r}}_k - \ddot{\boldsymbol{G}}\hat{\boldsymbol{r}}_k - 2\dot{\boldsymbol{G}}\dot{\hat{\boldsymbol{r}}}_k - \boldsymbol{G}\ddot{\hat{\boldsymbol{r}}}_k \\
-\beta(\dot{\boldsymbol{r}}_k - \dot{\boldsymbol{G}}\hat{\boldsymbol{r}}_k - \boldsymbol{G}\dot{\hat{\boldsymbol{r}}}_k) &= \frac{\dot{v}_k}{v_k}\dot{\boldsymbol{r}}_k + u_k \boldsymbol{R}_{\frac{\pi}{2}}\dot{\boldsymbol{r}}_k - \hat{u}_k \boldsymbol{G}\boldsymbol{R}_{\frac{\pi}{2}}\dot{\hat{\boldsymbol{r}}}_k - \ddot{\boldsymbol{G}}\hat{\boldsymbol{r}}_k - 2\dot{\boldsymbol{G}}\dot{\hat{\boldsymbol{r}}}_k \\
\frac{\dot{v}_k}{v_k}\dot{\boldsymbol{r}}_k + u_k \boldsymbol{R}_{\frac{\pi}{2}}\dot{\boldsymbol{r}}_k &= -\beta(\dot{\boldsymbol{r}}_k - \dot{\boldsymbol{G}}\hat{\boldsymbol{r}}_k - \boldsymbol{G}\dot{\hat{\boldsymbol{r}}}_k) + \hat{u}_k \boldsymbol{G}\boldsymbol{R}_{\frac{\pi}{2}}\dot{\hat{\boldsymbol{r}}}_k + \ddot{\boldsymbol{G}}\hat{\boldsymbol{r}}_k + 2\dot{\boldsymbol{G}}\dot{\hat{\boldsymbol{r}}}_k
\end{aligned}$$

Multiplying by the above equation by $\dot{\boldsymbol{r}}_k^T$ *and by* $\dot{\boldsymbol{r}}_k^T \boldsymbol{R}_{\frac{\pi}{2}}^T$ *both following expressions hold:*

$$\begin{aligned}
\dot{v}_k v_k &= -\beta v_k^2 + \beta \dot{\boldsymbol{r}}_k^T(\dot{\boldsymbol{G}}\hat{\boldsymbol{r}}_k + \boldsymbol{G}\dot{\hat{\boldsymbol{r}}}_k) + \hat{u}_k \dot{\boldsymbol{r}}_k^T \boldsymbol{G}\boldsymbol{R}_{\frac{\pi}{2}}\dot{\hat{\boldsymbol{r}}}_k + \dot{\boldsymbol{r}}_k^T \ddot{\boldsymbol{G}}\hat{\boldsymbol{r}}_k + 2\dot{\boldsymbol{r}}_k^T \dot{\boldsymbol{G}}\dot{\hat{\boldsymbol{r}}}_k \\
u_k v_k^2 &= \beta \dot{\boldsymbol{r}}_k^T \boldsymbol{R}_{\frac{\pi}{2}}^T(\dot{\boldsymbol{G}}\hat{\boldsymbol{r}}_k + \boldsymbol{G}\dot{\hat{\boldsymbol{r}}}_k) + \hat{u}_k \dot{\boldsymbol{r}}_k^T \boldsymbol{R}_{\frac{\pi}{2}}^T \boldsymbol{G}\boldsymbol{R}_{\frac{\pi}{2}}\dot{\hat{\boldsymbol{r}}}_k + \dot{\boldsymbol{r}}_k^T \boldsymbol{R}_{\frac{\pi}{2}}^T \ddot{\boldsymbol{G}}\hat{\boldsymbol{r}}_k + 2\dot{\boldsymbol{r}}_k^T \boldsymbol{R}_{\frac{\pi}{2}}^T \dot{\boldsymbol{G}}\dot{\hat{\boldsymbol{r}}}_k
\end{aligned}$$

By definition, this control law enforces exponential convergence of the tracking error dynamics away from the singularity $v_k = 0$. If condition (3.12) *is satisfied then, the control inputs of* (3.13) *are respectively obtained.*

Note that Theorem 3.2 presents a dynamic control law in which the control inputs are $(\dot{v}_k, u_k)$.

□

This result does not depend on the initial conditions of the reference system. Therefore, for any initial conditions of the original and reference system, $\theta_k(0)$ and $\psi_k(0)$ respectively, each vehicle k converges to an elastic motion defined by the transformation matrix $\mathbf{G}(t)$ applied to the unit circle.

Theorem 3.2 presents a general control law expressed in the a framework based on affine transformations, to stabilize a group of agents to an elastic motion. The matrix $\mathbf{G}$ is a given reference for all the agents. Note that each agent converges to the motion independently of the rest of the fleet. The following subsection presents a collaborative control to distribute the agents along a formation defined by $\mathbf{G}$.

3.3.5 Uniform distribution along elastic formations

This part is dedicated to the problem of homogenizing the distribution of the agents along elastic formations. The control law from Theorem 3.2 makes the fleet of agents converge to the same desired motion. Each agent converges independently to the same elastic motion, however the phase arrangement of the particles is arbitrary. The objective now is to stabilize the agents to an elastic *formation* in a cooperative way.

It is important to mention that, in the unit circle $\mathcal{C}_0$, the agents are uniformly distributed when the angular difference between adjacent vehicles is $2\pi/N$. The distribution of the agents along an elastic formation $\mathcal{F}$ depends on the transformation matrix $\mathbf{G}$ applied to $\mathcal{C}_0$.

Following the same cooperative control design presented in Chapter 2, a potential function $U(\psi)$ is included to reach this objective. Communication constraints are represented by means of the Lapalcian matrix of the associated communication graph $\mathcal{G}$. Recalling the matrix notation for the Laplacian matrix presented in previous Chapter 2 such that, $\bar{\mathbf{L}} = \mathbf{L} \otimes \mathbf{I}_2$ where $\otimes$ is the classical Kronecker product, and the matrix $\mathbf{B}_m = (\cos m\psi_1, \sin m\psi_1, ..., \cos m\psi_N, \sin m\psi_N)^T$ contains all the transformed heading angles.

Corollary 3.1 *(Extension of Briñón-Arranz et al. 2011 [21]) Let $\boldsymbol{G}$ be a twice differentiable matrix with bounded derivatives resulting of a sequence of affine transformations defined in* (3.2) *and $\mathcal{F} = \boldsymbol{G} \circ \mathcal{C}_0$ be the desired elastic formation. Let $\omega_0 \neq 0$,*

$\kappa > 0$,$\beta > 0$, and $K > 0$ be four control parameters and the condition (3.12) *be satisfied. Let $\mathcal{G}$ be the communication graph and $\boldsymbol{L}$ be its corresponding Laplacian matrix. Then the previous control law* (3.13) *with the closed-loop dynamics of the reference system imposed by:*

$$\begin{cases} \hat{u}_k = \omega_0 \left(1 + \kappa \dot{\hat{\boldsymbol{r}}}_k^T \hat{\boldsymbol{r}}_k\right) - \frac{\partial U}{\partial \psi_k} \\ U(\psi) = \frac{K}{N} \sum_{m=1}^{\lfloor N/2 \rfloor} \frac{1}{2m^2} \boldsymbol{B}_m^T \bar{\boldsymbol{L}} \boldsymbol{B}_m \end{cases} \tag{3.14}$$

where $\lfloor N/2 \rfloor$ is the largest integer less than or equal to $N/2$, makes all the agents defined by (3.1) *converge to the formation $\mathcal{F}$. The direction of rotation is determined by the sign of ω_0. Moreover, the splay pattern is an extremum point of the potential $U(\psi)$. If the communication graph is complete (all-to-all communication) the splay pattern is exponentially stable and the uniform distribution of the angles ψ_k along $\mathcal{C}_0$ is achieved. Therefore the agents are distributed in the formation $\mathcal{F}$, taking into account the transformation $\boldsymbol{G}$.*

Proof 3.3 *The proof is similar that in the previous Corollary 2.1. The stability is analyzed by the composed Lyapunov function $V(\hat{\boldsymbol{r}}, \psi) = \kappa S(\hat{\boldsymbol{r}}, \psi) + U(\psi)$ whose derivative is expressed as:*

$$\dot{V}(\hat{\boldsymbol{r}}, \psi) = \kappa \dot{S}(\hat{\boldsymbol{r}}, \psi) + \nabla U(\psi)$$

Based on the previous works [86, 150], the potential function $U(\psi)$ is invariant to rigid rotations. Therefore, using (3.14)*, the derivative of the Lyapunov function satisfies:*

$$\dot{V}(\hat{\boldsymbol{r}}, \psi) = -\sum_{k=1}^{N} \left(\kappa \omega_0 \hat{\boldsymbol{r}}_k^T \dot{\hat{\boldsymbol{r}}}_k - \frac{\partial U}{\partial \psi_k}\right)^2 \leq 0$$

If the communication graph is complete the splay state is the only critical point of $U(\psi)$ global exponentially stable. Therefore, thanks to LaSalle Principle, the system converges asymptotically to the elastic formation and the agents are distributed along $\mathcal{F}$ taking into account the transformation matrix $\boldsymbol{G}$.

□

Remark 3.2 *This result can be extended for the case of limited communication preserving the same formulation and considering the connectivity properties for the Laplacian matrix which correspond to several communication graphs [12, 111, 150].*

The cooperative control law (3.14) is an extension of the previous formation control law to get elastic formations. The splay pattern (uniform distribution) is an extremum of the potential function $U(\psi)$ which is added to the transformed control variable $\hat{u}_k$. The previous analysis provided in Chapter 2 in the case of limited communication rage can also be considered here. In this situation, a communication area ρ is introduced.

This means that each agent can only receive information from its close neighbors. However, the geometrical condition imposed to the critical communication radius ρ in order to guarantee the connectivity of the graph, introduced in Chapter 2, cannot be expressed with a simple equation for a general transformation matrix $\mathbf{G}$.

3.3.6 Particular cases and simulations

The elastic formation control law from Corollary 3.1 allows expressing a general control algorithm in a compact form in order to reach several kinds of formations. Afterwards, some particular examples of sequences of affine transformations are presented in order to clarify the previous Corollary 3.1. Firstly, it will be shown how the previous circular control laws can be obtained using this new formulation based on affine transformations. Then, another class of elastic formations are considered.

Fixed circular formation. The simplest case analyzed is when the transformation matrix is equal to the identity matrix $\mathbf{G} = \mathbf{I}_3$. In this case, the change of coordinates defined by (3.3) is equivalent to $\hat{\mathbf{r}}_k = \mathbf{r}_k$. Hence, the tracking objective can be expressed as follows:

$$\dot{\mathbf{r}}_k \to \dot{\hat{\mathbf{r}}}_k \quad \Longleftrightarrow \quad \dot{\mathbf{r}}_k \to \omega_0 \mathbf{R}^* \mathbf{r}_k$$

where the matrix $\mathbf{R}^* \in \mathbb{R}^{3\times 3}$ defined previously represents a rotation matrix through an angle $\frac{\pi}{2}$ but erasing the homogeneous coordinate. It corresponds to a circular motion centered at the origin of coordinates and with unit radius.

The general control law from Theorem 3.2 becomes:

$$\begin{aligned} \dot{v}_k =& -\beta v_k + \frac{\hat{u}_k \dot{\mathbf{r}}_k^T \mathbf{R}_{\frac{\pi}{2}} \dot{\hat{\mathbf{r}}}_k + \beta \dot{\mathbf{r}}_k^T \dot{\hat{\mathbf{r}}}_k}{v_k} \\ u_k =& \frac{\hat{u}_k \dot{\mathbf{r}}_k^T \dot{\hat{\mathbf{r}}}_k + \beta \dot{\mathbf{r}}_k^T \mathbf{R}_{\frac{\pi}{2}}^T \dot{\hat{\mathbf{r}}}_k}{v_k^2} \end{aligned}$$

This control law makes all the agents defined by (3.1) converge to the unit circle $\mathcal{C}_0$ which is centered at the origin of the reference frame and with unit radius.

In order to stabilize a fleet of vehicles to a circular formation with a desired radius $R > 0$ and centered at $\mathbf{c} = (c_x, c_y)^T$, the general transformation $\mathbf{G}$ is a sequence of a time-invariant translation and a time-invariant uniform scaling, *i.e.*, $s_x = s_y = R$, such that $\mathbf{G} = \mathbf{T}_c \mathbf{S}_R$. The change of coordinates defined by (3.3) is thus equivalent to

$$\hat{\mathbf{r}}_k = \mathbf{S}_{\frac{1}{R}} \mathbf{T}_{-c} \mathbf{r}_k = \frac{\mathbf{r}_k - \mathbf{c}^h}{R}$$

where $\mathbf{c}^h = (\mathbf{c}^T, 1)^T$ is the position vector of the center in homogeneous coordinates. Therefore, the tracking objective can be written such as:

$$\dot{\mathbf{r}}_k \to R\dot{\hat{\mathbf{r}}}_k \quad \Longleftrightarrow \quad \dot{\mathbf{r}}_k \to R\omega_0 \mathbf{R}_{\frac{\pi}{2}} \frac{\mathbf{r}_k - \mathbf{c}^h}{R}$$

This expression corresponds to a circular motion centered at $\mathbf{c}$ and with radius R. In this situation, the general control law is expressed as in previous particular case.

Previous works already cited [86, 149, 150] deal with the control problem of a fixed circular formation. As shown in Theorem 2.1, their approach is cooperative, such that the center of the final circular formation is not a given parameter for the controller but the result of a consensus algorithm. The final radius is equal to $1/|\omega_0|$. The control law presented previously for a fixed circular formation stabilize the agents to a fixed circular formation with desired and given center and radius. This is the first step to achieve the time-varying circular control.

Translation of a circular motion. The transformation matrix representing a translation of a circular formation corresponds logically to a time-varying translation matrix, such that $\mathbf{G}(t) = \mathbf{T}_{c(t)}$ where $\mathbf{c}(t) \in \mathbb{R}^2$ is the time-varying trajectory reference of the center of the circle. The relation between the transformed system and the original system defined by (3.3) becomes

$$\hat{\mathbf{r}}_k = \mathbf{T}_{-c(t)}\mathbf{r}_k = \mathbf{r}_k - \mathbf{c}^h(t)$$

In this case, the tracking objective is expressed by:

$$\dot{\mathbf{r}}_k \to \dot{\hat{\mathbf{r}}}_k + \dot{\mathbf{c}}^h \quad \Longleftrightarrow \quad \dot{\mathbf{r}}_k \to \omega_0 \mathbf{R}^*(\mathbf{r}_k - \mathbf{c}^h) + \dot{\mathbf{c}}^h$$

This expression represents the combined motion of a rotation and a translation, *i.e.*, a circular motion with time-varying center.

The elastic formation control law (3.13) becomes:

$$\dot{v}_k = -\beta v_k + \frac{\hat{u}_k \dot{\mathbf{r}}_k^T \mathbf{R}_{\frac{\pi}{2}} \dot{\hat{\mathbf{r}}}_k + \dot{\mathbf{r}}_k^T (\ddot{\mathbf{c}} + \beta(\dot{\hat{\mathbf{r}}}_k + \dot{\mathbf{c}}))}{v_k} \tag{3.16a}$$

$$u_k = \frac{\hat{u}_k \dot{\mathbf{r}}_k^T \dot{\hat{\mathbf{r}}}_k + \dot{\mathbf{r}}_k^T \mathbf{R}_{\frac{\pi}{2}}^T (\ddot{\mathbf{c}} + \beta(\dot{\hat{\mathbf{r}}}_k + \dot{\mathbf{c}}))}{v_k^2} \tag{3.16b}$$

where $\mathbf{c}^h$, $\dot{\mathbf{c}}^h$ and $\ddot{\mathbf{c}}^h$ are the references of the center and its first and second derivatives expressed in homogeneous coordinates respectively.

This is equivalent to the translation control law from Theorem 2.4 using the homogeneous coordinates. Note that, in this case, the agents are stabilized to a circular motion with unit radius.

Scaling of a circular motion. The second contribution dealing with time-varying circular formations presented in Chapter 2 is represented by a time-varying uniform scaling matrix, $\mathbf{G}(t) = \mathbf{S}_{R(t)}$, in which $s_x = s_y = R(t)$ where $R(t)$ is the desired reference of the radius. The change of coordinates defined by (3.3) is equivalent to

$$\hat{\mathbf{r}}_k = \mathbf{S}_{\frac{1}{R(t)}} \mathbf{r}_k = \frac{\mathbf{r}_k}{R(t)}$$

Therefore, the tracking objective can be written such as:

$$\dot{\mathbf{r}}_k \to \dot{R}\hat{\mathbf{r}}_k + R\dot{\hat{\mathbf{r}}}_k \quad \Longleftrightarrow \quad \dot{\mathbf{r}}_k \to \frac{\dot{R}}{R}\mathbf{r}_k + \omega_0 \mathbf{R}^* \mathbf{r}_k$$

This expression corresponds to a circular motion centered at the origin of the reference frame and the scaling term allows the circle to track the time-varying radius R.

The following control law obtained from (3.13) is equivalent to the scaling control law from Theorem 2.6 using the homogeneous coordinates:

$$\begin{aligned} \dot{v}_k =& -\beta v_k + \frac{\hat{u}_k R \dot{\mathbf{r}}_k^T \mathbf{R}_{\frac{\pi}{2}} \dot{\hat{\mathbf{r}}}_k + \frac{\ddot{R}+\beta\dot{R}}{R}\dot{\mathbf{r}}_k^T \mathbf{r}_k + (2\dot{R}+\beta R)\dot{\mathbf{r}}_k^T \hat{\mathbf{r}}_k}{v_k} \\ u_k =& \frac{\hat{u}_k R \dot{\mathbf{r}}_k^T \dot{\hat{\mathbf{r}}}_k + \frac{\ddot{R}+\beta\dot{R}}{R}\dot{\mathbf{r}}_k^T \mathbf{R}_{\frac{\pi}{2}}^T \mathbf{r}_k + (2\dot{R}+\beta R)\dot{\mathbf{r}}_k^T \mathbf{R}_{\frac{\pi}{2}}^T \dot{\hat{\mathbf{r}}}_k}{v_k^2} \end{aligned}$$

where R, $\dot{R}$ and $\ddot{R}$ are the reference of the radius and its first and second derivatives respectively.

This result is equivalent to the scaling control law from Theorem 2.6. Note that, in this case, the agents converge to a circular formation centered at the origin of the inertial frame.

Combined Motion of a circular motion. The new formulation presented in this chapter makes possible the combination of several transformations to define a complex time-varying motion in a more elegant manner. This is the case of the combined motion problem in which a circular formation with time-varying radius tracks a time-varying center. Consider the transformation $\mathbf{G}(t) = \mathbf{T}_{c(t)}\mathbf{S}_{R(t)}$ where the center of the desired formation $\mathbf{c}(t) : \mathbb{R} \to \mathbb{R}^2$ and its radius $R(t) : \mathbb{R} \to \mathbb{R}^+$ are twice differentiable functions with bounded first and second time-derivatives. Applying Corollary 3.1, the agents converge to a circular formation which follows the time-varying parameters of the transformation $\mathbf{G}(t)$. In this situation, the change of coordinates defined by (3.3) can be expressed by

$$\hat{\mathbf{r}}_k = \mathbf{S}_{\frac{1}{R(t)}}\mathbf{T}_{-c(t)}\mathbf{r}_k = \frac{\mathbf{r}_k - \mathbf{c}^h(t)}{R(t)}$$

Therefore, the tracking objective is equivalent to:

$$\dot{\mathbf{r}}_k \to \dot{R}\hat{\mathbf{r}}_k + R\dot{\hat{\mathbf{r}}}_k + \dot{\mathbf{c}}^h \quad \Longleftrightarrow \quad \dot{\mathbf{r}}_k \to \frac{\dot{R}}{R}(\mathbf{r}_k - \mathbf{c}^h) + \omega_0 \mathbf{R}^* \mathbf{r}_k + \dot{\mathbf{c}}^h$$

This expression represents the combined motion of a rotation, a translation and a scaling term, *i.e.*, a circular motion with time-varying radius tracking a time-varying center.

The following combined motion control law is obtained from (3.13):

$$\dot{v}_k = -\beta v_k + \frac{\hat{u}_k R \dot{\mathbf{r}}_k^T \mathbf{R}_{\frac{\pi}{2}} \dot{\hat{\mathbf{r}}}_k + \frac{\ddot{R}+\beta\dot{R}}{R} \dot{\mathbf{r}}_k^T \mathbf{r}_k + (2\dot{R}+\beta R)\dot{\mathbf{r}}_k^T \dot{\hat{\mathbf{r}}}_k + \dot{\mathbf{r}}_k^T(\ddot{\mathbf{c}}+\beta\dot{\mathbf{c}})}{v_k}$$

$$u_k = \frac{\hat{u}_k R \dot{\mathbf{r}}_k^T \dot{\hat{\mathbf{r}}}_k + \frac{\ddot{R}+\beta\dot{R}}{R} \dot{\mathbf{r}}_k^T \mathbf{R}_{\frac{\pi}{2}}^T \mathbf{r}_k + (2\dot{R}+\beta R)\dot{\mathbf{r}}_k^T \mathbf{R}_{\frac{\pi}{2}}^T \dot{\hat{\mathbf{r}}}_k + \dot{\mathbf{r}}_k^T \mathbf{R}_{\frac{\pi}{2}}^T(\ddot{\mathbf{c}}+\beta\dot{\mathbf{c}})}{v_k^2}$$

This control law make converge the fleet of vehicles to the same circular motion with time-varying radius $R(t)$ and tracking the time-varying center $\mathbf{c}(t)$.

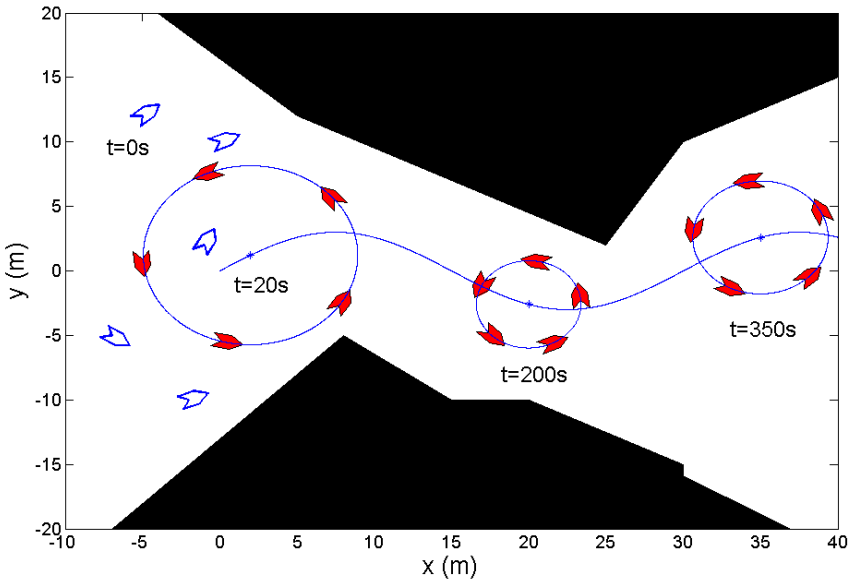

Figure 3.5: *Simulation of five agents governed by the control law* (3.13) *with* $\boldsymbol{G}(t) = \boldsymbol{T}_{c(t)}\boldsymbol{S}_{R(t)}$. *The circular formation, whose center tracks a time-varying reference, changes its radius in order to avoid the obstacles (black blocks).*

Figure 3.5 shows the simulation of five agents governed by the control law from Corollary 3.1 where $\mathbf{G}(t) = \mathbf{T}_{c(t)}\mathbf{S}_{R(t)}$. The control law parameters are $\omega_0 = \kappa = \beta = 1$ and $K = 0.1$. The time-varying reference of the radius is

$$R(t) = 5 + 2\cos\frac{2\pi}{500}t$$

and the reference tracked by the center corresponds to

$$\mathbf{c}(t) = (\frac{1}{10}t, 3\sin\frac{2\pi}{300}t)^T$$

The agents converge to the time-varying circular formation for any random initial conditions (position and heading of the agent) represented in the figure by the blue

void agents. This is an example of one possible application of the combined motion control law and a first step to achieve the final objective of designing a collaborative control to generate both references in a distributed way.

Moreover, the communication radius considered here is $\rho = 10$ which satisfies the geometrical condition

$$\rho > 2R_{max} \sin \frac{\pi}{N}$$

where R_{max} is the up-bound of the reference of the radius, in this case $R_{max} = 7$. Therefore the agents are distributed along the time-varying circular formation.

Elliptic formation. The general elastic formation control law is pertinent also to stabilize the fleet to non-circular formations as an ellipse. In this situation, the transformation is a non-uniform time-invariant scaling

$$\mathbf{G} = \mathbf{S} = \begin{pmatrix} a & 0 & 0 \\ 0 & b & 0 \\ 0 & 0 & 1 \end{pmatrix}$$

where $s_x = a \neq s_y = b$. In this situation, the change of coordinates defined by (3.3) can be expressed by

$$\hat{\mathbf{r}}_k = \mathbf{S}^{-1}\mathbf{r}_k = \begin{pmatrix} 1/a & 0 & 0 \\ 0 & 1/b & 0 \\ 0 & 0 & 1 \end{pmatrix} \mathbf{r}_k$$

Applying this transformation matrix to the control law from Theorem 3.2, following algorithm makes the agents converge to an ellipse centered at the origin which major axis is equal to a and the minor axis is equal to b:

$$\begin{aligned} \dot{v}_k =& -\beta v_k + \frac{\hat{u}_k \dot{\mathbf{r}}_k^T \mathbf{S}\mathbf{R}_{\frac{\pi}{2}} \dot{\hat{\mathbf{r}}}_k + \beta \dot{\mathbf{r}}_k^T \mathbf{S} \dot{\hat{\mathbf{r}}}_k}{v_k} \\ u_k =& \frac{\hat{u}_k \dot{\mathbf{r}}_k^T \mathbf{S} \dot{\hat{\mathbf{r}}}_k + \beta \dot{\mathbf{r}}_k^T \mathbf{R}_{\frac{\pi}{2}}^T \mathbf{S} \dot{\hat{\mathbf{r}}}_k}{v_k^2} \end{aligned}$$

Figure 3.6 shows a simulation of five agents with the controller designed in Corollary 3.1 and all-to-all communication assumption. The control law parameters are $\omega_0 = \kappa = \beta = 1$ and $K = 0.1$. The agents are stabilized to the elliptic formation defined by the non-uniform scaling $s_x = 5$, $s_y = 1$. Moreover the agents are distributed along the formation considering the transformation of the splay pattern which is stable in the unit circle (transformed system).

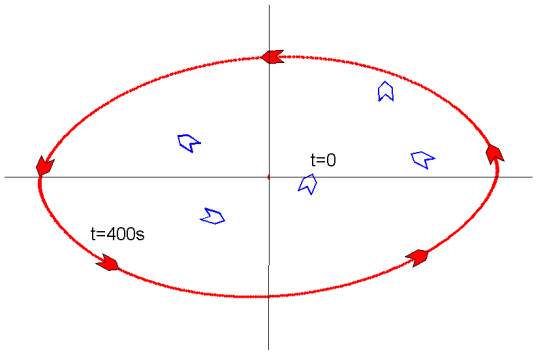

Figure 3.6: *Simulation of five agents stabilized in an elliptic formation. The red line represents the trajectory of the agents at the final state (elliptic formation). The figure shows two snapshots. The blue agents represent the initial conditions. The reds ones represent the final state at* $t = 400s$.

3.3.7 Distributed algorithm applied to elastic formation control

The first contribution of this chapter is the elastic motion control law presented in Theorem 3.2. This control law makes a group of agents converge to the curve defined by the transformation matrix $\mathbf{G}$. This matrix function is a given reference known to all the agents. Therefore, each agent converge independently to the curve. There is not cooperation between agents. However, the notion of formation here makes sense because all the agents converge to the same configuration. Moreover, the improved control law from Corollary 3.1 provides a collaborative solution to distribute the agents uniformly along the formation.

Nevertheless, the final objective of this thesis is to solve the source-seeking problem taking into account the underwater communication problems. In this context, the agents must be able to collaborate in order to decide the trajectory of the formation center. Therefore, the idea now is to implement a cooperative algorithm to make the fleet of vehicles converge to the same elastic formation considering that the transformation matrix $\mathbf{G}$ is unknown.

Consensus with a reference velocity. A first approach is to consider that each agent only knows the first and second derivatives of the matrix which defines the elastic formation. Then, the consensus protocol is designed to reach the same reference matrix $\mathbf{G}$ for all the agents.

For simplicity, the particular case of a time-varying circular formation is analyzed

in the sequel. The given reference is thus, the desired velocity of the center. The objective is for the agents to reach the same circular formation, it means, to reach a consensus on the center of the circle. Consensus problems with a reference velocity are already studied in [127, 128, 173] for double-integrator dynamics. In the context of a moving circle, the velocity of the center is a given reference denoted by $\mathbf{v}_c^{ref} \in \mathbb{R}^2$ known to all the vehicles. Besides, the acceleration represented by $\mathbf{a}_c^{ref} \in \mathbb{R}^2$ is also known to all the vehicles. Nevertheless, the center trajectory is not defined. This is coherent with a source-seeking situation in which the gradient of the scalar field of interest is the desired velocity of the formation center. This information could be a given reference for the agents, but the center of the circular formation is not a known parameter. In this situation, each agent computes:

- its own estimated position of the center of the circular formation represented by $\mathbf{p}_{ck} \in \mathbb{R}^2$
- its own estimated velocity of the center denoted by $\mathbf{v}_{ck} \in \mathbb{R}^2$
- its own estimated acceleration of the center represented by $\mathbf{a}_{ck} \in \mathbb{R}^2$

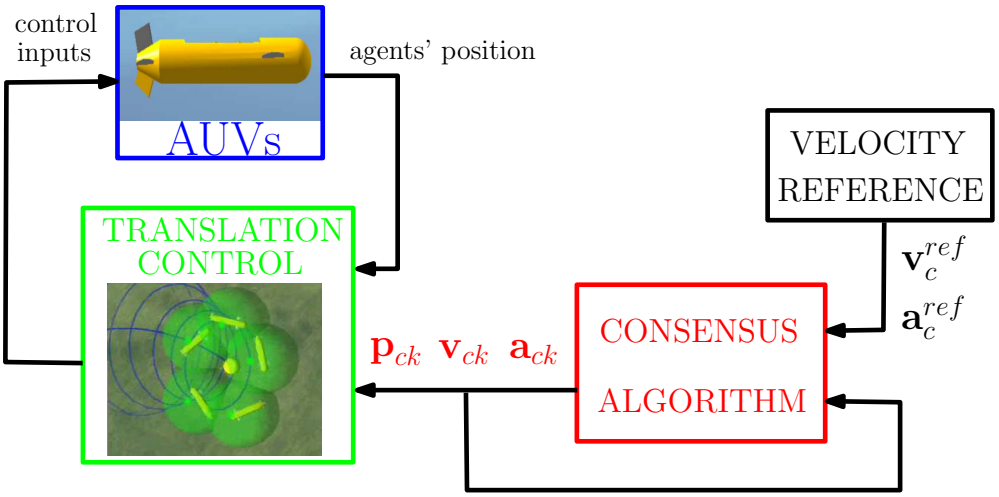

Figure 3.7: *Control strategy: consensus with a reference velocity*

In order to keep the formation, the position of the center calculated for all the vehicles must be the same. Summarizing, the proposed control strategy, which is explained schematically in Figure 3.7, is composed by the following steps:

1. Each agent computes its own estimated position of the center and its derivatives.
2. A distributed algorithm is implemented to reach consensus on the position of the formation center using the external references of the desired velocity of the center and its acceleration.

3. The inputs of the translation control law for each agent are obtained from the consensus algorithm.

In order to fulfil the previous items, a new dynamic variable to estimate the center of the formation is introduced. This variable representing the center of the circle computed by each agent, satisfies the following dynamics:

$$\dot{\mathbf{p}}_{ck} = \mathbf{v}_{ck} \tag{3.20a}$$

$$\dot{\mathbf{v}}_{ck} = \mathbf{a}_{ck} \tag{3.20b}$$

The dynamics of the estimated center $\mathbf{p}_{ck}$ correspond to a double-integrator model which was studied in the survey on multi-agent systems from Chapter 1. This choice comes from the fact that in the translation control approach presented here, the reference of the center and its first and second derivatives are needed to compute the control law (3.16). Therefore, to be consistent with (3.16), the double-integrator dynamics are the most appropriate.

As explained before, the main idea is to implement a consensus algorithm on the estimated position of the formation center in order to stabilize the fleet of agents to the same desired formation. Consensus is reached for (3.20) if for all $\mathbf{p}_{ck}(0)$ and $\mathbf{v}_{ck}(0)$, then $\mathbf{p}_{ck}(t) \to \mathbf{p}_{cj}(t)$ and $\mathbf{v}_{ck}(t) \to \mathbf{v}_c^{ref}(t)$ asymptotically as $t \to \infty$.

Based on [128, 131], the following consensus algorithm with a group reference velocity can be applied here:

$$\mathbf{a}_{ck} = \mathbf{a}_c^{ref} - \alpha(\mathbf{v}_{ck} - \mathbf{v}_c^{ref}) - \sum_{j \in \mathcal{N}_k} (\mathbf{p}_{ck} - \mathbf{p}_{cj}) \tag{3.21}$$

where α is a positive gain and $\mathcal{N}_k$ represents the neighborhood of agent k according to the communication graph. The author of [128] shows that this consensus algorithm converges when the directed communication graph has a spanning tree. This is a generalization of the results presented in [127] for directed graphs. In this chapter, the communication between the vehicles is considered undirected, such that the Laplacian matrix of the communication graph is always symmetric. Therefore all its eigenvalues are real and nonnegative, see Appendix A. In consequence, the result on consensus algorithms with a group reference velocity from [128] can be rewritten for undirected graphs as follows:

Theorem 3.3 *(Ren 2008 [128]) Consider the consensus algorithm* (3.21)*, if the undirected communication graph between the agents is connected and* $\alpha > 0$ *then* $\boldsymbol{p}_{ck}(t) \to \boldsymbol{p}_{cj}(t)$ *and* $\boldsymbol{v}_{ck}(t) \to \boldsymbol{v}_c^{ref}(t)$ *asymptotically as* $t \to \infty$ *for all* k, j*.*

Proof 3.4 *The details of the proof can be found in [128] for the general case of a directed graph. The principal properties of convergence of this algorithm can be also*

analyzed by a Lyapunov function. Rewriting the consensus algorithm with a group reference velocity in a vectorial form, previous equation (3.21) *becomes:*

$$\boldsymbol{a}_c = \boldsymbol{1} \otimes \boldsymbol{a}_c^{ref} - \alpha(\boldsymbol{v}_c - \boldsymbol{1} \otimes \boldsymbol{v}_c^{ref}) - \boldsymbol{L}\boldsymbol{p}_c \tag{3.22}$$

where $\boldsymbol{p}_c = (\boldsymbol{p}_{c1}^T, \ldots, \boldsymbol{p}_{cN}^T)^T$ *represents the vector of all the local positions of the center computed by each agent (analogically the vectors* $\boldsymbol{v}_c$ *and* $\boldsymbol{a}_c$*) and* $\boldsymbol{1} = (1, \ldots, 1)^T \in \mathbb{R}^N$ *is the vector of ones. Considering that* $\boldsymbol{p}_c^{ref}$ *represents the reference trajectory associated to the given* $\boldsymbol{v}_c^{ref}$*, a new variable* $\chi = (\chi_1, \ldots, \chi_N)^T$ *is introduced to express the following error equation:*

$$\chi = \boldsymbol{p}_c - \boldsymbol{1} \otimes \boldsymbol{p}_c^{ref}$$

By definition, the vector of ones $\boldsymbol{1}$ *is always a right eigenvector of the Laplacian matrix* $\boldsymbol{L}$ *corresponding to the eigenvalue* 0*. Using this property of the Laplacian matrix, the previous compact form of the consensus algorithm* (3.22) *can be rewritten as:*

$$\boldsymbol{a}_c - \boldsymbol{1} \otimes \boldsymbol{a}_c^{ref} = -\alpha(\boldsymbol{v}_c - \boldsymbol{1} \otimes \boldsymbol{v}_c^{ref}) - \boldsymbol{L}(\boldsymbol{p}_c - \boldsymbol{1} \otimes \boldsymbol{p}_c^{ref})$$

According to this equation, the dynamics of the error are expressed using the new variable χ*, and thus the following equation holds:*

$$\ddot{\chi} = -\alpha\dot{\chi} - \boldsymbol{L}\chi \tag{3.23}$$

which corresponds to a simple double-integrator consensus algorithm. Choosing the following Lyapunov function

$$V(\chi) = \frac{1}{2}\dot{\chi}^T\dot{\chi} + \frac{1}{2}\chi^T\boldsymbol{L}\chi \geq 0$$

At the equilibrium when $V(\chi) = 0$*, the dynamics of the equation error satisfy:*

$$\dot{\chi}^T\dot{\chi} + \chi^T\boldsymbol{L}\chi \equiv 0$$

If the communication graph is connected the vector of ones $\boldsymbol{1}$ *is the only eigenvector of* $\boldsymbol{L}$ *associated to the zero eigenvalue. Therefore, the zero minimum of the Lyapunov function is reached when:*

$$\dot{\chi} = 0 \quad \textit{and} \quad \chi = \chi_0\boldsymbol{1}$$

where χ_0 *is a constant value.*

Differentiating and taking into account equation (3.23)*, then*

$$\dot{V}(\chi) = \ddot{\chi}^T\dot{\chi} + \dot{\chi}^T\boldsymbol{L}\chi = -\alpha\dot{\chi}^T\dot{\chi} - \chi^T\boldsymbol{L}\dot{\chi} + \dot{\chi}^T\boldsymbol{L}\chi$$

The communication graph is undirected, hence the Laplacian matrix is symmetric. Therefore, the derivative of the Lyapunov function is given by:

$$\dot{V}(\chi) = -\alpha\dot{\chi}^T\dot{\chi} = -\alpha\|\dot{\chi}\|^2 \leq 0$$

In conclusion, for all $\chi_k(0)$ *and* $\dot{\chi}_k(0)$*, then* $\chi_k(t) \to \chi_j(t)$ *and* $\dot{\chi}_k(t) \to 0$ *asymptotically as* $t \to \infty$*. Therefore, for all* $\boldsymbol{p}_{ck}(0)$ *and* $\boldsymbol{v}_{ck}(0)$*,* $\boldsymbol{p}_{ck}(t) \to \boldsymbol{p}_{cj}(t)$ *and* $\boldsymbol{v}_{ck}(t) \to \boldsymbol{v}_c^{ref}(t)$ *asymptotically as* $t \to \infty$*.*

□

This previous consensus algorithm allows the agents to reach an agreement on the trajectory of the center of the circular formation from a given velocity reference known to all the agents. The center trajectory and its first and second derivatives computed for each agent are the inputs of the translation control law presented in Chapter 2. The transformed system is now defined by

$$\hat{\mathbf{r}}_k = \mathbf{r}_k - \mathbf{p}_{ck} \quad \forall k = 1, ..., N$$

where the dynamics of the transformed system $\dot{\hat{\mathbf{r}}}_k$ satisfy (3.4) and the closed-loop dynamics are imposed by the control law (3.6). Therefore, this previous control law developed to move the center of a circular formation following a given reference becomes:

$$\dot{v}_k = -\beta v_k + \frac{\hat{u}_k \dot{\mathbf{r}}_k^T \mathbf{R}_{\frac{\pi}{2}} \dot{\hat{\mathbf{r}}}_k + \dot{\mathbf{r}}_k^T (\mathbf{a}_{ck} + \beta(\dot{\hat{\mathbf{r}}}_k + \mathbf{v}_{ck}))}{v_k} \tag{3.24a}$$

$$u_k = \frac{\hat{u}_k \dot{\mathbf{r}}_k^T \dot{\hat{\mathbf{r}}}_k + \dot{\mathbf{r}}_k^T \mathbf{R}_{\frac{\pi}{2}}^T (\mathbf{a}_{ck} + \beta(\dot{\hat{\mathbf{r}}}_k + \mathbf{v}_{ck}))}{v_k^2} \tag{3.24b}$$

where the position of agent k is represented by $\mathbf{r}_k = (x_k, y_k)^T \in \mathbb{R}^2$, and the position of the center computed for agent k and its velocity and acceleration are $\mathbf{p}_{ck}$, $\mathbf{v}_{ck}$ and $\mathbf{a}_{ck}$ respectively, obtained from the consensus algorithm.

To formalize this new collaborative approach the following corollary holds.

Corollary 3.2 *Let* $\boldsymbol{v}^{ref}$ *and* $\boldsymbol{a}^{ref}$ *be the velocity and acceleration references of the desired center formation. Let* $\omega_0 \neq 0$*,* $\kappa > 0$*,* $\beta > 0$ *and* $\alpha > 0$ *be four control parameters such that the following condition is satisfied:*

$$v_k > 0 \quad \forall k = 1, \ldots, N$$

Then the control law (3.24) *makes each agent defined by* (3.1) *converge to a circular motion with unit radius and time-varying center* $\boldsymbol{p}_{ck}$*. Thanks to the consensus algorithm* (3.21) *applied to the center dynamics* (3.20)*, if the undirected communication graph is connected then all the centers reach a consensus asymptotically and their velocities follow the reference velocity* $\boldsymbol{v}^{ref}$*. The direction of rotation is determined by the sign of* ω_0*.*

Proof 3.5 *As it is shown in Figure 3.7, the whole system consists of two uncoupled systems. The first one is composed of the dynamics of the multi-agent system* (3.4) *and the translation control law which stabilize each agent* $k = 1, \ldots, N$ *to a circular motion whose center is defined by* $\boldsymbol{p}_{ck}$*. The translation control law uses the first and second derivatives of the reference of the center. Thanks to Theorem 2.3 from Chapter 2, the control law* (3.24) *makes each agent converge to a circular motion with center the time-varying reference* $\boldsymbol{p}_{ck}$*.*

In the other hand, the second system represents a consensus algorithm which is implemented to reach an agreement on the center of the formation for all the agents. Thanks to Theorem 3.3, the collaborative algorithm (3.21) *makes system* (3.20) *reach consensus asymptotically. Therefore, asymptotically, all the computed centers satisfy* $\boldsymbol{p}_{ck} = \boldsymbol{p}_{cj} = \boldsymbol{c}_0 \quad \forall k, j$*. Consequently, all the vehicles describes a circular motion following the time-varying center* $\boldsymbol{c}_0$*.*

□

Remark 3.3 *Note that this result can be applied to other time-varying elastic formations, such as circular formation with time-varying radius or an elliptic formation tracking a time-varying reference of its center. In these cases, the consensus algorithm will be applied to the time-varying parameters of the general transformation matrix* $\boldsymbol{G}$ *which defines the elastic formation.*

Simulation Results. The consensus algorithm (3.21) is implemented to generate the reference of the center circular formation in order to apply the translation control law (3.24). The group reference velocity is given by

$$\mathbf{v}_c^{ref} = (0.2, 0.24 \cos 0.08t)^T$$

and the initial conditions of the position of the center are different for each agent.

Figure 3.8 shows a simulation of five agents governed by the translation control law (3.24) with the consensus algorithm (3.21) to provide the reference of the center of the circular formation. The control parameters are $R = 2$, $\omega_0 = \kappa = \beta = 1$ and $\alpha = 0.1$. The communication graph is a ring, therefore is connected. The figure shows three snapshots, the initial conditions, and two states for $t = 45s$ and $t = 116s$. The red circles represent the circular motion corresponding to each agent at each instant. The black lines represent the trajectories of each estimated center. This simulation shows that the center of each agent achieve consensus, then the common center tracks the given reference velocity and the circular formation is kept.

Figure 3.9 displays the evolution of the trajectories of centers $\mathbf{p}_{ck}$ computed by each agent k for the same simulation of five agents. Starting from any initial condition, the collaborative algorithm (3.21) makes the agents reach consensus on the center position.

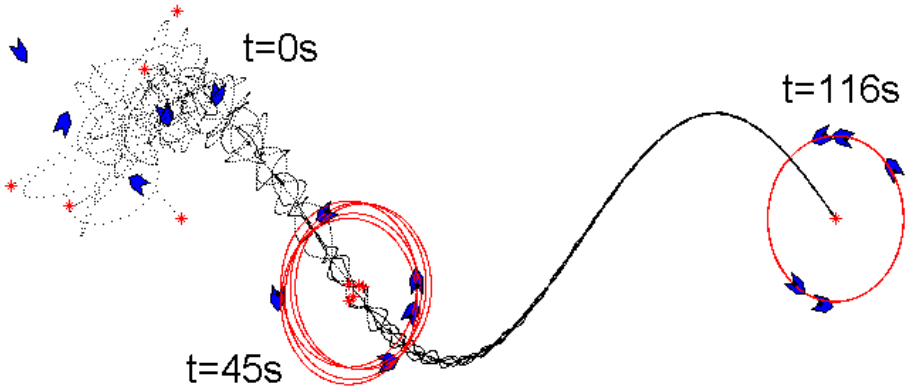

Figure 3.8: *Simulation of five agents governed by the control law* (3.24) *where the center computed by each agent results from the consensus algorithm* (3.21). *The black lines represent the centers' trajectories.*

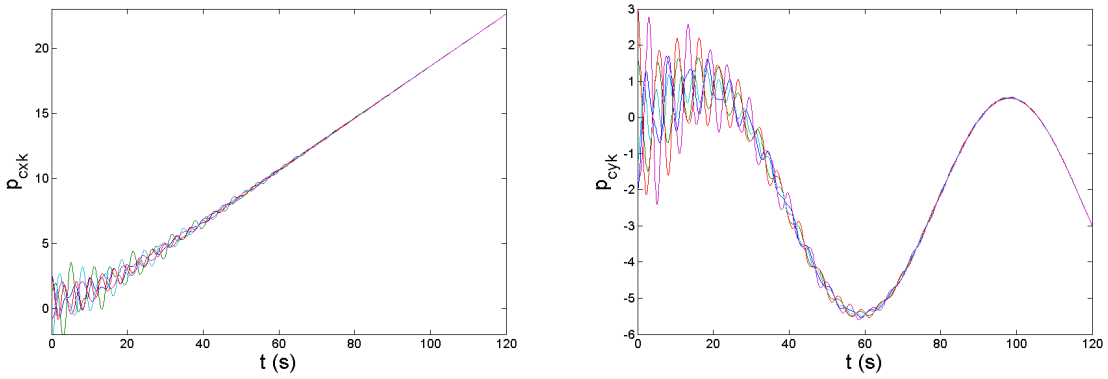

(a) X-coordinate of the centers' positions

(b) Y-coordinate of the centers' positions

Figure 3.9: *Evolution of the centers' positions* $\boldsymbol{p}_{ck} = (p_{cxk}, p_{cyk})^T$ *corresponding to the previous simulation of five agents shown in Figure 3.8.*

In Figure 3.10, the evolution of the centers' velocities $\mathbf{v}_{ck}$ computed by each agent k, is compared to the reference velocity $\mathbf{v}_c^{ref}$ represented by the black dashed line. For any initial conditions, all the centers' velocities converge asymptotically to the external reference.

Consensus with reference velocity corrupted by noise. Previous collaborative algorithm can be improved by considering that each agent receives the external reference velocity corrupted by noise. This assumption is more realistic in underwater scenarios, in which, the signals transmitted through water are exposed to some

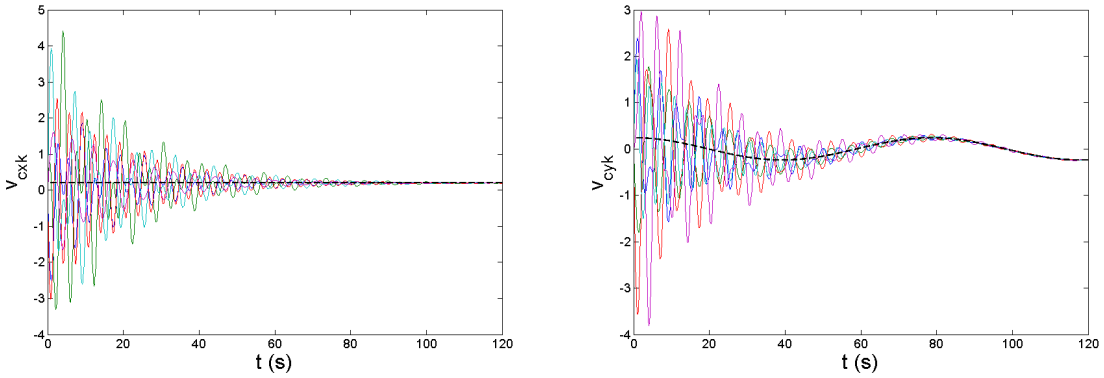

(a) X-coordinate of the centers' velocities (b) Y-coordinate of the centers' velocities

Figure 3.10: *Evolution of the centers' velocities* $\boldsymbol{v}_{ck} = (v_{cxk}, v_{cyk})^T$ *corresponding to the previous simulation of five agents shown in Figure 3.8 and the reference velocity* $\boldsymbol{v}_c^{ref} = (v_{cx}^{ref}, v_{cy}^{ref})^T$ *(black dashed line).*

perturbations such as currents and fading.

It is assumed that the external reference received for each agent is then $\mathbf{s}(t) = \mathbf{v}_c^{ref} + \mathbf{w}_1$, where $\mathbf{w}_1 \in \mathbb{R}^2$ is a vector whose components are Gaussian zero-mean noise. Based on previous corollary, an extension of the consensus with a group reference velocity is proposed.

Proposition 3.1 *Let* $\boldsymbol{v}^{ref}$ *and* $\boldsymbol{a}^{ref}$ *be the references of velocity and acceleration of the desired formation center, both corrupted by bounded zero-mean noise represented by* $\boldsymbol{w}_1$ *and* $\boldsymbol{w}_2$ *respectively. Let* $\omega_0 \neq 0$, $\kappa > 0$, $\beta > 0$ *and* $\alpha > 0$ *be four control parameters. Then the control law* (3.24) *makes each agent defined by* (3.4) *converge to a circular motion with unit radius and time-varying center* $\boldsymbol{p}_{ck}$*. Thanks to the consensus algorithm:*

$$\boldsymbol{a}_{ck} = \boldsymbol{a}_c^{ref} + \boldsymbol{w}_2 - \alpha(\boldsymbol{v}_{ck} - \boldsymbol{v}_c^{ref} - \boldsymbol{w}_1) - \sum_{j \in \mathcal{N}_k} (\boldsymbol{p}_{ck} - \boldsymbol{p}_{cj}) \tag{3.25}$$

all the centers reach a consensus asymptotically and their velocities follow the reference velocity $\boldsymbol{v}^{ref}$*. The direction of rotation is determined by the sign of* ω_0*.*

Intuitively, if the noise is bounded then, the previous algorithm reaches consensus in a closed ball centered at the consensus final value. However, the mathematical details of the proof of this proposition have to be analyzed formally.

Simulation Results. The reference of the center formation used in the translation control law (3.24) is generated from consensus algorithm (3.25). The group reference

velocity is the same that in previous case, and the initial conditions of the position of the center are different for each agent.

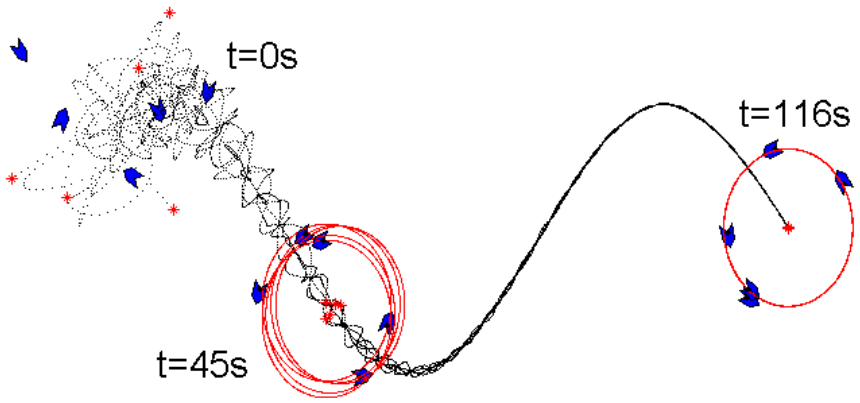

Figure 3.11: *Simulation of five agents governed by the control law* (3.24) *where the center computed by each agent results from the consensus algorithm* (3.25). *The black lines represent the centers' trajectories.*

Figure 3.11 shows a simulation of five agents governed by the translation control law (3.24) with the consensus algorithm (3.25) to provide the reference of the center of the circular formation. The control parameters are $R = 2$, $\omega_0 = \kappa = \beta = 1$ and $\alpha = 0.1$. The communication graph is a ring, therefore is connected. The figure shows three snapshots, the initial conditions, and two states for $t = 45s$ and $t = 116s$. The red circles represent the circular motion corresponding to each agent in each instant. The black lines represent the trajectories of each estimated center.

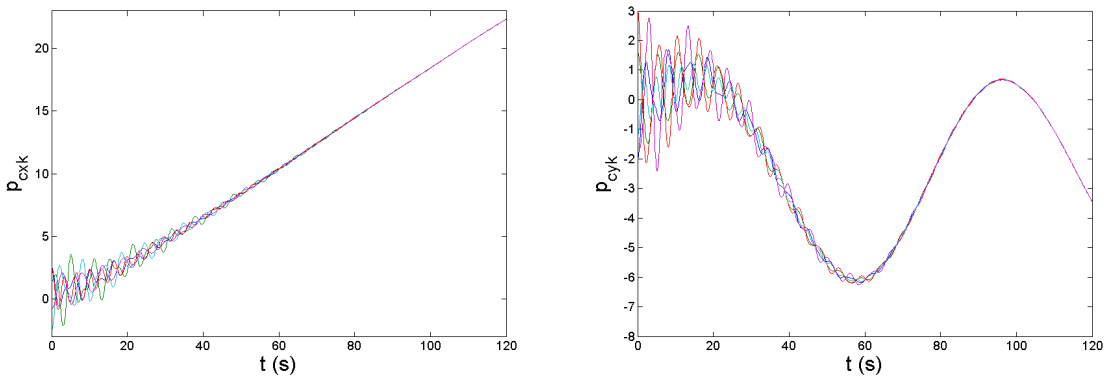

(a) X-coordinate of the centers' position (b) Y-coordinate of the centers' positions

Figure 3.12: *Evolution of the centers' positions* $\boldsymbol{p}_{ck} = (p_{cxk}, p_{cyk})^T$ *corresponding to the previous simulation of five agents shown in Figure 3.11.*

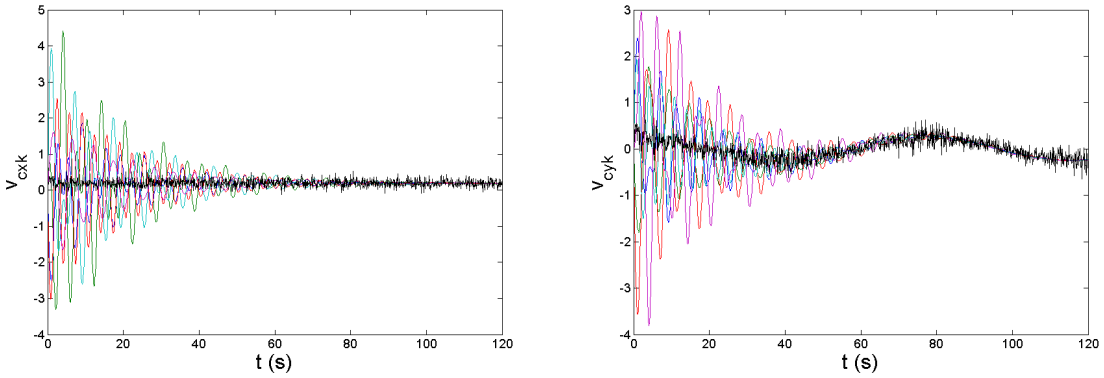

(a) X-coordinate of the centers' velocities (b) Y-coordinate of the centers' velocities

Figure 3.13: *Evolution of the centers' velocities* $\boldsymbol{v}_{ck} = (v_{cxk}, v_{cyk})^T$ *corresponding to the previous simulation of five agents shown in Figure 3.11 and the reference velocity* $\boldsymbol{v}_c^{ref} = (v_{cx}^{ref}, v_{cy}^{ref})^T$ *corrupted by noise.*

Figure 3.12 displays the evolution of the trajectories of centers $\mathbf{p}_{ck}$ computed by each agent k for the same simulation of five agents. Starting from any initial condition, the collaborative algorithm (3.21) makes the agents to reach consensus on the center position.

In Figure 3.13, the evolution of the centers' velocities $\mathbf{v}_{ck}$ computed by each agent k, is compared to the reference velocity $\mathbf{v}_c^{ref}$ represented by the dashed black line. For any initial conditions, all the centers' velocities converge asymptotically to the external reference corrupted by noise.

3.4 Motion-tracking based on affine transformations

The previous section presents a first result on formation control based on affine transformations. This approach provides a general framework very powerful in order to express a richer class of curves including time-varying formations. According to this new framework, a *motion-tracking* control design which use the affine transformations to define a desired reference velocity is presented in this section. The general control law proposed enables to track a reference velocity and to obtain several motions expressed with few time-varying parameters.

3.4.1 Definition of motion-tracking

Consider the standard vehicle model commonly used in the literature to model AUVs restricted kinematics presented before (3.1). It corresponds to a kinematic unicycle

fitting with model properties subject to a simple non-holonomic constraint. All the vectors are expressed in homogeneous coordinates, then $\mathbf{r}_k = (x_k, y_k, 1)^T$ is the position vector of the agent k expressed in homogeneous coordinates, θ_k the heading angle and $v_k, \dot{\theta}_k$ are the control inputs. Note that $\mathbf{v} \in \mathbb{R}^N$ and $\theta \in \mathbb{R}^N$ represent the vector of all velocities and the vector of all heading angles respectively.

The objective is for the agents to follow different reference velocities and to converge to different formations in a cooperative way. The idea is now to use the general transformation matrix $\mathbf{G}$ defined by (3.2) to characterize a class of motion. The desired trajectory of the motion is the result of applying the transformation matrix to a constant vector. Therefore, the idea is to relate some constant vector to a time-varying vector which point to the trajectory of the motion desired for the vehicles. This aim can be expressed as:

$$\mathbf{r}_k = \mathbf{G}\mathbf{r}_0$$

where $\mathbf{r}_0$ is a constant vector. The differentiation of previous equation leads to:

$$\dot{\mathbf{r}}_k = \dot{\mathbf{G}}\mathbf{r}_0 = \dot{\mathbf{G}}\mathbf{G}^{-1}\mathbf{r}_k \tag{3.26}$$

This equation represents the objective in terms of velocity. Therefore, we consider a dynamic control in the velocity in order to deal with this control problem. In previous section a definition of elastic formation based on affine transformations is provided. Now, *motion-tracking* is defined as a common motion of a group of agents so that all the agents follow the same kind of motion (circular, rectilinear, periodical) in terms of velocity. It is important to recall that this definition does not imply trajectory tracking because each agent describes a different trajectory. This can be considered as a *velocity tracking* due to the fact that the group of agents follows the same reference velocity.

3.4.2 Motion-tracking control design

The purpose is now to design a general and compact control law to stabilize a fleet of vehicles to several formation motions using the affine transformations.

With a view to analyze the stability of the system, the following Lyapunov function is proposed:

$$S(\mathbf{r}, \mathbf{v}, \theta) = \frac{1}{2}\sum_{k=1}^{N} \left\| \dot{\mathbf{r}}_k - \dot{\mathbf{G}}\mathbf{G}^{-1}\mathbf{r}_k \right\|^2 \geq 0 \tag{3.27}$$

Note that when $S(\mathbf{r}, \mathbf{v}, \theta) = 0$ the dynamics of the system satisfy $\dot{\mathbf{r}}_k = \dot{\mathbf{G}}\mathbf{G}^{-1}\mathbf{r}_k$ which is the objective defined in (3.26). Evaluating the derivative of $S(\mathbf{r}, \mathbf{v}, \theta)$ along the solutions of system (3.1) leads to:

$$\dot{S}(\mathbf{r}, \mathbf{v}, \psi) = \sum_{k=1}^{N} \left(\ddot{\mathbf{r}}_k - \ddot{\mathbf{G}}\mathbf{G}^{-1}\mathbf{r}_k - \dot{\mathbf{G}}\dot{\mathbf{G}}^{-1}\mathbf{r}_k - \dot{\mathbf{G}}\mathbf{G}^{-1}\dot{\mathbf{r}}_k \right)^T \left(\dot{\mathbf{r}}_k - \dot{\mathbf{G}}\mathbf{G}^{-1}\mathbf{r}_k \right)$$

In this case, a transformed system which dynamics have been enforced to have constant velocity is not considered. Unlike the previous cases of time-varying circular formations and elastic formations, the Lyapunov function depends on the position and velocity vector of the AUVs. Therefore, differentiating this Lyapunov function, the first derivative of the velocity v_k appears explicitly. Due to the expression of the second derivative of the position vector $\mathbf{r}_k$, such that

$$\ddot{\mathbf{r}}_k = \frac{\dot{v}_k}{v_k}\dot{\mathbf{r}}_k + \dot{\theta}_k \mathbf{R}^* \dot{\mathbf{r}}_k \tag{3.28}$$

where $\mathbf{R}^*$ is the rotation matrix through an angle $\frac{\pi}{2}$ but erasing the homogeneous coordinate, the two control inputs become $u_{1k} = \dot{v}_k$ and $u_{2k} = \dot{\theta}_k$. In consequence, a dynamic velocity control law is proposed in the following theorem:

Theorem 3.4 *(Briñón-Arranz et al. 2011 [18]) Let $\boldsymbol{G}$ be a twice differentiable matrix with bounded derivatives resulting from a sequence of affine transformations defined in* (3.2)*. Let $\kappa > 0$ be a control parameter and the condition $v_k \neq 0$ is satisfied. Then the control law:*

$$u_{1k} = -\kappa v_k + \frac{1}{v_k}\dot{\boldsymbol{r}}_k^T \dot{\boldsymbol{G}}\boldsymbol{G}^{-1}\dot{\boldsymbol{r}}_k + \frac{1}{v_k}\dot{\boldsymbol{r}}_k^T \left(\ddot{\boldsymbol{G}}\boldsymbol{G}^{-1} + \dot{\boldsymbol{G}}\dot{\boldsymbol{G}}^{-1} + \kappa\dot{\boldsymbol{G}}\boldsymbol{G}^{-1}\right)\boldsymbol{r}_k \tag{3.29a}$$

$$u_{2k} = \frac{1}{v_k^2}\dot{\boldsymbol{r}}_k^T \boldsymbol{R}^{*T}\dot{\boldsymbol{G}}\boldsymbol{G}^{-1}\dot{\boldsymbol{r}}_k + \frac{1}{v_k^2}\dot{\boldsymbol{r}}_k^T \boldsymbol{R}^{*T}\left(\ddot{\boldsymbol{G}}\boldsymbol{G}^{-1} + \dot{\boldsymbol{G}}\dot{\boldsymbol{G}}^{-1} + \kappa\dot{\boldsymbol{G}}\boldsymbol{G}^{-1}\right)\boldsymbol{r}_k \tag{3.29b}$$

makes all the agents defined by (3.1) *converge to the motion defined by the transformation $\boldsymbol{G}$ applied to the constant vector $\boldsymbol{r}_0$.*

Proof 3.6 *The Lyapunov function defined by* (3.27) *is positive semidefinite. Evaluating the derivative of the Lyapunov function along the solution of the resulted closed-loop system* (3.1) *and using the equation* (3.28)*, $\dot{S}(\boldsymbol{r}, \boldsymbol{v}, \psi)$ can be rewritten as:*

$$\dot{S}(\boldsymbol{r}, \boldsymbol{v}, \psi) = \sum_{k=1}^{N}\left(\frac{u_{1k}}{v_k}\dot{\boldsymbol{r}}_k + u_{2k}\boldsymbol{R}^*\dot{\boldsymbol{r}}_k - \ddot{\boldsymbol{G}}\boldsymbol{G}^{-1}\boldsymbol{r}_k - \dot{\boldsymbol{G}}\dot{\boldsymbol{G}}^{-1}\boldsymbol{r}_k - \dot{\boldsymbol{G}}\boldsymbol{G}^{-1}\dot{\boldsymbol{r}}_k\right)^T \cdot\left(\dot{\boldsymbol{r}}_k - \dot{\boldsymbol{G}}\boldsymbol{G}^{-1}\boldsymbol{r}_k\right)$$

Considering the previous control law (3.29) *the derivative of the Lyapunov function becomes:*

$$\dot{S}(\boldsymbol{r}, \boldsymbol{v}, \psi) = -\kappa\sum_{k=1}^{N}\left\|\dot{\boldsymbol{r}}_k - \dot{\boldsymbol{G}}\boldsymbol{G}^{-1}\boldsymbol{r}_k\right\|^2 = -2\kappa S(\boldsymbol{r}, v, \theta) \leq 0$$

Therefore $S(\boldsymbol{r}, \boldsymbol{v}, \theta)$ is nonincreasing along the solutions. The solutions thus converge to the largest invariant set, Λ, for which $\dot{S} = 0$. Then, system (3.1) *asymptotically reaches the conditions corresponding to the following dynamics of the vehicles:*

$$\dot{\boldsymbol{r}}_k = \dot{\boldsymbol{G}}\boldsymbol{G}^{-1}\boldsymbol{r}_k$$

which describe a formation motion defined by the transformation matrix $\boldsymbol{G}$.

□

Remark 3.4 *The control law presented in the previous theorem has a singular points when* $v_k = 0$. *A mathematical condition to avoid this situation in all cases cannot straightforward be obtained. Nevertheless, the simulation results for some particular cases presented in the following subsections, show that, if the initial velocities are positive for all the agents, and the time-varying formation motion represented by* $\boldsymbol{G}$ *varies slowly, the singular point is avoided.*

This previous theorem presents a general result to stabilize the agents to a motion whose characteristics (shape, speed) are defined by the matrix $\mathbf{G}$. The following subsections present particular types of motions to show the applicability of this new framework.

3.4.3 Particular cases and simulations

Velocity tracking. First of all, the simplest case when the transformation is the identity matrix, that is $\mathbf{G} = \mathbf{I}_3$, is studied. The objective becomes $\dot{\mathbf{r}}_k = 0$. Thus, the control inputs become:

$$u_{1k} = -\kappa v_k \tag{3.30}$$

$$u_{2k} = 0 \tag{3.31}$$

It is clear that in such situation, the objective only concerns the velocity and no constraint appears on the final position of the agents. These final positions depend on the initial conditions of the agents. This fact is important to understand the following cases.

The trajectory tracking problem can be expressed as a transformation, specifically a translation by the reference vector $\mathbf{r}_{ref} = (x_{ref}, y_{ref})$. Thus, the objective is:

$$\mathbf{r}_k = \mathbf{T}_{\mathbf{r}_{ref}} \mathbf{r}_0 = \begin{pmatrix} 1 & 0 & x_{ref} \\ 0 & 1 & y_{ref} \\ 0 & 0 & 1 \end{pmatrix} (0, 0, 1)^T = \mathbf{r}^h_{ref}$$

where $\mathbf{r}^h_{ref}$ is the reference position vector in homogeneous coordinates. This objective expressed in the new formulation presented before leads with:

$$\dot{\mathbf{r}}_k = \dot{\mathbf{T}}_{\mathbf{r}_{ref}} \mathbf{T}^{-1}_{\mathbf{r}_{ref}} \mathbf{r}_k = \dot{\mathbf{r}}^h_{ref}$$

Therefore, the system will be able to follow a reference velocity. According to Theorem 3.4, and considering $\mathbf{G} = \mathbf{T}_{\mathbf{r}_{ref}}$ then, the control law dealing with this problem is

written as:

$$u_{1k} = -\kappa v_k + \frac{1}{v_k}\dot{\mathbf{r}}_k^T(\ddot{\mathbf{r}}_{ref}^h + \kappa\dot{\mathbf{r}}_{ref}^h) \tag{3.32a}$$

$$u_{2k} = \frac{1}{v_k^2}\dot{\mathbf{r}}_k^T\mathbf{R}^{*T}(\ddot{\mathbf{r}}_{ref}^h + \kappa\dot{\mathbf{r}}_{ref}^h) \tag{3.32b}$$

Note that, the agents follow the reference velocity and not the exact reference trajectory. This is not a trajectory tracking or path following problem. The formulation of the problem allows the agents to track the same velocity. In this thesis, this result is defined as a velocity tracking, as shown in Figure 3.14. Note that parallel motion problem analyzed in [149] loads to a straight line reference. Here, the control law (3.32) allows considering more general class of planar motions. Nevertheless, our approach is not cooperative and each vehicle converge to the desired motion independently.

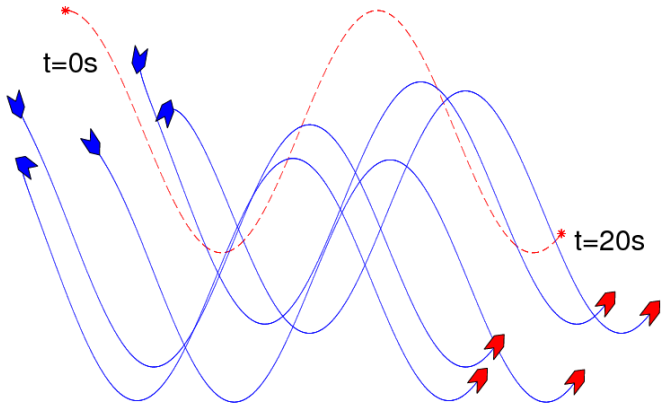

Figure 3.14: *Simulation of five agents governed by* (3.32). *The blue lines represent the trajectories of the agents following a reference velocity given by the red dashed line* $\dot{\boldsymbol{r}}_{ref} = (1, -2\sin\frac{t}{2})$. *The figure shows two snapshots. The blue agents represent the initial conditions. The red ones represent the final state at* $t = 20s$.

Circular trajectory. A circular trajectory centered at the origin of the reference frame and with unit radius is described using the following parametrization in time:

$$x(t) = \cos(\omega_0 t)$$
$$y(t) = \sin(\omega_0 t)$$

where $\omega_0 \neq 0$ is the angular velocity of the rotation. In this case, the transformation matrix $\mathbf{G}$ becomes a time-varying rotation by angle $\omega_0 t$, that is, $\mathbf{G} = \mathbf{R}_{\omega_0 t}$. Consequently, the objective can be expressed as:

$$\dot{\mathbf{r}}_k = \dot{\mathbf{R}}_{\omega_0 t}\mathbf{R}_{\omega_0 t}^{-1}\mathbf{r}_k = \omega_0\mathbf{R}^*\mathbf{r}_k$$

Adapting this objective to Theorem 3.4 the following control law is obtained:

$$u_{1k} = -\kappa v_k + \kappa \frac{\omega_0}{v_k} \dot{\mathbf{r}}_k^T \mathbf{R}^* \mathbf{r}_k \tag{3.33a}$$

$$u_{2k} = \omega_0 + \kappa \frac{\omega_0}{v_k^2} \dot{\mathbf{r}}_k^T \mathbf{r}_k \tag{3.33b}$$

Once more, this formulation ensures that the agents converge to a circular motion. This leads to the same problem analyzed in [118]. However, no conditions on its radius is stated for now. As in the previous case, the initial conditions will influence the final radius. Note that the radius of the final circle of each agent satisfies $R_k = v_{k\infty}/\omega_0$, where $v_{k\infty} = lim_{t\to\infty} v_k$ denotes the final velocity of agent $k = 1, \ldots, N$. According to equation (3.33), this final value $v_{k\infty}$ is related to the initial conditions of the agent. Therefore, the radius of the final circular motion of each agent depends of its initial conditions and thus, all vehicle converge to circular trajectories with different radius. Applying different sequences of transformations the agents can track a time-varying circular trajectories with a moving center and not constant radius. In order to achieve the same circle, and for more complex cases, for instance the same formation, a cooperative control is introduced later.

Not circular formations. A particular case of the contraction or scaling of a circular motion can be considered when the radius depends on the agent position. In this way, many curves can be expressed by scaling a circle. For example, a non-uniform time-invariant scaling, as previously presented in the definition of affine transformations, corresponds to

$$\mathbf{S} = \begin{pmatrix} a & 0 & 0 \\ 0 & b & 0 \\ 0 & 0 & 1 \end{pmatrix}$$

where a and b are some positive constant parameters which can define the mayor and minor axes of an ellipse respectively. In general, a scaling matrix depending on the position of the agent can be expressed as

$$\mathbf{S}_k = \begin{pmatrix} R_k & 0 & 0 \\ 0 & R_k & 0 \\ 0 & 0 & 1 \end{pmatrix}$$

where the uniform scaling parameter R_k is a function leading to:

$$\begin{aligned} R_k &= R(\alpha_k) \\ \tan \alpha_k &= \frac{y_k}{x_k} \end{aligned}$$

The transformation matrices dealing with these problems are $\mathbf{G} = \mathbf{S}\mathbf{R}_{\omega_0 t}$ and $\mathbf{G}_k = \mathbf{S}_k\mathbf{R}_{\omega_0 t}$ respectively. The following analysis focuses on this second formulation with a

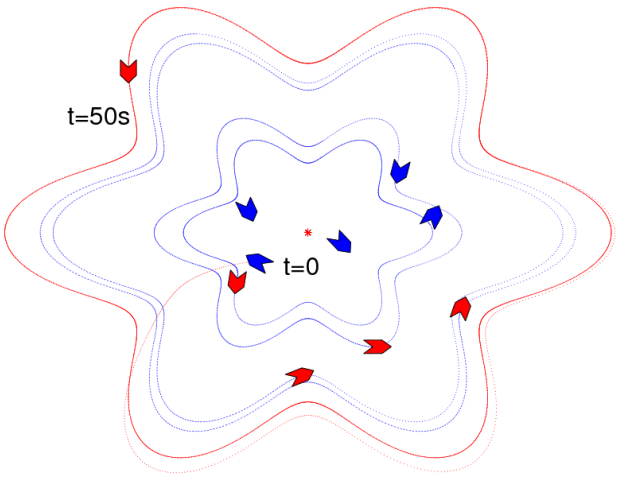

Figure 3.15: *Simulation of five agents governed by the control law* (3.34) *and the reference of the radius* $R_k = \cos 6\alpha_k + 5$. *The red line represents the trajectory of one agent and the blue ones represent the final curves achieves for each agent. The figure shows two snapshots. The blue agents represent the initial conditions. The red ones represent the final state* $t = 50s$.

transformation matrix depending on the position of the agent $\mathbf{G}_k$. Let $R : \mathbb{R} \to \mathbb{R}^+$ be a twice differentiable function with bounded first and second derivatives, as in (3.34) and denote $R_k = R(\alpha_k)$ the value of the function at position $\mathbf{r}_k$ of agent k. The previous control law (3.29) becomes:

$$u_{1k} = -\kappa v_k + \frac{\dot{R}_k}{R_k} v_k + \kappa \frac{\omega_0}{v_k} \dot{\mathbf{r}}_k^T \mathbf{R}^* \mathbf{r}_k + \frac{R_k \ddot{R}_k + \kappa R_k \dot{R}_k - \dot{R}_k^2}{v_k R_k^2} \dot{\mathbf{r}}_k^T \mathbf{r}_k \tag{3.34a}$$

$$u_{2k} = \omega_0 + \kappa \frac{\omega_0}{v_k^2} \dot{\mathbf{r}}_k^T \mathbf{r}_k + \frac{R_k \ddot{R}_k + \kappa R_k \dot{R}_k - \dot{R}_k^2}{v_k R_k^2} \dot{\mathbf{r}}_k^T \mathbf{r}_k \tag{3.34b}$$

Note that once more, the final trajectory of each agent is related to its final velocity which depends on the initial conditions. Therefore, each agent converge to a different curve but with the same shape and velocity of rotation, as shown in Figure 3.15.

In the sequel, a cooperative method which ensures that the trajectories of each agent converge to the same curve is presented. In this situation, the agents reach a consensus on some variable in order to achieve the same formation.

3.4.4 Cooperative control design

The general formulation presented in Theorem 3.4 allows us to govern a group of agents to follow a reference velocity or to converge to a time-varying motion defined by the matrix $\mathbf{G}$. Note that each agent converges to a different trajectory depending on the

initial conditions but with the same shape. The aim now is to develop a cooperative control to make the agents converge to the same formation.

This subsection presents collaborative control laws to obtain consensus on velocities and on the heading angles to reach the same formation and the uniform distribution of the agents along the formation respectively.

Consensus on velocities for circular formation. In a circular motion, there exists a relation between the linear velocity and the radius of the circle. Due to the relation $v = R\omega_0$, whose implications are extensively analyzed in Chapter 2, if the linear velocity of all the agents converge to the same value v_0 then, all the vehicles turn around the same circular trajectory with radius $R = v_0/\omega_0$. The conclusion is that, to reach the same circular formation, the agents need to reach the same final velocity. Consequently, a consensus algorithm is adding to the previous control law.

The following composed Lyapunov function is proposed to analyze the system:

$$V(\mathbf{r}, \mathbf{v}, \theta) = \kappa_1 S(\mathbf{r}, \mathbf{v}, \theta) + \kappa_2 Q(\mathbf{v}) \tag{3.35}$$

where $\kappa_1 > 0$, $\kappa_2 > 0$ are two control parameters, $S(\mathbf{r}, \mathbf{v}, \theta)$ is the previous Lyapunov function defined in (3.27) which is used in the analysis of the formation motion control design and the quadratic form $Q(\mathbf{v})$ is expressed by the following equation:

$$Q(\mathbf{v}) = \frac{1}{2}\mathbf{v}^T \mathbf{L}\mathbf{v}$$

where $\mathbf{L}$ represents the Laplacian matrix of the communication graph. According to the properties of the Laplacian matrix (see Appendix A), $\mathbf{L}$ is positive semidefinite because the communication graph considered is undirected. Hence, $Q(\mathbf{v})$ is nonnegative. Moreover, if the communication graph is connected then, the only eigenvector associated to the eigenvalue 0 is the vector of ones $\mathbf{1} \in \mathbb{R}^N$. Therefore, the quadratic form reaches its minimum only when $\mathbf{v} = v_0\mathbf{1}$ where v_0 is a constant value, that is, when all agents have the same linear velocity.

In the sequel, a cooperative control law which stabilizes a multi-agent system to circular formation is proposed. The idea is to introduce an additional control term to the previous control law (3.33) which assures a consensus on the velocities of all the agents.

Theorem 3.5 *(Briñón-Arranz et al. 2011 [18]) Let $\omega_0 \neq 0$, $\kappa_1 > 0$ and $\kappa_2 > 0$ be three control parameters and the condition $v_k \neq 0$ is satisfied. Let $\mathcal{G}$ be the communication graph and $\boldsymbol{L}$ be the corresponding Laplacian matrix, where $\boldsymbol{L}_k$ represents its k^{th} row.*

Then the control law:

$$u_{1k} = -\kappa_1 v_k + \kappa_1 \frac{\omega_0}{v_k} \dot{\boldsymbol{r}}_k^T \boldsymbol{R}^* \boldsymbol{r}_k - \kappa_2 \boldsymbol{L}_k \boldsymbol{v} \tag{3.36a}$$

$$u_{2k} = \omega_0 + \kappa_1 \frac{\omega_0}{v_k^2} \dot{\boldsymbol{r}}_k^T \boldsymbol{r}_k \tag{3.36b}$$

makes all the agents defined by (3.1) *converge to a circular motion centered at the origin and the direction of the rotation defined by the sign of* ω_0*. Moreover, if the communication graph* $\mathcal{G}$ *is connected, all the agents converge to the same circular formation whose radius is obtained through a consensus algorithm on the agents' velocities.*

Proof 3.7 *Consider the Lyapunov function* (3.35)*. Its derivative is expressed as follows:*

$$\dot{V}(\boldsymbol{r}, \boldsymbol{v}, \theta) = \kappa_1 \dot{S}(\boldsymbol{r}, \boldsymbol{v}, \theta) + \kappa_2 \dot{Q}(\boldsymbol{v})$$

Evaluating the derivative of $V(\boldsymbol{r}, \boldsymbol{v}, \theta)$ *along the solutions of system* (3.1) *and using the equation* (3.28) *leads to:*

$$\begin{aligned} \dot{V}(\boldsymbol{r}, v, \theta) &= \kappa_1 \sum_{k=1}^{N} \left(\ddot{\boldsymbol{r}}_k - \omega_0 \boldsymbol{R}^* \dot{\boldsymbol{r}}_k\right)^T \left(\dot{\boldsymbol{r}}_k - \omega_0 \boldsymbol{R}^* \boldsymbol{r}_k\right) + \kappa_2 \dot{\boldsymbol{v}}^T \boldsymbol{L} \boldsymbol{v} \\ &= \sum_{k=1}^{N} u_{1k} \left(\kappa_1 v_k - \kappa_1 \frac{\omega_0}{v_k} \dot{\boldsymbol{r}}_k^T \boldsymbol{R}^* \boldsymbol{r}_k + \kappa_2 \boldsymbol{L}_k \boldsymbol{v}\right) \\ &\quad + \kappa_1 \sum_{k=1}^{N} (\omega_0 - u_{1k}) \omega_0 \dot{\boldsymbol{r}}_k^T \boldsymbol{r}_k \end{aligned}$$

Considering the control law (3.36) *the previous equation leads to:*

$$\dot{V}(\boldsymbol{r}, v, \theta) = -\sum_{k=1}^{N} \left(\kappa_1 v_k - \kappa_1 \frac{\omega_0}{v_k} \dot{\boldsymbol{r}}_k^T \boldsymbol{R}^* \boldsymbol{r}_k - \kappa_2 \boldsymbol{L}_k \boldsymbol{v}\right)^2 - \kappa_1 \sum_{k=1}^{N} \left(\frac{\omega_0}{v_k} \dot{\boldsymbol{r}}_k^T \boldsymbol{r}_k\right)^2 \leq 0$$

Therefore, $V(\boldsymbol{r}, \boldsymbol{v}, \theta)$ *is a suitable Lyapunov function for this system. If the communication graph* $\mathcal{G}$ *is connected, the equilibrium point of the quadratic form* $Q(\boldsymbol{v})$ *is asymptotically stable, thus all the agents converge to the same circular formation.*

□

Previous works already cited [86, 149, 150] deal with the circular formation problem. The agents have unit velocity and converge to a circle of radius $R = 1/\omega_0$. In the control laws presented in Chapter 2 to stabilize the agents to time-varying circular motions, the radius is a parameter of the control law or a desired time-varying reference. In the approach presented in Theorem 3.5, the consensus algorithm provides the final radius of the circular formation. Therefore, the final radius of the circular formation depends on the initial velocities of the agents.

Remark 3.5 *Based on [111] and [150], if the graph is uniformly connected (see Appendix A), the collaborative control law from Theorem 3.5 makes the agents converge to the same circular formation considering time-varying and switched communication graphs.*

Uniform distribution along a circular formation. The methodology developed to accomplish the general control law presented in Theorem 3.4 does not make use of a transformed system. Hence, the potential function already defined in previous sections and applied to distribute the vehicles along a formation depends now on the real heading angle of the vehicles θ_k. We recall the matrix notation for the Laplacian matrix such that, $\bar{\mathbf{L}} = \mathbf{L} \otimes \mathbf{I}_2$ where $\otimes$ is the classical Kronecker product, and the matrix $\mathbf{B}_m = (\cos m\theta_1, \sin m\theta_1, ..., \cos m\theta_N, \sin m\theta_N)^T$ contains all the heading angles of the agents.

The following corollary adds a potential function to the control input u_{2k} whose minimum corresponds to the uniform distribution of the agents along the circular formation.

Corollary 3.3 *(Briñón-Arranz et al. 2011 [18]) Let $\omega_0 \neq 0$, $\kappa_1 > 0$, $\kappa_2 > 0$, and $K > 0$ be four control parameters. Let $\mathcal{G}$ be the communication graph and $\boldsymbol{L}$ be the corresponding Laplacian matrix. Then the control law:*

$$u_{1k} = -\kappa_1 v_k + \kappa_1 \frac{\omega_0}{v_k} \dot{\boldsymbol{r}}_k^T \boldsymbol{R}^* \boldsymbol{r}_k - \kappa_2 \boldsymbol{L}_k \boldsymbol{v} \tag{3.37a}$$

$$u_{2k} = \omega_0 + \kappa_1 \frac{\omega_0}{v_k^2} \dot{\boldsymbol{r}}_k^T \boldsymbol{r}_k - \frac{\partial U}{\partial \theta_k} \tag{3.37b}$$

and

$$U(\theta) = -\frac{K}{N} \sum_{m=1}^{\lfloor N/2 \rfloor} \frac{1}{2m^2} \boldsymbol{B}_m^T \bar{\boldsymbol{L}} \boldsymbol{B}_m \tag{3.38}$$

where $\lfloor N/2 \rfloor$ is the largest integer less than or equal to $N/2$, makes all the agents defined by (3.1) converge to a circular formation centered at the origin and the direction of the rotation defined by the sign of ω_0. Moreover, if the communication graph $\mathcal{G}$ is almost d_0-circular, the radius of the circle is obtained through a consensus algorithm on the agents' velocities and the uniform distribution of the agents along the circle is achieved.

Proof 3.8 *The stability is analyzed by the composed Lyapunov function*

$$V_1(\boldsymbol{r}, \boldsymbol{v}, \theta) = V(\boldsymbol{r}, \boldsymbol{v}, \theta) + U(\theta)$$

whose derivative is expressed as

$$\dot{V}_1(\boldsymbol{r}, \boldsymbol{v}, \theta) = \dot{V}(\boldsymbol{r}, \boldsymbol{v}, \theta) + \nabla U(\theta)$$

Based on previous works of [149, 150], the potential function $U(\theta)$ is invariant to rigid rotations. Therefore, using (3.37) *the derivative of the Lyapunov function satisfies $\dot{V}_1(\boldsymbol{r}, \boldsymbol{v}, \theta) \leq 0$ and the uniform distribution of the agents along the circular formation is locally exponentially stable. The details of the proof are similar than in previous Theorem 2.1 from Chapter 2.*

□

Simulation results. This paragraph presents the simulation results in order to show the performance of previous collaborative control laws. The control law (3.37) is applied to the multi-agent system (3.4) with $\omega_0 = 1$, $\kappa_1 = 0.1$, $\kappa_2 = 0.1$ and $K = 0.1$. The communication graph is a ring, therefore is connected.

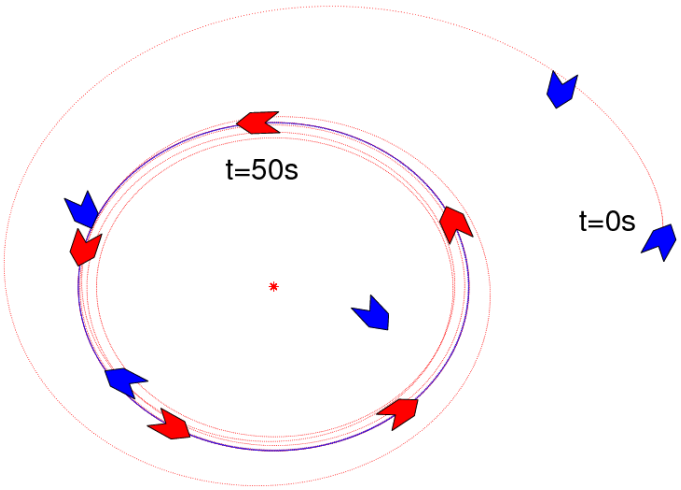

Figure 3.16: *Simulation of five agents governed by the control law* (3.37)*. The red line represents the trajectory of one agent. The same circular formation (blue line) with uniform distribution is reached. $t = 50s$.*

Figure 3.16 displays a simulation of five agents governed by (3.37). The figure shows two snapshots. The blue agents represent the initial conditions and the red ones represent the final state. The agents converge to the same circular motion with angular velocity ω_0. The radius of this circular formation is provided by the consensus term of the control law which enforce agreement on the linear velocity for all the agents.

Figure 3.17 shows the evolution of the linear velocities v_k of the agents from previous simulation. The consensus is reached asymptotically, therefore the agents are stabilized to the same circular formation. The radius of the formation is related to the consensus value for the velocities v_0, such that $R = v_0/\omega_0$.

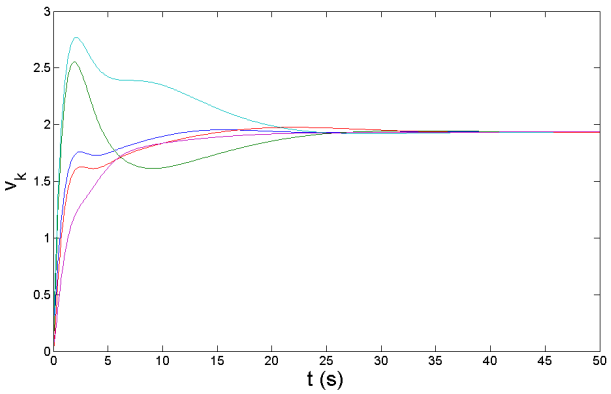

Figure 3.17: *Evolution of the agents' velocities corresponding to the simulation of Figure 3.16*

3.5 Conclusions

This chapter deals with the generalization of the previous results in circular formation control argued in Chapter 2. The main contribution consists in introducing the affine transformations in order to define a larger class of formations called elastic formations. This new formulation allows expressing previous results from Chapter 2 in a compact way and many class of configurations which can be non-circular and time-varying can be obtained.

An elastic motion is defined by a transformation matrix known to all the agents. It is considered as a given reference and its first and second derivatives are not influenced by delays, noise or any other constraints. Nevertheless, some extensions are developed taking into account communication limitations between the agents. The first one, tackle the problem of distributing the agents uniformly along the elastic formation in a collaborative way. A second distributed algorithm based on consensus protocols stabilizes the fleet of agents to a formation whose time-varying center is unknown but its velocity and acceleration are given references. This is the following step to achieve the source-seeking problem.

The new formulation based on affine transformations presented in this chapter is also exploited to elaborate a motion-tracking control law. This algorithm makes a group of agents converge to a time-varying configuration in terms of velocity. It means that all the vehicles follow the same kind of motion (same shape, same speed), defined by a transformation matrix, but not the same trajectory. This control law is improved with cooperative algorithms to make the agents converge to the same formation.

Chapter 4

Collaborative source-seeking

Previous Chapters 2 and 3 deal with the first objective addressed in this thesis: the formation control design of a fleet of autonomous underwater vehicles (AUVs). The contributions presented stabilize the vehicles to time-varying formations which change their shape and are able to follow a given reference of the formation center. The main contribution of this chapter is the design of control strategies in order to generate cooperatively the appropriate direction to move the center formation in order to achieve a source-seeking. The objective is to develop a novel decentralized algorithm which makes the agents agree on a common direction.

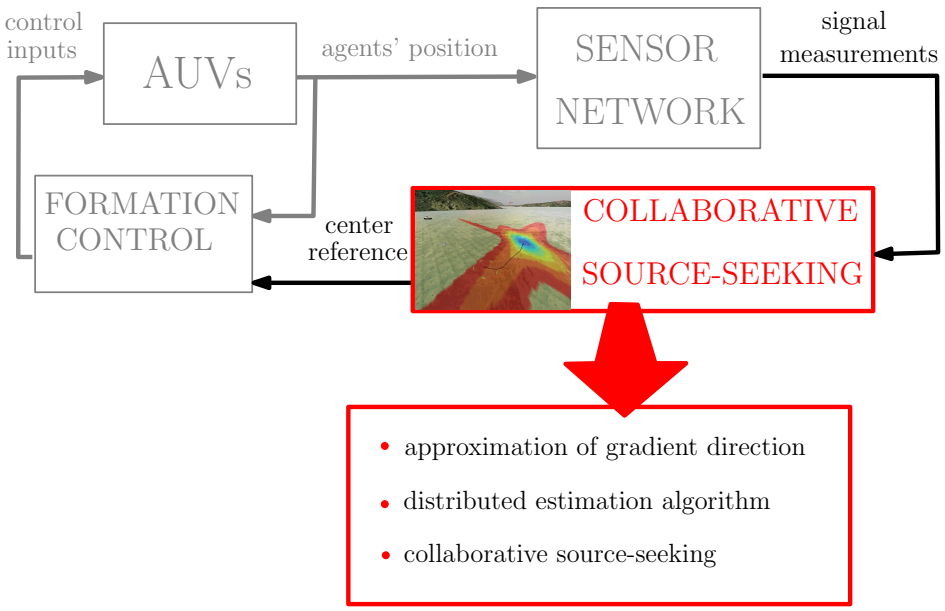

Figure 4.1: *Contributions of Chapter 4*

In particular, the problem of source-seeking using a multi-agent system is addressed here. In order to locate the source of a scalar field, the AUVs are equipped with sensors

which measure the field of interest such as, temperature, salinity, pollutant flow. In this situation, the fleet of vehicles can be seen as a mobile sensor network. The stabilization of the agents uniformly distributed along a circular formation is pertinent to tackle the source-seeking problem. According to previous results in formation control, this chapter focuses on obtaining the adequate reference of the center to steer the fleet of agents to the location of an underwater source, as explained in Figure 4.1.

A first contribution shows that collecting the sensor data from vehicles, which are uniformly distributed along a fixed circular formation, allows us to approximate the gradient of the signal distribution. Then, a distributed algorithm based on this result is proposed to estimate the gradient direction taking into account communication constraints. This approach combines the previous results on formation control exposed in Chapter 2 and existing results on consensus filters applied to this mobile sensor network situation. A modified algorithm which exploits the periodic properties of the circular formation is also proposed. Finally, a comparison of the two distributed algorithms is discussed and motivated by simulations.

4.1 Problem statement

This chapter deals with collaborative source-seeking algorithms in order to drive a formation of AUVs to the location of an underwater source. The problem is tackled in a 2-dimensional space, hence the configuration considered is a planar formation. As in previous chapters, it is assumed that the agents have no physical extension, *i.e.*, their positions are single points.

The following assumptions are considered in the sequel to deal with this new contribution:

- The fleet composed by N vehicles is stabilized to a circular formation with radius R and centered at $\mathbf{c}$. The vehicles are uniformly distributed along the circular formation.
- Each vehicle $k = 1, \ldots, N$ is able to measure the signal strength in the environment. It is assumed that the sensor has not dynamics.
- The communication topology of the fleet of vehicles is represented by an undirected graph $\mathcal{G}$.
- Communication constraints such as noise, packet loss and time delays are not considered.

This chapter takes into consideration several assumptions about the scalar field measured. The signal distribution representing the scalar field is continuous. This

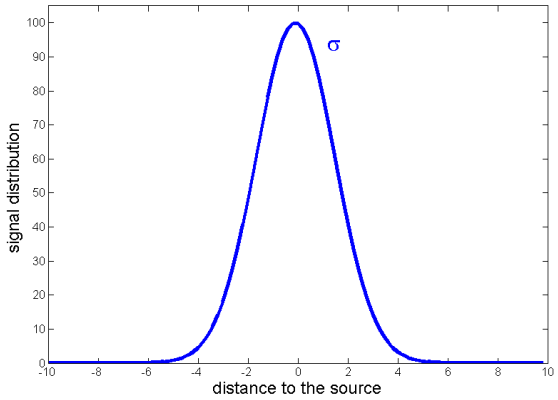

Figure 4.2: *Signal distribution modeled as a Gaussian function emitted by a single source.*

signal is emitted by a single source such that the source is the only maximum or minimum of the scalar field. The signal distribution is assumed to decay away from the position of the source. There are not local extremum thus, the signal distribution decreases or increases from the source, as shown in Figure 4.2.

Under these assumptions, this chapter presents distributed strategies to estimate the gradient direction of a signal distribution by a circular formation of agents. This direction can be used to steer the fleet to the maximum or minimum of the signal.

4.2 Survey on source-seeking

The source localization of a signal distribution is a problem considered in recent literature. There are different approaches to deal with this topic, but the common objective is to calculate the position of a source using measurements of the signal propagation. In mathematical terms, the signal distribution is a spacial function representing the scalar field with a maximum or minimum in the position where the source is located. The source could be a radio transmitter and the signal would be a radio frequency transmission, for instance. Alternatively, the source could be a point of chemical contamination and the signal would be that chemical's concentration in the environment.

Source-seeking algorithms are designed to steer a vehicle or a group of vehicles to the physical location of the source (or at least to the vicinity thereof). It means that some techniques to estimate the location of the source such as triangulation are not considered here. Several different approaches have been proposed in current literature. Some results dealing with odor source localization, based on swarms intelligence [38, 67, 175], present distributed algorithms which use measurements of the source plume and of the wind or flow that creates this plume. In an underwater context, usually, the vehicles

are only equipped with sensors which are able to take concentration measurements of the quantity of interest (salinity, pollutant or methane concentrations, for instance). The aim is thus, to drive the vehicles to the source avoiding the estimation of the real plume and eluding the computation of the function representing the scalar field.

Several source-seeking algorithms are based on gradient-descent methods. A comparison between gradient search and evolutionary algorithms is presented in [141]. These strategies are usually developed and applied in the field of Computer Sciences. In [34], a gradient method which converges in finite-time is developed. In this work the bases of the gradient search are presented. Consider a scalar function $f : \mathbb{R}^d \to \mathbb{R}$, where $d \in \mathbb{N}$ and the following gradient system:

$$\dot{x} = -\nabla f(x)$$

The minimum of function f is a stable equilibrium for this system and if the level sets of the function are bounded then, the trajectories converge asymptotically to the set of critical points of f. Note that, changing the sign of the algorithm the gradient-descent method makes the system converge to the maximum of the function. In conclusion, the computation of the gradient of the signal propagation allows steering a vehicle to the source location (if there only exists a minimum or a maximum of the signal distribution). If it is available, the gradient of the signal strength can be used to produce a gradient-decent algorithm for a vehicle or group of vehicles [4], but this information may not be available in reality. One alternative is to use spatially distributed measurements of the signal strength to approximate its gradient. In the literature there are two different strategies to collect distributed measurements. The fist one uses a single vehicle which changes its position over time in order to measure the signal propagation in different positions. The other option considers a group of vehicles collaborating to collect the measurements. A proposed classification of the different approaches to deal with the source-seeking problem is presented in the sequel.

One single vehicle

In this approach, one single vehicle (mobile sensor) measures a scalar field distribution during its motion. Spatially distributed measurements of the signal propagation are collected to estimate its gradient and steer the vehicle to the maximum or minimum of the scalar field. There exist different methodologies to estimate the gradient of a signal propagation. The following results tackle the source-seeking problem with a single vehicle.

a) Gradient-descent method

A first result concerning the location of a source with a single vehicle is presented

in [23]. In this work, an AUV obtains different measurements of a hydrothermal plume by a circle maneuvre. This technique allows estimating the two dimensional gradient and thanks to a least squares solution of the overall slop the vehicle is driven towards the source. A least square gradient estimation combined with a gradient-descent method is also used in [4] to steer a single vehicle to the maximum or minimum of a scalar field. A reactive control law for unicycle vehicles for ascending/descending along a potential field is presented in [6]. In this approach the control is related to the geometry of the potential field.

In [166], the gradient of the signal distribution is estimated in discrete time by a nonlinear optimization algorithm. In [123], an algorithm to achieve the location of a vapor-emitting source with a single mobile sensor is developed computing the gradients of the Cramér-Rao bound on the location error with respect to the sensor's coordinates.

b) Extremum seeking

The extremum seeking problem is an important contribution on the field of adaptive control [156]. This method is a non-model-based optimization which can be simply defined as tracking a maximum or minimum of a function. The first stability proof of the extremum seeking algorithm appears in [82]. This technique has been adopted to many different applications [3].

The extremum seeking method applied to the source-seeking problem consist in adding an excitatory input to the vehicle's steering control, using a special filter on the signal strength measurement to approximate its gradient, and using this information to drive the vehicle towards the source. This approach has been analyzed under different assumptions [28, 29, 30, 176]. In [100, 101], an hybrid controller is implemented to improve the extremum seeking performances according to the source localization task. In these works, an optimization method with successive line minimizations and heading changes, based on conjugate vectors, is developed. For a certain class of signal strength distributions, the resulting system is shown to be practically stable under perturbations. An extension to 3-dimensions is accomplished in [31]. Finally, a novel stochastic approach based on the clasical extremum seeking algorithm is introduced in [93] and [154].

Another interesting approach proposed in [99], presents a strategy belonging to the class of sliding mode control laws, but in this case, the single vehicle does not need to compute the gradient of the signal distribution to reach its source.

All these works consider a single vehicle collecting the measurements. The main disadvantage of these approaches is that in order to collect sufficient information, the

vehicle may have to travel over large distances. In this situation the vehicle's convergence to the source location may be delayed.

Multi-agent systems

A group of moving vehicles allows gathering sufficient information about the signal to carry out the source-seeking problem. Spatially distributed vehicles collecting measurements are considered in order to avoid sinusoidal excitation of a vehicle used in the extremum seeking method or the long distances traveled by a single mobile sensor, for instance. In the sequel, the principal results in source-seeking with multi-agent systems are detailed.

a) Gradient climbing

A first approach developed in [105], considers that each vehicle is able to measure the full gradient at its current position. The authors present an algorithm including a gradient-descent term and inter-vehicle forcing terms for a group of vehicles modeled with simple integrator dynamics. Another strategy consists in approximating the gradient value of the signal using concentration measurements of multiple vehicles at different locations [64]. In this work, a group of gilders equipped with sensors estimates the model parameters of the scalar field via collected measurements. A least square approximation is applied in order to steer the group of agents to the source location. In [55], a real application of previous approach is presented. A gradient-descent method is applied in [4] considering that each vehicle of the fleet is driven by an estimate of the local environmental gradient together with control forces that maintain uniformity in group geometry.

b) Extremum seeking

Based on previous results in extremum seeking for one vehicle, the authors of [13] are able to drive a formation of agents to the maximum or minimum of a scalar field. This approach considers one leader which implements the extremum seeking algorithm and the rest of agents follows the leader keeping a particular formation. Therefore, this is not a collaborative source-seeking algorithm, and the source localization is carried out only by the leader. In [61], the extremum seeking method is improved to make a group of agents accomplish the source-seeking task in 1-dimension in a collaborative way.

c) Stochastic approach

In [140], a group of chemical sensors placed at different locations, measures plume concentration values to estimate the source of that plume. The source localization is achieved using a stochastic approximation technique. This approach can

be considered as a distributed estimation method as in [124], which employs the sensor measurements to estimate the model parameters of the concentration plume.

A collaborative control law to steer a fleet of AUVs to the source of a signal distribution using only direct signal measurements by a circular formation of agents is presented in [104]. This work will be analyzed in detail in the previous section.

4.3 Preliminaries

The aim is here to locate the source of some signal distribution using a fleet of AUVs. In this situation, the vehicles are equipped with sensors which are able to measure the concentration of the quantity of interest. The fleet of agents becomes a mobile wireless sensors network. The contribution of this chapter focuses on designing a collaborative algorithm to chose an appropriate direction in order to steer a formation of AUVs to the source localisation. The control strategy proposed in this thesis is composed of two levels:

1. Estimation of the gradient direction of the signal distribution of the source.

2. Generation of a reference trajectory for the formation center based on the estimated gradient direction.

This chapter copes only with the first step: to provide an algorithm which estimates the gradient direction of a signal distribution by a formation of agents. In future research, this direction will be used to drive the formation center to the maximum or minimum of the scalar field.

Considering the source as a target, it seems interesting to use a circular formation to cope with the source-seeking problem. When the formation reach the source position, the vehicles will turn around this source. This strategy is suitable in the context of underwater source localization because, even if the source is fixed, the AUVs are always moving. This is convenient considering that the agents must to avoid zero speed. The same constraints appear in an aerial scenario in which a fleet of Unmanned Aerial Vehicles (UAVs) accomplishes a target tracking mission, for instance. Some results in target localization and circumnavigation (it means that the vehicles describes circular trajectories around the target) have been recently developed using bearing measurements [44]. This result are built on the idea that each agent can measure the bearing angle between its position and the target. The source-seeking problem considered in this thesis regards the previous approaches in the field in which the

source of a signal propagation is locate by the signal measurements. Therefore, the techniques using bearing measurements are not applicable in this context.

In Chapter 2, a control law which asymptotically stabilizes a group of vehicles modeled with unicycle kinematics, such as

$$\begin{aligned} \dot{x}_k &= v_k \cos\theta_k \\ \dot{y}_k &= v_k \sin\theta_k \\ \dot{\theta}_k &= u_k \end{aligned}$$

where $\dot{\mathbf{r}}_k = (\dot{x}_k, \dot{y}_k)^T$, to a circular formation around a dynamic center point $\mathbf{c}(t) = (c_x, c_y)^T$ with a uniform distribution (*i.e.*, with the agents evenly separated on the circle by $2\pi/N$ radians each) is presented. This translation control law from Corollary 2.1 is given by:

$$\dot{v}_k = -\beta v_k + \frac{\hat{u}_k \dot{\mathbf{r}}_k^T \mathbf{R}_{\frac{\pi}{2}} \dot{\hat{\mathbf{r}}}_k + \dot{\mathbf{r}}_k^T (\ddot{\mathbf{c}} + \beta(\dot{\hat{\mathbf{r}}}_k + \dot{\mathbf{c}}))}{v_k} \tag{4.1a}$$

$$u_k = \frac{\hat{u}_k \dot{\mathbf{r}}_k^T \dot{\hat{\mathbf{r}}}_k + \dot{\mathbf{r}}_k^T \mathbf{R}_{\frac{\pi}{2}}^T (\ddot{\mathbf{c}} + \beta(\dot{\hat{\mathbf{r}}}_k + \dot{\mathbf{c}}))}{v_k^2} \tag{4.1b}$$

where the closed-loop dynamics of the reference model $\dot{\hat{\mathbf{r}}}_k = (\dot{\hat{x}}_k, \dot{\hat{y}}_k)^T$ defined by

$$\begin{aligned} \dot{\hat{x}}_k &= R|\omega_0| \cos\psi_k \\ \dot{\hat{y}}_k &= R|\omega_0| \sin\psi_k \\ \dot{\psi}_k &= \hat{u}_k \end{aligned}$$

are imposed by

$$\begin{cases} \hat{u}_k = \omega_0(1 + \kappa \dot{\hat{\mathbf{r}}}_k^T \hat{\mathbf{r}}_k) - \frac{\partial U}{\partial \psi_k} \\ U(\psi) = \frac{K}{N} \sum_{m=1}^{\lfloor N/2 \rfloor} \frac{1}{2m^2} \mathbf{B}_m \bar{\mathbf{L}} \mathbf{B}_m \end{cases}$$

where the Laplacian matrix of the communication graph considered is $\bar{\mathbf{L}} = \mathbf{L} \otimes \mathbf{I}_2$, $b_{mk} = (\cos m\psi_k, \sin m\psi_k)^T$ represents the vector which contains the transformed orientation angle, $\mathbf{B}_m = (b_{m1}^T, \ldots, b_{mN}^T)^T$, and $\omega_0 \neq 0$, $\kappa > 0$, $\beta > 0$ are three control parameters.

This control law makes a fleet of agents modeled with unicycle kinematics, converge to a circular motion of radius R, and whose center tracks the time-varying reference $\mathbf{c}(t)$. The direction of rotation is determined by the sign of ω_0. Moreover, for $K > 0$, if the graph is d_0-circulant, the set of curve-phase arrangements that are balanced modulo $2\pi/N$ is locally exponentially stable.

In this situation, the center of the formation $\mathbf{c}(t)$ is an external reference known to all the agents. This result is a first step to deal with the source-seeking problem. To move the formation towards the location of the source, the objective now is to compute the trajectory of the formation center in a collaborative way taking into account the measurements of the signal distribution emitting by the source.

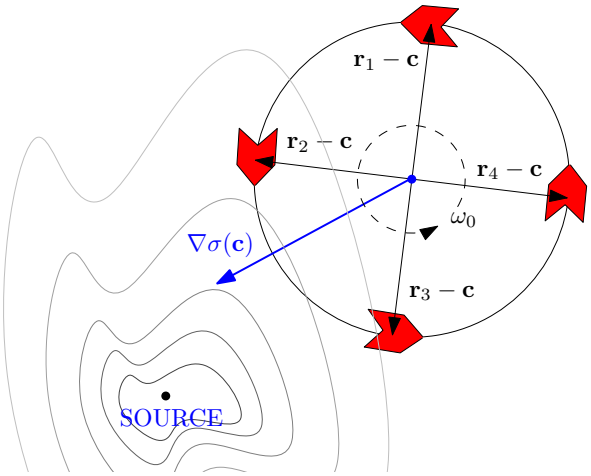

Figure 4.3: *Illustration of the source-seeking problem*

Thanks to previous control law (4.1), the vehicles are stabilized to a circular formation described by a center point $\mathbf{c}$, a radius R and an angle ϕ which is linearly increasing with time (*i.e.* $\phi = \omega_0 t$ for some angular speed $\omega_0 > 0$). In the sequel, the position of each agent k in the formation is given by the following equation:

$$x_k = c_x + R\cos\left(\phi + k\frac{2\pi}{N}\right) \tag{4.2a}$$

$$y_k = c_y + R\sin\left(\phi + k\frac{2\pi}{N}\right) \tag{4.2b}$$

This equation describes a formation where the agents are uniformly distributed along a circle of radius R. In the context of source-seeking problem, the objective is that the center of the formation $\mathbf{c}(t)$ follows a trajectory which converges to the maximum of a signal, that is usually its source.

4.3.1 Approximation of the gradient by a fixed circular formation

The first idea is to design an algorithm to estimate the gradient direction of the signal distribution based on the concentration measurements obtained by a circular formation of agents. Communication constraints between the vehicles are taken into account. This estimated direction will be the reference velocity of the formation center in order to steer the group of agents to the source position as represented in Figure 4.3.

Consider a fleet of N vehicles uniformly distributed along a circular formation. The position of each agent k is described by equation (4.2). In this first step of the control strategy previously detailed to deal with the source-seeking problem, the

circular formation is not moving. Only the estimation of gradient direction is addressed here.

Assumption 4.1 *The center of the circular formation* $\boldsymbol{c}$ *is fixed and known to all the agents.*

The distribution of the signal strength in the environment will be described by an unknown positive spatial mapping $\sigma : \mathbb{R}^2 \to \mathbb{R}^+$, and so agent k measures the signal strength at its position as $\sigma(\mathbf{r}_k)$. Let us consider a mobile sensor network, in which the position of the sensor k is given by (4.2), taking measurements of a signal distribution σ. Let $\nabla\sigma(\mathbf{c}) = (\nabla_x\sigma(\mathbf{c}), \nabla_y\sigma(\mathbf{c}))$ denote the gradient of function σ at the center of the circular formation $\mathbf{c}$. The following lemma is proposed:

Lemma 4.1 *(Briñón-Arranz et al. 2011 [20]) Let* σ *be a bounded function and* $\sigma(\boldsymbol{r}_k)$ *the measure obtained by agent* k *where* $\boldsymbol{r}_k$ *is its position vector given by* (4.2)*. Considering a fleet of* $N > 2$ *agents, if Assumption 4.1 is satisfied and the agents are uniformly distributed along the circle centered at* $\boldsymbol{c}$*, then:*

$$\frac{1}{N}\sum_{k=1}^{N}\sigma(\boldsymbol{r}_k)(\boldsymbol{r}_k - \boldsymbol{c}) = \frac{R^2}{2}\nabla\sigma(\boldsymbol{c})^T + o(R^2) \tag{4.3}$$

where $o(R^2)$ *is a vector such that* $\|o(R^2)\|$ *is negligible with respect to* R^2*.*

Proof 4.1 *To prove this result it is necessary to define the following equation:*

$$\sum_{k=0}^{N-1} z^k = \begin{cases} (1-z^N)/(1-z), & \text{if} \quad z \neq 1 \\ N & \text{if} \quad z = 1 \end{cases} \tag{4.4}$$

where $z \in \mathbb{C}$ *and* $N \in \mathbb{R}^+$*. This equation is satisfied according to some properties of telescoping series [22].*

According to the linear approximation of function σ *at a fixed location* $\boldsymbol{c}$ *the following equation holds:*

$$\sigma(\boldsymbol{r}_k) - \sigma(\boldsymbol{c}) = \nabla\sigma(\boldsymbol{c})(\boldsymbol{r}_k - \boldsymbol{c}) + o(R) \tag{4.5}$$

This expression is equivalent to the first two terms in the multi-variable Taylor series expansion of σ *at* $\boldsymbol{c}$*.*

Multiplying the previous equation (4.5) *by the relative vector* $(\boldsymbol{r}_k - \boldsymbol{c})$ *and summing over* $k = 1, \ldots, N$*, it yields:*

$$\frac{1}{N}\sum_{k=1}^{N}(\sigma(\boldsymbol{r}_k) - \sigma(\boldsymbol{c}))(\boldsymbol{r}_k - \boldsymbol{c}) = \frac{1}{N}\sum_{k=1}^{N}\left(\nabla\sigma(\boldsymbol{c})(\boldsymbol{r}_k - \boldsymbol{c})\right)(\boldsymbol{r}_k - \boldsymbol{c}) + o(R^2)$$

The first sum is equivalent to:

$$\frac{1}{N}\sum_{k=1}^{N}(\sigma(\boldsymbol{r}_k)-\sigma(\boldsymbol{c}))(\boldsymbol{r}_k-\boldsymbol{c}) = \frac{1}{N}\sum_{k=1}^{N}\sigma(\boldsymbol{r}_k)(\boldsymbol{r}_k-\boldsymbol{c}) - \sigma(\boldsymbol{c})\frac{1}{N}\sum_{k=1}^{N}(\boldsymbol{r}_k-\boldsymbol{c})$$

Considering the model defined in (4.2) *for the agents and using equation* (4.4) *when* $z = e^{i\frac{2\pi}{N}}$ *the following equality is satisfied if* $N > 1$*:*

$$\sum_{k=1}^{N}(\boldsymbol{r}_k-\boldsymbol{c}) = R\sum_{k=1}^{N}\left(e^{i\frac{2\pi}{N}}\right)^k = \frac{1-e^{i2\pi}}{1-e^{i\frac{2\pi}{N}}} = 0$$

Therefore the previous equation can be rewritten as:

$$\frac{1}{N}\sum_{k=1}^{N}\sigma(\boldsymbol{r}_k)(\boldsymbol{r}_k-\boldsymbol{c}) = \frac{1}{N}\sum_{k=1}^{N}\left(\nabla\sigma(\boldsymbol{c})(\boldsymbol{r}_k-\boldsymbol{c})\right)(\boldsymbol{r}_k-\boldsymbol{c}) + o(R^2)$$

Analyzing in terms of components and using (4.2) *to express the position of the agents* $\boldsymbol{r}_k$*, the right-hand side of the previous equation is given by:*

$$\sum_{k=1}^{N}\left(\nabla\sigma(\boldsymbol{c})(\boldsymbol{r}_k-\boldsymbol{c})\right)(\boldsymbol{r}_k-\boldsymbol{c}) = R^2\sum_{k=1}^{N}\begin{pmatrix}\nabla_x\sigma(\boldsymbol{c})\cos^2\phi_k + \nabla_y\sigma(\boldsymbol{c})\cos\phi_k\sin\phi_k \\ \nabla_x\sigma(\boldsymbol{c})\sin\phi_k\cos\phi_k + \nabla_y\sigma(\boldsymbol{c})\sin^2\phi_k\end{pmatrix}$$

where $\phi_k = \phi + k\frac{2\pi}{N}$*.*

Using trigonometric properties each component of the right sum is rewritten:

$$\nabla_x\sigma(\boldsymbol{c})\cos^2\phi_k + \nabla_y\sigma(\boldsymbol{c})\cos\phi_k\sin\phi_k = \nabla_x\sigma(\boldsymbol{c})\cos^2\phi_k + \frac{1}{2}\nabla_y\sigma(\boldsymbol{c})\sin 2\phi_k \quad (4.6a)$$

$$\nabla_x\sigma(\boldsymbol{c})\sin\phi_k\cos\phi_k + \nabla_y\sigma(\boldsymbol{c})\sin^2\phi_k = \frac{1}{2}\nabla_x\sigma(\boldsymbol{c})\sin 2\phi_k + \nabla_y\sigma(\boldsymbol{c})\sin^2\phi_k \quad (4.6b)$$

Consequently, there are two sums which need an exhaustively analysis:

$$\sum_{k=1}^{N}\sin^2\phi_k \quad \textit{and} \quad \sum_{k=1}^{N}\sin 2\phi_k$$

Using the trigonometric identity and other trigonometric properties, the first previous sum can be expressed as:

$$\begin{aligned}\sum_{k=1}^{N}\sin^2\phi_k &= \sum_{k=1}^{N}\frac{1-\cos 2\phi_k}{2} \\ &= \frac{N}{2} - \frac{1}{2}\sum_{k=1}^{N}\left(\cos(2\phi)\cos(k\frac{4\pi}{N}) - \sin(2\phi)\sin(k\frac{4\pi}{N})\right) \\ &= \frac{N}{2} - \frac{\cos(2\phi)}{2}\sum_{k=1}^{N}\cos(k\frac{4\pi}{N}) + \frac{\sin(2\phi)}{2}\sum_{k=1}^{N}\sin(k\frac{4\pi}{N})\end{aligned}$$

In order to determine the result of these new trigonometric sums, a detailed mathematical study is provided. According to the properties of the telescoping series (4.4)*, choosing* $z = e^{i\frac{4\pi}{N}}$*, the following equality is satisfied if* $N > 2$*:*

$$\sum_{k=1}^{N} \left(e^{i\frac{4\pi}{N}}\right)^k = \frac{1 - e^{i\frac{4\pi}{N}N}}{1 - e^{i\frac{4\pi}{N}}} = \frac{1 - e^{i4\pi}}{1 - e^{i\frac{4\pi}{N}}} = 0$$

In conclusion, due to the definition $e^{i\frac{4\pi}{N}} = \cos(\frac{4\pi}{N}) + i\sin(\frac{4\pi}{N})$*, the following trigonometric sums are equal to zero, if* $N > 2$*:*

$$\sum_{k=1}^{N} \cos(k\frac{4\pi}{N}) = 0 \quad \textit{and} \quad \sum_{k=1}^{N} \sin(k\frac{4\pi}{N}) = 0 \tag{4.7}$$

Therefore, the first sum studied here can be expressed as:

$$\sum_{k=1}^{N} \sin^2 \phi_k = \frac{N}{2} \tag{4.8}$$

In the sequel, the sum of the term corresponding to $\sin 2\phi_k$ *is studied:*

$$\begin{aligned} \frac{1}{N}\sum_{k=1}^{N} \sin 2\phi_k &= \frac{1}{N}\sum_{k=1}^{N} \sin\left(2\phi + k\frac{4\pi}{N}\right) \\ &= \frac{\sin 2\phi}{N}\sum_{k=1}^{N} \cos(k\frac{4\pi}{N}) + \frac{\cos 2\phi}{N}\sum_{k=1}^{N} \sin(k\frac{4\pi}{N}) \end{aligned}$$

Thanks to (4.7) *(i.e., due to the uniform distribution), if* $N \geq 2$ *then:*

$$\sum_{k=1}^{N} \sin(2\phi_k) = 0 \tag{4.9}$$

Since both equalities (4.8) *and* (4.9) *are satisfied and by the decomposition of previous components equations* (4.6)*, finally, the following equation holds:*

$$\frac{1}{N}\sum_{k=1}^{N} \left(\nabla\sigma(\boldsymbol{c})(\boldsymbol{r}_k - \boldsymbol{c})\right)(\boldsymbol{r}_k - \boldsymbol{c}) = \frac{R^2}{2}\nabla\sigma(\boldsymbol{c})^T$$

Thus, the equality (4.3) *presented in Lemma 4.1 is satisfied.*

□

Lemma 4.2 *(Briñón-Arranz et al. 2011 [20]) Let* σ *be a bounded function and* $\sigma(\boldsymbol{r}_k)$ *the measure obtained by agent* k *where* $\boldsymbol{r}_k$ *is its position vector given by* (4.2)*. Considering a limitless number of agents along the circular formation* ($N \to \infty$)*, if Assumption 4.1 is satisfied, then:*

$$\frac{1}{2\pi}\int_0^{2\pi} \sigma(\boldsymbol{r}_k)(\boldsymbol{r}_k - \boldsymbol{c})d\phi = \frac{R^2}{2}\nabla\sigma(\boldsymbol{c})^T + o(R^2) \tag{4.10}$$

Proof 4.2 *A similar analysis that it is followed in previous lemma, can be applied to this second case. Integrating along the circle (in the interval* $[0, 2\pi]$*) and multiplying by the relative positions of the agents* $\boldsymbol{r}_k - \boldsymbol{c}$*, the equation* (4.5) *becomes:*

$$\frac{1}{2\pi}\int_0^{2\pi}(\sigma(\boldsymbol{r}_k)-\sigma(\boldsymbol{c}))(\boldsymbol{r}_k-\boldsymbol{c})d\phi = \frac{1}{2\pi}\int_0^{2\pi}\left(\nabla\sigma(\boldsymbol{c})(\boldsymbol{r}_k-\boldsymbol{c})\right)(\boldsymbol{r}_k-\boldsymbol{c})d\phi + o(R^2)$$

In this case, considering (4.2) *when* $N \to \infty$*, it is easy to see that the following equation holds:*

$$\int_0^{2\pi}(\boldsymbol{r}_k-\boldsymbol{c})d\phi = R\int_0^{2\pi}e^{i\phi} = 0$$

In consequence the first expression is now rewritten as:

$$\frac{1}{2\pi}\int_0^{2\pi}\sigma(\boldsymbol{r}_k)(\boldsymbol{r}_k-\boldsymbol{c})d\phi = \frac{1}{2\pi}\int_0^{2\pi}\left(\nabla\sigma(\boldsymbol{c})(\boldsymbol{r}_k-\boldsymbol{c})\right)(\boldsymbol{r}_k-\boldsymbol{c})d\phi + o(R^2)$$

Hence, one more time the right-hand term of the previous equation have to be analyzed in detail. Using trigonometric properties the following integrals are solved:

$$\int_0^{2\pi}\sin^2\phi d\phi = \pi \quad \textit{and} \quad \int_0^{2\pi}\cos\phi\sin\phi d\phi = 0 \tag{4.11}$$

Thanks to these equalities (4.11) *the following equation holds:*

$$\frac{1}{2\pi}\int_0^{2\pi}\left(\nabla\sigma(\boldsymbol{c})(\boldsymbol{r}_k-\boldsymbol{c})\right)(\boldsymbol{r}_k-\boldsymbol{c})d\phi = \frac{R^2}{2}\nabla\sigma(\boldsymbol{c})^T \tag{4.12}$$

and (4.10) *is straightforwardly obtained.*

□

Both results provide an approximation of the gradient of the signal distribution at the center of the circular formation. A similar result can be obtained for a moving source (which is equivalent to a time-varying signal propagation function in the space), such that the signal distribution σ depends both on position and time, *i.e.* $\sigma(\mathbf{r}_k, t)$. Consider a fleet of agents given by (4.2) taking measurements of a signal distribution σ. An extension of the previous Lemma 4.1 is proposed in the sequel to cope with this time-varying signal distribution.

Lemma 4.3 *(Briñón-Arranz et al. 2011 [19]) Let* σ *be a bounded function and* $\sigma(\boldsymbol{r}_k, t)$ *the measure obtained at time* t *by agent* k*, where* $\boldsymbol{r}_k$ *is its position vector given by* (4.2)*. If Assumption 4.1 is satisfied and the agents are uniformly distributed along the circular formation centered at* $\boldsymbol{c}$*, then for a fleet of* $N > 2$ *agents, the following equation is satisfied:*

$$\frac{1}{N}\sum_{k=1}^{N}\sigma(\boldsymbol{r}_k,t)(\boldsymbol{r}_k-\boldsymbol{c}) = \frac{R^2}{2}\nabla\sigma(\boldsymbol{c},t)^T + o(R^2) \tag{4.13}$$

Proof 4.3 *The proof is similar to the one of Lemma 4.1. According to the linear approximation of the function σ at a fixed location $\boldsymbol{c}$ the following equation holds:*

$$\forall t \quad \sigma(\boldsymbol{r}_k, t) - \sigma(\boldsymbol{c}, t) = \nabla\sigma(\boldsymbol{c}, t)(\boldsymbol{r}_k - \boldsymbol{c}) + o(R)$$

Multiplying this equation by the relative vector $(\boldsymbol{r}_k - \boldsymbol{c})$ and summing over $k = 1, \ldots, N$, it yields:

$$\forall t \quad \frac{1}{N}\sum_{k=1}^{N}(\sigma(\boldsymbol{r}_k, t) - \sigma(\boldsymbol{c}, t))(\boldsymbol{r}_k - \boldsymbol{c}) = \frac{1}{N}\sum_{k=1}^{N}\left(\nabla\sigma(\boldsymbol{c}, t)(\boldsymbol{r}_k - \boldsymbol{c})\right)(\boldsymbol{r}_k - \boldsymbol{c}) + o(R^2)$$

Considering the model defined in (4.2) *for the agents and using equation* (4.4) *when $z = e^{i\frac{2\pi}{N}}$ the following equality is satisfied if $N > 1$:*

$$\forall t \quad \sum_{k=1}^{N}(\boldsymbol{r}_k - \boldsymbol{c}) = R\sum_{k=1}^{N}\left(e^{i\frac{2\pi}{N}}\right)^k = \frac{1 - e^{i2\pi}}{1 - e^{i\frac{2\pi}{N}}} = 0$$

Therefore, the previous equation can be rewritten as:

$$\forall t, \quad \frac{1}{N}\sum_{k=1}^{N}\sigma(\boldsymbol{r}_k, t)(\boldsymbol{r}_k - \boldsymbol{c}) = \frac{1}{N}\sum_{k=1}^{N}\left(\nabla\sigma(\boldsymbol{c}, t)(\boldsymbol{r}_k - \boldsymbol{c})\right)(\boldsymbol{r}_k - \boldsymbol{c}) + o(R^2)$$

The rest of the proof follows the same steps that in previous one from Lemma 4.1 taking into account that function σ depends now on time. Using trigonometric properties equation (4.13) *is obtained.*

□

The previous three lemmas show that the gradient direction of a signal distribution can be approximated via collected measurements obtained by a fixed circular formation of vehicles. Following sections will make use of this result to built collaborative algorithms to estimate the direction of the gradient in order to steer the formation of agents to the source position.

4.3.2 Centralized approach

A first result in collaborative source-seeking by a circular formation of agents is accomplished in [104]. The authors consider here a stable circular formation of N mobile agents in the plane. The agents are stabilized by the previous translation control law (4.1) presented in Chapter 2. An outer-loop control that steers the formation by determining $\dot{\mathbf{c}}(t)$ in a collaborative way is provided. In this case the source-seeking is achieved by a time-varying circular formation. That is to say that the system is considered as the two dimensional single integrator such that:

$$\dot{\mathbf{c}} = u \tag{4.14}$$

The control signal u will be based on measurements of signal strength taken by the individual agents. The following control law is proposed:

$$u = \lambda \sum_{k=1}^{N} \sigma(\mathbf{r}_k)(\mathbf{r}_k - \mathbf{c}) \tag{4.15}$$

which is a sum of the agents' current normalized displacement vectors from the center of the formation, $\mathbf{r}_k - \mathbf{c}$, weighted by their individual signal strength measurements, $\sigma(\mathbf{r}_k)$, and a common possibly time-varying gain factor, $\lambda > 0$. This control law steers the formation in the direction of an estimate of the gradient of σ at the point $\mathbf{c}$ based on the signal strength measurements taken by the agents distributed uniformly about $\mathbf{c}$.

The stability of system (4.14) under the control law (4.15) is analized in two cases: signal distributions with circular level sets and signal distributions with elliptical level sets. This result does not takes into account the previous Lemma 4.1, hence the authors of [104] only study the convergence of this centralized algorithm if the level sets of the signal distribution are convex. Note that, Lemma 4.1 only addresses the case of a fixed formation.

Signal distributions with circular level sets: The first result presented in [104] deals with a simple case in which the level sets of the signal distribution are circular, it means that the source plume has a Gaussian profile.

Theorem 4.1 *(Moore and Canudas-de-Wit 2010 [104]) Assume that the signal strength is a continuously differentiable mapping and satisfies the following property:*

$$\|\boldsymbol{p}_1 - \boldsymbol{p}^*\| > \|\boldsymbol{p}_2 - \boldsymbol{p}^*\| \Rightarrow \sigma(\boldsymbol{p}_1) < \sigma(\boldsymbol{p}_2) \tag{4.16}$$

where $\boldsymbol{p}_j \in \mathbb{R}^2$ represents an arbitrary point in the 2-D space. The previous inequality means that the signal strength has a maximum at some point $\boldsymbol{p}^*$ and is strictly decreasing as the Euclidean distance from $\boldsymbol{p}^*$ increases (and thus has circular level sets). Under the control input of (4.15) *the point $\boldsymbol{c} = \boldsymbol{p}^*$ is an asymptotically stable equilibrium of system* (4.14)*.*

Proof 4.4 *To analyze the stability of the system the following Lyapunov function is defined:*

$$V(\boldsymbol{c}) = \sigma(\boldsymbol{p}^*) - \sigma(\boldsymbol{c}) \tag{4.17}$$

which is zero at $\boldsymbol{c} = \boldsymbol{p}^*$ and positive otherwise. This Lyapunov function has the time derivative

$$\dot{V}(\boldsymbol{c}) = -\nabla\sigma(\boldsymbol{c})\dot{\boldsymbol{c}} \tag{4.18}$$

Substituting the control formula (4.15) *for* $\dot{\boldsymbol{c}}$ *in* (4.18) *yields*

$$\dot{V}(\boldsymbol{c}) = -\nabla\sigma(\boldsymbol{c})\lambda\sum_{k=1}^{N}\sigma(\boldsymbol{r}_k)(\boldsymbol{r}_k-\boldsymbol{c}) = -\lambda\sum_{k=1}^{N}\sigma(\boldsymbol{r}_k)\nabla\sigma(\boldsymbol{c})(\boldsymbol{r}_k-\boldsymbol{c}) \tag{4.19}$$

The assumption (4.16) *about* σ *means that its gradient can be expressed as follows*

$$\nabla\sigma(\boldsymbol{c})^T = \alpha(\|\boldsymbol{c}-\boldsymbol{p}^*\|)\frac{\boldsymbol{c}-\boldsymbol{p}^*}{\|\boldsymbol{c}-\boldsymbol{p}^*\|}$$

which is to say that $\nabla\sigma(\boldsymbol{c})^T$ *points from* $\boldsymbol{c}$ *towards* $\boldsymbol{p}^*$ *with a magnitude determined by a function* α *of the distance from* $\boldsymbol{c}$ *to* $\boldsymbol{p}^*$*. Because of the assumptions about* σ*, this magnitude function* α *is continuous and satisfies*

$$\alpha(0)=0 \quad \text{and} \quad \alpha(d)>0, \quad \forall\, d>0$$

Substituting the expression for $\nabla\sigma(\boldsymbol{c})$ *into* $\dot{V}(\boldsymbol{c})$*,*

$$\dot{V}(\boldsymbol{c}) = -\lambda\frac{\alpha(\|\boldsymbol{c}-\boldsymbol{p}^*\|)}{\|\boldsymbol{c}-\boldsymbol{p}^*\|}\sum_{k=1}^{N}\sigma(\boldsymbol{r}_k)(\boldsymbol{c}-\boldsymbol{p}^*)^T(\boldsymbol{r}_k-\boldsymbol{c})$$

In order to determine a bound on $\dot{V}(\boldsymbol{c})$*, define a time-varying set of agents* $\mathcal{M}$ *to be those agents whose displacement from the formation center, has a positive projection onto the vector* $\boldsymbol{c}-\boldsymbol{p}^*$ *such that:*

$$\mathcal{M} = \{k : (\boldsymbol{c}-\boldsymbol{p}^*)^T(\boldsymbol{r}_k-\boldsymbol{c})>0\} \tag{4.20}$$

Now separate the sum in $\dot{V}(\boldsymbol{c})$ *as follows,*

$$\begin{aligned}\dot{V}(\boldsymbol{c}) \;=\; & -\lambda\frac{\alpha(\|\boldsymbol{c}-\boldsymbol{p}^*\|)}{\|\boldsymbol{c}-\boldsymbol{p}^*\|}\sum_{k\in\mathcal{M}}\sigma(\boldsymbol{r}_k)(\boldsymbol{c}-\boldsymbol{p}^*)^T(\boldsymbol{r}_k-\boldsymbol{c}) \\ & -\lambda\frac{\alpha(\|\boldsymbol{c}-\boldsymbol{p}^*\|)}{\|\boldsymbol{c}-\boldsymbol{p}^*\|}\sum_{k\notin\mathcal{M}}\sigma(\boldsymbol{r}_k)(\boldsymbol{r}-\boldsymbol{p}^*)^T(\boldsymbol{r}_k-\boldsymbol{c})\end{aligned} \tag{4.21}$$

Due to the geometry of the situation (circular level sets of the signal strength mapping and a circular formation of the agents) we know that if $\boldsymbol{c}\neq\boldsymbol{p}^*$ *then the agents in* $\mathcal{M}$ *are all closer to the source* $\boldsymbol{p}^*$ *than those agents not in* $\mathcal{M}$ *(see Figure 4.4).*

Hence any agent from $\mathcal{M}$ *has a higher signal measurement than any agent not from* $\mathcal{M}$ *and there must be some middle value between them both. Mathematically speaking, it means that:*

$$\forall k\in\mathcal{M}, m\notin\mathcal{M},\ \exists\,\delta>0 \quad \textit{such that} \quad \sigma(\boldsymbol{r}_k)>\delta>\sigma(\boldsymbol{r}_m) \tag{4.22}$$

Applying this inequality to the summation terms in (4.21) *then*

$$k\in\mathcal{M} \Rightarrow \underbrace{\sigma(\boldsymbol{r}_k)}_{>\delta}\underbrace{(\boldsymbol{c}-\boldsymbol{p}^*)^T(\boldsymbol{r}-\boldsymbol{c})}_{>0} > \delta(\boldsymbol{c}-\boldsymbol{p}^*)^T(\boldsymbol{r}_k-\boldsymbol{c}) \tag{4.23}$$

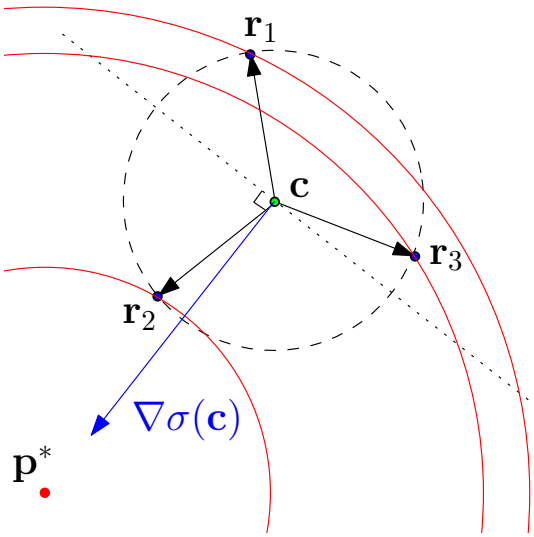

Figure 4.4: *Illustration of vectors used in the proof of Theorem 4.1. Level curves of σ are shown in red. In this situation the set $\mathcal{M}$ contains only agent 2.*

and

$$k \notin \mathcal{M} \Rightarrow \underbrace{\sigma(\boldsymbol{r}_k)}_{<\delta} \underbrace{(\boldsymbol{c}-\boldsymbol{p}^*)^T(\boldsymbol{r}_k-\boldsymbol{c})}_{\leq 0} \geq \delta(\boldsymbol{c}-\boldsymbol{p}^*)^T(\boldsymbol{r}_k-\boldsymbol{c}) \tag{4.24}$$

Assuming that $\mathcal{M}$ is not empty (which is guaranteed if $N \geq 3$), the sum in (4.21) can be bounded from below as

$$\sum_{k\in\mathcal{M}} \sigma(\boldsymbol{r}_k)(\boldsymbol{c}-\boldsymbol{p}^*)^T(\boldsymbol{r}_k-\boldsymbol{c}) + \sum_{k\notin\mathcal{M}} \sigma(\boldsymbol{r}_k)(\boldsymbol{c}-\boldsymbol{p}^*)^T(\boldsymbol{r}_k-\boldsymbol{c}) > \delta(\boldsymbol{c}-\boldsymbol{p}^*)^T \sum_{k=1}^{N}(\boldsymbol{r}_k-\boldsymbol{c})$$

Due to the uniform distribution of the agents, this previous sum is equal to zero and since λ is positive and $\alpha(\|\boldsymbol{c}-\boldsymbol{p}^*\|_2)/\|\boldsymbol{c}-\boldsymbol{p}^*\|_2$ is non-negative the conclusion is that $\dot{V}(\boldsymbol{c}) < 0$ for all $\boldsymbol{c} \neq \boldsymbol{p}^*$ whenever $\mathcal{M}$ is not empty.

The only situation where $\mathcal{M}$ is empty occurs when $N = 2$ and the agents' displacement vectors from the center of the formation, $\boldsymbol{r}_1 - \boldsymbol{c}$ and $\boldsymbol{r}_2 - \boldsymbol{c}$, are orthogonal to $\boldsymbol{c}-\boldsymbol{p}^*$. In this instance, due to the symmetry of σ it must be the case that $\sigma(\boldsymbol{r}_1) = \sigma(\boldsymbol{r}_2)$ and thus $u = 0$. Since ϕ keeps increasing, $\dot{V}(\boldsymbol{c})$ will immediately become negative again so these situations do not constitute an invariant set. Thus by LaSalle's principle [75], the point $\boldsymbol{c} = \boldsymbol{p}^*$ is an asymptotically stable equilibrium of the system (4.14) *under control law* (4.15).

□

Figure 4.5 shows the trajectory of the formation center for three simulations for different number of agents in the fleet, $N = 2$ in blue, $N = 3$ in red and $N = 4$ in green.

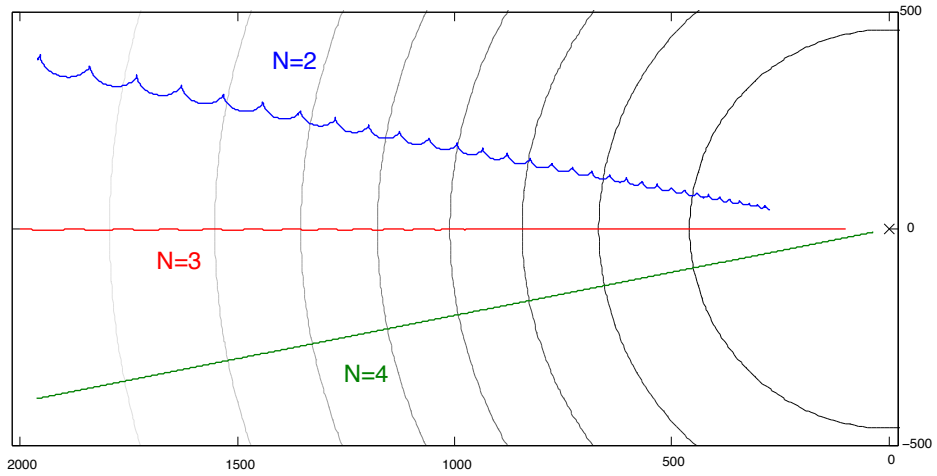

Figure 4.5: *Trajectories of the formation center* $\boldsymbol{c}$ *for different numbers of agents* N *when* σ *has circular level sets. Location of source is denoted by the* $\times$*. Image courtesy of Brandon J. Moore.*

For this simulation from [104], $\sigma(z) = e^{-5x10^{-7}(x^2+y^2)}$, $R = 200m$, and $\omega_0 = 0.01rad/s$. In all cases, the algorithm from Theorem 4.1 steers the center of the circular formation to the source position.

Signal distributions with elliptical level sets: Following theorem presents a similar result that previous one but considering elliptical level sets of the signal propagation. In simulation, the authors of [104] obtain also successful results when the level sets are a combination of a three ellipsis, but the theoretical analysis is not provided in the paper.

Theorem 4.2 *(Moore and Canudas-de-Wit 2010 [104]) Assume that the signal strength is a continuously differentiable mapping and satisfies the following property*

$$(\boldsymbol{p}_2-\boldsymbol{p}^*)^T\mathbf{A}(\boldsymbol{p}_2-\boldsymbol{p}^*)>(\boldsymbol{p}_1-\boldsymbol{p}^*)^T\mathbf{A}(\boldsymbol{p}_1-\boldsymbol{p}^*) \Longrightarrow \sigma(\boldsymbol{p}_1)<\sigma(\boldsymbol{p}_2) \tag{4.24}$$

for some positive definite matrix $\mathbf{A}$*. This is to say that the signal strength has a maximum at some point* $\boldsymbol{p}^*$ *and has compact elliptical level sets. If the number of agents* N *is even, then under the control input of* (4.15) *the point* $\boldsymbol{c} = \boldsymbol{p}^*$ *is an asymptotically stable equilibrium of system* (4.14)*.*

The proof is similar than in the case of a signal distributions with circular level sets. The details of the proof can be found in [104].

The control law (4.15) allows the formation to move such that its center converges to the source position, if the signal distribution decreases around the source in such a way

that level sets are circles or ellipses centered on the maximum or minimum of the signal distribution. The main constraint of this algorithm is the all-to-all communication assumption. The control law proposed by the authors is centralized, in consequence communication constraints are not considered. This constitutes a first result to solve the source-seeking problem by a circular formation of agents in a collaborative way. Nevertheless, this centralized approach is not realistic according to the underwater communication problems presented in Chapter 1, and the objective of this thesis is to extend this result towards a distributed approach.

4.4 Collaborative estimation of gradient direction by a fixed circular formation

The objective of this section focuses on the fist step of the control strategy previously exposed in the problem formulation. The idea is to develop an algorithm to estimate the gradient direction of the signal distribution of the source. As explained before, this estimation will be achieved by a circular formation of AUVs. Thanks to Lemmas 4.1 and 4.2, the gradient of a signal strength distribution can be approximated by the measurements obtained from a fixed circular formation of agents uniformly distributed. A first centralized algorithm based on this result is addressed in [104]. Nevertheless, in order to consider communication constraints between the agents, a distributed algorithm is developed in this section to estimate the direction of the gradient by a fixed circular formation.

In this situation, each agent calculates its own estimation of the gradient direction computing its own measurement of the signal distribution and the measurements of its neighbors. Consequently, each agent computes a different gradient direction. With a view to obtain the same estimated direction for all the agents, a consensus algorithm is included. This algorithm allows the agents to converge to the same estimated gradient direction, taking into account the communication topology of the system.

4.4.1 Fixed source

The simplest case, when the circular formation is fixed and the source is also fixed is analyzed here. The presence of currents is not considered. A fixed source implies that the signal distribution is time-invariant. The idea is to develop a distributed algorithm to estimate the gradient direction of the signal distribution σ at the center $\mathbf{c}$ of a circular formation of agents.

Communication constraints are taken into account by a communication graph $\mathcal{G}$. Due to these communication restrictions each agent estimates its own gradient direction

$\mathbf{z}_k$ using the information of its neighbors according to the communication topology. The objective is to make all estimated directions $\mathbf{z}_k$ converge to the mean direction defined as:

$$\mathbf{u}^* = \frac{1}{N}\sum_{k=1}^{N}\mathbf{u}_k; \quad \mathbf{u}_k = \sigma_k(\mathbf{r}_k - \mathbf{c}) \tag{4.25}$$

where $\mathbf{u}_k$ is the relative position vector of agent k weighted by its concentration measurement $\sigma_k = \sigma(\mathbf{r}_k)$. Thanks to Lemma 4.1, this mean vector $\mathbf{u}^*$ approximates the gradient direction of the signal distribution at the center of the formation $\mathbf{c}$. A consensus algorithm is implemented to reach an agreement on the estimated gradient direction of the signal distribution for all the agents.

Distributed algorithm design

This paragraph presents some notations used in the sequel. Let $\mathcal{G} = (V, E)$ be an undirected graph with adjacency matrix $\mathcal{A} = [a_{kj}]$ that specifies the communication topology of the multi-agent system. If agents k, j are connected then $a_{kj} = 1$ and $a_{kj} = 0$ otherwise. Let $\mathcal{N}_k = \{j \in V : a_{kj} \neq 0\}$ be the set of neighbors of agent k and $\mathcal{J}_k = \mathcal{N}_k \cup \{k\}$. The Laplacian matrix $\mathbf{L}$ of graph $\mathcal{G}$ is defined as $\mathbf{L} = \Delta - \mathcal{A}$ where Δ is the diagonal matrix which contains the degree of each agent, *i.e.*, $\Delta_{kk} = d_k = \sum_j a_{kj}$. More details of graph theory can be found in Appendix A. In the sequel, $\otimes$ denotes the Kronecker product and, for simplicity, the following notation is defined $\mathbf{M}_2 = \mathbf{M} \otimes \mathbf{I}_2$ where $\mathbf{M}$ is a square matrix and $\mathbf{I}_N$ is the identity matrix of order N.

The fixed formation of agents taking concentration measurements can be considered as a sensor network. The mission of this sensor network is to estimate the gradient direction of the signal propagation measured in a collaborative way. Based on consensus filters for sensor networks presented in [112], the following consensus algorithm for the multi-agents system is proposed:

$$\dot{\mathbf{z}}_k = \kappa \sum_{j \in \mathcal{N}_k}(\mathbf{z}_j - \mathbf{z}_k) + \sum_{j \in \mathcal{J}_k}(\mathbf{u}_j - \mathbf{z}_k)$$

where $\kappa > 0$ is a control parameter which is introduced to make the algorithm more flexible. The consensus variable is the vector $\mathbf{z}_k \in \mathbb{R}^2$ which represents the estimated gradient direction by agent k. The input $\mathbf{u}_k = \sigma_k(\mathbf{r}_k - \mathbf{c}) \in \mathbb{R}^2$, depends on the concentration measurements and the position of the agent in the formation. The main difference to the consensus filter from [112] is that the input of the algorithm is not a given signal known to all the agents corrupted by noise, but a different vector for each agent.

Using the Laplacian matrix of the communication topology of the multi-agent sys-

tem the previous equation can be rewritten in a matrix way:

$$\begin{aligned}\dot{\mathbf{z}} &= -\kappa\mathbf{L}\otimes\mathbf{I}_2\mathbf{z} + \mathbf{I}_N\otimes\mathbf{I}_2(\mathbf{u}-\mathbf{z}) + \mathcal{A}\otimes\mathbf{I}_2\mathbf{u} - \Delta\otimes\mathbf{I}_2\mathbf{z} \\ &= -(\mathbf{I}_N + \Delta + \kappa\mathbf{L})_2\mathbf{z} + (\mathbf{I}_N + \mathcal{A})_2\mathbf{u} \end{aligned} \tag{4.26}$$

where $\mathbf{z} = (\mathbf{z}_1^T, \mathbf{z}_2^T, \ldots, \mathbf{z}_N^T)^T$ and $\mathbf{u} = (\mathbf{u}_1^T, \mathbf{u}_2^T, \ldots, \mathbf{u}_N^T)^T$ are vectors of dimension $2N$, and $\mathbf{I}_N$ the identity matrix of order N. Let $\mathbf{A}_\kappa = (\mathbf{I}_N + \Delta + \kappa\mathbf{L})_2$, and $\mathbf{B} = (\mathbf{I}_N + \mathcal{A})_2$. Note that by definition, $\mathbf{A}_\kappa$ is a positive definite matrix. Then, the previous equation becomes:

$$\dot{\mathbf{z}} = -\mathbf{A}_\kappa\mathbf{z} + \mathbf{B}\mathbf{u} \tag{4.27}$$

The objective of the consensus algorithm is to make all the estimated directions $\mathbf{z}_k$ converge to the mean direction $\mathbf{u}^*$. Consider the vector of dimension $2N$

$$\mathbf{u}_\mathbf{1}^* = \mathbf{1}\otimes\mathbf{u}^* = (\mathbf{u}^{*T}, \ldots, \mathbf{u}^{*T})^T$$

where $\mathbf{1} = (1, \ldots, 1)^T \in \mathbb{R}^N$ is the vector of ones that is always a right eigenvector of $\mathbf{L}$ corresponding to the eigenvalue 0. Therefore, the error equation is $\eta = \mathbf{z} - \mathbf{u}_\mathbf{1}^*$. Using equation (4.27), the dynamics of the error can be written as:

$$\begin{aligned}\dot{\eta} &= -\mathbf{A}_\kappa\mathbf{z} + \mathbf{B}\mathbf{u} - \dot{\mathbf{u}}_\mathbf{1}^* + (\mathbf{I}_N + \Delta + \kappa\mathbf{L})_2\mathbf{u}_\mathbf{1}^* - (\mathbf{I}_N + \Delta)_2\mathbf{u}_\mathbf{1}^* \\ \dot{\eta} &= -\mathbf{A}_\kappa\eta + \mathbf{B}(\mathbf{u} - \mathbf{u}_\mathbf{1}^*) - \dot{\mathbf{u}}_\mathbf{1}^* \end{aligned} \tag{4.28}$$

The stability of this algorithm is analyzed using the Lyapunov function given by:

$$V(\eta) = \frac{1}{2}\eta^T\mathbf{A}_\kappa\eta \tag{4.29}$$

which is a nonnegative function because the matrix $\mathbf{A}$ is positive definite. At the equilibrium, when $V(\eta) = 0$ the following equation is satisfied:

$$\eta^T\mathbf{A}_\kappa\eta \equiv 0$$

Therefore, the minimum of the Lyapunov function corresponds to $\eta = 0$. This is equivalent to the expression $\mathbf{z} = \mathbf{u}_\mathbf{1}^*$, which represents the initial objective.

Differentiating the previous Lyapunov function (4.29):

$$\dot{V}(\eta) = -\eta^T\mathbf{A}_\kappa^T\mathbf{A}_\kappa\eta + (\mathbf{u} - \mathbf{u}_\mathbf{1}^*)^T\mathbf{B}^T\mathbf{A}_\kappa\eta - \dot{\mathbf{u}}_\mathbf{1}^{*T}\mathbf{A}_\kappa\eta$$

According to the previous matrix definitions and the mixed-product property of the Kronecker product, it yields:

$$\dot{\mathbf{u}}_\mathbf{1}^{*T}\mathbf{A}_\kappa = \mathbf{1}^T\otimes\dot{\mathbf{u}}^{*T}(\mathbf{I}_N + \Delta + \kappa\mathbf{L})_2 = \mathbf{1}^T(\mathbf{I}_N + \Delta + \kappa\mathbf{L})\otimes\dot{\mathbf{u}}^{*T}\mathbf{I}_2$$

Using the properties of the Laplacian matrix the previous equation becomes:

$$\dot{\mathbf{u}}_{\mathbf{1}}^{*T}\mathbf{A}_\kappa = (1+d_1,\ldots,1+d_N)\otimes\dot{\mathbf{u}}^{*T}$$

It is assumed that the distribution of the signal strength in the environment considered here varies softly, it means that the derivative of the signal propagation is bounded. Let $\|\dot{\mathbf{u}}_{\mathbf{1}}^*\| \leq \nu$, due to the soft variation of the concentration levels of the signal distribution. Therefore, the following inequality holds:

$$\|\dot{\mathbf{u}}_{\mathbf{1}}^{*T}\mathbf{A}_\kappa\| \leq \|\dot{\mathbf{u}}^*\|\sqrt{\sum_{k=1}^{N}(1+d_k)^2} \leq \nu\sqrt{N}(1+d_{max})$$

Hence, previous derivative of the Lyapunov function (4.30) can be bounded by:

$$\dot{V}(\eta) \leq -\lambda_{min}^2(\mathbf{A}_\kappa)\|\eta\|^2 + \nu\sqrt{2N}(1+d_{max})\|\eta\| + \|(\mathbf{u}-\mathbf{u}_{\mathbf{1}}^*)^T\mathbf{B}^T\mathbf{A}_\kappa\eta\|$$

It is plausible to assume that a bound on maximal signal concentration is known from the problem setting. Therefore, $\|(\mathbf{u}-\mathbf{u}_{\mathbf{1}}^*)\| \leq \alpha$ where α depends on the radius of the circular formation and on the greatest concentration measurement obtained by the agents. For simplicity, let γ be a bound of the following matrix norm $\left\|\mathbf{B}^T\mathbf{A}_\kappa\right\| \leq \gamma$. Taking these considerations into account the following equation holds:

$$\|(\mathbf{u}-\mathbf{u}_{\mathbf{1}}^*)^T\mathbf{B}^T\mathbf{A}_\kappa\| \leq \alpha\gamma$$

The derivative of the Lyapunov function is bounded by:

$$\dot{V}(\eta) \leq -\lambda_{min}^2(\mathbf{A}_\kappa)\|\eta\|^2 + \left(\nu\sqrt{N}(1+d_{max}) + \alpha\gamma\right)\|\eta\|$$

Based on the proof of Proposition 2 from [112] a closed ball B_β centered at $\eta = 0$ is defined with radius

$$\beta = \frac{\nu\sqrt{N}(1+d_{max}) + \alpha\gamma}{\lambda_{min}^2(\mathbf{A}_\kappa)}$$

Let $\Omega_m = \{\eta : V(\eta) \leq m\}$ be a level set of the Lyapunov function $V(\eta)$ with $m = \frac{1}{2}\lambda_{max}(\mathbf{A}_\kappa)\beta^2$. Then, B_β is contained in Ω_m because

$$\|\eta\| \leq \beta \Longrightarrow V(\eta) = \frac{1}{2}\eta^T\mathbf{A}_\kappa\eta \leq \frac{1}{2}\lambda_{max}(\mathbf{A}_\kappa)\beta^2 = m,$$

and thus $\eta \in \Omega_m$. As a result, any solution of (4.28) starting in the set $\mathbb{R}^{2N}\backslash\Omega_m$ satisfies $\dot{V}(\eta) < 0$. Thus, it enters Ω_m in some finite time and remains in Ω_m thereafter. This guarantees global asymptotic ϵ-stability of $\eta = 0$ with a radius $\epsilon = \beta\lambda_{max}(\mathbf{A}_\kappa)/\lambda_{min}(\mathbf{A}_\kappa)$. To show this, note that

$$\frac{1}{2}\lambda_{min}(\mathbf{A}_\kappa)\|\eta\|^2 \leq V(\eta) \leq \frac{1}{2}\lambda_{max}(\mathbf{A}_\kappa)\beta^2$$

Thus, the solutions enter the region

$$\|\eta\| \leq \beta \sqrt{\frac{\lambda_{max}(\mathbf{A}_\kappa)}{\lambda_{min}(\mathbf{A}_\kappa)}}$$

which implies the radius of ϵ-stability is

$$\epsilon = \frac{\nu\sqrt{N}(1+d_{max})+\alpha\gamma}{\lambda^2_{min}(\mathbf{A}_\kappa)} \sqrt{\frac{\lambda_{max}(\mathbf{A}_\kappa)}{\lambda_{min}(\mathbf{A}_\kappa)}}$$

The ϵ-stability of $\eta = 0$ implies ϵ-tracking of the mean vector $\mathbf{u}_\mathbf{1}^*$ by every agent, therefore ϵ-consensus is asymptotically reached.

After the previous detailed analysis this result can be presented as a theorem:

Theorem 4.3 *(Briñón-Arranz et al. 2011 [20]) Consider a circular formation of N agents defined by (4.2) with a connected communication graph $\mathcal{G}$ and Assumption 4.1 is satisfied. Let $\sigma : \mathbb{R}^2 \to \mathbb{R}^+$ be a bounded function and the mean vector $\boldsymbol{u}^*$ defined in (4.25) satisfies $\|\dot{\boldsymbol{u}}^*\| \leq \nu$. Then, $\boldsymbol{z}^*(t) = \boldsymbol{1} \otimes \boldsymbol{u}^*$ is a globally asymptotically ϵ-stable equilibrium of the dynamics of the distributed algorithm given by*

$$\dot{\boldsymbol{z}} = -\kappa \boldsymbol{L}_2 \boldsymbol{z} - \boldsymbol{L}_2 \boldsymbol{u} + (\boldsymbol{I}_N + \Delta)_2(\boldsymbol{u} - \boldsymbol{z}) \tag{4.30}$$

with $\boldsymbol{u} = (\sigma_1(\boldsymbol{r}_1 - \boldsymbol{c})^T, \ldots, \sigma_N(\boldsymbol{r}_N - \boldsymbol{c})^T)^T$ and

$$\epsilon = \frac{(\nu\sqrt{N}(1+d_{max})+\alpha\gamma)\lambda^{\frac{1}{2}}_{max}(\boldsymbol{A}_\kappa)}{\lambda^{\frac{5}{2}}_{min}(\boldsymbol{A}_\kappa)}$$

where the matrix $\boldsymbol{A}_\kappa$ and the constants α and γ are previously defined.

Remark 4.1 *Analyzing the linear system (4.27), it seems straightforward that the control parameter κ has an important role in the convergence of the algorithm. The simulation results show that taking $\kappa >> 1$, the amplitude of oscillations of the estimated gradient directions $\boldsymbol{z}_k$ are smaller. Therefore, the error η is also reduced.*

Simulations

In order to show the performances of this distributed algorithm some simulation results are presented. All simulations show a fixed circular formation of five agents with radius $R = 1m$ and angular velocity of $\omega_0 = 1rad/s$. The communication graph is a ring (d_1-circulant graph).

In Figures 4.6 and 4.7, the source-seeking consensus algorithm (4.30) from Theorem 4.3 is implemented with $\kappa = 50$. For these simulations, the function σ representing the signal distribution centered at the origin has circular level sets:

$$\sigma(x, y) = 100e^{-(x^2+y^2)/10}$$

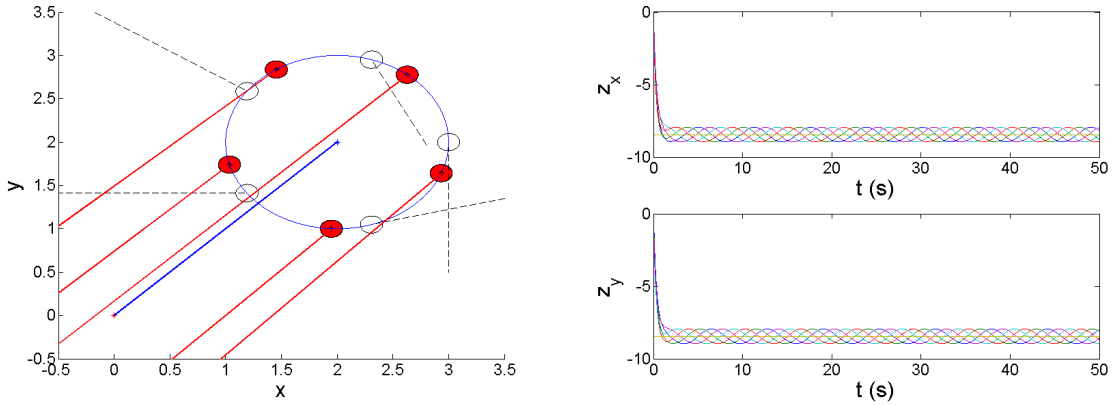

(a) Estimated directions $\mathbf{z}_k$ for $t = 0s$ (black dashed lines) and for $t = 50s$ (red lines)

(b) X and Y coordinates of estimated directions $\mathbf{z}_k$

Figure 4.6: *Simulation of a circular formation of five agents centered at* $\boldsymbol{c} = (2, 2)^T$. *The function* σ *representing the signal distribution centered at the origin has circular level sets. The consensus algorithm of Theorem 4.3 is implemented with* $\kappa = 50$.

Therefore, the gradient vector $\nabla\sigma(\mathbf{c})$ provides the adequate direction to steer the formation to the source location. Both Figures 4.6(a) and 4.7(a) show two snapshots. The void circles represent the initial conditions and the black dashed lines the initial estimated direction $\mathbf{z}_k$ of each agent. The red circles represent the position of the agents at $t = 50s$ and the red lines are the estimated gradient directions at that time. The blue line is the real direction of the gradient at center $\mathbf{c}$. Both Figures 4.6(b) and 4.7(b) show the components of the consensus variable $\mathbf{z}_k$ and the mean vector $\mathbf{u}^*$. The estimated directions $\mathbf{z}_k$ oscillate around the vector $\mathbf{u}^*$ which approximates the true gradient direction for any initial conditions.

In Figure 4.6 the circular formation of agents is centered at $\mathbf{c} = (2, 2)^T$ and the oscillations of the estimated gradient directions $\mathbf{z}_k$ are smaller than in Figure 4.7 where the formation is centered at source location. In this second case, the mean of the directions is equal to zero but, the convergence region of radius ϵ leads to completely wrong gradient direction estimations.

Conclusions and limitations of the algorithm

The final gradient direction $\mathbf{z}_k$ estimated by each agent oscillates with period $T = 2\pi/\omega_0$. The amplitude of these oscillations depends on the concentration measurements σ_k. When the formation is close to the source location, the measurements are greater, thus, the amplitude of oscillations are greater as well. Moreover, as the gradient is close to zero in the neighborhood of the source (at least with the Gaussian profile used in

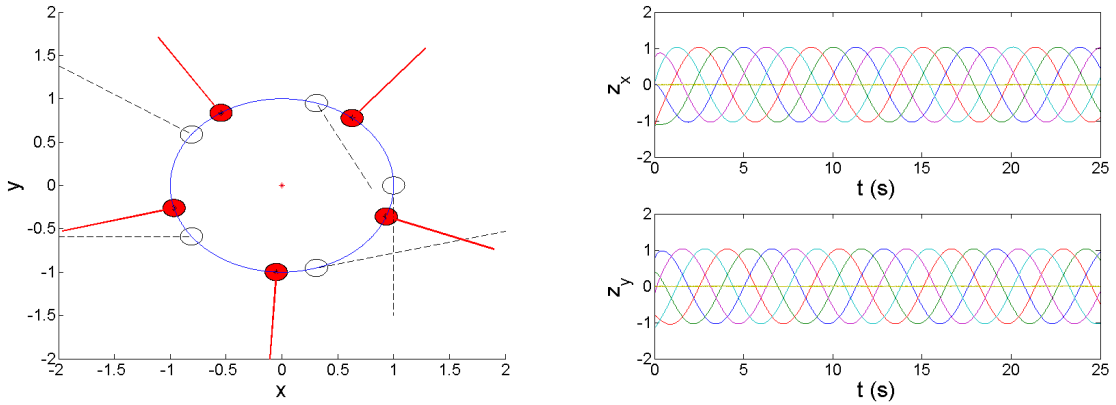

(a) Estimated directions $\mathbf{z}_k$ for $t = 0s$ (black dashed lines) and for $t = 50s$ (red lines)

(b) X and Y coordinates of estimated directions $\mathbf{z}_k$

Figure 4.7: *Simulation of a circular formation of five agents centered at* $\boldsymbol{c} = (0, 0)^T$. *The function* σ *representing the signal distribution centered at the origin has circular level sets. The consensus algorithm* (4.30) *is implemented with* $\kappa = 50$.

these simulations), a ball of radius ϵ around 0 leaves the gradient direction essentially unknown; thus Theorem 4.3 does not guarantee good behaviour in the neighborhood of the source.

Another limitation of the consensus algorithm (4.30) is that the radius ϵ depends on the constants α and γ which cannot necessarily be small values. In order to avoid these problems, an averaging approach is presented in the sequel.

Input-averaging

With a view to improve the distributed algorithm presented before, the periodic properties of the situation assumed in the problem formulation are studied.

The agents describe a periodic movement, it means that $\mathbf{r}_k(t) = \mathbf{r}_k(t + T)$ with $T = 2\pi/\omega_0$. Therefore, the measurements σ_k obtained by agent k are a periodic map because $\sigma(\mathbf{r}_k(t)) = \sigma(\mathbf{r}_k(t + T))$. In conclusion, the input variable of the consensus algorithm $\mathbf{u}_k = \sigma_k(\mathbf{r}_k - \mathbf{c})$ is a T-periodic function with $T = 2\pi/\omega_0$. Estimated directions $\mathbf{z}_k$ obtained by the consensus algorithm (4.30) shown in Figures 4.6 and 4.7 are also periodic. The average of these solutions approximates the gradient direction of the source. Thanks to these observations, an analysis of the average properties of the input variable $\mathbf{u}_k$ seems adequate. The idea now is to improve the previous distributed consensus algorithm using the periodic properties of the measurements $\sigma(\mathbf{r}_k)$.

The input vector $\mathbf{u}_k$ in previous consensus algorithm is replaced by its mean value

over one period $T = 2\pi/\omega_0$ which is defined as:

$$\bar{\mathbf{u}}_k = \frac{1}{T}\int_{t-T}^{t} \sigma_k(\mathbf{r}_k(\tau) - \mathbf{c})d\tau \tag{4.31}$$

Therefore, thanks to Lemma 4.2 the new mean vector $\bar{\mathbf{u}}^*$ approximates the gradient of the signal propagation σ at the center of the circular formation:

$$\bar{\mathbf{u}}^* = \frac{1}{N}\sum_{k=1}^{N} \bar{\mathbf{u}}_k \tag{4.32}$$

The new input variable of the improved algorithm based on (4.30), is the mean vector $\bar{\mathbf{u}} = (\bar{\mathbf{u}}_1^T, \bar{\mathbf{u}}_2^T, \ldots, \bar{\mathbf{u}}_N^T)^T$, and the objective is defined as $\bar{\mathbf{u}}_\mathbf{1}^* = \mathbf{1} \otimes \bar{\mathbf{u}}^*$. Following the analysis developed previously, assumed that the signal distribution varies softly, thus, following inequality $\|(\bar{\mathbf{u}} - \bar{\mathbf{u}}_\mathbf{1}^*)\| \leq \bar{\alpha}$ is satisfied. Using these considerations, a new algorithm is proposed in the following corollary:

Corollary 4.1 *(Briñón-Arranz et al. 2011 [20]) Consider a circular formation of N agents defined by* (4.27) *with a connected communication graph $\mathcal{G}$ and Assumption 4.1 is satisfied. Let $\sigma : \mathbb{R}^2 \to \mathbb{R}^+$ be a bounded function and the mean vector $\bar{\boldsymbol{u}}^*$ defined in* (4.32) *satisfies $\|\dot{\bar{\boldsymbol{u}}}^*\| \leq \bar{\nu}$. Then, $\boldsymbol{z}^*(t) = \boldsymbol{1} \otimes \bar{\boldsymbol{u}}^*$ is a globally asymptotically $\bar{\epsilon}$-stable equilibrium of the dynamics of the distributed algorithm given by*

$$\dot{\boldsymbol{z}} = -\kappa \boldsymbol{L}_2 \boldsymbol{z} - \boldsymbol{L}_2 \bar{\boldsymbol{u}} + (\boldsymbol{I}_N + \Delta)_2(\bar{\boldsymbol{u}} - \boldsymbol{z}) \tag{4.33}$$

with

$$\bar{\epsilon} = \frac{(\bar{\nu}\sqrt{N}(1 + d_{max}) + \bar{\alpha}\gamma)\lambda_{max}^{\frac{1}{2}}(\boldsymbol{A}_\kappa)}{\lambda_{min}^{\frac{5}{2}}(\boldsymbol{A}_\kappa)}$$

where the matrix $\boldsymbol{A}_\kappa$ and the constants $\bar{\alpha}$ and γ are previously defined.

Considering Assumption 4.1 (the circular formation is fixed) by definition, the mean input $\bar{\mathbf{u}}$ is a constant vector after a time period T. Therefore, the input variable $\bar{\mathbf{u}}$ converges to the mean vector $\bar{\mathbf{u}}_\mathbf{1}^*$ and moreover, its derivative is equal to zero. It means that:

$$\bar{\nu} \to 0 \quad \text{and} \quad \bar{\alpha} \to 0$$

It implies that the radius of the convergence region $\bar{\epsilon}$ converges to zero after a period T, the consensus is achieved and all the agents estimate the mean vector $\bar{\mathbf{u}}^*$ which approximates the gradient direction at the center of the formation.

The gradient direction estimated by the agents will be the reference velocity of the formation center to steer the fleet of agents to the source location. If the formation is moving, the gradient of the signal distribution in the circle center becomes time-varying and the concentration measurements does not satisfy the periodic properties anymore.

Therefore, the consensus algorithm makes that the agents estimate the gradient direction before a period T. A detailed investigation of our algorithms when the formation moves along the estimated gradient direction towards the source location is the next research goal discussed later.

Simulations

The simulations show the same circular formation of five agents from the previous ones. In Figures 4.8 and 4.9 the improved distributed algorithm (4.33) from Corollary 4.1 is implemented with $\kappa = 1$ by a circular formation centered at $\mathbf{c} = (2, 2)^T$ and at source location, respectively. The measured signal is the same as in previous simulations. Due to the circular level sets of the signal propagation the gradient vector $\nabla\sigma(\mathbf{c})$ provides the adequate direction to steer the formation to the source location.

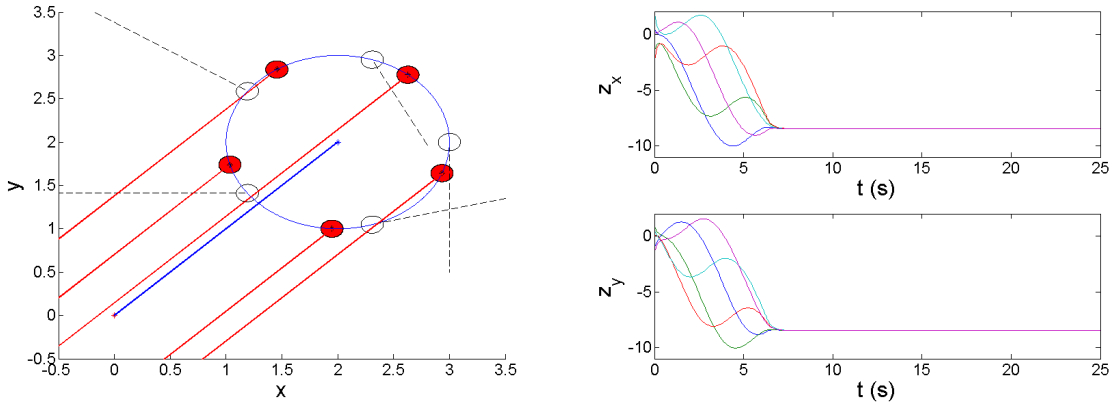

(a) Estimated directions $\mathbf{z}_k$ for $t = 0s$ (black dashed lines) and for $t = 50s$ (red lines)

(b) Components of estimated directions $\mathbf{z}_k$

Figure 4.8: *Simulation of a circular formation of five agents centered at* $\mathbf{c} = (2, 2)^T$. *The function* σ *representing the signal distribution centered at the origin has circular level sets. The mean input consensus algorithm* (4.33) *is implemented.*

Both Figures 4.8(a) and 4.9(a) show two snapshots, the initial conditions and the stable situation at $t = 50s$. Both Figures 4.8(b) and 4.9(b) show the components of consensus variable $\mathbf{z}_k$. This algorithm allows us to remove the oscillations and the final vectors for all the agents $\mathbf{z}_k$ (red lines) are parallel to the gradient direction (blue line). The problem of oscillations when the formation is centered at source location is also solved and the final directions $\mathbf{z}_k$ are equal to zero, *i.e.*, the formation decides to stay in the desired location. The estimated directions $\mathbf{z}_k$ converge to the gradient direction approximated by the mean vector $\bar{\mathbf{u}}^*$ for any initial conditions.

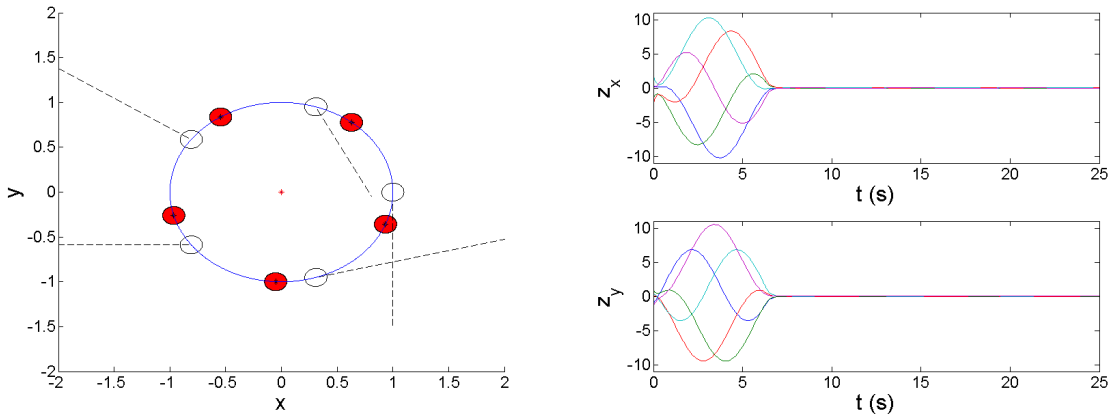

(a) Estimated directions $\mathbf{z}_k$ for $t = 0s$ (black dashed lines) and for $t = 50s$ (red lines)

(b) Components of estimated directions $\mathbf{z}_k$

Figure 4.9: *Simulation of a circular formation of five agents centered at* $\boldsymbol{c} = (0, 0)^T$. *The function* σ *representing the signal distribution centered at the origin has circular level sets. The mean input consensus algorithm of* (4.33) *is implemented.*

In Figure 4.10 the same algorithm (4.33) is implemented with an elliptical signal distribution defined by

$$\sigma(x, y) = 100e^{-(x^2/10+y^2/2)/10}$$

The estimated directions $\mathbf{z}_k$ converge to the gradient direction $\nabla\sigma(\mathbf{c})$. In this case, this direction will not directly steer the formation to the source location, but a formation moving along the respective gradient direction will be progressively steered towards the source over several consecutive steps, as in a gradient-descent method, see [34].

4.4.2 Time-varying source

In this section a time-varying source is considered. In this situation, the signal distribution in the environment becomes a time-varying function, such that σ depends both on the position and time, *i.e.* $\sigma(\mathbf{r}_k, t)$.

The previous Lemma 4.3 shows that a fleet of $N > 2$ agents uniformly distributed along a fixed circular formation is able to approximate the gradient direction of a scalar field varying with time. A direct consequence of this lemma is that the distributed estimation algorithm from Theorem 4.3 with the u_k's defined in (4.25) also holds in the case of time-varying signal distribution.

However the extension presented in Lemma 4.2 to time-varying signal distributions is not straightforward. Indeed, if the signal distribution depends on the time variable, equation (4.12) is not valid anymore.

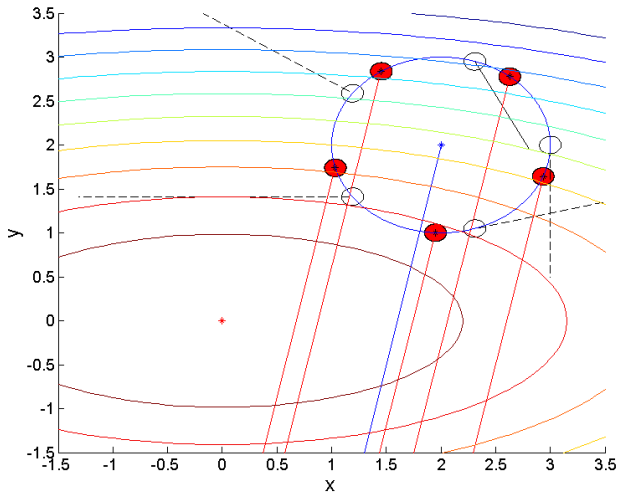

Figure 4.10: *Simulation of the distributed algorithm* (4.33) *by a circular formation of five agents centered at* $\boldsymbol{c} = (2, 2)^T$. *The function* σ *representing the signal propagation centered at the origin has elliptical level sets.*

Simulations

The same circular formation of five agents from the previous simulations is still considered. Figure 4.11 shows the simulation results of the gradient estimation of a time-varying signal distribution. The distribution is given by

$$\sigma((x, y), t) = 100e^{-((x-2cos(t/10))^2+y^2)/10}$$

In order to compare the directions of the effective gradient and of the resulting estimations, we consider the angle (in radians) between the $\nabla\sigma(\mathbf{c}, t)^T$ (and $\mathbf{z}_k$, respectively) and $(1, 0)^T$. In Figure 4.11 (a), one can see that each estimated direction, obtained by the algorithm (4.30) from Theorem 4.3 with $\kappa = 100$, oscillates around the effective gradient direction. Figure 4.11 (b) shows the same situation but implementing the algorithm from Corollary 4.1 with $\kappa = 100$. In this case, a consensus on the estimates is clearly reached. However there exists an error (on time) between the estimated direction and the effective one. This delay, equal to the period T, is due to the fact that with the input-averaging algorithm each agent needs one period in order to compute the direction $\mathbf{u}_k$ defined by (4.31).

4.5 Conclusions

The source-seeking problem is considered in this chapter. By way of introduction, an exhaustive study of different approaches proposed in the recent literature, which deal

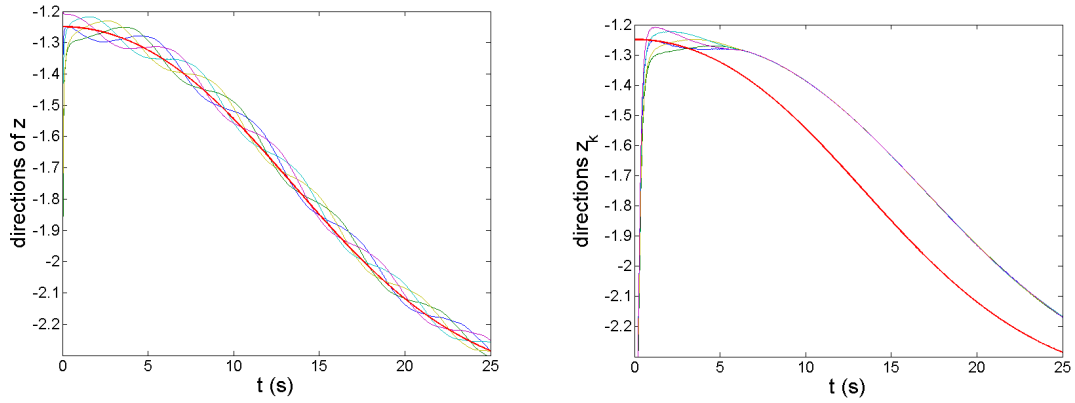

(a) Simulation results using the algorithm from Theorem 4.3

(b) Simulation results using the algorithm from Corollary 4.1

Figure 4.11: *Evolution of the direction, given in radians of the estimates (soft lines) and the real gradient (red bold line) for a time-varying signal distribution.*

with the source-seeking problem, is provided. There are only a few works that consider a collaborative strategy.

In this context, the main contributions presented in this chapter, are the three lemmas presented in Subsection 4.3.1, which prove that the measurements of a signal distribution, obtained by a group of sensors uniformly distributed along a fixed circular formation, allow us to approximate the gradient direction of the signal at the center of the formation. Based on this result, a distributed algorithm is developed to estimate the gradient direction of a signal by a circular formation of AUVs. Communication constraints are considered via a communication graph. This new collaborative strategy is based on a consensus filter algorithm in order to make the agents reach an agreement on the estimated gradient direction. The estimated directions oscillate around the real direction of the gradient.

According to the periodic properties of the measurements obtained by the circular formation of agents, the previous distributed algorithm is modified. Using the average of the directions computed by each agent and applying the previous consensus algorithm, the agents reach a consensus on the gradient direction asymptotically. Both algorithms are analyzed when the source emitting the signal distribution is time-varying.

The estimated gradient direction will be used to drive the fleet of AUVs to the source position thanks to a gradient-descent approach. A control strategy, based on several results presented in this dissertation, will be developed to achieve the source-seeking in future researches.

Chapter 5

Conclusion and Future works

The purpose of this chapter is to summarize the contributions presented in the dissertation and introduce some perspectives of future research to complete and improve this work.

5.1 Review of the contributions and conclusions

Cooperative control is an important issue due to its large number of applications. Collaborative behavior of a group of agents means that there exist several interconnections between them in order to reach a common objective. In the context of this thesis, the agents represent autonomous underwater vehicles (AUVs) and the common goal is to locate and follow an underwater source (fresh water, pollutant flow, chemical source). To achieve the final aim, the collaborative mission is structured in several phases. Firstly, the vehicles reach a desired formation thanks to a feedback control. The main contribution is to stabilize the fleet to time-varying formations. Besides, a cooperative control law distributes the AUVs uniformly along the formation, tacking into account the communication constraints. These results constitute the support to tackle the source-seeking problem. A distributed algorithm is developed to estimate the gradient direction of a signal by a group of vehicles in formation. This estimated direction will steer the fleet of AUVs to the source location.

5.1.1 Formation control tracking time-varying references

Feedback control laws to stabilize the vehicles to time-varying formations are developed. The vehicles are modeled by unicycle kinematics as is detailed in Chapter 2. Collective motions, particularly circular motions, have been studied in recent literature. The main contribution according to the field of formation control, is that the vehicles are stabilized to a formation which is defined by time-varying parameters. The

first control law developed in this thesis allows the AUVs to describe a circular trajectory whose center is an external time-varying reference. The main idea is to change the coordinates reference frame to a relative frame which is invariant with respect to the time-varying center. The coordinates transformation is appropriate to take into account some properties of the new manifold, in which the multi-agent system is expressed. Based on the same idea, a control law is presented to govern the AUVs in order to converge to circular motions with time-varying radius.

Consequently, the following contribution, presented in Chapter 3, deals with the generalization of both previous control laws using the same idea, *i.e.*, by transforming the reference frame. As result, a new framework is developed to express a large class of motions by deforming a unit circle. The three main transformations which can be applied to a formation in order to change its shape, position and orientation, are the scaling, translation and rotation, respectively. Therefore, a sequence of affine transformations applied to the unit circle defines a new formation which results from deforming that circle. The configurations obtained with this methodology are called elastic formations in this thesis. Thanks to a coordinates transformation, a new general formation control law is developed to stabilize a group of vehicles to elastic formations defined by affine transformations. Moreover, this new formulation allows us to specify several class of motions defined by a velocity reference. A new algorithm based also on affine transformations, makes a group of agents converge to a time-varying configuration in terms of velocity.

5.1.2 Collaborative algorithms to formation control

The notion of formation is introduced in the survey from Chapter 1. An important characteristic of formation control is that the agents collaborate between them. Therefore, several cooperative algorithms are included to the control laws presented in both Chapters 2 and 3 in order to achieve different objectives. The first cooperative approach deals with the distribution of the vehicles along formations. The agents have to exchange some information: in this case, their heading angle or their transformed heading angle with respect to a relative frame. Hence, interconnections between agents must be taking into account. The communication topology of the network is represented by an undirected graph. The convergence of collaborative algorithms presented in this dissertation, is related to the connectivity properties of graphs studied in detail in Appendix A.

The first contribution is to consider a graph in which the interconnections depend on the relative position of the vehicles. It means that, each vehicle can only communicate with its spacial neighbors, *i.e.*, two vehicles are connected if the distance between them is smaller than a certain value. This value, called critical communication radius,

defines the communication region. Previous control laws to stabilize the agents to a uniformly distribution along a circular formation are considered now under this new communication approach. Moreover, this collaborative algorithm is also applied in the case of elastic formations.

Another contribution deals with the application of consensus algorithms to the previous formation control laws developed in this thesis. Note that, the time-varying parameters which define the formations, are considered external references and are known to all the vehicles. The objective of the cooperative approach is to relax this assumption. A particular case, when the center reference of a circular formation is unknown, is analyzed. In this situation, the velocity and acceleration of the desired center trajectory are given references and thanks to a consensus algorithm the agents reach consensus on the center position of the circular formation. This result, can be seen as a preliminary step to achieve the source-seeking problem.

5.1.3 Distributed estimation of the gradient direction

Several control techniques have been developed in the last years in order to locate the source of a signal distribution. Source-seeking strategies are designed to steer a single vehicle or a group of vehicles to the source location. The vehicles are equipped with sensors which are able to measure the scalar signal originating from the source. Nevertheless, the sensor does not have the capability of sensing the position of the source.

In this context, our main contribution is to prove mathematically that the gradient direction of a signal distribution can be approximated by the measurements obtained by a group of agents uniformly distributed along a fixed circular formation. The sensors do not have any knowledge of the functional form of the field. This is an important result because the gradient direction could be used to drive the center of the formation to the desired location of the source.

Taking into account communication constraints between the vehicles, a distributed algorithm based on consensus filters, which exploits the previous mathematical result, is developed. This collaborative method allows estimating the gradient direction of the signal distribution at the center of a circular formation of AUVs. Due to the circular motion of the agents, the measurements obtained are periodical. Therefore, the estimated directions oscillate around the real direction of the gradient. Using the average of the computed directions, an improved distributed algorithm is presented in order to reduce these oscillations. In this second case, exactly consensus is reached and all the agents estimate the same gradient direction.

Several simulations are provided to support these results and to analyze the performances of both algorithms. Moreover, the performance of both strategies, when the

source emitting the signal distribution is time-varying, is evaluated by simulations.

5.2 Ongoing and future works

This dissertation proposes control strategies to carry out several challenges present in cooperative underwater missions. The main contributions previously presented have been developed considering several assumptions related to the model of the vehicles, precision of sensors, communication constraints, model of the environment, etc. Consequently, the futures research directions focus on relax previous assumptions in order to consider more realistic situations.

5.2.1 Perspectives in formation control design

All formation control laws developed in this thesis take into consideration that the vehicles know their absolute position vector with respect to the inertial frame. This assumption is consistent to the fact that the vehicles are equipped with a precise inertial measurement unit for navigation. Nevertheless, according to previously cited works dealing with circular formation control [69, 86, 120, 149, 150], it seems very appropriate to consider that each vehicle is only able to compute the relative distance with respect to its neighbors. In this situation, the time-varying circular control laws from Chapter 2 and the elastic formation control design presented in Chapter 3 will be improved by cooperative algorithms in order to take into account the relative positions between the vehicles instead of their absolute positions.

Another research direction copes with extending the control strategies studied in this dissertation with a view to stabilize a fleet of autonomous underwater vehicles to time-varying formations in the presence of currents. The authors of [120, 121] provides control laws to stabilize a group of vehicles to circular formations in a time-invariant and estimated time-varying flowfield respectively. Following the same reasoning of these works, and thanks to the ideas presented in this thesis, cooperative control laws will be developed to make the vehicles converge to time-varying elastic formations in a flowfield.

Throughout this thesis, we assume a two-dimensional kinematic model of the vehicles. In consequence, the motions and formations obtained are planar, *i.e.*, the vehicles are moving in a 2-D framework. In the literature, different control strategies are proposed to obtain coordinated motion in three-dimensions of a group of vehicles, see [91] and [69] for instance. A logical extension of the results studied in this dissertation considers the possibility of develop three-dimensional time-varying formation control laws.

Finally, another future work to improve the presented formation control laws deals with collision and obstacle avoidance. The cooperative control proposed in Chapters 2 and 3 to distribute uniformly the vehicles along a formation can be seen as a collision avoidance method. The potential term added to the formation control law allows the vehicles to avoid collisions with their neighbors in the formation. However, we cannot assure collision avoidance until the vehicles are stabilized to the final configuration. Therefore, some techniques based on cooperative strategies [47, 98] can be applied in order to guarantee that vehicles do not impact each other. In the same way, potential terms can be added to the formation control laws to achieve obstacle avoidance during the motion of the fleet [108].

5.2.2 Perspectives in source-seeking algorithms

Chapter 4 tackles the source-seeking problem from a collaborative point of view. A mathematical result demonstrates that a group of sensors uniformly distributed along a fixed circular configuration taking measurement of a scalar field can approximate the gradient of the signal distribution of that field at the center of the circular formation. The first obvious research direction is to analyze the implications of a time-varying center of the formation.

Based on this previous result, two distributed algorithms are developed to estimate the gradient direction of the signal by a circular formation of autonomous underwater vehicles. The idea is to use this direction in order to steer the formation to the location of the source, *i.e.*, to the maximum or minimum of the scalar field. A collaborative approach merging time-varying formation control, consensus with reference velocity algorithms and the estimated gradient direction will be considered in future works to reach the source localization.

We assume perfect communication between two connected vehicles. With a view to analyze the performance of the control algorithms studied in this dissertation in the presence of more realistic communication constraints, cooperative approaches dealing with packet loss, noise and time delays can be considered in further research.

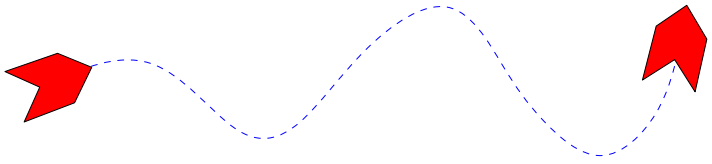

Appendix A

Fundamentals of graph theory

The present appendix looks forward to provide a sufficient detailed description of the area of graph theory which mathematical properties have been used in this thesis.

This following exposition is based on both excellent talks *Distributed Control of Robotic Networks: A Mathematical Approach to Motion Coordination Algorithms*[1] presented by Francesco Bullo, Jorge Cortés and Sonia Martínez at the 47th IEEE Conference on Decision and Control at Cancun, Mexico in December 2008 and *Consensus, flocking and opinion dynamics*[2] given by Antoine Girard during the International summer school of Automatic Control at Grenoble, France in September 2010. The reader can also refer to the book *Algebraic Graph Theory* [12], for an exhaustive and complete dissertation on the field. In addition, the PhD Thesis of Sarlette [142] presents very detailed mathematical preliminaries in graph theory and the PhD Thesis of Hendrickx [68] study the proprieties of graphs for the analysis of multi-agent systems.

A.1 Definition of Graph

Definition A.1 *A **direct graph** or digraph is defined as a couple $\mathcal{G} = (V, E)$ consisting of a set of with N elements called vertices, denoted by $V = \{1, 2, \ldots, N\}$ and a set of ordered pair of vertices called edges, represented by $E \subseteq V \times V$. The pair (k, j) denotes an edge from the element k to j.*

Definition A.2 *An **undirected graph** consists of a set of vertices V and a set of edges E which satisfies for all pair of elements $k, j \in V$, if and only if $(k, j) \in E$ then $(j, k) \in E$.*

[1] The slides of the authors can be found at http://coordinationbook.info/pdfs/CDC08workshop-DCRN-BulloCortesMartinez-lecture1.pdf

[2] The corresponding slides can be found in the Antoine Girard webpage: http://www-ljk.imag.fr/membres/Antoine.Girard/Talks/auto-school.pdf

The graphs usually represent the interconnections in a group of elements also called nodes. In this thesis, an edge between two nodes symbolizes that these elements can communicate. In this situation, the notion of neighbors and neighborhood are very useful to understand the mathematical notation dealing with graph theory.

Definition A.3 *The **neighborhood** of a vertex $k \in V$ is the set*

$$\mathcal{N}_k = \{j \in V | (k, j) \in E\}$$

Therefore, all the elements $j \in \mathcal{N}_k$ are called the neighbors of element k. This means that there is a edge from node k to each node j which belongs to the neighborhood.

Definition A.4 *The **degree** of a vertex $k \in V$ is the number its neighbors, such that*

$$d_k = |\mathcal{N}_k|$$

In a visual representation of an undirected graph, the edges between neighbors are symbolized by bidirectional arrows or usually by non-oriented segments. Figure A.1 shows a directed and an undirected graph with $N = 5$ nodes. In the case of the directed graph, the degree of node 1 is $d_1 = |\mathcal{N}_1| = 2$ because the nodes 2 and 5 are the only vertices which belong to its neighborhood. Note that, the edges $(1, 2), (1, 5) \in E$. In the other example, the vertex 1 in the undirected graph has three neighbors such that, vertices $2, 3, 5 \in \mathcal{N}_1$, thus the degree of vertex 1 is $d_1 = 3$.

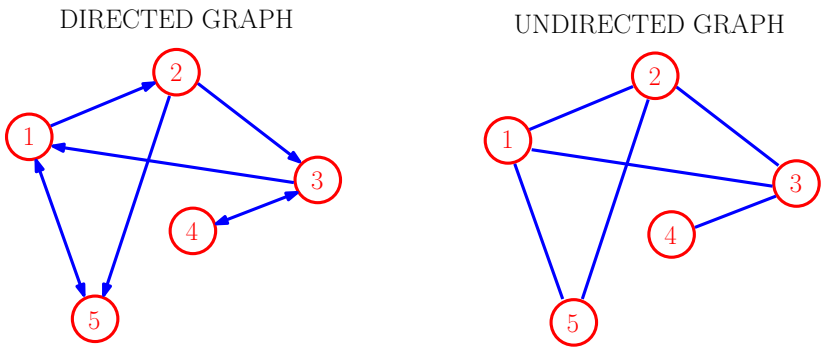

Figure A.1: *Directed and undirected graphs*

Definition A.5 *A graph $\mathcal{G}' = (V', E')$ is a **subgraph** of $\mathcal{G} = (V, E)$ if its set of vertices and its set of edges are subsets of the corresponding sets of graph $\mathcal{G}$ respectively, such that, $V' \subset V$ and $E' \subset E$.*
In addition, if $V' = V$ then $\mathcal{G}'$ is a spanning subgraph of $\mathcal{G}$.

Definition A.6 *A **spanning subgraph** is a subgraph in which $V' \equiv V$.*

Definition A.7 *A **direct tree** is a digraph in which there is a vertex, called root, such that any other vertex of the digraph can be reached by one and only one path starting at the root.*

Definition A.8 *A **direct spanning tree** is a spanning subgraph in which there is a vertex, called root, such that any other vertex of the digraph can be reached by one and only one path starting at the root.*

Definition A.9 *A digraph is **balanced** if each vertex $k \in V$ has the same number of incoming and outgoing edges.*

In particular, an undirected graph is balanced.

A.2 Connectivity of a graph

In this section connectivity notions and several properties of the graphs are presented. The stability of an algorithm, which use a graph in order to represent the interconnections between the different systems evolved in the algorithm, is directly related to the connectivity properties of the graph. An example with consensus algorithms will be analyzed in the sequel.

Consider a digraph $\mathcal{G} = (V, E)$ which vertices are denoted by $V = \{k_1, k_2, \ldots, k_N\}$. In order to analyze the connectivity properties of the graphs, the notion of direct path is introduced as follows:

Definition A.10 *A **direct path** in a digraph $\mathcal{G} = (V, E)$ is an ordered sequence of vertices $(k_1, k_2)(k_2, k_3)\ldots(k_{m-1}, k_m)$ such that any ordered pair of vertices appearing consecutively in the sequence is an edge of the digraph, i.e., $(k_{p-1}, k_p) \in E$ for all $p = 1, \ldots, m$, where $m \leq N$.*

The notion of connectivity is associated to the idea of that the information transmitted by one node in the graph can be received for the rest of the nodes of the communication graph. A vertex of a digraph is globally reachable if it can be reached from any other vertex by traversing a direct path.

Definition A.11 *A digraph $\mathcal{G} = (V, E)$ is **strongly connected** if every vertex is globally reachable, such that, for all $k \in V$ there is a direct path starting from each other vertex $j \in V, j \neq k$ which finish in k.*

For undirected graphs the notion of connectivity is expressed as follows. If for all $k, j \in V$, there exist a path (non-ordered sequence) joining k and j (its means they are connected), then the undirected graph is **connected**.

In Figure A.1 the directed graph is strongly connected because all its vertices are globally reachable. In other words, starting from every node, there exist a direct path to reach the rest of nodes. The undirected graph of Figure A.1 is connected because all its vertices are connected.

A.2.1 Adjacency matrix

The adjacency matrix allows to represent in a simple numeric form the interconnections in a graph. The connectivity of a graph is directly related to several properties of this matrix, such that its eigenvalues. The relationship between a graph and the eigenvalues and eigenvectors of its adjacency matrix is studied in spectral graph theory.

Definition A.12 *The* ***adjacency matrix*** *of a digraph* $\mathcal{G} = (V, E)$ *is the* $N \times N$ *matrix* $\mathcal{A} = (a_{kj})$ *given for all* $j, k \in V$ *by:*

$$a_{kj} = \begin{cases} 1, & \textit{if} \quad (k,j) \in E \\ 0 & \textit{otherwise} \end{cases}$$

In the case of undirected graphs, by definition, the adjacency matrix is symmetric. Note that, in this appendix self-loops are not considered, therefore all diagonal elements of the adjacency matrix are equal to zero.

For illustration, the adjacency matrix of both directed and undirected graphs displayed in Figure A.1 can be written as follows:

$$\mathcal{A}_{directed} = \begin{pmatrix} 0 & 1 & 0 & 0 & 1 \\ 0 & 0 & 1 & 0 & 1 \\ 1 & 0 & 0 & 1 & 0 \\ 0 & 0 & 1 & 0 & 0 \\ 1 & 0 & 0 & 0 & 0 \end{pmatrix} \quad \mathcal{A}_{undirected} = \begin{pmatrix} 0 & 1 & 1 & 0 & 1 \\ 1 & 0 & 1 & 0 & 1 \\ 1 & 1 & 0 & 1 & 0 \\ 0 & 0 & 1 & 0 & 0 \\ 1 & 1 & 0 & 0 & 0 \end{pmatrix}$$

A diagonal matrix, called also degree matrix, is defined in order to represent, in a matrix form, the number of neighbors of each agent.

Definition A.13 *The* ***degree matrix*** *of a digraph* $\mathcal{G} = (V, E)$ *is the* $N \times N$ *matrix* $\Delta = (d_{kj})$ *given for all* $j, k \in V$ *by:*

$$d_{kj} = \begin{cases} d_k, & \textit{if} \quad k = j \\ 0 & \textit{otherwise} \end{cases}$$

By definition, each diagonal element of the degree matrix is equal to the sum of elements of its corresponding row in the adjacency matrix. Hence, the degree matrix of both

graphs can be expressed as:

$$\Delta_{directed} = \begin{pmatrix} 2 & 0 & 0 & 0 & 0 \\ 0 & 2 & 0 & 0 & 0 \\ 0 & 0 & 2 & 0 & 0 \\ 0 & 0 & 0 & 1 & 0 \\ 0 & 0 & 0 & 0 & 1 \end{pmatrix} \quad \Delta_{undirected} = \begin{pmatrix} 3 & 0 & 0 & 0 & 0 \\ 0 & 3 & 0 & 0 & 0 \\ 0 & 0 & 3 & 0 & 0 \\ 0 & 0 & 0 & 1 & 0 \\ 0 & 0 & 0 & 0 & 2 \end{pmatrix}$$

Note that, for digraphs, two different degree matrices can be defined. The first one, is also called the out-degree matrix and it is defined as $(\Delta_{out})_{kk} = \sum_{j=1}^{N} a_{kj}$. This diagonal matrix is the same which has been determined in Definition A.13. The other one, is the in-degree matrix, expressed as $(\Delta_{in})_{kk} = \sum_{j=1}^{N} a_{jk}$.

A.2.2 Laplacian matrix of a graph

According to these previous adjacency and degree matrices, a new matrix is built in order to analyze the connectivity properties of graphs using the matrix theory.

Definition A.14 *The **Laplacian matrix** of a digraph $\mathcal{G} = (V, E)$ is the $N \times N$ matrix $\boldsymbol{L} = (l_{kj})$ given for all $j, k \in V$ by:*

$$l_{kj} = \begin{cases} d_k, & \text{if} \quad k = j \\ -1, & \text{if} \quad (k, j) \in E \\ 0 & \text{otherwise} \end{cases}$$

Consequently, the Laplacian matrix is also defined as $\mathbf{L} = \Delta - \mathcal{A}$.

The Laplacian matrix of a digraph has several interesting properties, especially with a view to study the connectivity of the graph. The following list summarizes some of the most important:

- The vector of ones $\mathbf{1} = (1, \ldots, 1)^T \in \mathbb{R}^N$ is always an eigenvector of the Laplacian matrix with eigenvalue zero, such that, $\mathbf{L1} = \mathbf{0}$, where $\mathbf{0} = (0, \ldots, 0)^T \in \mathbb{R}^N$ represents the vector of zeros.

- All the eigenvalues of $\mathbf{L}$ have nonnegative real parts, such that:

$$0 = \lambda_0 \leq \lambda_1 \leq \ldots \leq \lambda_{N-1}$$

- The digraph $\mathcal{G}$ contains a vertex globally reachable if and only if the rank of its Laplacian matrix is equal to $N - 1$.

- The quadratic expression $x^T \mathbf{L} x$, where $x \in \mathbb{R}^N$, is positive semidefinited if and only if the digraph associated $\mathcal{G}$ is balanced.

Following with both examples of Figure A.1, the corresponding Laplacian matrices of the directed and undirected graph can be expressed as:

$$\mathbf{L}_{directed} = \begin{pmatrix} 2 & -1 & 0 & 0 & -1 \\ 0 & 2 & -1 & 0 & -1 \\ -1 & 0 & 2 & -1 & 0 \\ 0 & 0 & -1 & 1 & 0 \\ -1 & 0 & 0 & 0 & 1 \end{pmatrix} \quad \mathbf{L}_{undirected} = \begin{pmatrix} 3 & -1 & -1 & 0 & -1 \\ -1 & 3 & -1 & 0 & -1 \\ -1 & -1 & 3 & -1 & 0 \\ 0 & 0 & -1 & 1 & 0 \\ -1 & -1 & 0 & 0 & 2 \end{pmatrix}$$

In the case of undirected graphs, the Laplacian matrix has additional interesting properties:

- The Laplacian matrix of an undirected graph $\mathcal{G}$ is symmetric. Therefore, all its eigenvalues are real.
- The Laplacian matrix of an undirected graph $\mathcal{G}$ is positive semidefinite.
- The quadratic expression $x^T\mathbf{L}x = \frac{1}{2}\sum_{j\in\mathcal{N}_k}^{N}(x_k - x_j)^2$, for all $x \in \mathbb{R}^N$.

The properties of the Laplacian matrix provide information about the connectivity of its associated graph. In the case of undirected graphs, these properties are stronger than for directed graphs.

Definition A.15 *The second smallest eigenvalue λ_1 of the Laplacian matrix $\boldsymbol{L}$ is referred to as the **algebraic connectivity** of the undirected graph $\mathcal{G}$.*

And it can be proved that this second eigenvalue is positive $\lambda_1 > 0$ if and only if the is connected. This result is equivalent to:

- If the digraph $\mathcal{G}$ is strongly connected then 0 is a simple eigenvalue of $\mathbf{L}$.
- The algebraic multiplicity of the eigenvalue 0 of $\mathbf{L}$ is equal to the number of connected components in the undirected graph $\mathcal{G}$.

A.3 Time-varying graphs

It is of both theoretical and practical interest to consider time-varying communication topologies. During a coordinated motion or a collaborative task, the interconnections between the agents that conform the network can evolve such that, new communication links are created and others are broken. In this situation, the links of the network are represented by a time-varying graph. It means that the set of edges E depends on time and consequently the adjacency matrix is time-varying too.

Time-varying communication topologies are described by a time-varying δ-digraph $\mathcal{G}(t) = (V, E(t))$, where the elements of its adjacency matrix $\mathcal{A}(t)$ are bounded and satisfy some threshold $\delta > 0$, that is, $akj(t) = 0$ in the absence of a communication link and $a_{kj}(t) \geq \delta$ in the presence of a communication link.

Definition A.16 *Consider a time-varying graph $\mathcal{G}(t) = (V, E(t))$ with adjacency matrix $\mathcal{A}$, and let $\bar{\mathcal{G}}(t) = (\bar{V}, \bar{E}(t))$ be the graph in which $\bar{E}(t)$ contains all edges that appear in $\mathcal{G}(\tau)$ for $\tau \in [t, t+T]$ and its adjacency matrix is defined as $\bar{\mathcal{A}} = \int_t^{t+T} \mathcal{A}(\tau)d\tau$. A node k is said to be connected to node $j \neq k$ in the interval $[t, t+T]$ if there is a path from vertex k to j, which respects the orientation of the edges for the directed graph $\bar{\mathcal{G}}$. Then, $\mathcal{G}(t)$ is said to be* ***uniformly connected*** *if there exists an index k and a time horizon $T > 0$ such that, for all t, node k is connected to all the other nodes across $[t, t+T]$.*

A.4 Circulant graphs

A circulant graph is an undirected graph in which, the adjacency matrix is circulant and all the vertices $k = 1, \ldots, N$ of the graph have the same degree $d_k = d_0 > 1$. It means that the graph has a cyclic group of symmetries that includes a symmetry taking any vertex to any other vertex, see Figure A.2.

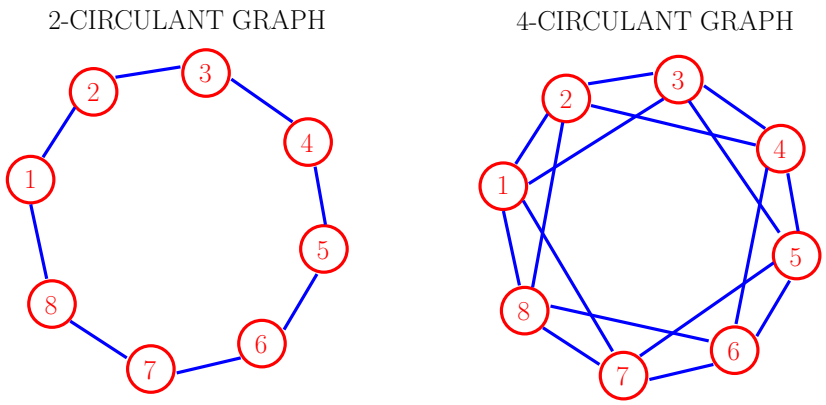

Figure A.2: *Circulant graphs*

A d_0-circulant graph is a circulant graph in which each node is connected to d_0 other nodes, where d_0 is a fixed integer in the interval $[2, N-1]$. All d_0-circulant graphs are d_0-regular, which means that $d_k = d_0$ for all k. Both adjacency and Laplacian matrices of a circulant graph are circulant, *i.e.*, they are completely defined by their first row [41]. Each subsequent row of a circulant matrix is the previous row shifted one position

to the right with the first element equal to the last element of the previous row. For example, the complete graph (all-to-all communication) is $(N-1)$-circulant and the cyclic graph (ring topology) is 2-circulant. Note that, by definition, all d_0-circulant graphs are connected [150].

The Laplacian matrix of the 2-circulant graph shown in Figure A.2 is written as follows:

$$\mathbf{L}_{2-circulant} = \begin{pmatrix} 2 & -1 & 0 & \cdots & 0 & -1 \\ -1 & 2 & -1 & \cdots & 0 & 0 \\ \vdots & \vdots & \vdots & \ddots & \vdots & \vdots \\ 0 & 0 & 0 & \cdots & 2 & -1 \\ -1 & 0 & 0 & \cdots & -1 & 2 \end{pmatrix}$$

In the same manner, the corresponding Laplacian matrix of the 4-circulant graph from Figure A.2 is expressed by:

$$\mathbf{L}_{4-circulant} = \begin{pmatrix} 4 & -1 & -1 & \cdots & -1 & -1 \\ -1 & 4 & -1 & \cdots & 0 & -1 \\ \vdots & \vdots & \vdots & \ddots & \vdots & \vdots \\ -1 & 0 & 0 & \cdots & 4 & -1 \\ -1 & -1 & 0 & \cdots & -1 & 4 \end{pmatrix}$$

Appendix B

Resumé en français

B.1 Introduction

L'exploration sous-marine est le processus relativement récent d'enquêter sur les profondeurs de la mer pour comprendre ses caractéristiques physiques et chimiques et approfondir nos connaisances sur les formes de vie qui peuplent cet environnement. L'exploration sous-marine est un phénomène nouveau (par rapport à beaucoup d'autres sciences), car la technologie nécessaire pour assurer la sécurité humaine dans les eaux profondes n'a été que dévelopée récemment. Au cours des dernières décennies, des technologies alternatives, qui utilisent des véhicules sans équipage, tels que flotteurs avec capteurs immergés, véhicules télécommandés (ROV pour le sigle en anglais) et véhicules autonomes sous-marins (AUV pour le sigle en anglais), ont émergé pour compléter les techniques de détection existantes. Tous ces véhicules sont équipés de différents capteurs afin de recueillir les informations d'une région d'intérêt. Ces informations fournissent un soutien fondamental à la compréhension des processus des océans d'un point de vue biologique (productivité de l'écosystème), ou à prédire les propriétés physiques de l'océan, comme la température et les courants. À cette fin, des stratégies de contrôle pour la commande des véhicules mobiles doivent être développées pour orienter les véhicules vers les endroits où leurs données seraient les plus utiles [39].

Les réseaux de capteurs mobiles sont souvent utilisés dans des applications environnementales telles que l'échantillonnage des océans, la surveillance, la cartographie, l'exploration spatiale et de la communication, voir [39, 86, 167, 177] et les références incluses. Dans ces sortes de missions, les capteurs mobiles sont commandés pour mesurer un champ scalaire inconnu. Par exemple, une concentration de produits chimiques, un polluant, ou la température. Comme chaque capteur ne peut prendre qu'une mesure à la fois, les capteurs doivent se déplacer dans une formation pour estimer le champ d'intérêt. Il semble approprié que le groupe de véhicules collabore afin de mener à bien la tâche d'exploration tout en optimisant le temps et l'énergie. *Collaboration* signifie

que chaque véhicule est capable de communiquer certaines informations pour le reste du groupe et ces données sont utilisées pour déterminer une action ou un comportement particulier pour accomplir la tâche d'exploration.

Dans ce contexte, la présente thèse aborde le problème d'une mission d'exploration sous-marine effectuée par un groupe d'AUVs de façon coopérative. L'objectif est de concevoir des stratégies de contrôle pour accomplir les différents défis scientifiques trouvés dans ces missions :

Commande de systèmes multi-agent : Un système multi-agent, défini plus précisément dans la Section 1.2, est un système composé par un groupe d'individus autonomes qui interagissent les uns avec les autres. Par conséquent, une flotte d'AUVs peut être traitée comme un système multi-agents dans lequelle chaque véhicule est considéré comme un agent avec des capacités de communication.

Contrôle d'une formation : Afin d'accomplir une tâche d'exploration, un choix raisonnable est de coordonner les agents pour former une configuration particulière. Les algorithmes de contrôle pour atteindre ce but doivent assurer certaines performances, telles que l'inter-distance entre les véhicules dans la formation. L'objectif le plus important est de déplacer le groupe de véhicules tout en gardant la formation.

Algorithms de contrôle avec contraintes de communication : Dans une mission collaborative, les individus échangent des informations pour atteindre une tâche particulière. Les données transmises sont soumises à différents problèmes de communication dus au canal de communication, tout particulièrement dans les environnements sous-marins, comme le bruit dans le signal transmis, les pertes de paquets, les retards lors de la transmission et les problèmes d'affaiblissement de la puissance du signal.

Cette thèse traite de ces problèmes dans le contexte d'une mission sous-marine dans laquelle une flotte de AUVs doit collaborer pour localiser une source.

B.1.1 Contexte de la thèse

Cette thèse s'inscrit dans le cadre de deux projets de recherche : le projet européen FeedNetBack[1] et le projet français CONNECT[2], financé par l'ANR (Agence Nationale de la Recherche). Les deux projets traitent de systèmes commandés en réseau (NCS pour le sigle en anglais) et ils sont particulièrement intéressés par le problème du contrôle des systèmes multi-agents, c'est-à-dire, des systèmes composés de plusieurs

[1] http ://www.feednetback.eu/

[2] http ://www.gipsa-lab.inpg.fr/projet/connect/

sous-systèmes interconnectés par un réseau de communication hétérogène. Le défi principal de ces projets est d'apprendre à concevoir des contrôleurs en prenant en compte des contraintes sur la topologie du réseau et la possibilité de partager des ressources informatiques au cours du fonctionnement du système, tout en préservant la stabilité du système en boucle fermée.

Le projet FeedNetBack regroupe plusieurs partenaires académiques, et aussi des participants industriels en vue de réaliser les applications technologiques. Le cas d'étude commun à ces deux projets se concentre sur la commande coopérative d'un groupe de véhicules marins sans pilote, c'est-à-dire, véhicules autonomes sous-marins (AUV) et navires de surface autonomes (ASV). Ce cas d'étude, détaillé plus tard, concerne le partenaire IFREMER[3] qui est chargé des aspects techniques relatifs à des véhicules sous-marins. Il permettra d'accomplir une démonstration utilisant des véhicules réels. Un des participants universitaires qui se concentre sur les innovations techniques de cette étude de cas, est l'institut de recherche INRIA (Institut National de Recherche en Informatique et en Automatique) à travers de l'équipe NeCS[4], au coeur de laquelle, cette thèse a été faite. Le projet CONNECT considère également la possibilité d'évaluer les structures de contrôle proposées par le biais d'une interface graphique développée par PGES et des simulations effectuées avec un simulateur complexe qui est construit par PROLEXIA.

Cas d'étude

The proposed case study copes with a main mission whose objective is to carry out a gradient search and following an underwater source by a fleet of AUVs. The nature of the source to be detected, can be very different : fresh water, a chemical source, methane vent, etc. The technical details corresponding to this case study are reported in

Les systèmes multi-agents en réseau, en particulier les systèmes sous-marins, qui sont actuellement utilisés ou développés par l'industrie et la recherche marine, sont soumis à de sévères contraintes technologiques. L'avantage d'utiliser plusieurs véhicules simples au lieu d'un système complexe, coûteux et de haute capacité, est que la flotte est capable de réaliser des tâches qui ne peuvent pas être facilement obtenues par un seul véhicule. Ce cas d'étude comprend des véhicules hétérogènes marins (de surface et sous-marins tels que des embarcations autonomes, AUVs ou planeurs sous-marins) afin de réaliser une mission scientifique composée de plusieurs phases (exploration et recherche, échantillonnage des données par des capteurs). Le cas d'étude proposé traite d'une mission dont l'objectif est d'effectuer une recherche de gradient et de suivre une

[3]Institut français de recherche pour l'exploitation de la mer, http ://wwz.ifremer.fr/institut
[4]http ://necs.inrialpes.fr/

source sous-marine avec une flotte de AUVs. La nature de la source à détecter, peut être très différente : de l'eau douce, une source chimique, du méthane, etc. Les détails techniques correspondant à ce cas d'étude sont détaillés dans [113].

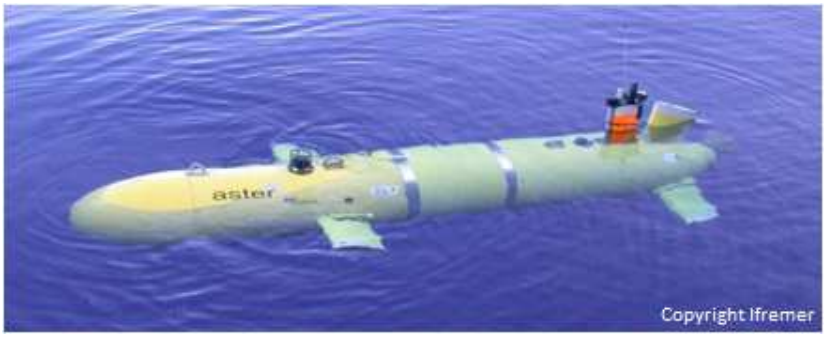

FIGURE B.1 – *Le véhicule sous-marin AsterX*

AsterX : Le véhicule sous-marin pris en compte dans ce cas d'étude et, par conséquent, dans cette thèse, est l'AsterX, qui appartient à l'IFREMER (voir Figure B.1). L'AsterX est un véhicule autonome sous-marin qui est actionné par une hélice principale destinée au déplacement dans la direction longitudinale. La direction du véhicule autour de ses angles de roulis, tangage et lacet est assurée par deux ailettes dans la partie avant du véhicule (ailettes de canard), et deux couples d'ailettes à l'arrière du véhicule (plan horizontal et vertical). En fonction de la charge utile, son poids est compris entre 580 et 800 kg dans l'air, avec une profondeur de plongée de 3000 mètres. Sa vitesse de croisière est comprise entre $0,5$ et $2,5$ mètres par seconde. La longueur du véhicule est de $4,5$ mètres et son autonomie est de 11 heures [135].

Ce AUV a plusieurs capteurs de navigation : un système Doppler pour mesurer la vitesse, une centrale inertielle (composée d'un gyroscope, d'accéléromètres et de magnétomètres) pour calculer en temps réel son attitude (roulis, tangage et l'angle de lacet) et mettre à jour sa position, et également un capteur acoustique pour le positionnement absolu.

Mission et scénario sous-marin : L'objectif de la mission est de localiser et de suivre une source en prenant en compte les données mesurées fournies par des capteurs situés à bord des AUVs, qui mesurent la concentration de l'écoulement de la source. La configuration des véhicules doit être telle que des estimations spatiales de le gradient de la concentration peuvent être calculés d'une façon coopérative. Les lois de commande coopérative conçues pour atteindre cet objectif devraient prendre en compte les contraintes de communication dues au scénario sous-marin.

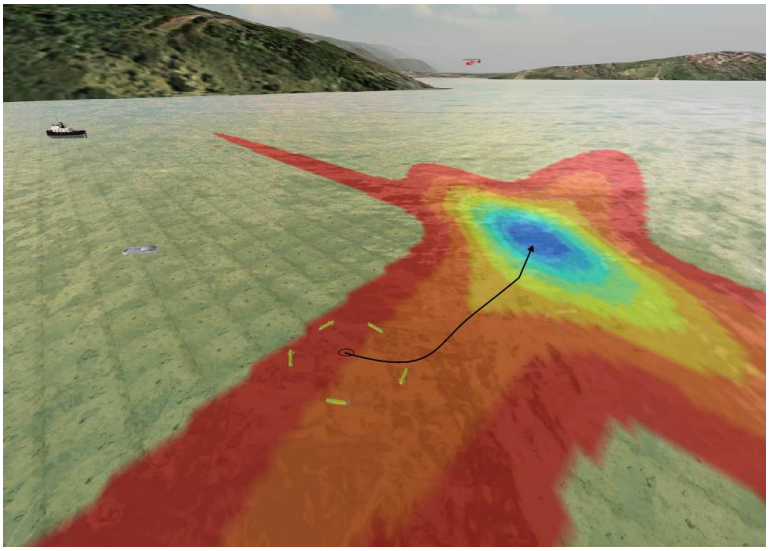

FIGURE B.2 – *Détection et suivi d'une source sous-marine*

Pour effectuer des missions impliquant plusieurs véhicules, le mouvement coordonné est nécessaire, surtout lorsque l'objectif de la mission est de diriger des capteurs. Dans le cas présenté ici, la détection de la source peut être réalisée avec les informations des capteurs recueillies par les véhicules en mesurant la concentration dans la zone de diffusion de la source, comme le montre la Figure B.2. Cette image représente l'objectif du cas d'étude et elle a été produite par l'interface graphique développée par PGES et le simulateur qui est fourni par PROLEXIA. Les formes colorées elliptiques symbolisent les courbes de niveau du champ scalaire d'intérêt. La flotte d'AUVs, organisée dans une formation particulière, calcule de manière collaborative la meilleure direction pour déplacer le centre de la formation vers l'emplacement de la source. La flotte doit manoeuvrer afin de rechercher la région de concentration la plus élevée de la distribution du signal, et donc, procéder à la localisation de la source.

Etapes de la mission et défis : Ces dernières années, il peut être remarqué la détérioration des eaux marines due à de multiples polluants. Ce cas d'étude, dévéloppé en coordination avec l'IFREMER, vise à localiser les sources des fuites, à la suite d'un naufrage, ou, inversement, les sources d'eau douce pour la consommation domestique. Les différentes étapes considérées pour atteindre cet objectif sont détaillées ci-dessous.

La configuration initiale est une flottille composée de cinq véhicules autonomes sous-marins équipés de capteurs de salinité, qui doivent trouver une source d'eau douce, sans intervention humaine. Les stratégies de coopération avec la mise en commun d'informations provenant de chaque véhicule, doivent être développées pour exploiter les avantages de l'utilisation d'une flotte de véhicules et pour réduire le temps de l'explo-

ration.

Un premier défi est dû à la difficulté d'établir une communication fiable dans un environnement sous-marin. C'est un point clé pour assurer une coopération efficace. En effet, le débit de données est seulement de quelques centaines de $bits/s$, le délai de transmission est d'environ une seconde et environ 10% de paquets sont perdus. Dans cette situation, toutes les stratégies de contrôle développées doivent prendre en compte les contraintes de communication.

La localisation d'une source sera effectuée en deux phases. Par conséquent, un deuxième défi concerne la conception des lois de commande d'une formation appropriées pour atteindre les objectifs de chaque phase. La première correspond à la phase d'exploration. Au cours de cette étape d'exploration, les véhicules se déplacent dans une formation en forme de V [103], dans le but de recueillir des informations et pour détecter la distribution de signal émise par la source. Une fois qu'un agent détecte un changement significatif de la salinité, il transmet cette information aux autres. Puis la flotte commence une phase de consolidation.

Dans cette deuxième phase, la flotte se regroupe dans une forme particulière, par exemple circulaire. Avec une telle formation, le mouvement pourrait être plus lent que lors de la formation en V. Toutefois, une formation circulaire a une plus grande souplesse pour se déplacer dans toutes les directions. En outre, la répartition des AUVs le long de la formation est pertinente pour recueillir des mesures distribuées spatialement qui peuvent permettre une localisation plus précise de la source. Il est également possible d'envisager un grand nombre de formations : il peut être intéressant de déformer la formation pour l'adapter à l'environnement, de suivre un chemin ou pour éviter des obstacles.

En vue de former et de maintenir cette formation, les véhicules doivent échanger des messages en fonction de leur position par rapport au centre de la formation. Une conception centralisée peut être considérée où un véhicule de surface fournit toutes les informations nécessaires à la flotte. Les échanges de données entre les AUVs permettent d'envisager une approche décentralisée dans laquelle aucun véhicule n'est consideré comme un leader. Afin de prendre en compte les contraintes de communication, telles qu'une zone limitée de communication pour les AUVs, seuls les voisins les plus proches sont pris en compte pour échanger des informations.

Afin d'atteindre l'objectif de la recherche d'une source, un algorithme de décision doit être développée. Il sera également basé sur les échanges de données entre voisins pour assurer la même robustesse que dans le cas des contraintes de communication. L'objectif de cette dernière tâche est de permettre à tous les véhicules de se mettre d'accord sur une orientation de la formation pour se déplacer vers la source en utilisant les mesures collectées par les véhicules. On peut imaginer d'étendre ce type d'algo-

rithmes pour d'autres applications telles que la definition des contours qui cherche à délimiter l'étendue et l'évolution d'une zone polluée.

Objectifs généraux

Les objectifs généraux communs aux deux projects FeedNetBack et CONNECT, correspondant au cas d'étude des véhicules sous-marins déjà présenté, se concentrent sur les cinq défis principaux suivants :

Architecture : La nécessité de coordonner les actions des véhicules sur des canaux de capacité limitée.

Contrôle et Complexité : Stratégies de contrôle centralisées contre décentralisées, qui sont au coeur de cette application.

Contrôle et Communication : La bande passante disponible est très limitée (quelques bits par seconde), la communication est soumise à des retards de propagation longs et variables, des multi-trajets, de la décoloration et des taux élevés d'erreurs de transmissions.

Contrôle et Calcul : Le cas d'étude fera usage des stratégies d'échantillonnage adaptatif et de calcul collaboratif distribué.

Contrôle et Énergie : Dans cette application la puissance des batteries est limitée et généralement les batteries ne peuvent pas être rechargées pendant une mission. Les ressources énergétiques doivent être partagées entre les différentes fonctions.

Conformément à ces objectifs généraux, la stratégie de contrôle suivante, basée sur un rapport technique du projet FeedNetBack [152], pour parvenir à la recherche collaborative d'une source sous-marine à l'aide d'une flotte de AUVs est proposée dans cette thèse. Le premier défi est de décrire une architecture adéquate pour faire face à une approche coopérative en prenant en compte tous les éléments de la formulation du problème et toutes les contraintes. En conséquence, trois boucles de contrôle principales sont prises en considération, comme le montre la Figure B.3. Sachant que ce projet vise à étudier des flottes de véhicules qui travaillent ensemble pour atteindre un objectif commun, en termes de contrôle et de coordination des flottes, cette thèse considère que la flotte est composée d'un ensemble homogène de véhicules, *c'est-à-dire*, tous les véhicules ont le même modèle dynamique.

Le premier objectif est de développer une boucle de régulation locale, appelée commande robuste, qui stabilise chaque AUV. Cette loi de commande prend en compte le modèle dynamique des véhicules, afin de contrôler leur orientation, la vitesse et la

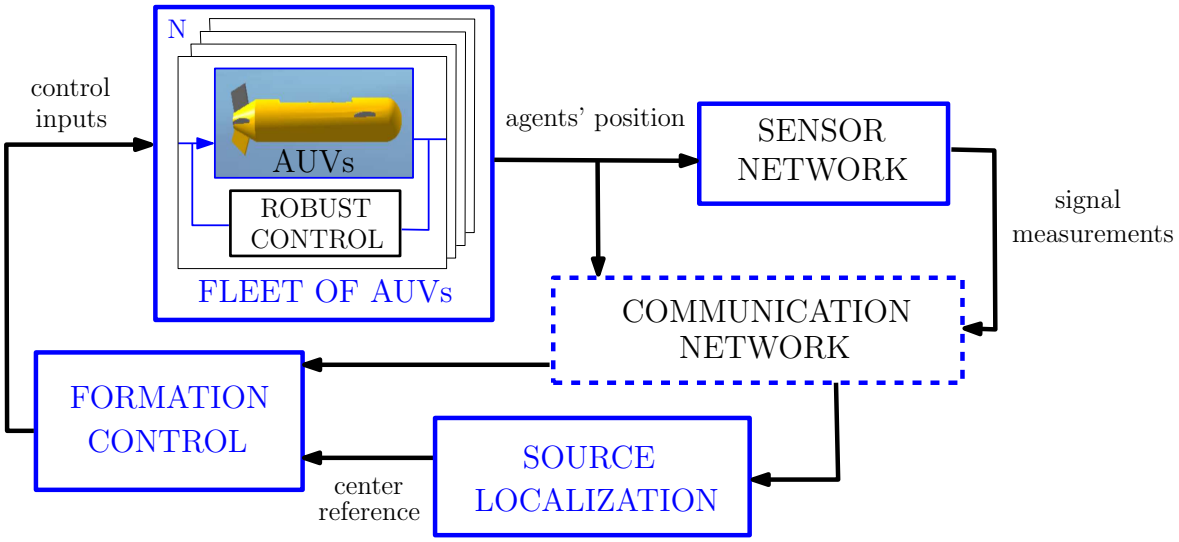

FIGURE B.3 – *Architecture de la stratégie du contrôle*

profondeur. Le mouvement le long des trois axes est découplé de telle sorte que, trois contrôleurs différents sont calculés pour le contrôle de la vitesse d'avancement, l'angle de lacet et de l'altitude respectivement. La thèse de Roche [136], qui fait également partie des projets FeedNetBack et CONNECT, s'occupe de la conception robuste des commandes pour le suivi de trajectoire d'un seul AUV par une approche d'échantillonnage variable.

En considérant plusieurs véhicules identiques, la boucle externe effectue la tâche de recherche. Un contrôle coopératif est mis en oeuvre pour atteindre un mouvement coordonné de la flotte de telle sorte que le groupe des AUVs est disposé dans une configuration particulière. La formation souhaitée est définie par plusieurs paramètres tels que son centre et son rayon dans le cas d'une formation circulaire. Une loi de commande collaborative stabilise la flotte vers une formation qui suit des paramètres variant dans le temps. Ce travail est réalisé en deux dimensions, par conséquent, il est supposé que tous les véhicules se déplacent à la même profondeur. La vitesse linéaire et l'orientation sont les variables de contrôle qui dépendent de l'état de l'AUV (sa position et sa vitesse) et des références externes qui définissent la formation désirée. La distribution uniforme des véhicules le long de la formation est également considérée. Afin de prendre en compte les contraintes de communication, un algorithme décentralisé est conçu pour stabiliser les véhicules vers la configuration désirée (distribution uniforme), en utilisant uniquement les informations de leurs voisins les plus proches.

Enfin, la trajectoire du centre de la formation est obtenue par une commande distribuée en utilisant les mesures du signal collectées par la flotte de AUVs. Les données attendues sont mesurées par des capteurs de détection. La trajectoire à suivre par

la flotte passe d'une configuration de recherche prédéfinie à un contrôle de suivi de trajectoire basé sur les données des capteurs afin de détecter la source des données mesurées.

La mise en oeuvre des boucles de régulation sur un réseau de contrôleurs numériques induit des perturbations supplémentaires par rapport à la conception initiale à temps continu, plus précisément en raison de l'échantillonnage, les retards, la quantification et de la perte de données. Par conséquent, il convient de prendre en compte ces contraintes de communication afin de concevoir les différentes stratégies de contrôle définies précédemment.

B.1.2 Contributions de la thèse

La communauté d'automatique a spécialement porté son attention sur les systèmes multi-agents dans les vingt dernières années. Les différents aspects présentés dans l'état de l'art précédent ont été largement étudiés à cause des avantages des systèmes multi-agents, par rapport à l'utilisation d'un seul véhicule ou d'un capteur, dans un grand nombre d'applications.

Dans le contexte de l'exploration sous-marine, la conception des missions collaboratives permet la collecte d'informations provenant de zones étendues dans un temps plus court. Le principal avantage d'utiliser plusieurs systèmes dans un mouvement coordonné est d'augmenter la portée d'un capteur par rapport à sa zone de couverture. Ceci est particulièrement important si les propriétés qui doivent être mesurées fluctuent avec le temps.

Selon le cas d'étude présenté dans cette introduction, les principaux défis abordés dans cette thèse sont résumés comme suit :

- Contrôle d'une formation de AUVs
- Commande coopérative
- Recherche d'une source
- Algorithmes du contrôle avec contraintes de communication

La figure B.4 présente les principaux objectifs qui seront discutés dans cette thèse. La première boucle de commande correspond au problème de contrôle d'une formation. Le système multi-agents, dans ce cas représenté par un groupe d'AUVs, est régi par une loi de commande qui utilise les positions des agents et leurs orientations, et qui dépendt de paramètres de références externes pour la formation. Cet algorithme stabilise la flotte vers des formations variant dans le temps. Ces formations suivent des paramètres de références externes qui définissent la configuration souhaitée, comme son centre,

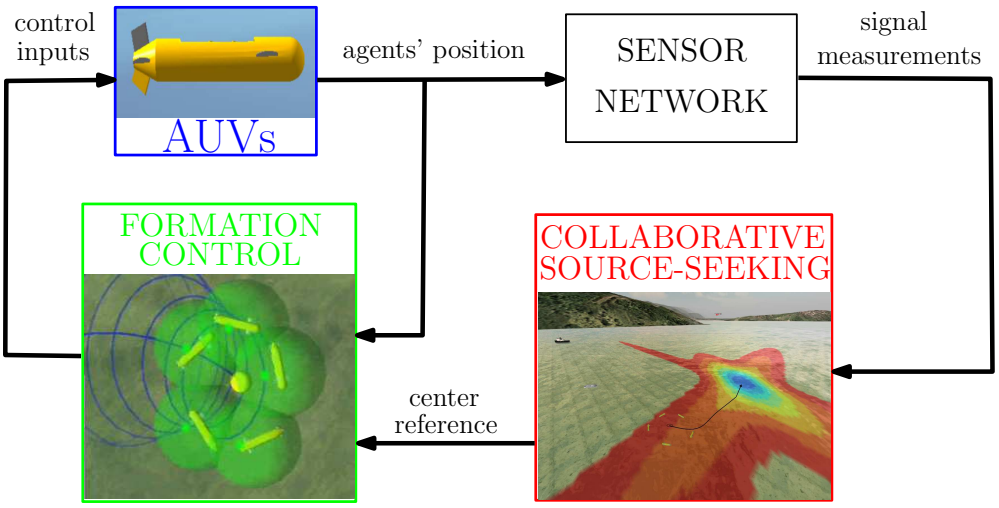

FIGURE B.4 – *Contributions de cette thèse*

par exemple. Par ailleurs, nous avons développé des algorithmes collaboratifs pour distribuer les véhicules autour de la formation d'une façon particulière.

La deuxième boucle de commande est conçue pour atteindre l'objectif final, la localisation et le suivi collaboratif d'une source. Les AUVs sont maintenant considérés comme un réseau de capteurs mobiles pour obtenir des mesures d'un champ scalaire. Ces mesures seront utilisées pour calculer un algorithme distribué pour réaliser la recherche d'une source. Enfin, cet algorithme fournit la référence adéquate pour déplacer la formation vers la localisation de la source.

A la fin de cette thèse, nous verrons comment plusieurs outils du domaine de l'Automatique nous permetent de trouver une solution pour les problèmes discutés au début de cette introduction.

B.2 Contrôle d'une formation circulaire variant dans le temps

Afin de faire face aux défis mentionnés dans l'introduction, la stratégie de contrôle élaborée dans cette thèse est structurée en trois phases. La première étape se concentre sur le problème du contrôle d'une formation. Cette section traite de la conception des lois de commande d'une formation pour une flotte de véhicules autonomes sous-marins. Une formation est une configuration composée par un groupe de véhicules capables de communiquer, dans lequel les véhicules collaborent pour atteindre un objectif commun. Cette première contribution se concentre sur la conception de lois de commande pour obtenir des formations circulaires.

Le cercle a plusieurs propriétés symétriques intéressantes et sa forme géométrique peut être simplement caractérisée par son centre et son rayon. Pour cette raison, le mouvement circulaire des véhicules est un sujet très vastement analysé dans la littérature. Il y a plusieurs approches qui abordent cette question. Par example, la stratégie collaborative appellée *poursuite cyclique* étudiée dans [95], *circumnavigation* d'un seul véhicule présenté dans [44] ou les mouvements circulaires collectifs dans [86].

Sur la base des résultats précédents sur le contrôle d'une formation circulaire étudiés dans la littérature, plusieurs lois de commande sont développées dans cette section pour stabiliser une flottille d'agents vers des formations circulaires variant dans le temps. D'une part, le contrôle de convergence de véhicules vers un mouvement circulaire dont le centre suit une référence variant dans le temps est présenté. Dans un second temps, les agents sont stabilisés vers un mouvement circulaire qui change son rayon selon une référence externe. Les deux lois de commande sont améliorées en ajoutant une fonction potentiel afin de distribuer les agents autour de la formation dans un esprit collaboratif.

B.2.1 Formulation du problème

Dans cette section, on considère des formations circulaires d'agents autonomes dans un espace à 2 dimensions. Il est supposé que les agents n'ont pas d'extension physique, *c'est-à-dire*, que leurs positions sont de simples points. Considérons un groupe de N véhicules identiques modélisés avec une cinématique unicycle soumise à une simple contrainte non-holonomique, adéquate pour les véhicules sous-marins, tels que la dynamique des agents, où $k = 1, \ldots, N$, est définie par :

$$\dot{x}_k = v_k \cos\theta_k \tag{B.1a}$$

$$\dot{y}_k = v_k \sin\theta_k \tag{B.1b}$$

$$\dot{\theta}_k = u_k \tag{B.1c}$$

où $\mathbf{r}_k = (x_k, y_k)^T \in \mathbb{R}^2$ est le vecteur position de l'agent k, $\theta_k \in S^1$ est son angle du cap et v_k, u_k sont les variables d'entrée de la commande.

L'objectif est de concevoir des stratégies de contrôle pour faire converger le groupe d'AUVs, représenté par le système (B.1), vers des formations circulaires, dont les paramètres, centre et rayon, sont variant dans le temps. Les hypothèses suivantes sont prises en compte dans la suite pour établir à cette première contribution :

- Chaque véhicule $k = 1, \ldots, N$ connaît son vecteur de position absolute $\mathbf{r}_k$ par rapport au système de référence inertiel.
- Les références variant dans le temps qui définissent les paramètres de la formation circulaire, *c'est-à-dire*, son centre et son rayon, sont connus par tous les véhicules.

- Chaque véhicule est capable de communiquer dans une région délimitée par une distance de communication critique ρ. Ce rayon est le même pour tous les véhicules.

- Les problèmes de communication tels que, le bruit, la perte de paquets et les délais, ne sont pas considérés.

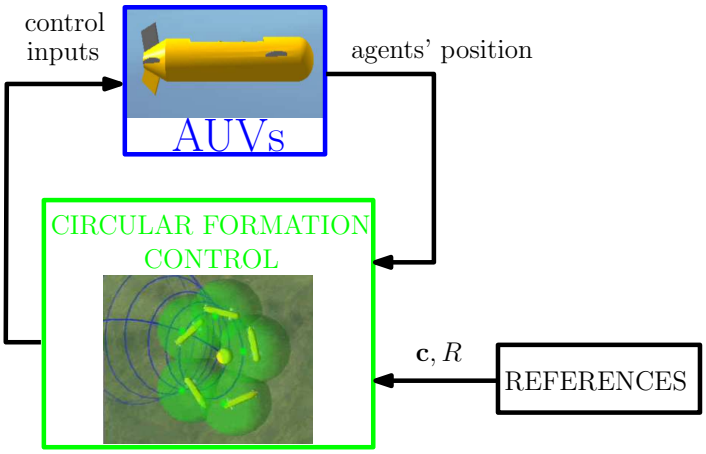

FIGURE B.5 – *Formulation du problème de la section B.2*

Sous ces hypothèses, cette section présente des lois de commande pour stabiliser un groupe de véhicules vers des mouvements circulaires qui suivent des références variant dans le temps, comme le représente la Figure B.5. De plus, un algorithme collaboratif permet de distribuer les véhicules dans une configuration désirée autour de la formation.

B.2.2 Translation d'un mouvement circulaire

Sur la base des travaux précédents sur les formations circulaires de multi-agents [86, 118, 149, 150], cette subsection présente une première contribution dans le domaine du contrôle d'une formation et une première étape pour résoudre le problème de recherche d'une source.

Le déplacement d'une formation d'agents est pertinent pour certaines applications où les agents doivent exécuter des tâches collaboratives nécessitant que la formation se déplace vers une direction a priori inconnue. Par exemple, dans les applications de recherche d'une source, la formation est dirigée en suivant la direction du gradient de la source (qui est calculée en ligne, et implémentée comme une boucle externe supplémentaire) [64, 104]. Le problème de la poursuite de cible nécessite également de considérer des formations variant dans le temps. Dans cette application, les agents tentent d'entourer la cible. Par conséquent, une formation circulaire dont le centre

est situé sur l'objectif, semble particulièrement appropriée au problème du suivi d'une cible. Certaines approches coopératives pour atteindre ce défi en utilisant une flotte de véhicules ont été étudiées dans la littérature [80, 117]. Par conséquent, une formation circulaire peut être utile pour suivre la trajectoire d'une cible variant dans le temps [85].

Cette subsection présente une stratégie de contrôle de telle sorte qu'un système multi-agent définie par (B.1) converge vers un mouvement circulaire qui suit un centre variant dans le temps. À la première étape, on suppose que le centre désiré variant dans le temps $\mathbf{c}(t)$ est une référence externe donnée qui est connue par tous les agents de la formation.

Pour résoudre le problème de déplacement d'une formation circulaire, on doit se concentrer sur les deux questions suivantes :

a) L'amélioration du contrôle circulaire précédemment presenté dans [118] pour stabiliser la flotte d'agents vers le même mouvement circulaire variant dans le temps.

b) Définir la classe des fonctions $\mathbf{c}(t)$ pour lesquelles le déplacement du mouvement circulaire est possible.

Introduction d'un nouveau système de coordonnées

Nous voulons stabiliser le système (B.1) vers un mouvement circulaire de rayon R et de centre $\mathbf{c}(t)$ variant deans le temps suivant une référence donnée. L'idée principale et donc, la principale contribution, consiste à exprimer le système multi-agents dans un cadre relatif dont l'origine est le centre désiré variant dans le temps $\mathbf{c} = (c_x, c_y)^T$. Ce système transformé, dans lequel la position des agents est exprimée par rapport au centre du cercle, sera stabilisé vers un mouvement circulaire centré sur $\mathbf{c}$ et de rayon R, en se basant sur le contrôle d'une formation circulaire presenté dans [118].

On considère que le système transformé est une référence pour le système original. Le système transformé est stabilisé vers un mouvement circulaire fixe. Le problème de concevoir une loi de commande devient un problème de suivi entre les deux systèmes. Cette stratégie suit trois phases :

- **Modèle de référence :** une relation entre le système original (vecteur de position de chaque agent) et le système de référence (vecteur de position relative) est déterminée.
- **Contrôle d'un cercle fixe :** le système de référence est stabilisé vers un mouvement circulaire avec centre fixe grâce à la loi de commande de [118].
- **Suivi du modèle :** les entrées de commande du système original sont définies par un procédé de suivi de référence.

Afin d'exprimer le vecteur position $\mathbf{r}_k$ de chaque agent k dans le cadre relatif qui se déplace suivant le centre du mouvement circulaire $\mathbf{c}$, le changement de coordonnées suivant est défini :

$$\hat{\mathbf{r}}_k = \mathbf{r}_k - \mathbf{c} \tag{B.2}$$

où $\hat{\mathbf{r}}_k \in \mathbb{R}^2$ représente le vecteur de position relative.

La loi de commande de [118] peut être appliquée à un système multi-agent modélisé par (B.1) avec une vitesse constante $v_k = v$. Par conséquent, pour appliquer cette loi de commande circulaire au système transformé, exprimé dans le système de référence relatif par rapport au centre mobile, la dynamique des positions relatives doit avoir une vitesse constante. Les agents *virtuels* définis par le système transformé convergent vers un mouvement circulaire avec rayon $R = v/|\omega_0|$ où $\omega_0 \neq 0$ est la vitesse angulaire. Ensuite, on impose une vitesse linéaire constante égale à $v = R|\omega_0|$ au système transformé. En conséquence, nous imposons au système transformé la dynamique suivantes :

$$\dot{\hat{x}}_k = R|\omega_0| \cos\psi_k \tag{B.3a}$$
$$\dot{\hat{y}}_k = R|\omega_0| \sin\psi_k \tag{B.3b}$$
$$\dot{\psi}_k = \hat{u}_k \tag{B.3c}$$

où ψ_k représente l'angle d'orientation du veteur position transformé $\dot{\hat{\mathbf{r}}}_k = (\dot{\hat{x}}_k, \dot{\hat{y}}_k)^T$.

Le système résultant transformé, est invariant dans le temps car le centre est fixe dans le nouveau cadre de référence transformé. Par conséquent, on peut appliquer la loi de commande pour un mouvement circulair de [118]. L'objectif est donc de contrôler une flotte d'agents fictifs modélisés par (B.3), de telle sorte que ces agents virtuels convergent vers un mouvement circulaire centré à l'origine du système de coordonnées transformé. La loi de commande suivante garantit que le système (B.3) converge vers un mouvement circulaire :

$$\hat{u}_k = \dot{\psi}_k = \omega_0(1 + \kappa\dot{\hat{\mathbf{r}}}_k^T\hat{\mathbf{r}}_k) \tag{B.4}$$

Translation d'un mouvement circulaire

Le système transformé défini par (B.2) est considéré comme un système de référence. La dynamique du système de référence satisfait (B.3) et la dynamique en boucle fermée est imposée par la loi de commande (B.4). Dans cette situation, le théorème suivant présente le résultat principal de cette section.

Théorème B.1 *Considerons une fonction deux fois différentiable $\mathbf{c}(t) : \mathbb{R} \to \mathbb{R}^2$, avec ses première et seconde dérivés bornées. Le rayon du mouvement circulaire désiré est*

représenté par $R > 0$, les paramètres de contrôle sont tels que $\omega_0 \neq 0$, $\kappa > 0$, $\beta > 0$ et que la condition suivante est satisfaite :

$$v_k > 0 \tag{B.5}$$

Alors, la loi de commande

$$\dot{v}_k = -\beta v_k + \frac{\hat{u}_k \dot{\boldsymbol{r}}_k^T \boldsymbol{R}_{\frac{\pi}{2}} \dot{\hat{\boldsymbol{r}}}_k + \dot{\boldsymbol{r}}_k^T (\ddot{\boldsymbol{c}} + \beta(\dot{\hat{\boldsymbol{r}}}_k + \dot{\boldsymbol{c}}))}{v_k} \tag{B.6a}$$

$$u_k = \frac{\hat{u}_k \dot{\boldsymbol{r}}_k^T \dot{\hat{\boldsymbol{r}}}_k + \dot{\boldsymbol{r}}_k^T \boldsymbol{R}_{\frac{\pi}{2}}^T (\ddot{\boldsymbol{c}} + \beta(\dot{\hat{\boldsymbol{r}}}_k + \dot{\boldsymbol{c}}))}{v_k^2} \tag{B.6b}$$

où $\dot{\hat{\boldsymbol{r}}}_k$ et $\hat{u}_k$ sont définies par (B.3) *and* (B.4) *respectivement, fait converger tous les agents définis par* (B.1) *vers un mouvement circulair de rayon R, et dont le centre suit la référence variant dans le temps $\boldsymbol{c}(t)$. La direction de rotation est déterminée par le signe de ω_0.*

B.2.3 Contraction d'un cercle

Après le premier résultat concernant la translation d'un mouvement circulaire proposé précédemment, on considère aussi le problème de concevoir une loi de commande de telle sorte que le groupe des AUVs forme un cercle dont le centre $\mathbf{c}$ est fixe et dont le rayon suit une référence variant dans le temps $R(t)$. En utilisant la même idée que dans le cas de la translation, cette extension à la contraction et l'expansion d'une formation circulaire est l'étape logique suivante en prenant en compte du fait que les principaux paramètres d'un cercle sont son centre et son rayon. Une loi de commande similaire à (B.6) est proposée pour ce cas de contraction d'un mouvement circulaire.

B.2.4 Répartition uniforme autour d'une formation circulaire

Les deux lois de contrôle précédentess ne prennent pas en considération les contraintes de communication, car chaque agent converge indépendamment vers le mouvement circulaire désirée. Par conséquent, la disposition des particules autour du cercle est arbitraire. En d'autres termes, afin de stabiliser les agents à une *formation* circulaire des lois de commande pour la translation et la contraction doivent inclure un terme coopératif pour distribuer les agents autour du même cercle en suivant un schéma particulier. En outre, dans le contexte de la recherche d'une source avec véhicules sous-marins, faire en sorte que les agents soient répartis uniformément le long de la formation pourrait être plus approprié pour produire des mouvements de recherche efficaces.

Considérer des graphes de communication fixes n'est pas réaliste car la distance entre deux agents connectés n'est pas considérée, [109, 111, 130]. Dans le cas de communication sous-marine, la qualité de la transmission est fortement affectée par la distance

entre deux agents [155]. Par conséquent, dans un scénario sous-marin, il pourrait être plus intéressant de considérer des graphes de communication dépendants de la distance. Cela signifie que chaque agent peut seulement recevoir des informations de ses voisins proches. Ainsi, une région de communication pour chaque véhicule est introduite dans notre approche. La région de communication pour n'importe quel agent est définie par ρ, qui est la distance de communication critique donnée par les caractéristiques des dispositifs de communication et de l'environnement des AUVs. Pour la suite, le rayon ρ délimite une région de communication circulaire pour chaque véhicule. Cependant, nous supposons qu'il existe une communication parfaite à l'intérieur de cette région.

Le graphe de communication, qui dépend de la distance, est maintenant variant dans le temps parce que la position des véhicules évolue dans le temps. En se basant sur la théorie des graphes, la matrice Laplacienne variant dans le temps $\mathbf{L}(t)$ qui correspond à un graphe de communication dépendant de la distance est définie comme suit :

$$L_{k,j} = \begin{cases} d_k, & \text{si} \quad k = j \\ -1, & \text{si} \quad \|\mathbf{r}_k - \mathbf{r}_j\| \leq \rho \\ 0 & \text{autrement} \end{cases} \tag{B.7}$$

La formulation de la notation suivante est introduite. La matrice Laplacienne considérée est $\bar{\mathbf{L}} = \mathbf{L} \otimes \mathbf{I}_2$ où $\otimes$ est le produit de Kronecker et $\mathbf{I}_N \in \mathbb{R}^{N\times N}$ est la matrice indentité. Le vecteur $b_{mk} = (\cos m\psi_k, \sin m\psi_k)^T$ contient les angles d'orientation des agents fictifs et $\mathbf{B}_m = (b_{m1}^T, \ldots, b_{mN}^T)^T$ contient tous les angles de cap du système transformé.

Le contrôle coopératif pour la translation d'une formation circulaire avec l'hypothèse de communication dépendant de la distance est présenté dans le corollaire suivant :

Corollaire B.1 *(Extension de Briñón-Arranz et al. 2009 [16]) Considerons une function deux fois dérivable $\boldsymbol{c}(t) : \mathbb{R} \to \mathbb{R}^2$, avec ses dérivées, première et seconde, bornées et le rayon de la formation désiré est $R > 0$. Les paramètres de contrôle sont tels que $\omega_0 \neq 0$, $\kappa > 0$, $\beta > 0$, et la condition* (B.5) *est satisfaite. Le graphe de communication est representé par $\mathcal{G}(t)$, $\boldsymbol{L}(t)$ est sa matrice Laplacienne correspondante et le rayon de communication ρ satisfait :*

$$\rho > 2R \sin \frac{\pi}{N} \tag{B.8}$$

Donc, la loi de commande (B.6) *avec*

$$\begin{cases} \hat{u}_k = \omega_0(1 + \kappa \dot{\hat{\boldsymbol{r}}}_k^T \hat{\boldsymbol{r}}_k) - \frac{\partial U}{\partial \psi_k} \\ U(\psi) = \frac{K}{N} \sum_{m=1}^{\lfloor N/2 \rfloor} \frac{1}{2m^2} \boldsymbol{B}_m \bar{\boldsymbol{L}} \boldsymbol{B}_m \end{cases} \tag{B.9}$$

fait converger tous les agents définis par (B.1) *vers une formation circulaire de rayon R et de centre $\boldsymbol{c}(t)$ qui est une référence variant dans le temps. En outre, pour $K > 0$,*

la distribution uniforme des agents autour de la formation est le seul point critique de $U(\psi)$ exponentiellement stable.

Simulations

La simulation montrée dans la Figure B.6, présente un groupe de six agents régis par la loi de commande pour la translation du Corollaire B.1. Les paramètres de contrôle sont $\omega_0 = \kappa = \beta = 1$ et $K = 0.1$. Le rayon de la formation circulaire désiré est $R = 2$ et la référence du centre $\mathbf{c}(t)$ est donnée par :

$$\mathbf{c}(t) = (0.2t, 3\sin(0.08t))^T$$

Le rayon de communication essentiel $\rho = 3$ satisfait la condition (B.8). Par conséquent, les agents sont distribués uniformément le long du cercle.

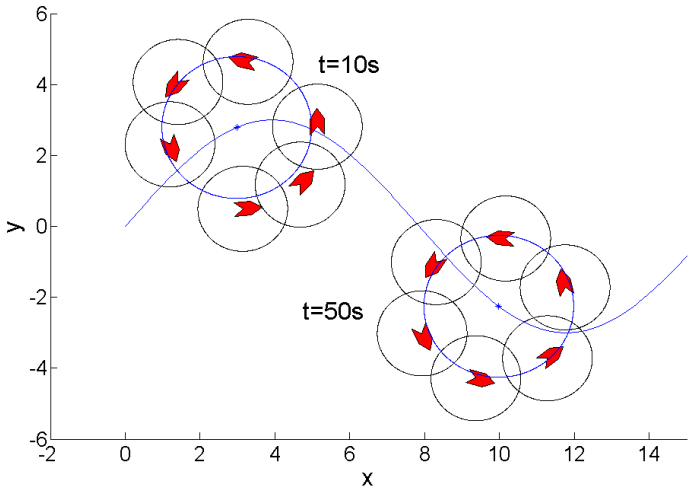

FIGURE B.6 – *Simulation de six agents régis par la coi de commande du Corollaire B.1 qui suit la référence du centre de la formation en bleu. Les cercles noirs représentent la région de communication des agents. La figure montre deux moments correspondant à des instants différents, à $t = 10s$ la distribution uniforme n'a pas encore été obtenue et à $t = 50s$ les agents sont distribués uniformement autour du cercle.*

B.3 Contrôle d'une formation basé sur les transformations affines

La section précédente présente deux contributions dans le domaine de contrôle d'une formation : la translation et la mise à l'échelle (contraction et expansion) d'une formation circulaire. Même si ces deux éléments sont fondamentaux pour l'objectif final, la

recherche d'une source, il peut être intéressant de ne pas restreindre les lois de commande à des formations circulaires. Afin d'exprimer les contributions précédentes sous une forme compacte et en vue d'étendre ces résultats à des formations plus complexes variant dans le temps, un nouveau cadre de travail basé sur des transformations affines est introduit.

Cette section se concentre sur la conception de nouvelles lois de commande d'une formation utilisant une approche différente. L'objectif est de généraliser les lois de commande précédentes, utilisant des transformations affines. Dans la suite, une nouvelle loi générale de commande d'une formation est développée pour stabiliser un groupe de véhicules vers plusieurs types de formations, non plus uniquement circulaire, ansi que des formations variant dans le temps. La configuration de la formation est définie par une matrice de transformation qui est une référence donnée et connue par tous les agents de la flotte. En outre, un contrôle coopératif est prévu pour distribuer les agents uniformément le long de la formation en prenant en compte des contraintes de communication. Enfin, des algorithmes distribués sont conçus pour améliorer la loi de commande d'une formation générale dans le cas où la référence du centre de la formation est inconnu.

Les transformations affines sont utilisées dans les domaines de l'informatique et de la robotique, [2, 70, 72, 107]. Elles sont très utiles pour definir d'une manière plus simple les coordonnées d'un robot manipulateur [58] ou pour relier le cadre de référence local d'une caméra vidéo à un autre système de coordonnées, par exemple. En général, une transformation affine est composée de transformations linéaires, tels que la rotation et l'homothétie, et les translations. Puisque une translation est une transformation affine, mais pas une transformation linéaire, les coordonnées homogènes sont normalement utilisées pour représenter l'opérateur translation par une matrice, et donc, pour le rendre linéaire.

Les trois principales transformations affines sont la translation, la rotation et l'homothétie. Pour exprimer ces transformations de façon matricielle, les coordonnées homogènes sont définis, voir [56]. Les coordonnées homogènes d'un vecteur $\mathbf{z} = (z_x, z_y)^T \in \mathbb{R}^2$ peuvent être simplement définies comme le nouveau vecteur $\mathbf{z}^h = (z_x, z_y, 1)^T$. Le vecteur de position de l'agent k en coordonnées homogènes est maintenant défini comme $\mathbf{r}_k = (x_k, y_k, 1)^T$.

Definition de formation élastique

Une formation circulaire dans le plan peut être définie par trois paramètres, son centre, son rayon et la vitesse angulaire de rotation. Pour modifier ces paramètres, les transformations affines sont introduites. L'objectif maintenant est de définir une formulation mathématique pour les *formations élastiques*. En considerant les contributions

précédentes, la translation et la contraction d'un cercle, l'idée principale est de déformer le cercle unité afin d'obtenir la *formation élastique* désirée. Dans ce contexte, le cercle unité $\mathcal{C}_0$ est définie comme une circonférence centrée à l'origine du système de référence et de rayon unité.

Des séquences de transformations affines, qui sont générées par une combinaison de translations, homothéties et rotations, est définie comme suit :

$$\mathbf{G} = \prod_{i}^{I} \prod_{j}^{J} \prod_{k}^{K} \mathbf{S}_i \mathbf{R}_{\alpha_j} \mathbf{T}_{c_k} \tag{B.10}$$

Ici, les indices représentent les différentes transformations du même type qui sont appliquées. Notez que le produit de matrices n'est pas commutatif.

Chaque combinaison de transformations affines, exprimée par une matrice générale $\mathbf{G}$, définit une formation élastique $\mathcal{F}$.

Définition B.1 *Une formation élastique $\mathcal{F}$ est une courbe qui résulte de l'application d'une séquence de transformations affines $\boldsymbol{G}$ définie par* (B.10)*, au cercle unité $\mathcal{C}_0$ de telle sorte que :*

$$\mathcal{F} = \boldsymbol{G} \circ \mathcal{C}_0$$

Contrôle d'une formation élastique

La première étape pour concevoir une nouvelle loi de commande consiste à exprimer le vecteur position dans le système de référence transformé. Selon la définition d'une formation élastique $\mathcal{F} = \mathbf{G} \circ \mathcal{C}_0$ la transformation des coordonnées suivante est introduit :

$$\hat{\mathbf{r}}_k = \mathbf{G}^{-1} \mathbf{r}_k \tag{B.11}$$

où $\hat{\mathbf{r}}_k = (\hat{x}_k, \hat{y}_k, 1)^T$ est le vecteur de position transformé exprimé en coordonnées homogènes.

Afin d'utiliser la loi de commande pour une formation circulaire fixe, le nouveau système transformé doit avoir une vitesse linéaire constante égale à $|\omega_0|$. Le raisonnement est le même que dans la section précédente pour la translation et contraction du cercle. Par définition, la vitesse linéaire d'un point dans le cercle unité fixe est $v = R_0|\omega_0|$. Par conséquent, la dynamique du vecteur position transformé est imposée comme suit :

$$\dot{\hat{x}}_k = |\omega_0| \cos \psi_k \tag{B.12a}$$

$$\dot{\hat{y}}_k = |\omega_0| \sin \psi_k \tag{B.12b}$$

$$\dot{\psi}_k = \hat{u}_k \tag{B.12c}$$

où ψ_k représente l'angle d'orientation du vecteur vitesse transformé $\dot{\hat{\mathbf{r}}}_k$. Le vecteur des nouvelles entrées de contrôle pour le système transformé est $\dot{\psi} = (\dot{\psi}_1, \ldots, \dot{\psi}_N)^T$.

En utilisant les définitions précédentes d'une formation élastique et la matrice générale de transformation, une nouvelle loi de commande générale est proposé dans le théorème suivant :

Théorème B.2 *(Extension de Briñón-Arranz et al. 2011 [21]) La matrice $\boldsymbol{G}$ est deux fois dérivable avec des dérivés bornées résultant d'une séquence de transformations affines définie comme* (B.10) *et $\mathcal{F} = \boldsymbol{G} \circ \mathcal{C}_0$ est la formation élastique désirée. Les paramètres du contrôle sont $\omega_0 \neq 0$, $\kappa > 0$, $\beta > 0$ et la condition suivante est satisfaite :*

$$v_k > 0 \tag{B.13}$$

Donc, la loi de commande :

$$\dot{v}_k = -\beta v_k + \frac{\hat{u}_k \dot{\boldsymbol{r}}_k^T \boldsymbol{G} \boldsymbol{R}_{\frac{\pi}{2}} \dot{\hat{\boldsymbol{r}}}_k + \dot{\boldsymbol{r}}_k^T \left(\ddot{\boldsymbol{G}} \boldsymbol{G}^{-1} \boldsymbol{r}_k + \beta \dot{\boldsymbol{G}} \boldsymbol{G}^{-1} \boldsymbol{r}_k + 2 \dot{\boldsymbol{G}} \dot{\hat{\boldsymbol{r}}}_k + \beta \boldsymbol{G} \dot{\hat{\boldsymbol{r}}}_k) \right)}{v_k} \tag{B.14a}$$

$$u_k = \frac{\hat{u}_k \dot{\boldsymbol{r}}_k^T \boldsymbol{R}_{\frac{\pi}{2}}^T \boldsymbol{G} \boldsymbol{R}_{\frac{\pi}{2}} \dot{\hat{\boldsymbol{r}}}_k + \dot{\boldsymbol{r}}_k^T \boldsymbol{R}_{\frac{\pi}{2}}^T \left(\ddot{\boldsymbol{G}} \boldsymbol{G}^{-1} \boldsymbol{r}_k + \beta \dot{\boldsymbol{G}} \boldsymbol{G}^{-1} \boldsymbol{r}_k + 2 \dot{\boldsymbol{G}} \dot{\hat{\boldsymbol{r}}}_k + \beta \boldsymbol{G} \dot{\hat{\boldsymbol{r}}}_k) \right)}{v_k^2} \tag{B.14b}$$

où $\dot{\hat{\boldsymbol{r}}}_k$ et $\hat{u}_k$ sont définis par (B.12) *et* (B.9) *respectivement, stabilise tous les agents définis par* (B.1) *vers la formation élastique définie par $\mathcal{F}$. Le sens de rotation est déterminé par le signe de ω_0. En plus, pour $K > 0$, la distribution uniforme autour du cercle unité est le seul point critique de $U(\psi)$ exponentiellement stable. Par conséquent, les agents sont répartis dans la formation $\mathcal{F}$, en prenant en compte la transformation $\boldsymbol{G}$.*

Simulations

La Figure B.7 montre la simulation de cinq agents régis par la loi de commande du Theorème B.2 où $\mathbf{G}(t) = \mathbf{T}_{c(t)}\mathbf{S}_{R(t)}$. Les paramètres de contrôle sont $\omega_0 = \kappa = \beta = 1$ and $K = 0.1$. La référence du rayon variant dans le temps est

$$R(t) = 5 + 2\cos\frac{2\pi}{500}t$$

et la référence suivie par le centre correspond à

$$\mathbf{c}(t) = (\frac{1}{10}t, 3\sin\frac{2\pi}{300}t)^T$$

Les agents convergent vers la formation circulaire variant dans le temps pour toutes les conditions initiales aléatoires (position et le cap de l'agent) représentés dans la figure par les agents bleu vides. Ceci est un exemple d'une application possible de la loi de

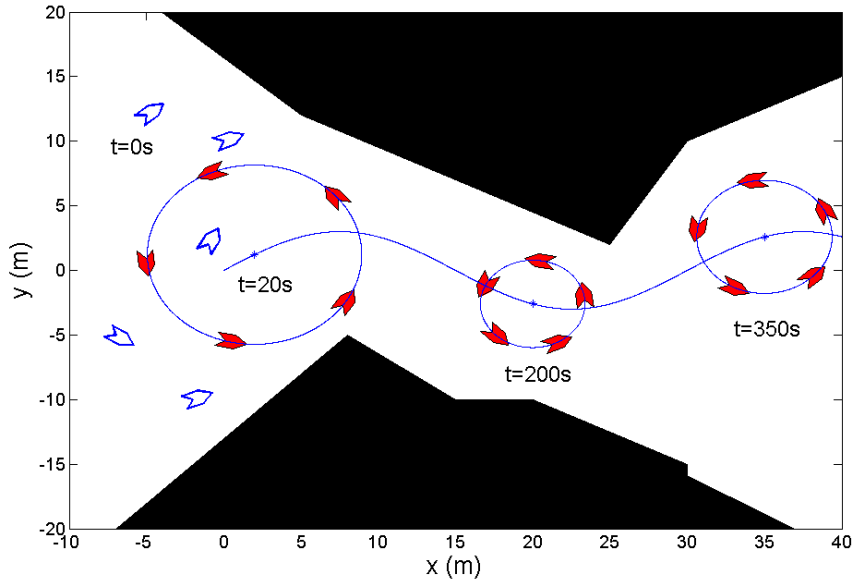

FIGURE B.7 – *Simulation de cinq agents régis par la loi de commande* (B.14) *avec* $\boldsymbol{G}(t) = \boldsymbol{T}_{c(t)}\boldsymbol{S}_{R(t)}$. *La formation circulaire, dont le centre suit une référence variant dans le temps, change de rayon, afin d'éviter les obstacles (blocs noirs).*

commande d'un mouvement combiné et une première étape pour atteindre l'objectif final de la conception d'un contrôle collaboratif pour générer les deux références d'une manière distribuée.

En plus, le rayon de communication considéré ici est $\rho = 10$, ce qui satisfait la condition géométrique

$$\rho > 2R_{max} \sin \frac{\pi}{N}$$

où R_{max} est la borne supérieur de la référence du rayon, dans ce cas $R_{max} = 7$. Par conséquent, les agents sont distribués autour de la formation circulaire variant dans le temps.

B.4 Recherche collaborative d'une source

Les sections précédents B.2 et B.3 traitent du premier objectif abordée dans cette thèse : la conception des lois de commande pour une formation d'une flotte de véhicules autonomes sous-marins (AUVs). Les contributions présentées stabilisent les véhicules vers des formations variant dans le temps qui changent sa forme et qui sont capables de suivre une référence donnée du centre de la formation. La principale contribution de cette section est la conception de stratégies de contrôle qui permetent de générer de

façon coopérative la direction appropriée pour déplacer le centre de la formation afin d'atteindre la recherche d'une source. L'objectif est de développer un nouvel algorithme décentralisé pour que les agents se mettent d'accord sur une orientation commune.

Le problème principal abordé ici est celui de la recherche d'une source en utilisant un système multi-agent. Afin de localiser la source d'un champ scalaire, les AUVs sont équipés de capteurs qui mesurent le champ d'intérêt tel que la température, la salinité, les flux de polluants. Dans cette situation, la flotte de véhicules peut être vue comme un réseau de capteurs mobiles. La stabilisation des agents uniformément répartis le long d'une formation circulaire est pertinente pour aborder le problème de la recherche d'une source. En fonction des résultats précédents dans le domaine du contrôle d'une formation, cette section se concentre sur l'obtention de la référence appropriée du centre afin de diriger la flotte d'agents vers l'emplacement d'une source sous-marine.

Une première contribution montre que la collecte des données à partir des capteurs des véhicules, qui sont uniformément réparties le long d'une formation circulaire fixe, permet de rapprocher le gradient d'un signal. Ensuite, un algorithme distribué basé sur ce résultat est proposé pour estimer la direction du gradient en prenant en compte des contraintes de communication. Cette approche combine les résultats précédents en matière de contrôle d'une formation exposés dans la section B.2 et les résultats existants sur des algorithms de consensus appliqués à la situation d'un réseau de capteurs mobiles. Un algorithme modifié qui exploite les propriétés périodiques de la formation circulaire est également proposé. Enfin, une comparaison des deux algorithmes distribués est discuté et motivée par des simulations.

B.4.1 Formulation du problème

Cette section prend en considération plusieurs hypothèses sur le champ scalaire mesuré. Le signal qui représente le champ scalaire est continu. Ce signal est émis par une source de telle sorte que la source est le maximum ou le minimum du champ scalaire. On suppose que la distribution de signal décroît à partir de la position de la source.

L'objectif est localiser la source d'un signal à l'aide d'une flotte d'AUVs. Dans ce cas, les véhicules sont équipés de capteurs qui sont capables de mesurer la concentration de la quantité d'intérêt. La flotte d'agents devient un réseau sans fil de capteurs mobiles. La contribution de cette section se concentre sur la conception d'un algorithme collaboratif pour choisir une direction appropriée afin de diriger une formation d'AUV vers la position de la source. La stratégie de contrôle proposée dans cette thèse se compose de deux niveaux :

1. Estimation de la direction du gradient du signal emis par la source.

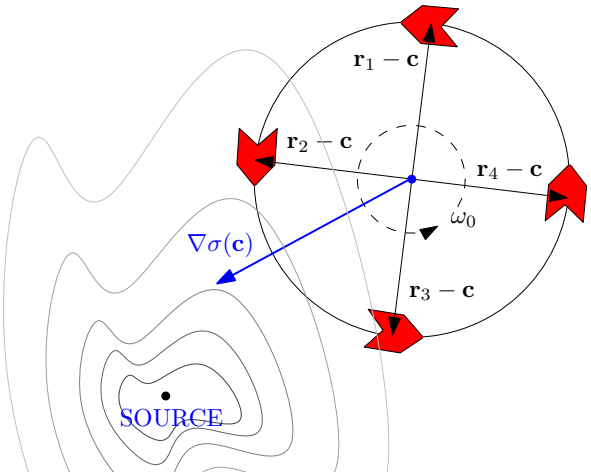

FIGURE B.8 – *Représentation de la recherche d'une source*

2. Génération d'une trajectoire de référence pour le centre de la formation en considerant la direction estimée du gradient.

Cette section ne considére que la première étape : fournir un algorithme qui estime la direction du gradient d'un signal par une formation d'agents. Dans des recherches futures, cette direction sera utilisée pour diriger le centre de la formation vers la valeur maximale ou minimale du champ scalaire, comme le montre la Figure B.8

Si l'on considère la source comme une cible, il semble intéressant d'utiliser une formation circulaire pour faire face au problème de la recherche d'une source. Lorsque la formation atteindra la position de la source, les véhicules vont tourner autour de cette source. Cette stratégie est adaptée dans le contexte de la localisation d'une source sous-marine car, même si la source est fixe, les AUVs sont toujours en mouvement. Les agents doivent éviter une vitesse nulle. Les mêmes contraintes apparaissent dans un scénario aérien dans lequel une flotte de véhicules aériens autonomes (UAVs par le sigle en anglais) accomplit une mission de suivi d'une cible, par exemple. Quelques résultats dans le contexte de localisation de cibles et de circumnavigation (cela signifie que les véhicules décrivent des trajectoires circulaires autour de la cible) ont été récemment mis au point en utilisant des *"bearing"* mesures [44]. Ce résultat est construit sur l'idée de que chaque agent peut mesurer l'angle entre sa position et la position de la cible. Le problème de recherche d'une source de cette thèse considère les approches précédentes dans ce domaine dans lequel la source d'un signal est localisée par les mesures de ce signal. Par conséquent, les techniques utilisant des *bearing* mesures ne sont pas applicables dans ce contexte.

Approximation du gradient par une formation circulaire fixe

La première idée est de concevoir un algorithme pour estimer la direction du gradient du signal sur la base des mesures de concentration obtenues par une formation circulaire d'agents. Les contraintes de communication entre les véhicules sont prises en compte. Cette direction estimé du gradient sera la vitesse de référence du centre de la formation afin de diriger le groupe de véhicules vers la position de la source.

Grâce à la loi de commande précédente (B.9), les véhicules sont stabilisés vers une formation circulaire décrite par un point central $\mathbf{c}$, un rayon R et un angle ϕ, ce qui est linéairement croissant dans le temps (*c'est-à-dire* $\phi = \omega_0 t$ pour une certaine vitesse angulaire $\omega_0 > 0$). En suite, la position de chaque agent k dans la formation est donnée par l'équation suivante :

$$x_k = c_x + R\cos\left(\phi + k\frac{2\pi}{N}\right) \tag{B.15a}$$

$$y_k = c_y + R\sin\left(\phi + k\frac{2\pi}{N}\right) \tag{B.15b}$$

Cette équation décrit une formation dans laquelle les agents sont distribués uniformément autour d'un cercle de rayon R. Dans le contexte de la recherche d'une source, l'objectif est que le centre de la formation $\mathbf{c}(t)$ suive une trajectoire qui converge vers le maximum d'un signal, qui est généralement sa source.

La distribution du signal dans l'environnement sera décrite par une fonction spatiale inconnue $\sigma : \mathbb{R}^2 \to \mathbb{R}^+$, de telle sorte que l'agent k mesure le signal à sa position $\sigma(\mathbf{r}_k)$. On consière un réseau de capteurs mobiles, dans lequel la position du capteur k est donnée par (B.15). Chaque capteur obtient des mesures du signal σ. Le gradient de la fonction σ au centre de la formation circulaire $\mathbf{c}$ est représenté par $\nabla\sigma(\mathbf{c}) = (\nabla_x\sigma(\mathbf{c}), \nabla_y\sigma(\mathbf{c}))$. Les lemmes suivants sont proposés :

Lemme B.1 *(Briñón-Arranz et al. 2011 [20]) La fonction σ est bornée et $\sigma(\boldsymbol{r}_k)$ représente la mesure obtenue par l'agent k où $\boldsymbol{r}_k$ est son verteur position donné par* (B.15)*. On considère une flotte de $N > 2$ agents uniformement distribués atour d'un cercle dont le centre $\boldsymbol{c}$ est fixe, alors :*

$$\frac{1}{N}\sum_{k=1}^{N}\sigma(\boldsymbol{r}_k)(\boldsymbol{r}_k - \boldsymbol{c}) = \frac{R^2}{2}\nabla\sigma(\boldsymbol{c})^T + o(R^2) \tag{B.16}$$

où $o(R^2)$ est un vecteur tel que $\|o(R^2)\|$ est négligeable par rapport à R^2.

Lemme B.2 *(Briñón-Arranz et al. 2011 [20]) La fonction σ est bornée et $\sigma(\boldsymbol{r}_k)$ représente la mesure obtenue par l'agent k où $\boldsymbol{r}_k$ est son verteur position donné par* (B.15)*. On*

considère un nombre illimité d'agents atour de la formation circulaire dont le centre est fixe, alors :

$$\frac{1}{2\pi}\int_0^{2\pi}\sigma(\boldsymbol{r}_k)(\boldsymbol{r}_k-\boldsymbol{c})d\phi=\frac{R^2}{2}\nabla\sigma(\boldsymbol{c})^T+o(R^2) \tag{B.17}$$

Les deux résultats fournissent une approximation du gradient du signal au centre de la formation circulaire.

B.4.2 Estimation collaborative de la direction du gradient par une formation circulaire fixe

L'objectif de cette partie se concentre sur la première étape de la stratégie du contrôle exposée précédemment dans la formulation du problème. L'idée est de développer un algorithme d'estimation de la direction du gradient du signal émis par la source. Comme c'était expliqué précédemment, cette estimation sera réalisée par une formation circulaire d'AUVs. Grâce aux Lemmes B.1 et B.2, le gradient d'un signal peut être approchée par les mesures obtenues à partir d'une formation circulaire fixe d'agents répartis uniformément. Un premier algorithme centralisé basé sur ce résultat est abordé dans [104]. Néanmoins, afin de prendre en compte des contraintes de communication entre les agents, un algorithme distribué est développé pour évaluer cette direction du gradient par une formation circulaire fixe.

Dans cette situation, chaque agent calcule sa propre estimation de la direction du gradient avec ses propres mesures du signal et les mesures de ses voisins. En conséquence, chaque agent calcule une direction différente. Afin d'obtenir la même direction estimée pour tous les agents, un algorithme de consensus est inclus. Cet algorithme permet aux agents de converger vers la même direction estimée du gradient, en prenant en compte la topologie du graphe de communication.

Source fixe

Les contraintes de communication sont prises en compte par un graphe de communication $\mathcal{G}$. En raison de ces restrictions de communication chaque agent estime que son propre direction du gradient $\mathbf{z}_k$ en utilisant l'information de ses voisins en fonction du graphe de communication. L'objectif est de faire converge toutes les directions estimées $\mathbf{z}_k$ vers la direction moyenne définie comme suit :

$$\mathbf{u}^*=\frac{1}{N}\sum_{k=1}^{N}\mathbf{u}_k;\quad \mathbf{u}_k=\sigma_k(\mathbf{r}_k-\mathbf{c}) \tag{B.18}$$

où $\mathbf{u}_k$ est le vecteur position relative de l'agent k étant pondéré par sa mesure de la concentration $\sigma_k=\sigma(\mathbf{r}_k)$. Grâce au Lemme 4.1, ce vecteur $\mathbf{u}^*$ est une bonne estimation

de la direction du gradient du signal au centre $\mathbf{c}$ de la formation. Un algorithme de consensus est mis en oeuvre pour atteindre un accord sur la direction estimée du gradient par tous les agents.

Il est plausible de supposer qu'une borne maximal de la concentration du signal est connue pour ce problème. Par conséquent, $\|\mathbf{u} - \mathbf{1} \otimes \mathbf{u}^*\| \leq \alpha$ où α dépend du rayon de la formation circulaire et de la mesure de concentration la plus grande obtenue par les agents.

Théorème B.3 *(Briñón-Arranz et al. 2011 [20]) Considerons une formation circulaire de N agents définie par* (B.15) *avec un graphe de communication connecté $\mathcal{G}$ et le centre de la formation est fixe. La foncion $\sigma : \mathbb{R}^2 \to \mathbb{R}^+$ est bornée et le vecteur $\boldsymbol{u}^*$ défini dans* (B.18) *satisfait $\|\dot{\boldsymbol{u}}^*\| \leq \nu$. Donc, $\boldsymbol{z}^*(t) = \boldsymbol{1} \otimes \boldsymbol{u}^*$ est un équilibre global asymptotiquement ϵ-stable de*

$$\dot{\boldsymbol{z}} = -\kappa \boldsymbol{L}_2 \boldsymbol{z} - \boldsymbol{L}_2 \boldsymbol{u} + (\boldsymbol{I}_N + \Delta)_2 (\boldsymbol{u} - \boldsymbol{z}) \tag{B.19}$$

avec $\boldsymbol{u} = (\sigma_1(\boldsymbol{r}_1 - \boldsymbol{c})^T, \ldots, \sigma_N(\boldsymbol{r}_N - \boldsymbol{c})^T)^T$ et

$$\epsilon = \frac{(\nu\sqrt{N}(1 + d_{max}) + \alpha\gamma)\lambda_{max}^{\frac{1}{2}}(\boldsymbol{A}_\kappa)}{\lambda_{min}^{\frac{5}{2}}(\boldsymbol{A}_\kappa)}$$

où les matrices $\boldsymbol{A}_\kappa = (\boldsymbol{I}_N + \Delta + \kappa \boldsymbol{L})_2$ et $\boldsymbol{B} = (\boldsymbol{I}_N + \mathcal{A})_2$ satisfont la relation suivante $\left\|\boldsymbol{B}^T \boldsymbol{A}_\kappa\right\| \leq \gamma$ et la constante α a été définie précédemment.

Simulations

Afin de montrer les performances de cet algorithme distribué des résultats de simulations sont présentés. La simulation montre une formation circulaire fixe de cinq agents de rayon $R = 1m$ et vitesse angulaire de $\omega_0 = 1rad/s$. Le graphe de communication est un anneau (d_1 graphe circulant). Dans la Figure B.9 l'algorithme de consensus pour la recherche d'une source (B.19) d'après le Théorème 4.3 est mis en oeuvre avec $\kappa = 50$. Pour cette simulation, la fonction σ qui représente le signal dont la source est à l'origine, a des courbes de niveau circulaires :

$$\sigma(x, y) = 100e^{-(x^2+y^2)/10}$$

Par conséquent, le vecteur gradient $\nabla\sigma(\mathbf{c})$ fournit l'orientation adéquate pour diriger la formation à l'emplacement de la source.

La Figure B.9(a) montre deux instants différents. Les cercles vides représentent les conditions initiales et les lignes noires pointillés la direction initiale estimée z_k par chaque agent. Les cercles rouges représentent la position des agents à $t = 50$ et les lignes rouges sont les directions du gradient estimées à ce moment là. La ligne bleue est

la vraie direction du gradient au centre $\mathbf{c}$. La Figure 4.6(b) montre les composants de la variable du consensus $\mathbf{z}_k$ et le vecteur $\mathbf{u}^*$. Les directions estimées $\mathbf{z}_k$ oscillent autour du vecteur $\mathbf{u}^*$, ce qui est une bonne estimation de la vrai direction du gradient, pour toutes les conditions initiales.

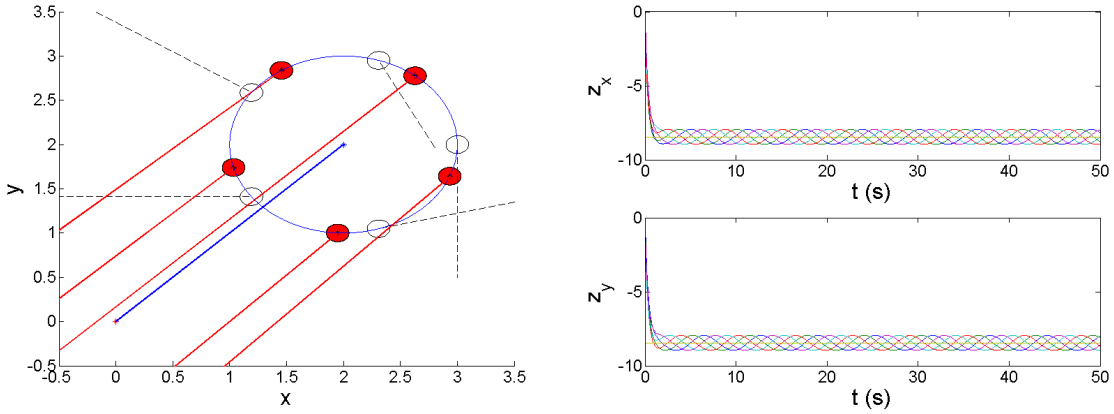

(a) Directions estimées $\mathbf{z}_k$ à $t = 0s$ (lignes noires(b) Coordonnées X et Y des directions estimées $\mathbf{z}_k$ pointillés) et à $t = 50s$ (lignes rouges)

FIGURE B.9 – *Simulation d'une formation circulaire fixe de cinq agents centrée à* $\boldsymbol{c} = (2, 2)^T$. *La fonction* σ *qui représente le signal dont la source est à l'origine a courbes de niveau circulaires. L'algorithme de consensus du Théorème 4.3 est appliqué avec* $\kappa = 50$.

Afin d'améliorer l'algorithme distribué présenté précédemment, les propriétés périodiques de la situation supposé dans la formulation du problème sont étudiés.

Les agents décrivent un mouvement périodique, cela signifie que $\mathbf{r}_k(t) = \mathbf{r}_k(t + T)$ avec $T = 2\pi/\omega_0$. Pour cette raison, les mesures σ_k obtenues par l'agent k sont une fonction périodique car $\sigma(\mathbf{r}_k(t)) = \sigma(\mathbf{r}_k(t + T))$. En conclusion, la variable d'entrée de l'algorithme de consensus $\mathbf{u}_k = \sigma_k(\mathbf{r}_k - \mathbf{c})$ est une fonction T-périodique avec $T = 2\pi/\omega_0$. Les directions estimées $\mathbf{z}_k$ obtenues par l'algorithme de consensus (B.19) sont périodiques aussi. La moyenne de ces solutions se rapproche de la direction du gradient du signal emis par la source. Grâce à ces observations, une analyse des propriétés moyennes de la variable d'entrée $\mathbf{u}_k$ semble adéquate. Maintenant l'idée est d'améliorer l'algorithme de consensus distribué précédent en utilisant les propriétés périodiques des mesures $\sigma(\mathbf{r}_k)$.

Le vecteur d'entrée $\mathbf{u}_k$ dans l'algorithme de consensus précédent est remplacée par sa valeur moyenne sur une période $T = 2\pi/\omega_0$, ce qui est défini comme suit :

$$\bar{\mathbf{u}}_k = \frac{1}{T}\int_{t-T}^{t} \sigma_k(\mathbf{r}_k(\tau) - \mathbf{c})d\tau \tag{B.20}$$

Donc, grâce au Lemme B.2 le nouveau vecteur $\bar{\mathbf{u}}^*$ approche le gradient du signal σ au centre de la formation circulaire :

$$\bar{\mathbf{u}}^* = \frac{1}{N}\sum_{k=1}^{N} \bar{\mathbf{u}}_k \tag{B.21}$$

La nouvelle variable d'entrée de l'algorithme amélioré basé sur (B.19), est le vecteur $\bar{\mathbf{u}} = (\bar{\mathbf{u}}_1^T, \bar{\mathbf{u}}_2^T, \ldots, \bar{\mathbf{u}}_N^T)^T$, et l'objetif est défini par $\bar{\mathbf{u}}_\mathbf{1}^* = \mathbf{1} \otimes \bar{\mathbf{u}}^*$. Suite à l'analyse développée précédemment, supposons que la distribution du signal varie doucement, donc, la inégalité suivante est satisfaite $\|(\bar{\mathbf{u}} - \bar{\mathbf{u}}_\mathbf{1}^*)\| \leq \bar{\alpha}$. Partant de ces considérations, un nouvel algorithme est proposé dans le corollaire suivant :

Corollaire B.2 *(Briñón-Arranz et al. 2011 [20]) Considerons une formation circulaire de N agents définie par* (4.27) *avec un graphe de communication connecté $\mathcal{G}$ et le centre de la formation est fixe. La fonction $\sigma : \mathbb{R}^2 \to \mathbb{R}^+$ est bornée et le vecteur $\bar{\boldsymbol{u}}^*$ est défini par* (B.21) *satisfait $\|\dot{\bar{\boldsymbol{u}}}^*\| \leq \bar{\nu}$. Alors, $\boldsymbol{z}^*(t) = \boldsymbol{1} \otimes \bar{\boldsymbol{u}}^*$ est un équilibre global asymptotiquement $\bar{\epsilon}$-stable de*

$$\dot{\boldsymbol{z}} = -\kappa \boldsymbol{L}_2 \boldsymbol{z} - \boldsymbol{L}_2 \bar{\boldsymbol{u}} + (\boldsymbol{I}_N + \Delta)_2(\bar{\boldsymbol{u}} - \boldsymbol{z}) \tag{B.22}$$

avec

$$\bar{\epsilon} = \frac{(\bar{\nu}\sqrt{N}(1 + d_{max}) + \bar{\alpha}\gamma)\lambda_{max}^{\frac{1}{2}}(\boldsymbol{A}_\kappa)}{\lambda_{min}^{\frac{5}{2}}(\boldsymbol{A}_\kappa)}$$

où la matrice $\boldsymbol{A}_\kappa$ et les constantes $\bar{\alpha}$ et γ ont été définies précédemment.

Simulations

La simulation montre la même formation circulaire de cinq agents de la simulation précédente. Dans la Figure B.10 l'algorithme distribué amelioré (B.22) du Corollaire B.2 est implementé avec $\kappa = 1$ par une formation circulaire centée à $\mathbf{c} = (2, 2)^T$. Le signal mesuré est le même que dans la simulation précédente. La Figure B.10(a) montre deux instants différents, les conditions initiales et la situation stable à $t = 50s$. La Figure B.10(b) montre les composants de la variable de consensus $\mathbf{z}_k$. Cet algorithme nous permet d'éliminer les oscillations et les vecteurs finaux de tous les agents $\mathbf{z}_k$ (lignes rouges) sont parallèles à la vrai direction du gradient (ligne bleue).

B.5 Conclusions et Travaux à venir

Le but de ce chapitre est de résumer les contributions présentées dans le manuscrit et d'introduire quelques perspectives de futures recherches pour compléter et améliorer ce travail.

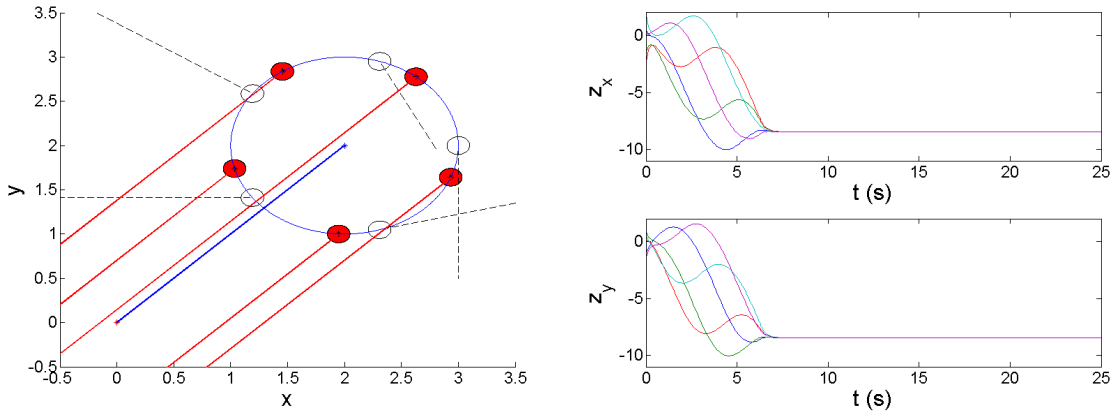

(a) Directions estimées $\mathbf{z}_k$ à $t = 0s$ (lignes noires pointillés)et à $t = 50s$ (lignes rouges)

(b) Composants des directions estimées $\mathbf{z}_k$

FIGURE B.10 – *Simulation d'une formation circulaire de cinq agents centrée à* $\boldsymbol{c} = (2, 2)^T$. *La fonction* σ *qui représente le signal dont la source est à l'origine a courbes de niveau circulaires. En ce cas, le nouveau algorithme de consensus* (4.33) *est appliqué.*

B.5.1 Resumé des contributions et conclusions

Le contrôle coopératif est un enjeu important en raison de son grand nombre d'applications. Le comportement collaboratif d'un groupe d'agents signifie qu'il existe plusieurs interconnexions entre eux afin d'atteindre un objectif commun. Dans le cadre de cette thèse, les agents représentent des véhicules autonomes sous-marins (AUVs) et l'objectif commun est de localiser et de suivre une source sous-marine (d'eau douce, de flux polluant, de produits chimiques). Pour atteindre l'objectif final, la mission collaborative est structurée en plusieurs phases. Premièrement, les véhicules atteignent une formation souhaitée grâce à un asservissement de position. La contribution principale est de stabiliser la flotte vers des formations variant dans le temps. Par ailleurs, une loi de commande coopérative distribue les AUVs uniformément autour de la formation, en prenant en compte des contraintes de communication. Ces résultats constituent le support pour attaquer le problème de recherche d'une source. Un algorithme distribué est élaboré pour estimer la direction du gradient d'un signal par un groupe de véhicules en formation. Cette direction estimée dirigera la flotte d'AUVs vers l'emplacement de la source.

Commande d'une formation qui suit des réferences variant dans le temps

Nous avons développé différents lois de commande pour stabiliser les véhicules vers une formation variant dans le temps. Les véhicules sont modélisés par une cinématique unicycle. Les mouvements collectifs, en particulier des mouvements circulaires, ont été

étudiés dans la littérature récente. La principale contribution de cette thèse au domaine du contrôle d'une formation, est que les véhicules sont stabilisés vers une formation qui est défini par des paramètres variant dans le temps. La première loi de commande développée dans cette thèse permet à chaque AUV décrire une trajectoire circulaire dont le centre est une réference externe variant dans le temps. L'idée principale est de changer le système de référence par un systeme de coordonnées relatives qui est invariant par rapport au centre. La transformation de coordonnées est appropriée pour prendre en compte certaines propriétés de la nouvelle variété, dans laquelle le système multi-agent est exprimé. Basée sur la même idée, une loi de commande est présentée pour gouverner les AUVs, afin de converger vers des mouvements circulaires avec un rayon variant dans le temps.

En conséquence, la contribution suivante, présentée dans la section B.3, traite de la généralisation des deux lois de commande précédentes en utilisant la même idée, c'est-à-dire, en transformant le système de référence. Comme résultat, un nouveau cadre est développé pour exprimer une grande classe de mouvements en déformant un cercle unitaire. Les trois principales transformations qui peuvent être appliquées à une formation afin de changer sa forme, sa position et son orientation, sont la homotethie, la translation et la rotation, respectivement. Par conséquent, une séquence de transformations affines appliquées au cercle unité définit une nouvelle formation qui résulte de la déformation de ce cercle. Les configurations obtenues avec cette méthode sont appelées formations élastiques dans cette thèse. Grâce à une transformation de coordonnées, une nouvelle loi de commande générale est conçue pour stabiliser un groupe de véhicules vers des formations élastiques qui sont définies par les transformations affines. Par ailleurs, cette nouvelle formulation nous permet de spécifier plusieurs classes de mouvements définies par une référence de vitesse. Un nouvel algorithme basé aussi sur des transformations affines, permet à un groupe d'agents de converger vers une configuration variant dans le temps en termes de vitesse.

Algorithmes collaboratifs pour le contrôle d'une formation

Une caractéristique importante du contrôle d'une formation est que les agents collaborent entre eux. Par conséquent, plusieurs algorithmes coopératifs sont inclus dans les lois de commande présentées dans les deux sections B.2 et B.3 afin d'atteindre différents objectifs. La première approche coopérative traitée est la répartition des véhicules autour d'une formation. Les agents doivent échanger des informations : dans ce cas, leur angle de cap ou leur angle transformé par rapport à un système de coordonnées relatives. Par conséquent, les interconnexions entre les agents doivent être prises en compte. La topologie de communication du réseau est représentée par un graphe non orienté. La convergence des algorithmes collaboratifs présentés dans cette thèse est liée aux

propriétés de connectivité des graphes, étudiées en détail dans l'Annexe A.

La première contribution est de considérer un graphe dans lequel les interconnexions dépendent de la position relative des véhicules. Cela signifie que, chaque véhicule ne peut communiquer qu'avec ses voisins proches, c'est-à-dire, deux véhicules sont connectés, si la distance entre eux est plus petite qu'une certaine valeur. Cette valeur, appelée rayon maximal de communication, définit la région de communication. Les lois de commande précédentes pour stabiliser les agents vers une formation circulaire uniformement distribuée autour du cercle sont considérées désormais sous cette approche de communication. Par ailleurs, cet algorithme collaboratif est également appliqué dans le cas des formations élastiques.

Une autre contribution traite de l'application des algorithmes de consensus à des lois de commande précédentes développées dans cette thèse pour contrôler une formation. Notez que les paramètres variant dans le temps qui définissent les formations, sont considérés comme des références externes et sont connus par tous les véhicules. L'objectif de l'approche coopérative est d'assouplir cette hypothèse. Le cas particulier lorsque le centre de référence d'une formation circulaire est inconnue est analysée. Dans cette situation, la vitesse et l'accélération de la trajectoire désirée du centre sont des références données et grâce à un algorithme de consensus les agents atteignent un consensus sur la position du centre de la formation circulaire. Ce résultat, peut être vu comme une étape préliminaire pour atteindre l'objectif de recherche d'une source.

Estimation distribuée de la direction du gradient

Plusieurs techniques de contrôle ont été développées ces dernières années afin de localiser la source d'un signal. Les stratégies de recherche d'une source sont conçues pour piloter un seul véhicule ou un groupe de véhicules vers l'emplacement de la source. Les véhicules sont équipés de capteurs qui sont capables de mesurer le signal scalaire provenant de la source. Néanmoins, le capteur n'a pas la capacité de détection de la position de la source.

Dans ce contexte, notre principale contribution est de prouver mathématiquement que la direction du gradient d'un signal peut être approchée par les mesures obtenues par un groupe d'agents répartis uniformément autour d'une formation circulaire fixe. Les capteurs n'ont pas de connaissance de la forme fonctionnelle du champ. C'est un résultat important parce que la direction du gradient pourrait être utilisée pour déplacer le centre de la formation vers l'endroit désiré où se trouve la source.

Prenant en compte des contraintes de communication entre les véhicules, nous avons développé un algorithme distribué basé sur *consensus filters* qui exploite le résultat mathématique précédent. Cette méthode collaborative permet d'estimer la direction du gradient du signal au centre d'une formation circulaire d'AUVs. Grâce au mou-

vement circulaire des agents, les mesures obtenues sont périodiques. Par conséquent, les directions estimées oscillent autour de la direction réelle du gradient. En utilisant la moyenne des directions calculées, nous avons présenté un algorithme amélioré qui a pour but de réduire ces oscillations. Dans ce deuxième cas, le consensus est atteint exactement et tous les agents estiment la même direction du gradient.

Plusieurs simulations sont fournis pour appuyer ces résultats et pour analyser les performances des deux algorithmes. Par ailleurs, les performances des deux stratégies, lorsque la source émettrice du signal est variant dans le temps, sont évaluées par simulation.

B.5.2 Travaux en cours et à venir

Cette thèse propose des stratégies de contrôle pour effectuer plusieurs défis présents dans les missions coopératives sous-marines. Les principales contributions présentées précédemment ont été développés en envisageant plusieurs hypothèses relatives au modèle des véhicules, à la précision des capteurs, aux contraintes de communication, au modèle de l'environnement, etc. Par conséquent, les futures directions de recherche se concentrent sur l'assouplissement des hypothèses précédentes afin d'analyser des situations plus réalistes.

Perspectives dans le contrôle d'une formation

Toutes les lois de commande pour contrôler une formation développées dans cette thèse prennent en considération le fait que les véhicules connaissent leur vecteur de position absolue par rapport au système de réference inertiel. Cette hypothèse est conforme au fait que les véhicules sont équipés d'une centrale à inertie pour la navigation très précise. Néanmoins, selon plusieurs travaux cités précédemment qui portent sur le contrôle d'une formation circulair [69, 86, 120, 149, 150], il semble très approprié de considérer que chaque véhicule est seulement capable de calculer la distance relative par rapport à ses voisins. Dans cette situation, les lois de commande pour une formation circulaire variant dans le temps presentées dans la section B.2 et le contrôle de formations élastiques présenté dans la section B.3 seront améliorés par des algorithmes coopératifs afin de prendre en compte les positions relatives entre les véhicules au lieu de leurs positions absolues.

Une autre direction de recherche s'occupe de l'extension des stratégies de contrôle étudiés dans cette thèse en vue de stabiliser une flotte de véhicules autonomes sous-marins vers des formations variant dans le temps en présence de courants. Les auteurs de [120, 121] fournissent différentes lois de commande pour stabiliser un groupe de véhicules vers des formations circulaires en présence de courants constants et variant

dans le temps respectivement. Suivant le même raisonnement de ces travaux, et grâce à des idées présentées dans cette thèse, nous allons développer des lois de commande coopératives pour faire converger les véhicules vers des formations élastiques variant dans le temps en présence de courants.

Tout au long de cette thèse, nous supposons un modèle cinématique bidimensionnel du véhicule. En conséquence, les trajectoires et les formations obtenues sont planes, c'est-à-dire, les véhicules sont en mouvement dans un cadre en 2-D. Dans la littérature, différentes stratégies de contrôle sont proposées pour obtenir un mouvement coordonné en trois dimensions d'un groupe de véhicules, voir [91] et [69] par exemple. Une extension logique des résultats étudiés dans cette thèse considère la possibilité de développer des lois de commande d'une formation variant dans le temps en trois dimensions.

Enfin, un futur travail pour améliorer les algorithmes de contrôle d'une formation présentés traite sur l'évitement d'obstacles et de collisions entre les véhicules. Le contrôle coopératif proposé dans les sections B.2 et B.3 pour répartir uniformément les véhicules autour d'une formation peut être considéré comme une méthode d'évitement des collisions. Le terme potentiel ajouté à la loi de commande permet à ces véhicules d'éviter les collisions avec leurs voisins dans la formation. Cependant, nous ne pouvons assurer l'évitement des collisions jusqu'à ce que les véhicules soient stabilisés vers la configuration finale. Par conséquent, certaines techniques basées sur les stratégies coopératives [47, 98] peuvent être appliquées afin de garantir que les véhicules ne s'heurtent pas les uns avec les autres. De la même manière, différents termes potentiels peuvent être ajoutés à la loi de commande pour contrôler la formation afin d'atteindre l'évitement d'obstacles pendant le mouvement de la flottille [108].

Perspectives dans la recherche d'une source

La section B.4 aborde le problème de la recherche d'une source sous une perspective collaborative. Un premier résultat mathématique démontre que les mesures collectées par un groupe de capteurs uniformément répartis autour d'une configuration circulaire fixe peuvent servir à rapprocher le gradient du signal d'un champ scalair au centre de la formation circulaire. Le premier axe de recherche évident est d'analyser les implications si le centre de la formation est variant dans le temps.

Nous avons développé deux algorithmes distribués, basés sur ce résultat précédent, pour estimer la direction du gradient du signal par une formation circulaire des véhicules autonomes sous-marins. L'idée est d'utiliser cette direction afin de diriger la formation vers l'emplacement de la source, c'est-à-dire, au maximum ou minimum du champ scalaire. Une approche collaborative qui fusionne le contrôle d'une formation variant dans le temps, des algorithmes de consensus avec une réference de vitesse et la direction du gradient estimé sera prise en compte dans les travaux futurs pour atteindre la

localisation de la source.

Nous supposons une communication parfaite entre deux véhicules connectés. En vue d'analyser la performance des algorithmes de contrôle étudiés dans cette thèse en présence de contraintes de communication plus réalistes, des approches coopératives concernants la perte de paquets, les problèmes de bruit et les délais de communication peuvent être envisagées dans d'autres recherches.

Bibliography

[1] H. Ando, Y. Oasa, Suzuki, and M. Yamashita. Distributed memoryless point convergence algorithm for mobile robots with limited visibility. *IEEE Transactions on Robotics and Automation*, 15:818–828, 1999.

[2] J. Angeles. *Fundamentals of robotic mechanical systems: theory, methods, and algorithms*. Springer, 2007.

[3] K. B. Ariyur and M. Krstić. *Real-time optimization by extremum-seeking control*. IEEE Control Systems Magazine, 2003.

[4] R. Bachmayer and N. E. Leonard. Vehicle networks for gradient descent in a sampled environment. In *Proceedings of the 41st IEEE Conference on Decision and Control, Las Vegas, NV, USA*, pages 112–117, 2002.

[5] T. Balch and R. C. Arkin. Behavior-based formation control for multirobot teams. *IEEE Transactions on Robotics and Automation*, 14(6):926–939, December 1998.

[6] D. Baronov and J. Baillieul. Autonomous vehicle control for ascending/descending along a potential field with two applications. In *Proceedings of the 2008 American Control Conference, Seattle, Washington, USA*, pages 678–683, 2008.

[7] M. Baseggio, A. Cenedese, P. Merlo, M. Pozzi, and L. Schenato. Distributed perimeter patrolling and tracking for camera networks. In *Proceedings on the 49th IEEE Conference on Decision and Control, Atlanta, USA*, pages 2093–2098, 2010.

[8] D. Bauso, L. Giarre, and R. Pesenti. Attitude alignment of a team of UAVs under decentralized information structure. In *In Proceedings of 2003 IEEE Conference on Control Applications, Istanbul, Turkey*, volume 1, pages 486 – 491, 2003.

[9] R. W. Beard, J. Lawton, and F. Y. Hadaegh. A feedback architecture for formation control. In *Proceedings of the 2000 American Control Conference, Chicago, IL, USA*, volume 6, pages 4087–4091, 2000.

[10] R. W. Beard, J. Lawton, and F. Y. Hadaegh. A coordination architecture for spacecraft formation control. *IEEE Transactions on Control Systems Technology*, 9:777–790, 2001.

[11] D. P. Bertsekas and J. Tsitsiklis. *Parallell and Distributed Computation*. Upper Saddle River, 1989.

[12] N. Biggs. *Algebraic Graph Theory*. Cambridge University Press, 1994.

[13] E. Biyik and M. Arcak. Gradient climbing in formation via extremum seeking and passivity-based coordination rules. *Asian Journal of Control, Special Issue on Collective Behavior and Control of Multi-Agent Systems*, 10(2):201–211, 2008.

[14] V. Borkar and P. Varaiya. Asymptotic agreement in distributed estimation. *IEEE Transactions on Automatic Control*, 27(3):650–655, 1982.

[15] M. Bowling and M. Veloso. Multiagent learning using a variable learning rate. *Artificial Intelligence*, 136:215–250, 2002.

[16] L. Briñón-Arranz, A. Seuret, and C. Canudas-de-Wit. Translation control of a fleet circular formation of AUVs under finite communication range. In *Proceedings of the 48th IEEE Conference on Decision and Control held jointly with the 28th Chinese Control Conference, Shanghai, China*, pages 8345–8350, 2009.

[17] L. Briñón-Arranz, A. Seuret, and C. Canudas-de-Wit. Contraction control of a fleet circular formation of AUVs under limited communication range. In *Proceedings of the IEEE 2010 American Control Conference, Baltimore, MD, USA*, 2010.

[18] L. Briñón-Arranz, A. Seuret, and C. Canudas-de-Wit. General framework using affine transformations to formation control design. In *Proceedings of the 2nd IFAC Workshop on Distributed Estimation and Control in Networked Systems, Annecy, France*, 2010.

[19] L. Briñón-Arranz, A. Seuret, and C. Canudas-de-Wit. Collaborative estimation of gradient direction by a formation of AUVs. In *5th International ICST Conference on Performance Evaluation Methodologies and Tools, 2011 Cachan, France*, 2011.

[20] L. Briñón-Arranz, A. Seuret, and C. Canudas-de-Wit. Collaborative estimation of gradient direction by a formation of AUVs under communication constraints. In *Proceedings of the 50th IEEE Conference on Decision and Control, held jointly with the European Control Conference, Orlando, FL, USA*, pages 5583–5588, 2011.

[21] L. Briñón-Arranz, A. Seuret, and C. Canudas-de-Wit. Elastic formation control based on affine transformations. In *Proceedings of the 2011 American Control Conference, San Francisco, CA, USA*, pages 3984–3989, 2011.

[22] T. J. I. Bromwich. *An introduction to the theory of infinite series.* London Macmillan, 1908.

[23] E. Burian, D. Yoerger, A. Bradley, and H. Singh. Gradient search with autonomous underwater vehicles using scalar measurements. In *Proceedings of the 1996 Symposium on Autonomous Underwater Vehicle Technology*, pages 86–98, 1996.

[24] Z. Cao, L. Xie, B. Zhang, S. Wang, and M. Tan. Formation constrained multi-robot system in unknown environments. In *Proceedings of the 2003 IEEE International Conference on Robotics and Automation, Taipei, Taiwan*, volume 1, pages 735–740, 2003.

[25] J. Chen, D. Sun, J. Yang, and H. Chen. Leader-follower formation control of multiple non-holonomic mobile robots incorporating a receding-horizon scheme. *The International Journal of Robotics Research*, 29(6):727–747, May 2010.

[26] Y. Q. Chen and Z. Wang. Formation control: a review and a new consideration. In *Proceedings of the 2005 IEEE/RSJ International Conference on Intelligent Robots and Systems, Edmonton, Alberta, Canada*, pages 3181–3186, 2005.

[27] N. Chopra and M. W. Spong. On exponential synchronization of kuramoto oscillators. *IEEE Transactions on Automatic Control*, 54:353–357, 2009.

[28] J. Cochran and M. Krstić. Source seeking with a nonholonomic unicycle without position measurements and with tuning of angular velocity Part I: Stability analysis. In *Proceedings of 46th IEEE Conference on Decision and Control, New Orleans, LA, USA*, pages 6009–6016, 2007.

[29] J. Cochran and M. Krstić. Nonholonomic source seeking with tuning of angular velocity. *IEEE Transactions on Automatic Control*, 54(4):717–731, 2009.

[30] J. Cochran, A. Siranosian, N. Ghods, and M. Krstić. Source seeking with a nonholonomic unicycle without position measurements and with tuning of angular velocity Part II: Applications. In *Proceedings of 46th IEEE Conference on Decision and Control, New Orleans, LA, USA*, pages 1951–1956, 2007.

[31] J. Cochran, A. Siranosian, N. Ghods, and M. Krstić. 3-d source seeking for underactuated vehicles without position measurement. *IEEE Transactions on Robotics*, 25(1):117–129, 2009.

[32] L. Consolinia, F. Morbidib, D. Prattichizzo, and M. Tosques. On the control of a leader-follower formation of nonholonomic mobile robots. In *Proceedings of the 45th IEEE Conference on Decision and Control, San Diego, CA, USA*, pages 5992–5997, 2006.

[33] L. Consolinia, F. Morbidib, D. Prattichizzo, and M. Tosques. Leader-follower formation control of nonholonomic mobile robots with input constraints. *Automatica*, 44:1343–1349, May 2008.

[34] J. Cortés. Achieving coordination tasks in finite time via nonsmooth gradient flows. In *Proceedings of the 44th IEEE Conference on Decision and Control and 2005 European Control Conference, Seville, Spain*, 2005.

[35] J. Cortés, S. Martínez, T. Karataş, and F. Bullo. Coverage control for mobile sensing networks. *IEEE Transactions on Robotics and Automation*, 20(2):243–255, 2004.

[36] J. Cortés, S. Martínez, and F. Bullo. Robust rendezvous for mobile autonomous agents via proximity graphs in arbitrary dimensions. *IEEE Transactions on Automatic Control*, 51:1289–1298, 2006.

[37] I. D. Couzin, J. Krause, N. R. Franks, and S. A. Levin. Effective leadership and decision-making in animal groups on the move. *Nature*, 433:513–516, 2005.

[38] X. Cui, C. T. Hardin, R. K. Ragade, and A. S. Elmaghraby. A swarm approach for emission sources localization. In *16th IEEE International Conference on Tools with Artificial Intelligence, Boca Raton, FL, USA*, pages 424–430, 2004.

[39] T. B. Curtin, J. G. Bellingham, J. Catipovic, and D. Webb. Autonomous oceanographic sampling networks. *Oceanography*, 6(3):86–94, 1993.

[40] P. Davidsson. Agent based social simulation: A computer science view. *Journal of Artificial Societies and Social Simulation*, 5(1), 2002.

[41] P. J. Davis. *Circulant matrices*. John Wiley & Sons, Inc., 1979.

[42] M. Defoort, T. Floquet, A. Kökösy, and W. Perruquetti. Sliding-mode formation control for cooperative autonomous mobile robots. *IEEE Transactions on Industrial Electronics*, 55:3944–3953, 2008.

[43] M. Defoort, A. Kokosy, T. Floquet, W. Perruquettic, and J. Palos. Motion planning for cooperative unicycle-type mobile robots with limited sensing ranges: A distributed receding horizon approach. *Robotics and Autonomous Systems*, 57:1094–1106, 2009.

[44] M. Deghat, I. Shames, B. D. O. Anderson, and C. Yu. Target localization and circumnavigation using bearing measurements in 2d. In *Proceedings of the 49th IEEE Conference on Decision and Control, Atlanta, GA, USA*, 2010.

[45] J. P. Desai, J. Ostrowski, and V. Kumar. Controlling formations of multiple mobile robots. In *Proceedings of the 1998 IEEE International Conference on Robotics and Automation, Leuven, Belgium*, volume 4, pages 2864–2869, 1998.

[46] D. V. Dimarogonas and K. J. Kyriakopoulos. On the rendezvous problem for multiple nonholonomic agents. *IEEE Transactions on Automatic Control*, 52:916–922, 2007.

[47] D. V. Dimarogonas, S. G. Loizou, K. J. Kyriakopoulos, , and M. M. Zavlanos. A feedback stabilization and collision avoidance scheme for multiple independent non-point agents. *Automatica*, 42:229–243, 2006.

[48] D. D. Dudenhoeffer and M. P. Jones. A formation behavior for large-scale microrobot force deployement. In *Proceedings of the 32nd Conference on Winter simulation, Orlando, FL, USA*, pages 972–982, 2000.

[49] D. B. Edwards, T. A. Bean, D. L. Odell, and M. J. Anderson. A leader-follower algorithm for multiple auv formations. *IEEE/OES Autonomous Underwater Vehicles*, pages 40–46, 2004.

[50] M. Egerstedt and X. Hu. Formation constrained multi-agent control. *IEEE Transactions on Robotics and Automation*, 17:947–951, 2001.

[51] J. A. Fax and R. M. Murray. Graph laplacians and stabilization of vehicle formations. In *Proceedings of the 15th IFAC World Conference, Barcelona, Spain*, July 2002.

[52] J. A. Fax and R. M. Murray. Information flow and cooperative control of vehicle formations. *IEEE Transactions on Automatic Control*, 49:1465–1476, 2004.

[53] J. Ferber. *Multi-Agent System: An Introduction to Distributed Artificial Intelligence*. Addison Wesley Longman, 1999.

[54] C. Ferrari, E. Pagello, J. Ota, and T. Arai. Multirobot motion coordination in space and time. *Robotics and Autonomous Systems*, 25:219–229, 1998.

[55] E. Fiorelli, P. Bhatta, N. E. Leonard, and I. Shulman. Adaptive sampling using feedback control of an autonomous underwater glider fleet. In *Proceedings of 13th International Symposium on Unmanned Untethered Submersible Technology (UUST)*, pages 1–16, 2003.

[56] J. D. Foley, A. van Dam, S. K. Feiner, J. F. Hughes, and R. L. Phillips. *Introduction to Computer Graphics*. Addison-Wesley Publishing Co., 1994.

[57] E. Frazzoli, M. A. Dahleh, and E. Feron. Robust hybrid control for autonomous vehicle motion planning. *Proceedings of the 39th IEEE Conference on Decision and Control*, pages 821–826, 2000.

[58] M. Fruchard, P. Morin, and C. Samson. A framework for the control of nonholonomic mobile manipulators. *International Journal of Robotic Research*, 25:745–780, 2006.

[59] S. S. Ge, C.-H. Fua, and K. W. Lim. Multi-robot formations: queues and artificial potential trenches. In *Proceedingsof the 2004 IEEE International Conference on Robotics and Automation, New Orleans, LA, USA*, volume 4, pages 3345–3350, 2004.

[60] R. Ghabcheloo, A. Pascoal, C. Silvestre, and I. Kaminer. Coordinated path following control of multiple wheeled robots with directed communication links. In *Proceedings of the 44th IEEE Conference on Decision and Control, and the European Control Conference 2005, Seville, Spain*, 2005.

[61] N. Ghods and M. Krstić. Multi-agent deployment around a source in one dimension by extremum seeking. In *Proceedings of the 2010 American Control Conference, Baltimore, MD, USA*, pages 4794–4799, 2010.

[62] S. Glavaski, M. Chaves, R. Day, P. Nag, A. Williams, and W. Zhang. Vehicle networks: achieving regular formation. In *Proceedings of the 2003 American Control Conference, Minneapolis, MN, USA*, volume 5, pages 4095–4100, 2003.

[63] M. F. Z. Goldgeier and P. S. Krishnaprasad. Control of small formations using shape coordinates. In *Proceedings of the 2003 IEEE International Conference on Robotics and Automation, Taipei, Taiwan*, pages 2510–2515, 2003.

[64] P. Ögren, E. Fiorelli, and N. E. Leonard. Cooperative control of mobile sensor networks: Adaptive gradient climbing in a distributed environment. *IEEE Transactions on Automatic Control*, 49:1292–1302, 2004.

[65] M. Greytak and F. S. Hover. Motion planning with an analytic risk cost for holonomic vehicles. In *Proceedings of the 48th IEEE Conference on Decision and Control held jointly with the 28th Chinese Control Conference, Shanghai, China*, 2009.

[66] V. Gupta, B. Hassibi, and R. M. Murray. Stability analysis of stochastically varying formations of dynamic agents. In *In Proceedings of the 42nd IEEE Conference on Decision and Control, Maui, Hawai*, volume 1, pages 504–509, 2003.

[67] A. T. Hayes, A. Martinoli, and R. M. Goodman. Distributed odor source localization. *IEEE Sensors Journal*, 2:260–271, 2002.

[68] J. M. Hendrickx. *Graphs and Networks for the Analysis of Autonomous Agent Systems*. PhD thesis, Université catholique de Louvain, Ecole Polytechnique de Louvain, Département d'Ingénierie Mathématique, 2008.

[69] S. Hernandez and D. A. Paley. Three-dimensional motion coordination in a time-invariant flowfield. In *Proceedings of the 48th IEEE Conference on Decision and Control held jointly with the 28th Chinese Control Conference, Shanghai, China*, pages 7043–7048, 2009.

[70] B. Horn. *Robot Vision*. The MIT Press, 1986.

[71] A. Jadbabaie, J. Lin, and A. S. Morse. Coordination of groups of mobile autonomous agents using nearest neighbor rules. *IEEE Transactions on Automatic Control*, 48(6):988–1001, June 2003.

[72] A. Jain. *Fundamentals of digital image processing*. Prentice-Hall, 1986.

[73] M. Ji and M. Egerstedt. Distributed coordination control of multiagent systems while preserving connectedness. *IEEE Transactions on Robotics*, 23:693–703, 2007.

[74] E. Justhand and P.Krishnaprasad. Equilibria and steering laws for planar formations. *Systems & Control Letters*, 52(1):25–38, 2004.

[75] H. Khalil. *Nonlinear Systems*. Prentice Hall, third edition 2002.

[76] A. Kibangou, C. Siclet, and L. Ros. Doppler estimation and data detection for underwater acoustic zf-ofdm receiver. In *7th International Symposium on Wireless Communication Systems, York, United Kingdom*, pages 591–595, 2010.

[77] A. Kibangou, C. Siclet, and L. Ros. Joint channel and doppler estimation for multicarrier underwater communications. In *2010 IEEE International Conference on Acoustics, Speech, and Signal Processing, Dallas, TX, USA*, pages 5630–5633, 2010.

[78] B. C. Kim and I. T. Lu. Parameter study of OFDM underwater communications system. In *Proceedings of OCEANS 2000 MTS/IEEE Conference and Exhibition*, volume 2, pages 1251–1255, 2000.

[79] T.-H. Kim and T. Sugie. Cooperative control for target-capturing task based on a cyclic pursuit strategy. *Automatica*, 43:1426–1431, 2007.

[80] D. J. Klein and K. A. Morgansen. Controlled collective motion for trajectory tracking. In *Proceedings of the 2006 American Control Conference, Minneapolis, MN, USA*, pages 5269–5275, June 2006.

[81] D. Kostic, S. Adinandra, J. Caarls, N. V. D. Wouw, and H. Nijmeijer. Collision-free tracking control of unicycle mobile robots. In *Proceedings of the 48th IEEE Conference on Decision and Control held jointly with the 28th Chinese Control Conference, Shanghai, China*, 2009.

[82] M. Krstić and H.-H. Wang. Stability of extremum seeking feedback for general nonlinear dynamic systems. *Automatica*, 36:595–601, 2000.

[83] Y. Kuramoto. Self-entrainment of a population of coupled non-linear oscillators. In *International Symposium on Mathematical Problems in Theoretical Physics*, volume 39 of *Lecture Notes in Physics*, pages 420–422. Springer Berlin / Heidelberg, 1975.

[84] A. Kwok and S. Martínez. Unicycle coverage control via hybrid modeling. *IEEE Transactions on Automatic Control*, 55:528–532, 2010.

[85] Y. Lan, Z. Lin, M. Cao, and G. Yan. A distributed reconfigurable control law for escorting and patrolling missions using teams of unicycles. In *Proceedings of the 49th IEEE Conference on Decision and Control, Atlanta, GA, USA*, pages 5456–5461, 2010.

[86] N. E. Leonard, D. A. Paley, F. Lekien, R. Sepulchre, D. M. Frantatoni, and R. E. Davis. Collective motion, sensor networks and ocean sampling. *Proceedings of the IEEE*, 95:48–74, 2007.

[87] M. A. Lewis and K.-H. Tan. High precision formation control of mobile robots using virtual structures. *Autonomous Robots*, 4(4):387–403, 1997.

[88] J. Lin, A. S. Morse, and B. D. O. Anderson. The multi-agent rendezvous problem. In *Proceedings of the 42nd IEEE Conference on Decision and Control, Maui, Hawaii*, volume 2, pages 1508 – 1513, 2003.

[89] J. Lin, A. S. Morse, and B. D. O. Anderson. The multi-agent rendezvous problem. Part 1: The synchronous case. *SIAM Journal on Control Optimization*, 46:2096–2119, 2007.

[90] J. Lin, A. S. Morse, and B. D. O. Anderson. The multi-agent rendezvous problem. Part 2: The asynchronous case. *SIAM Journal on Control Optimization*, 46:2120–2147, 2007.

[91] P. Lin, K. Qin, Z. Li, and W. Ren. Collective rotating motions of second-order multi-agent systems in three-dimensional space. *Systems & Control Letters*, 60:365–372, 2011.

[92] Z. Lin, M. Broucke, and B. Francis. Local control strategies for groups of mobile autonomous agents. *IEEE Transactions on Automatic Control*, 2004.

[93] S.-J. Liu and M. Krstic. Stochastic source seeking for nonholonomic unicycle. *Automatica*, 46:1443–1453, 2010.

[94] J.-M. Luna, R. Fierro, C. Abdallah, and J. Wood. An adaptive coverage control algorithm for deployment of nonholonomic mobile sensors. In *Proceedings of the 49th IEEE Conference on Decision and Control, Atlanta, GA, USA*, pages 1250–1256, 2010.

[95] J. A. Marshall, M. E. Broucke, and B. A. Francis. Formations of vehicles in cyclic pursuit. *IEEE Transactions on Automatic Control*, 2004.

[96] S. Martínez and F. Bullo. Optimal sensor placement and motion coordination for target tracking. *Automatica*, 42:661–668, 2006.

[97] S. Martínez, J. Cortés, and F. Bullo. Motion coordination with distributed information. *IEEE Control Systems Magazine*, 27:75–88, 2007.

[98] S. Mastellone, D. M. Stipanović, C. R. Graunke, K. A. Intlekofer, and M. W. Spong. Formation control and collision avoidance for multi-agent non-holonomic systems: Theory and experiments. *The International Journal of Robotics Research*, 27:107–126, 2008.

[99] A. S. Matveev, H. Teimoori, and A. V. Savkin. Navigation of a unicycle-like mobile robot for environmental extremum seeking. *Automatica*, 47(1):85–91, 2011.

[100] C. G. Mayhew, R. G. Sanfelice, and A. R. Teel. Robust source-seeking hybrid controllers for autonomous vehicles. In *Proceedings of the 2007 American Control Conference, New York City, USA*, pages 1185–1190, 2007.

[101] C. G. Mayhew, R. G. Sanfelice, and A. R. Teel. Robust hybrid source-seeking algorithms based on directional derivatives and their approximations. In *Proceedings of the 47th IEEE Conference on Decision and Control, Cancun, Mexico*, pages 1735–1740, 2008.

[102] S. Monteiro and E. Bicho. A dynamical systems approach to behavior-based formation control. In *Proceedings of the 2002 IEEE International Conference on Robotics and Automation, Washington D.C., USA*, volume 3, pages 2606–2611, 2002.

[103] B. J. Moore and C. Canudas-de-Wit. Formation control via distributed optimization of alignment error. In *Proceedings of the 48th IEEE Decision and Control held jointly with the 28th Chinese Control Conference, Shanghai, China*, pages 3075–3080, 2009.

[104] B. J. Moore and C. Canudas-de-Wit. Source seeking via collaborative measurements by a circular formation of agents. In *Prooceedings of the 2010 IEEE American Control Conference, Baltimore, USA*, pages 6417–6422, 2010.

[105] L. Moreau, R. Bachmayer, and N. E. Leonard. Coordinated gradient descent: A case study of lagrangian dynamics with projected gradient information. *IFAC Lagrangian and Hamiltonian Methods in Nonlinear Control*, pages 57–62, 2003.

[106] Y. Moreno and A. F. Pacheco. Synchronization of kuramoto oscillators in scale-free networks. *Europhysics Letters*, 68(4), 2004.

[107] M. E. Mortenson. *Mathematics for Computer Graphics Applications*. Industrial Press Inc, 1999.

[108] R. Olfati-Saber. Flocking for multi-agent dynamic systems: Algorithms and theory. *IEEE Transactions on Automatic Control*, 51:401–420, 2006.

[109] R. Olfati-Saber, J. A. Fax, and R. M. Murray. Consensus and cooperation in networked multi-agent systems. *Proceedings of the IEEE*, 95:215–233, 2007.

[110] R. Olfati-Saber and R. M. Murray. Graph rigidity and distributed formation stabilization of multi-vehicle systems. In *Proceedings of 41st IEEE Conference on Decision and Control, Las Vegas, Nevada, USA*, 2002.

[111] R. Olfati-Saber and R. M. Murray. Consensus problems in networks of agents whit switching topology and time-delays. *IEEE Transactions on Automatic Control*, 2004.

[112] R. Olfati-Saber and J. S. Shamma. Consensus filters for sensor networks and distributed sensor fusion. In *Proceedings of the 44th IEEE Conference on Decision and Control, and the European Control Conference 2005, Seville, Spain*, pages 6698–6703, 2005.

[113] J. Opderbecke, M. Drogou, and M. E. Bouhier. D8.1 description of the scientific mission scenario(s) to be investigated for the marine application. Technical report, Ifremer, FeedNetBack project, 2009.

[114] R. Oung, A. Ramezani, and R. D'Andrea. Feasibility of a distributed flight array. In *Proceedings of the 48th IEEE Conference on Decision and Control held jointly with the 28th Chinese Control Conference, Shanghai, China*, 2009.

[115] D. A. Paley. *Cooperative control of collective motion for ocean sampling with autonomous vehicles*. PhD thesis, Princeton University, 2007.

[116] D. A. Paley and N. E. Leonard. Collective motion of self-propelled particles: Stabilizing symmetric formations on closed curves. In *Proceedings of the 45th IEEE Conference on Decision and Control, San Diego, CS, USA*, pages 5067–5072, 2006.

[117] D. A. Paley, N. E. Leonard, and R. Sepulchre. Collective motion: Bistability and trajectory tracking. In *Proceedings of the 43th IEEE Conference Decision and Control, Paradise Island, Bahamas*, 2004.

[118] D. A. Paley, N. E. Leonard, and R. Sepulchre. Oscillator models and collective motion: Splay state stabilization of self-propelled particles. In *Proceedings of the 44th IEEE Conference on Decision and Control, and the European Control Conference 2005, Seville, Spain*, pages 3935–3940, December 2005.

[119] D. A. Paley, N. E. Leonard, and R. Sepulchre. Stabilization of symmetric formations to motion around convex loops. *Systems & Control Letters*, 57:209–215, 2008.

[120] D. A. Paley and C. Peterson. Stabilization of collective motion in a time-invariant flowfield. *Journal of Guidance, Control, and Dynamics*, 32:771–779, 2009.

[121] C. Peterson and D. A. Paley. Multivehicle coordination in an estimated time-varying flowfield. *Jornal of Guidance, control, and dynamics*, 34(1):177–191, 2011.

[122] L. Pimenta, V. Kumar, R. Mesquita, and G. Pereira. Sensing and coverage for a network of heterogeneous robots. In *47th IEEE Conference on Decision and Control*, pages 3947–3952, Cancun, Mexico, 2008.

[123] B. Porat and A. Nehorai. Localizing vapor-emitting sources by moving sensors. *IEEE Transactions on Signal Processing*, 44:1018–1021, 1996.

[124] M. Rabbat and R. Nowak. Distributed optimization in sensor networks. In *Proceedings of the 3rd International symposium on Information processing in sensor networks, Berkeley, CA, USA*, pages 20–27, 2004.

[125] R. L. Raffard, C. J. Tomlin, and S. P. Boyd. Distributed optimization for cooperative agents: Application to formation flight. In *Proceedings of 43rd IEEE Conference on Decision and Control, Paradise Islands, The Bahamas*, volume 3, pages 2453–2459, 2004.

[126] J. H. Reif and H. Wang. Social potential fields: A distributed behavioral control for autonomous robots. *Robotics and Autonomous Systems*, 27:171–194, May 1999.

[127] W. Ren. Consensus strategies for cooperative control of vehicle formations. *IET Control Theory & Applications*, 1(2):505–512, 2007.

[128] W. Ren. On consensus algorithms for double-integrator dynamics. *IEEE Transactions on Automatic Control*, 2008.

[129] W. Ren and E. Atkins. Distributed multi-vehicle coordinated control via local information exchange. *International Journal on Robust Nonlinear Control*, 17:1002–1033, 2007.

[130] W. Ren and R. W. Beard. Consensus seeking in multi-agents systems under dynamically changing interaction topologies. *IEEE Transactions on Automatic Control*, 50:655–661, 2005.

[131] W. Ren and R. W. Beard. *Distributed Consensus in Multi-vehicle Cooperative Control*. Communication and Control Engineering. Springer, 2007.

[132] W. Ren, R. W. Beard, and E. M. Atkins. A survey of consensus problems in multi-agent coordination. In *Proceedings of the 2005 American Control Conference, Portland, OR, USA*, pages 1859–1864, 2005.

[133] A. Renzaglia, L. Doitsidis, A. Martinelli, and E. Kosmatopoulos. Adaptive-based distributed cooperative multi-robot coverage. In *Proceedings of the 2011 American Control Conference, San Francisco, CA, USA*, pages 468–473, 2011.

[134] C. W. Reynolds. Flocks, herds, and schools: A distributed behavioral model. In *Proceedings of the 14th annual conference on Computer graphics and interactive techniques, Anaheim, CA, USA*, volume 21, July 1987.

[135] V. Rigaud, J. L. Michel, J. S. Ferguson, J. M. Laframboise, T. Crees, P. Leon, J. Opderbecke, and Y. Chardard. First steps in Ifremer's autonomous underwater vehicle program-a 3000m depth operational survey auv for environmental monitoring. In *Proceedings of the 14th International Offshore and Polar Engineering Conference, Tolon, France*, pages 203–208, 2004.

[136] E. Roche. *Commande à échantillonnage variable pour les systèmes LPV: application à un sous-marin autonome*. PhD thesis, Université de Grenoble, 2011.

[137] A. Rogers, E. David, J.Schiff, and . N.R. Jennings. The effects of proxy bidding and minimum bid increments within ebay auctions. *ACM Transactions on the Web*, 74:572–581, 2007.

[138] L. Sabattini, C. Secchi, and C. Fantuzzi. Potential based control strategy for arbitrary shape formations of mobile robots. In *Proceedings of the 2009 IEEE/RSJ International conference on Intelligent robots and systems, St. Louis, MO, USA*, pages 3762–3767, 2009.

[139] L. Sabattini, C. Secchi, and C. Fantuzzi. Arbitrarily shaped formations of mobile robots: artificial potential fields and coordinate transformation. *Autonomous Robots*, 30:385–397, 2011.

[140] S. S. Sahyoun, S. M. Djouadi, and H. Qi. Dynamic plume tracking using mobile sensors. In *Proceedings of the 2010 American Control Conference, Baltimore, MD, USA*, pages 2915–2920, 2010.

[141] R. Salomon. Evolutionary algorithms and gradient search: similarities and differences. *IEEE Transactions on Evolutionary Computation*, 2:45–55, 1998.

[142] A. Sarlette. *Geometry and Symmetries in Coordination Control*. PhD thesis, Université de Liège, Faculté des Sciences Appliquées, 2009.

[143] A. Sarlette, S. Bonnabel, and R. Sepulchre. Coordinated motion design on Lie groups. *IEEE Transactions on Automatic Control*, 55(5):1047–1058, 2010.

[144] N. Schurr, J. Marecki, M. Tambe, and P. Scerri. The future of disaster response: Humans working with multiagent teams using defacto. In *In AAAI Spring Symposium on AI Technologies for Homeland Security*, 2005.

[145] M. Schwager, J. McLurkin, and D. Rus. Distributed coverage control with sensory feedback for networked robots. In *Proceedings of Robotics: Science and Systems*, Philadelphia, PA, USA, 2006.

[146] R. Sepulchre. Consensus on nonlinear spaces. In *Proceedings of the 8th IFAC Symposium on Nonlinear Control Systems, Bologna, Italy*, 2010.

[147] R. Sepulchre. Consensus on nonlinear spaces. *Annual Reviews in Control*, 35:56–64, 2011.

[148] R. Sepulchre, D. A. Paley, and N. E. Leonard. Group coordination and cooperative control of steered particles in the plane. *Lecture Notes in control and Information Sciences*, 2006.

[149] R. Sepulchre, D. A. Paley, and N. E. Leonard. Stabilization of planar collective motion: All-to-all communication. *IEEE Transactions on Automatic Control*, 2007.

[150] R. Sepulchre, D. A. Paley, and N. E. Leonard. Stabilization of planar collective motion with limited communication. *IEEE Transactions on Automatic Control*, 53:706–719, 2008.

[151] A. Seuret, D. V. Dimarogonas, and K. H. Johansson. Consensus under communication delays. In *Proceedings of the 47th IEEE Conference on Decision and Control, Cancun, Mexico*, pages 4922–4927, 2008.

[152] A. Seuret, D. Simon, E. Roche, L. Briñón-Arranz, and G. R. de Campos. Multiagent systems architecture. d01.03 building blocks and architectures. Technical report, NeCS Team, INRIA Rône-Alpes, FeedNetBack project, February 2010.

[153] S. Spry and J. K. Hedrick. Formation control using generalized coordinates. In *Proceedings of the 43rd IEEE Conference on Decision and Control, Paradis Island, Bahamas*, pages 2441–2446, 2004.

[154] M. S. Stanković and D. M. Stipanović. Extremum seeking under stochastic noise and applications to mobile sensors. *Automatica*, 46:1243–1251, 2010.

[155] M. Stojanovic. Recent advances in high-speed underwater acoustic communications. *IEEE Journal of Oceanic Engineering*, 21, 1996.

[156] K. J. Åström and B. Wittenmark. *Adaptive control*. Addison Wesley, 1995.

[157] S. H. Strogatz. From kuramoto to crawford: exploring the onset of synchronization in populations of coupled oscillators. *Physica: Nonlinear Phenomena*, 143:1–20, 2000.

[158] S. H. Strogatz. *SYNC: the emerging science of spontaneous order*. Theia, 2003.

[159] H. Su, X. Wang, and G. Chen. Rendezvous of multiple mobile agents with preserved network connectivity. *Systems & Control Letters*, 59:313–322, 2010.

[160] K. Sugihara and I. Suzuki. Distributed motion coordination of multiple mobile robots. In *Proceedings of the 5th IEEE International Symposium on Intelligent Control*, 1990.

[161] R. Sun and I. Naveh. Simulating organizational decision-making using a cognitively realistic agent model. *Journal of Artificial Societies and Social Simulation*, 7(3), 2004.

[162] H. Takahashi, H. Nishi, and K. Ohnishi. Autonomous decentralized control for formation of multiple mobile robots considering ability of robot. *IEEE Transactions on Industrial Electronics*, 51(6):1272–1279, 2004.

[163] K.-H. Tan and M. A. Lewis. Virtual structures for high-precision cooperative mobile robotic control. In *Proceedings of the 1996 IEEE/RSJ International Conference on Intelligent Robots and Systems, Osaka, Japan*, volume 1, pages 132–139, 1996.

[164] H. G. Tanner, A. Jadbabaie, and G. J. Pappas. Stable flocking of mobile agents, part I: Fixed topology. In *Proceedings of the 42nd IEEE Conference on Decision and Control, Maui, Hawaii*, volume 2, pages 2010–2015, 2003.

[165] H. G. Tanner, A. Jadbabaie, and G. J. Pappas. Stable flocking of mobile agents, part II: Dynamic topology. In *Proceedings of the 42nd IEEE Conference on Decision and Control, Maui, Hawaii*, volume 2, pages 2016–2021, 2003.

[166] A. R. Teel and D. Popovic. Solving smooth and nonsmooth multivariable extremum seeking problems by the methods of nonlinear programming. In *Proceedings of the 2001 American Control Conference, Arlington, VA , USA*, number 3, pages 2394–2399, 2001.

[167] W. Truszkowski, H. L. Hallock, C. Rouff, J. Karlin, J. Rash, M. Hinchey, and R. Sterritt. *Autonomous and Autonomic Systems: With Applications to NASA Intelligent Spacecraft Operations and Exploration Systems*, chapter Swarms in Space Missions, pages 207–221. NASA Monographs in Systems and Software Engineering, 2009.

[168] J. N. Tsitsiklis. *Problems in Decentralized Decision Making and Computation*. PhD thesis, Department of EECS, Laboratory for Information and Decision Systems, MIT, 1984.

[169] J. N. Tsitsiklis, D. P. Bertsekas, and M. Athans. Distributed asynchronous deterministic and stochastic gradient optimization algorithms. *IEEE Transactions on Automatic Control*, 31(9):803–812, 1986.

[170] N. Ukita and T. Matsuyama. Real-time cooperative multi-target tracking by communicating active vision agents. *Computer Vision and Image Understanding*, 97:137–179, 2005.

[171] P. Wieland, J.-S. Kimb, and F. Allgöwer. On topology and dynamics of consensus among linear high-order agents. *International Journal of Systems Science*, 42, 2011.

[172] P. Wieland, R. Sepulchre, and F. Allgöwer. An internal model principle is necessary and sufficient for linear output synchronization. *Automatica*, 47:1068–1074, 2011.

[173] G. Xie and L. Wang. Consensus control for a class of networks of dynamic agents. *International Journal of Robust and Nonlinear Control*, 17(10-11):941–959, 2007.

[174] J. Yu, S. M. L. Valle, and D. Liberzon. Rendezvous without coordinates. *IEEE Transactions on Automatic Control, accepted. Available from http://ieeexplore.ieee.org/stamp/stamp.jsp?tp=&arnumber=5783895.*

[175] D. Zarzhitsky, D. F. Spears, and W. M. Spears. Swarms for chemical plume tracing. In *Proceedings of the 2005 IEEE Swarm Intelligence Symposium, Pasadena, CA, USA*, pages 49–256, 2005.

[176] C. Zhang, D. Arnold, N. Ghods, A. Siranosian, and M. Krstić. Source seeking with non-holonomic unicycle without position measurement and with tuning of forward velocity. *Systems & Control Letters*, 56:245–252, 2007.

[177] F. Zhang and N. E. Leonard. Cooperative filters and control for cooperative exploration. *IEEE Transactions on Automatic Control*, 55:650–663, 2010.